

AD-A128 084

LOCKHEED-CALIFORNIA CO BURBANK PYE CANYON RESEARCH LAB
EFFECT OF LOAD HISTORY ON FATIGUE LIFE.(U)

F/6 11/4

DEC 81 J T RYDER K N LAURAITIS

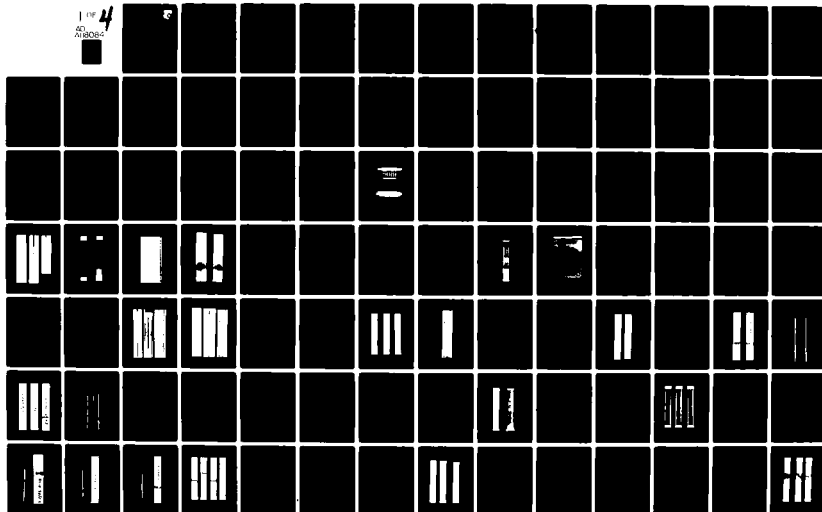
F33615-78-C-5090

UNCLASSIFIED

LR-29586-1

AFWAL-TR-81-4155

NL



AD A118084

AFWAL-TR-81-4155



EFFECT OF LOAD HISTORY ON FATIGUE LIFE

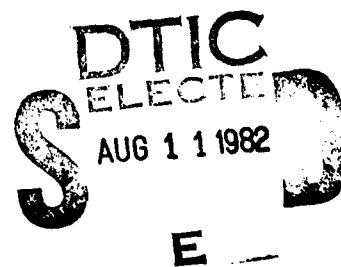
J. T. Ryder, K. N. Lauraitis
Lockheed-California Company
Rye Canyon Research Laboratory
Burbank, California 91520

December, 1981

Task II Final Report January 1980 - April 1981

Approved for public release: Distribution unlimited

Materials Laboratory
Air Force Wright Aeronautical Laboratories
Air Force Systems Command
Wright-Patterson Air Force Base, Ohio 45433



DTIC FILE COPY


82 08 11 004

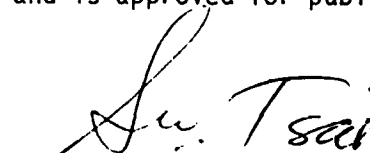
NOTICE

When Government drawings, specifications, or other data are used for any purpose other than in connection with a definitely related Government procurement operation, the United States Government thereby incurs no responsibility nor any obligation whatsoever; and the fact that the Government may have formulated, furnished, or in any way supplied the said drawings, specifications, or other data, is not to be regarded by implication or otherwise as in any manner licensing the holder or any other person or corporation, or conveying any rights or permission to manufacture, use, or sell any patented invention that may in any way be related thereto.


This report has been reviewed by the Office of Public Affairs (ASD/PA) and is releasable to the National Technical Information Service (NTIS). At NTIS, it will be available to the general public, including foreign nations.

This technical report has been reviewed and is approved for publication.


JAMES M. WHITNEY, Project Engineer
Mechanics & Surface Interactions Branch
Nonmetallic Materials Division


STEPHEN W. TSAI, Chief
Mechanics & Surface Interactions Branch
Nonmetallic Materials Division

FOR THE COMMANDER


FRANKLIN D. CHERRY, Chief
Nonmetallic Materials Division

"If your address has changed, if you wish to be removed from our mailing list, or if the addressee is no longer employed by your organization please notify AFWAL/MLBM, W-PAFB, Ohio 45433 to help us maintain a current mailing list.

Copies of this report should not be returned unless return is required by security considerations, contractual obligations, or notice on a specific document.

Unclassified

SECURITY CLASSIFICATION OF THIS PAGE (When Data Entered)

REPORT DOCUMENTATION PAGE		READ INSTRUCTIONS BEFORE COMPLETING FORM
1. REPORT NUMBER AFWAL-TR-81-4155	2. GOVT ACCESSION NO. AD-A118 084	3. RECIPIENT'S CATALOG NUMBER
4. TITLE (and Subtitle) EFFECT OF LOAD HISTORY ON FATIGUE LIFE		5. TYPE OF REPORT & PERIOD COVERED Final Technical, Task II 1 Jan 1980 - 30 April 1981
		6. PERFORMING ORG. REPORT NUMBER LR 29586-1
7. AUTHOR(s) J. T. Ryder K. N. Lauraitis		8. CONTRACT OR GRANT NUMBER(s) F33615-78-C-5090
9. PERFORMING ORGANIZATION NAME AND ADDRESS Lockheed-California Company Division of Lockheed Corporation Burbank, California 91502		10. PROGRAM ELEMENT, PROJECT, TASK AREA & WORK UNIT NUMBERS
11. CONTROLLING OFFICE NAME AND ADDRESS Materials Laboratory (AFWAL/MLBM) Air Force Wright Aeronautics Laboratory Wright-Patterson AFB, Ohio 45433		12. REPORT DATE December, 1981
		13. NUMBER OF PAGES 281
14. MONITORING AGENCY NAME & ADDRESS (if different from Controlling Office)		15. SECURITY CLASS. (of this report) UNCLASSIFIED
		15a. DECLASSIFICATION/DOWNGRADING SCHEDULE
16. DISTRIBUTION STATEMENT (of this Report) Approved for public release: Distribution unlimited		
17. DISTRIBUTION STATEMENT (of the abstract entered in Block 20, if different from Report)		
18. SUPPLEMENTARY NOTES		
19. KEY WORDS (Continue on reverse side if necessary and identify by block number) Composites, Graphite/Epoxy, Fatigue, NDI		
20. ABSTRACT (Continue on reverse side if necessary and identify by block number) The primary objectives of this program were to: (1) investigate the effects of mechanical load history on the response of laminated graphite/epoxy composites; and (2) to analyze the results in a manner such that an expanded foundation is laid for formulating cumulative damage concepts. The research investigation was divided into three tasks: Task I, Diagnostic Experimentation; Task II, Effect of Loading Parameters; and Task III, Data Analysis and Reporting. The results of the investigational effort conducted during Task I were previously (over)		

DD FORM 1 JAN 73 1473

EDITION OF 1 NOV 65 IS OBSOLETE

Unclassified

SECURITY CLASSIFICATION OF THIS PAGE (When Data Entered)

Unclassified

SECURITY CLASSIFICATION OF THIS PAGE(When Data Entered)

reported in June 1980 as AFML-TR-80-4044. This report covers the results of the Task II effort.

In Task I, the laminate of interest was selected as a quasi-isotropic layup of T300/5208 graphite/epoxy material. The unidirectional properties of the material were characterized at room temperature and at 82.2°C (180°F) in both an as-received and a high moisture content condition. Moisture absorption and thermal expansion properties of the laminate were obtained. Static tension and compression properties of the quasi-isotropic laminate as well as those for unidirectional laminates were determined. The effect of strain rate was investigated. Baseline fatigue data were obtained at four stress ratios: +0.5, 0.0, -0.5, -1.0. An evaluation of NDI techniques was conducted to select procedures for use in Task II. A conceptual context for evaluating and analyzing the results of Task II was established.

During Task II, different types of mechanical load histories were applied, at room temperature, to coupons of the selected quasi-isotropic laminate. Distributions of either monotonic strength or cyclic life, which ever was appropriate, were obtained for the various applied load histories. In addition, the evidence of resultant matrix cracking and delamination was recorded by edge replication and enhanced x-ray NDI techniques and by photomicrographs of coupon cross-sections. The mechanical property and damage accumulation data were combined and analyzed in order to infer the nature of the materials response to the applied mechanical load. Analytical emphasis was not on the strength or life distributions themselves or on any particular load induced event, such as fracture, but upon the dynamic process of change that the material/structure was undergoing due to the input of external energy (mechanical load). Therefore the laminate and the loading environment were viewed as a single energy system within which a dynamic process of energy exchange was taking place. The nature of the process of change within the laminate was found to be dependent on amount, rate, form, and repeated input of externally applied energy in a manner qualitatively similar to that of metals. This qualitative similarity of response was attributed to the fundamental principle that all things change under the influence of force and energy. The reasons for quantitative response differences were explained based upon the anisotropic, polymeric and fibrous structural nature of the materials. That structural nature was found to be of key importance because it determines the manner in which energy is stored, dissipated, and transmitted. The energy state change process was found to be essentially independent of the magnitude of prior energy input. This property is quite different than that of metals and was found to be due to the structural nature of a laminate graphite/epoxy composite. Understanding the manner in which the process of state change depends on material structure was suggested as a basis for developing damage tolerance and cumulative damage methodology.

Unclassified

SECURITY CLASSIFICATION OF THIS PAGE(When Data Entered)

FOREWORD



Accession For	NTIS GR&I	<input checked="" type="checkbox"/>	<input type="checkbox"/>
	DTIC TAB		
	Unannounced		
	Justification		
By			
Distribution/			
Availability Codes			
Avail and/or			
Dist Special			
			A

This report describes the results of the second part of an investigation of the effects of load history on the mechanical response of a graphite/epoxy laminate. Included in this report are the partial results of Task II and a summary of the pertinent results of Task I previously reported in detail in AFWAL-TR-80-4044 published June, 1980. The results of Task II are incomplete because the program was terminated at the convenience of the government due to government budgetary reductions. The Air Force Project Engineer was originally Dr. S. W. Tsai and, subsequently, Dr. J. M. Whitney, both of the Mechanics and Surface Interactions Branch, Nonmetallics Materials Division, Air Force Wright Aeronautical Laboratory, Materials Laboratory, Wright-Patterson Air Force Base, Ohio. Dr. J. T. Ryder was the Principal Investigator at Lockheed.

The program was conducted through the Structures and Materials Laboratory Department of the Lockheed California Company. The technical support and contributions of D. E. Pettit of the Fatigue and Fracture Laboratory are gratefully acknowledged as are those of J. R. Crocker, Jr., of the Non-destructive Test and Research Department and of R. C. Young and S. Krystkowiak of the Materials Laboratory. To D. R. Diggs, also of the Fatigue and Fracture Laboratory, goes our heartfelt thanks for his careful direction of the experimentation throughout the Task II portion of the research program. The experimental testing efforts of F. Pickel, P. Mohr, W. Renslen, L. Gray, L. Silvas, C. Spratt, W. Stevenson, C. Grove, and L. Reed, all of the Fatigue and Fracture Laboratory, are heartily appreciated. The authors also extend their appreciation and warm regards to D. Riley for her sustained typing and layout effort without which no manuscript would be possible. Lastly, but of at least equal importance, the authors thank E. K. Walker of the Structures Branch for providing the initial impetus for Lockheed work in this technical area and for his most helpful conversations throughout the course of the program.

TABLE OF CONTENTS

<u>Section No.</u>		<u>Page</u>
1	INTRODUCTION	1
	1.1 PROGRAM OBJECTIVE	1
	1.2 CONCEPTUAL APPROACH	2
	1.3 NATURE OF LAMINATED COMPOSITE ENERGY STATES	8
	1.4 EXPERIMENTAL INTERPRETATION	12
2	EXPERIMENTAL RESULTS	19
	2.1 REFERENCE DATA, MONOTONIC AND CYCLIC	25
	2.1.1 Monotonic Loading	25
	2.1.2 Cyclic Loading	39
	2.2 LOAD HISTORY EXPERIMENTAL RESULTS	59
	2.2.1 Relationship Between Monotonic and Fatigue Load Results	60
	2.2.1.1 Progressive Loading Experiments	60
	2.2.1.2 Trapezoidal Wave Loading	70
	2.2.2 Structural Dependence on the State Change Process	77
	2.2.2.1 Preload Experimental Results	80
	2.2.2.2 Block Load Experiments	81
	2.2.3 Overload Experiments	92
3	DISCUSSION	103
	3.1 CONCEPTUAL IMPLICATIONS	105
	3.2 EXPERIMENTAL DESIGN AND INTERPRETATION	112
	3.3 THOUGHTS ON IMPLICATIONS	124
4	CONCLUSIONS AND RECOMMENDATIONS	127
	4.1 DETAILED CONCLUSIONS	128

4.1.1	General Concept	129
4.1.2	Nature of the State Change Process	131
4.1.3	State Change Manifestation Characteristics	133
4.1.4	Thoughts on Implications	134
4.2	RECOMMENDATIONS	136
	REFERENCES	139
APPENDIX A		
	Material Selection and Quality Assurance	145
APPENDIX B		
	Experimental Procedures	173
APPENDIX C		
	Material Characterization	197
APPENDIX D		
	Summary of Test Data	219

LIST OF FIGURES

<u>Figure No.</u>		<u>Page</u>
1	Fixture Used for Compression-Compression Fatigue Loading	21
2	Matrix Cracks at Various Monotonic Load Levels	29
3	Enhanced X-Ray Photographs of Monotonic Tension Coupons Just Prior to Fracture, 2VX1403-B15 and 1VX1403-B22 at Approximately 97.5% of Their Ultimate Strength	30
4	Appearance of Matrix Cracking and Delamination of a Coupon Under Monotonic Tension at Approximately 97.5% of the Average Ultimate Strength Showing Delamination Between the Outer 0° and +45° Plies	31
5	External Appearance of Failed Coupon 2VX1391-A29 Subjected to Monotonic Tension Loading Showing +45° Delamination Fracture Region	32
6	Enhanced X-ray Photographs of Failed Coupons Monotonically Loaded in Compression Fatigue Fixture	37
7	Typical Photomicrographs of Sections Taken Near the Edge (Approximately 0.25mm (0.01 in.) away) of Coupons Loaded to Failure in Monotonic Compression	38
8	Constant Amplitude Fatigue, Stress-Life Results at $R = 0.0$ Showing Extent of Data Scatter	40
9	Comparison of Constant Amplitude Fatigue Data of T300/5208 and T300/934 Laminated Composites in Room Temperature, Laboratory Air at $R = 0.0$	41
10	Constant Amplitude Fatigue, Stress-Life Results at $R = -1.0$ Showing Extent of Data Scatter	43

LIST OF FIGURES

<u>Figure No.</u>		<u>Page</u>
11	Constant Amplitude Stress-Life Results at $R = -\infty$ Showing Extent of Data Scatter	44
12	Edge Replication of Matrix Cracks and Delamination Due to Fatigue Loading at a Maximum Stress of 310 MPa (45 ksi) at $R = 0.0$	45
13	Edge Replication of Matrix Cracks and Delamination Due to Fatigue Loading at a Maximum Stress of 414 MPa (60 ksi) at $R = 0.0$	46
14	Enhanced X-ray Photographs of Delamination Extension Due to Fatigue Loading	49
15	Edge Replication of Coupon Fatigue Loaded at 414 MPa (60 ksi) Maximum Stress at $R = 0.0$ Showing Delamina- tion Between the Outer 0° and $+45^\circ$ Plies	50
16	Diagram of Delamination and Matrix Cracking	51
17	Diagram of Outer 0° Ply Fracture at $+45^\circ$ Angle	52
18	Photographs of Failed Fatigue Loaded Coupons Showing $+45^\circ$ Fracture of Outer 0° Plies (Maximum Stress 310 MPa (45 ksi), $R = 0.0$)	53
19a	Appearance of Coupons Which Failed Under Compression Load (Monotonic Load)	55
19b	Appearance of Coupons Which Failed Under Compression Load (Monotonic Load)	56
19c	Appearance of Coupons Which Failed Under Compression Load (Fatigue Load, $R = -\infty$ $\sigma_{\min} = -310$ MPa (-45 ksi)	57
19d	Appearance of Coupons Which Failed Under Compression Load (Fatigue Load, $R = -\infty$ $\sigma_{\min} = -310$ MPa (-45 ksi)	58
20	Loading Waveforms Used in Progressive Load Experiments	62

LIST OF FIGURES

<u>Figure No.</u>		<u>Page</u>
21	Enhanced X-Rays Photographs of Failed Monotonic and Progressively Tensile Loaded Coupons Showing Absence of Delamination Prior to Failure	65
22	Enhanced X-Ray Photographs of Coupons Progressively Loaded to Failure in One Hour Showing Extensive Delamination at 98% or Greater of their Failure Load	68
23a	Coupons Monotonically and Progressively Loaded to Failure in Compression (Failure in One Minute Progressive Load)	71
23b	Coupons Monotonically and Progressively Loaded to Failure in Compression (Failure in One Hour Progressive Load)	72
23c	Coupons Monotonically and Progressively Loaded to Failure in Compression (Failure in Monotonic Load in One Minute)	73
24	Enhanced X-Ray Photographs of Failed Coupons Progressively Loaded in Compression	74
25	Results of Time at Load Experiments	76
26	Enhanced X-Ray Photographs of Time at Load Coupons Unfailed After 10 000 Cycles	78
27	Enhanced X-Ray Photographs of Coupons Fatigue Cycled to Failure at 414 MPa (60 ksi) With and Without Preload at 497 MPa (72 ksi)	84
28	Enhanced X-ray Photographs of Coupons Fatigue Cycled to Failure at 310 MPa (45 ksi) With and Without Preload at 497 MPa (72 ksi) or 625 MPa (76 ksi)	85
29	Loading Waveforms Used in Block Load Experiments	88

LIST OF FIGURES

<u>Figure No.</u>		<u>Page</u>
30	Enhanced X-Ray Photographs of Coupons Cycled at 310 MPa (45 ksi) to Approximately the 95% Probability of Survival Level (200 000 Cycles) Prior to Cycling at 414 MPa (60 ksi)	93
31	Loading Waveforms Used in Overload Experiments	95

LIST OF TABLES

<u>Table No.</u>		<u>Page</u>
1	Investigative Questions Concerning Nature of Dynamic Energy States	22
2	Summary of Quasi-Isotropic Static Tension Test Results at Room Temperature	26
3	Summary of Weibull Parameters for Quasi-Isotropic Static Tension Results at Room Temperature	26
4	Summary of Quasi-Isotropic Static Compression Test Results at Room Temperature	27
5	Summary of Weibull Parameters for Quasi-Isotropic Static Compression Results at Room Temperature	27
6	Monotonic Tension Test, NDI Data Matrix Cracking as Detected by Edge Replication	33
7	Comparison of Compression Failure Strengths of Coupons Which Failed in the Compression Fatigue Fixture at Various Loading Rates	35
8	Matrix Cracking and Delamination Under Fatigue Loading ($R = 0.0$)	47
9	Summary of the Effect of Progressive Load ($R=0$) on Tensile Strength	64
10	Non-Parametric Statistical Study of T-T Progressive Loading Data	67
11	Summary of the Effect of Progressive Load ($R = -\infty$) On Compressive Buckling Strength	69
12	Summary of Tension Preload Experimental Results	82

LIST OF TABLES

<u>Table No.</u>		<u>Page</u>
13	Summary of the Results of Statistical Comparison of Preload and Unpreloaded Populations	83
14	Summary of Block Loading Data	90
15	Summary of Conclusions Concerning Block Loading	91
16	Summary of Single Cycle Overload Experimental Results	97
17	Summary of Multiple Cycle Overload Experiments	99

SECTION 1

INTRODUCTION

1.1 PROGRAM OBJECTIVES

From an engineering point of view, a principal requirement of coherent design is ensurance of structural integrity. Satisfaction of this requirement necessitates awareness as to how the materials selected for a particular application will change under load and environment inputs. The purpose of this program is to aid in the development of that necessary awareness for graphite/epoxy laminates. The principal program objectives were to determine which loading parameters primarily influence material/structural changes (damage accumulation), to characterize the nature of the changes, and to elucidate the associated mechanical responses such as distributions in fatigue life and monotonic strength . To accomplish these objectives, simple but discriminatory load histories were selected to clarify the mechanics of the damage accumulation process in laboratory size coupons. The data generated in the program are intended not only as an aid for understanding laminated composite behavior, but also to help in evaluating changes in selected materials or laminates for a particular application and as a basis for future development of qualitative or quantitative fatigue life prediction capabilities.

The results of the research effort are published in two volumes. The first report¹ contained the Task I experimental results which consisted of the baseline lamina and laminate monotonic load data and the laminate, constant amplitude fatigue data. In addition the report discussed both the results and the process undertaken to select NDI procedures used for documenting damage accumulation in the experiments to be performed in later tasks.

This report presents the results and interpretation of the load history experiments conducted under room temperature laboratory air conditions using un-notched coupons. These experiments constituted the Task II effort of the program. A further report of Task III results, on geometric (notch) and environmental perturbational influences, was intended, but will not be forthcoming because governmental budgetary restrictions precluded performance of the experiments. The generality of the conclusions reached in this report are, therefore, somewhat limited because of the lack of the Task III results, the fact that the compression-compression fatigue investigation conducted in Task II was left incomplete, and that the NDI study was severely restricted. Despite these limitations, the program objectives are believed to have been met, although naturally not to the extent hoped for originally.

The remainder of this introductory section summarizes the conceptual approach which was taken towards the experiments conducted in Task II to meet the program objectives. In Section 2, the experimental results themselves are summarized. The remaining two sections are: 1) a discussion of the inferences which were reached based on the experimental results; and 2) a summary/conclusion presentation. The appendices of the report contain the rationale for laminate and coupon selection, manufacturing details, experimental procedures, pertinent Task I experimental results, and detailed tabulation of the individual Task II experimental results.

1.2 CONCEPTUAL APPROACH

The development of durability and cumulative damage concepts for metallic materials over the past 20 years have followed a now classic pattern. That pattern consists of: 1) recognition of an undesirable material response; 2) experimental investigation to ascertain what input parameters produce the undesired effect; 3) an attempt to gain a fundamental understanding of the physical phenomena; and 4) development of engineering tools to "forecast"

the conditions that will yield the undesired response and thus allow its avoidance. The last step is accomplished by using the information gathered in the second and third steps. For metals, the micromechanics of the changes in the material induced by fatigue loading were found to be so complex as to pose great difficulties for relating experimental data to structural application. Fortunately the engineering aspects of the phenomena can often be handled quite well without resorting to a micromechanical approach. The reason for this fact is the structural nature of the material which has two fundamental properties. First, the crystalline structure is such that a condition of isotropy can often be safely assumed even in small components. Second, that same crystalline nature allows large scale inelastic deformation to occur. These two properties permit many engineering structures to be designed without a constant awareness of the material structure.

Laminated composites are, in contrast to metals, highly anisotropic with polymeric and fibrous phases. This anisotropic and non-crystalline structure is such that, even in large components, structural/geometric interactions are highly important and cannot be ignored. The fact that essentially there is never a level at which the structure of the material can be overlooked dictates the awareness that the application of laminated composites requires an understanding normally associated more with structures than with materials. For this reason, the classic procedure being developed for metallic materials for ensuring durability would be expected to require some variation for the case of laminated graphite/epoxy composites.

None of this is to say that the structure of metals is unimportant. The reverse is clearly true and widely recognized. In fact, without a keen awareness of metallic structure, the recent advances in structural efficiency would be impossible. However, the need to include an awareness of the structural nature of laminated composites in all levels of a

research investigation or of a design application thrusts the structural nature of all materials forward in importance.

Because of the need for an increased awareness of the structural nature of materials, a note of warning concerning semantics is considered to be necessary. In common language, structures are made from materials, but for fiber/epoxy composites (and for that matter, wood, reinforced concrete, and human flesh and muscle) the line of demarcation between a structure and a material is not clear. In the common use of the terms "structure" and "material" can be found the rationale for thinking of graphite fiber composites as materials. But, just as a tree trunk is both a structure and a material, composites are, in the authors opinion, much better understood if they are thought of as structures more than as materials. Therefore, "like Humpty-Dumpty, when we use the word material in this book [report], it will mean whatever we want it to mean."² Throughout this report, the term material/structure is often used to emphasize this problem of understanding.

Once the recognition ensues that laminated composites must be thought of as a material/structure, the question of material response to external energies and forces must be reexamined. The necessity for this is clear when one realizes that the energy absorbing response of laminated composites is such that general matrix cracking and delamination may result, but a single dominant, macrosized crack does not easily develop as can occur in a metallic material; or further, when one also realizes that the acuity of notches is observed to decrease with fatigue cycling not increase^{3,4,5} again unlike metals. The entire material/structure response to various forms of energy input clearly constitutes an entirely different set of processes requiring our comprehension.

In this report, a specific conceptual approach to experimental design and interpretation was used which allowed development of an understanding of

the importance of material structure. That the structure of laminated composites is important is, of course, well recognized, but the significance of that structure for engineering application or conceptual understanding is less obvious. The conceptual approach is described in this subsection, but before proceeding to that description a further reason for using the concept requires explanation.

In the development of the technical communities present understanding of metallic materials, rather a static viewpoint has taken root. Despite the fact that what is happening to a material during the application of mechanical load and/or environment is clearly a dynamic process of change, this fact is often (usually?) ignored. This has led to the collection of many static "snapshots" of the process and, at times, an emphasis on sequence, but not to an effort to develop an inclusive comprehension of the process. That this quasi-static viewpoint is highly detrimental to the progress of both an intellectual understanding and a practical application is becoming widely recognized^{6,7}. Developing an awareness of the dynamic nature of all phenomena is now seen to be important in many fields of scientific endeavor. R. Walsh comments in the field of brain research:

"If we refine our perceptual sensitivity, if we examine the very large or the very small, matter or mind, we find nothing solid, nothing fixed, only external ceaseless motion. Any object, when examined closely enough, turns out to be dynamic and alive, a process rather than an event."⁸

The point of view of this report rests upon an attempt to maintain attention upon the dynamic process referred to by Dr. Walsh.

The concept used for the current program was founded first on the idea that all things ceaselessly change. That change is due to internal processes and to the external input of energy. Second, and of equal importance, the structure of the material was seen as determining how the inputted energy will be stored, dissipated, transformed, and transmitted. Therefore, a

specific approach was used to allow for a developing comprehension of the qualitative nature of the material's dynamic process of change. The reasons for the appearance of macroscale phenomena associated with material change were addressed based upon an understanding of the structural nature of the material. Finally the significance of that structural nature for understanding observed transmission of inputted energy and of associated mechanical properties was emphasized by use of the conceptual approach.

The conceptual approach was that a material/structure subjected to external loads and environment is best thought of as a specific energy state existing in an open system condition. The term state is used here to mean, for a laminated composite, that sum total physical/chemical condition (atomic, molecular) at any time, of the fiber and matrix material and inherently includes the layup itself and all micro/macro discontinuities (cracks, delaminations and fiber breakage) which may be present. Energy state further implies that the state should be thought of as an energy field whose existence and nature is manifested and defined by the physical/chemical condition and micro/macro discontinuities. The concept as indicated by the words, open system, includes the idea that external energy inputs (load, environment) must produce a dynamic continuous change in state within the material/structure subjected to the input. The change in state is often called damage accumulation based on the experience that the mechanical response of the material/structure will ultimately be altered, usually in an undesired fashion. However, substantial state changes can occur, as evidenced by large numbers of cracks, without any change in strength or sometimes even in fatigue life distribution (see Reference 9 and Section 2).

The emphasis in this report is upon energy state and sequence of state change and not upon strength or fatigue life per se, since these are but the manifestations of the process of change. The reason for this emphasis,

in the words of Professor Gordon, is the belief that "a deep intuitive appreciation of the inherent cussedness of materials and structures is one of the most valuable accomplishments an engineer can have."¹⁰ Thinking of composites in terms of energy states will, we believe, add in the development of this holistic intuitive appreciation. A corollary of this reason for thinking in terms of energy states was also expressed by Professor Gordon: "To make strong structures without the benefit of metals requires an instinct for the distribution and direction of stresses which is by no means possessed by modern engineers; for the use of metals, which are so conveniently tough and [relatively] uniform, has taken some of the intuition and also some of the thinking out of engineering."¹¹ Composites are forcing us to think in a composite or holistic fashion. The energy state concept is brought forward as a hopefully fruitful means of aiding in a conscious restoration of that holistic, but unconscious thinking of the "primitive" fashioner of such composite structures as bows, spears and chariot wheels.

Conceiving of the material/structure as an energy state in an open system, and awareness that the state is continuously changing, is believed to be of practical value in both the design of structures and the approach taken to experimental research studies. For example, the concept allows the engineer to improve structural design by considering three pertinent questions. First, the designer can evaluate whether the new state that will be reached during service will be associated with unacceptable deviations in structural response. Second, if such future states are of concern, procedures for reducing the amount or type of state change can be assessed. Third, in order to successfully develop such procedures, the engineer may now focus upon those specific details of the change in state (damage) process to allow determination of what in the process needs to be altered. The process itself is altered by changes in material selection, structural design, or load and environmental conditions.

The advantage of such a three step approach is that emphasis is placed upon the fact that structures fail because they were loaded too high for too long, not because cracks develop per se. Therefore, to prevent failure, either the material must be changed or the state change sequence altered. Knowledge as to the potential state changes, and the associated response deviations, which can occur under external energy input are hopefully provided by the research engineer. Ultimately the concept of an energy state is intended to be used not in a mathematical modeling form, but instead as a basis for deriving a pool of knowledge for the designer available to be drawn from to the depth required for a particular need. This research program was conducted in a manner intended to partially supply that knowledge.

In the following subsection, the manner in which the state, and changes therein, of laminated composites are presently thought of is discussed. The perceived advantages of the energy/state concept to the experimental investigator, and thus ultimately to the designer, are discussed in Section 1.4 and are demonstrated by the experimental results of Section 2. In this program application of the concept was used to dictate the quantification of selected experimental parameters, to interpret the relationship among (meaning of) observed effects, and to infer the significance of the experimental results.

1.3 NATURE OF LAMINATED COMPOSITE ENERGY STATES

The state of a material structure at any time and the nature of subsequent changes is, to understate, difficult to assess. To have precise knowledge would require extensive detail concerning the molecular and atomic energy field relationships among all constituents of the state at all time under any external energy input. The development of such knowledge is not only impractical, but not considered to be necessary. Instead, a more "engineering type" knowledge of both the state at any time and the sequence

of possible changes is considered to be adequate. Essentially this type of knowledge consists of three ideas. First, all materials can be thought of as being formed of atoms and molecules inherently bound together by energy fields which they themselves constitute. Secondly, that because all external and internal energies and forces are inherently dynamic (at least from the point of view of physics, although not necessarily of practical significance), the state is continually changing. Third, that fundamentally, the nature of events which make up the change in state process is the same for both metals and composites (whether under external tensile or compressive load), namely, the extension of molecular or atomic bonds sometimes resulting in tensile fracture of those bonds (often with re-formation).

An important implication of the energy state concept is that, because all states and state changes are the results of external energy application or internal energy equilibration, such phenomena as temperature variations, component deformations, cracks (micro or macro), and ultimately fracture or buckling are manifestations of energy dissipation. To say that the state has changed is simply to say that a different energy field now exists, the state of which depends on the manner in which energy is absorbed and dissipated. In many practical situations, the fact that energy is dissipated could be unimportant since the new state may have no associated change in response of engineering concern.

In this energy state view, therefore, such things as cracks do not cause stiffness change, but, instead both the nature of the cracking pattern and stiffness measurement can equally be used as measures of the present state of a material structure. They can also be used to infer the sequence of events which constituted the change in state process and thus can be used to detect whether the states or state change processes which occurred under different external inputs are the same. In fact, sufficient knowledge and understanding (for engineering practice) of the state at any time and of

the changes in state is believed to be obtained by observing the manifestation of such states and state changes as measured by numbers, distribution, and geometries of cracks, component deformations, stiffness variations, and distributions of component strengths or fatigue lives.

For metallic materials, as is well known, the small size of both the repeating atomic structure and that of the individual metallic grains relative to the size of most engineering components allows them to be considered as homogeneous, continuous, and isotropic at small dimensions (generally at any dimension greater than 1 or 2 mm). Because of this physical structure the dissipation of energy and associated state changes (extension and re-formation or fracture of atomic bonds) manifest as such microscopic phenomena commonly labeled as slip, twinning, cleavage, and grain level microcracking. This level of material change is usually not of engineering significance unless deformation characteristics are the controlling design parameters. For most applications, the importance of microscopic manifestations is not apparent until they coalesce into a macroscopic discontinuity or crack.

Laminated graphite/epoxy composite materials differ from metallic materials in two fundamental ways. The first is that one phase (fiber) is considerably more resistant, in stiffness and strain to failure, to imposed extension than the other phase (matrix). This manifests as large differences in strength and stiffness and must result in general fiber breakage eventuating significantly later than matrix cracking. The second difference is that their method of formation results in a state where conditions of isotropy occur at macroscopic levels (at least centimeters for chopped random fiber composites if not meters for oriented continuous fiber composites). In many practical applications of oriented fiber laminated composites, an isotropic condition suitable for modeling both state and change in state is not actually achieved in a direction perpendicular to the plies.

The highly non-isotropic nature of the composite on a macroscale is, of course, due to the large size of the fibers relative to structural dimensions, as well as to their ordered alignment and directionality. In metals, significant macroscale anisotropy does not normally arise despite the fact that usually two or more material phases are present. This is partially due to the fact that the phases do not have properties as dissimilar as those which occur in composites. These facts are supportive of the premise that consideration of laminated composites as structures is believed to be more fruitful than simply acknowledging them to be anisotropic materials.

Consideration of the structural nature of laminated composites (large differences between the two constituent phases, highly anisotropic) leads to several important realizations. First, for qualitative understanding of potential states and change in state and for anticipation of associated mechanical response, up to the onset of fiber breakage, observations of matrix cracking (both inter and intra lamina) are the primary measurements required. Second, since every laminate is unique, the sequence of state change, and hence matrix crack manifestation, must be peculiar to each laminate despite the fact that the sequence may be dependent on loading type, environment, or geometry. Third, the mechanical response of the material structure must be highly geometry dependent since state changes are geometry dependent because of the high anisotropy. In practical applications, both quantity and quality of the response of a material when fashioned as one geometry, for example a flat coupon, will often not be directly related to another, such as a wide panel or tube. Fourth, concepts such as notch acuity and fracture mechanics can not generally be used in the fashion commonly employed for metals. This does not preclude their use, but the macroscale anisotropic nature of laminated composites does dictate a significant change in form of application.

For engineering purposes the major considerations believed to be pertinent

to understanding the nature of the state at any time, and subsequent changes in state, for laminated graphite/epoxy composites are as follows.

1. There are two major constituents.
2. One constituent (fiber) is considerably more resistant to extension than the other (matrix).
3. Anisotropy exists because of ordered fiber alignment and directionality (considering composites to be structures appears to be valuable).
4. The material/structural state continuously changes due to internal and external forces and energies.
5. Inter and intralamina matrix cracking and fiber breakage constitute the three principal manifestations (exclusive of changes in mechanical response) that the state has changed.
6. Fiber breakage must generally occur significantly after the onset of matrix cracking.
7. Environment (for example, chemical atmosphere and temperature) principally affects the amount of energy required for changes to occur, and thus for cracks to manifest, but not the general scenario.
8. The manner in which state changes occur is characteristic of each laminate.

1.4 EXPERIMENTAL INTERPRETATION

The energy state approach used in this program is seen to be helpful for interpreting experimental results. As one example, an approach commonly taken to understand laminated composites is to consider them as brittle materials subjected to stress fields. In this stress/brittle material approach, the application of a monotonic tensile load to a coupon is expected to result in "damage" (cracks). However, unloading and reloading the coupon is not always anticipated to result in further damage unless the original load is exceeded. This conclusion assumes that every addition of energy must be dissipated in some manner and is essentially non-recover-

rable, at least theoretically. The stress approach thus concludes that the loading and unloading of a coupon to higher loads on each cycle (progressive loading) cannot lead to states any different than those which would be reached under a single monotonic loading to the same maximum level. The strength distributions of the two different loading types (monotonic, progressive) are often thus expected to be the same. If however, differences in strength distributions are detected, our reaction is to look for the unexpected "mechanism" that causes the effect. This has been hypothesized to be a creep effect;¹² i.e., the strength distribution is changed because additional time at load causes more damage. The stress/brittle material view has led on to consideration of constant amplitude block loading where changes in strength distribution are attributed to "material memory" and to "stress level interaction" mechanisms¹³.

From the energy state point of view, the stress/brittle material approach puts the cart before the horse. The approach has to resort to the rather artificial concept of "mechanisms" to explain experimental results which is unduly complicated and is not believed to be necessary. In the energy state approach, the unloading and reloading of a coupon adds energy to the initial state which must be dissipated. At a high enough load level, the energy is dissipated by fast tensile fracture of atomic and molecular bonds manifesting as the commonly observed cracking (inter or intra laminar or fiber). Progressive cyclic loading would thus be expected to result in a different state at fracture than monotonic loading and therefore the different strength distributions are anticipated. No appeal to a time at load creep "mechanism" appears to be necessary to explain the data. In essence, the energy state view discards the concept of mechanism.

Creep in the energy state view is not a mechanism, but only a name for a process in which time at load causes state changes. Fatigue block loading experiments, in the energy state view, are not used to determine whether a "material memory mechanism"¹³ exists, but to evaluate whether the magnitude

of the load variation influences the state that can be reached. In metals, this is known to happen; a high cyclic stress amplitude results in a state which cannot be reached by a low cyclic stress amplitude. Whether the effect is true for laminated composites is less clear.

The energy state concept is not a "black box" approach in which the material is viewed as an object to which energy is applied and resultant response obtained without regard to microscale details. The approach is instead to use the concept to focus upon the process itself and not upon failure, or fracture, or mechanical properties, per se, all of which are viewed as aspects of the process. The idea is advanced of using the holistic, intuitive appreciation of the process gained from integrating both microscale and macroscale observations as a guide for determining what should be mathematically modeled or should be changed in a particular application. There is, therefore, no ignoring of the details of what is physically occurring within the material nor is there any avoidance of the experimentalist's desire to understand, but instead an emphasis on that understanding in a manner useful both to the researcher and to the designer.

The approach is, however, perceived as different than present approaches which focus on only a small aspect of the dynamic process of change such as fracture or failure and which might therefore be termed mechanistic. They are mechanistic in the sense that having focused on a particular aspect, other aspects are seen as potential causes of the one of interest. This results in a confused relation between cause and effect. For example, there is, in the point of view adopted here, no cause and effect relationship between microscale and macroscale phenomenon. Instead, they are simply the appearance of the same dynamic process at different levels of observation. Similarly, recall, that creep is not seen as a cause of failure, but a label for a rather complex phenomenon differing in nature within different materials. This is not to say that creep does not exist,

but only that it does not "cause" fracture. Fracture is instead an aspect, or can be, of the phenomenon called creep.

The results of terming such phenomena as creep or cracks to be mechanisms of failure splits a holistic process into separated aspects. The confusion which results by this separation is apparent in the long futile search to find "the mechanism" of fatigue in metals and in the fact that mechanistically oriented research reports always become descriptions (often frustrated ones) of observed events¹⁴. The unnatural separation of the aspects of a single process prevents efficient development of the necessary holistic understanding of the process of material state change under external energy input. The energy concept is seen as a means of avoiding artificial separation by focusing upon the process as a whole using all available micro and macroscale experimental observations. The need for both levels of observation is not negated, but is transformed in nature. An initial and restricted attempt to demonstrate the concept was viewed as the experimental investigational and data interpretation tasks of this program.

What is required experimentally is to determine whether the state reached, the state change sequence, and rate of state change of a particular material differ under different energy inputs. The assumption is made that if this knowledge and the associated mechanical response data are combined with appropriate representations of laminate geometry, correct decisions can be made as to what changes (in load, environment, layup, etc.) are best to achieve the mechanical response intended. Sufficient knowledge of energy states (nature, sequence and rate of change) is believed to be obtainable by documentation of such indications of state as cracks, rate of crack formation, cracking pattern, and mechanical response (strength, stiffness, fatigue life, etc.) Essentially, therefore, experiments are viewed as probes to answer specific questions, the sum of which allow

sufficient understanding as to the nature of a continuously changing energy state.

The use of experimental probes for delineating the nature of energy state requires two thoughts to be kept in mind. First, certain types of mechanical response may be identical even though laminate energy states are different. For example, the stiffness and strength distributions of a 2/3 0° graphite/epoxy laminate have been shown to be identical when subjected to monotonic tension load with and without prior fatigue cycling⁴. This lack of response difference occurred despite the fact that the coupons subjected to fatigue cycling often displayed severe delaminations with numerous 0° fiber fractures. Therefore, mechanical response alone cannot be used to determine if states differ under different energy inputs, but can only indicate whether their significance depends on particular loading conditions. Second, the nature of the experiment being conducted and the type of data to be obtained must carefully be considered to determine if at a particular time, say at tensile fracture, the state itself, the sequence of state changes or the rate of change in state is being evaluated. The different distribution of cyclic lives obtained by applying different stress magnitudes of constant amplitude fatigue loading cannot, of themselves, be used to determine whether the state at fracture, sequence of state change or rate of state change is different. Non-destructive inspection (NDI), such as thermography, enhanced x-ray or edge replication, would have to be used to distinguish changes. The different cyclic life distributions would only indicate that a difference existed. The above two thoughts are the reason that extensive use of NDI is required.

The energy state approach was used to interpret the results of the experiments of this program. Answers to research questions were inferred by combining both the strength and life distribution data with the NDI data. The experiments of Task I, as discussed in Section 2, were used to answer questions concerning the effects of monotonic and cyclic loading on the

dynamic process of state change. These results were combined with the Task II load history data to infer the relationship between monotonic and cyclic loading. The first three load histories applied in Task II allowed investigation of the effects of repeated energy input (progressive loading), energy storage (time at load), and the nature of energy storage and dissipation (preload). Block load and overload experimental results were used to confirm and extend the range of validity of previous conclusions concerning the nature of the state change process.

SECTION 2

EXPERIMENTAL RESULTS

In this section only that information considered pertinent to understanding the experimental results is presented. Details concerning material properties, coupon manufacture, experimental procedures, and test results are given in the report appendices A through D, respectively.

The experimentation was conducted using un-notched 25 mm (1 in.) wide coupons with a 150 mm (6 in.) gage length test section. Lamina properties of the T300/5208 material were established in Task I using 0° and 90° unidirectional and $\pm 45^\circ$ coupons tested at room temperature in the as-received condition and at elevated temperature in an as-received and a high moisture content condition. The laminate selected for investigating the effects of loading history on material/structure state changes was a quasi-isotropic configuration of the following layup: $(0/45/90/-45_2/90/45/0)_s$. The laminate panel layups were designed and test coupons cut out so that no tape edges in the 0° or 90° plies lay within the coupon test sections. All of the experiments using the selected laminate structure and discussed in this report were conducted at room temperature in ambient air conditions. Baseline monotonic and cyclic data for the laminates were reported in the Task I final report¹ and are summarized in Appendix C. The as-received moisture content of the coupons was determined to be between 0.3 and 0.6 weight percent.

The manifestation of energy states and changes in state which occurred in the form of matrix cracks and delamination within the coupons were documented during Task II using DIB enhanced x-ray and edge replication techniques. These two procedures were selected based upon the results of the Task I investigation¹. The NDI data, the acoustic emission data of Task I,

and photomicrographs of coupon sections (taken parallel to the 0° ply direction) were combined to give an impression of the material state. Unfortunately, the NDI data obtained were limited by the early termination of the program; however, the data obtained were adequate for confirming many of the conclusions inferred based on the results obtained under the various loading conditions.

Monotonic tension properties of the laminate coupons were determined using procedures similar to ASTM D3039 - 74. Tension results were obtained at two strain rates, 0.01 and 6.0 mm/mm/min. The higher rate is equivalent to that which occurs in a constant amplitude fatigue test at 10 HZ. Compression properties were obtained using coupons tested in both the fully supported condition and using the fixture designed for compression-compression (C-C) fatigue testing. The test fixture used for the C-C fatigue testing is shown in Figure 1. The fixture was a six-bay column buckling restraint type designed so that the end conditions approximated an infinitely rigid end.

In Task I, monotonic tension data and constant amplitude fatigue data were obtained which were used both as a baseline reference for the experimental results of Task II and to infer the answer to initial questions asked concerning energy states. Additional data were obtained in Task II in order to establish population distributions at several stress levels for the fatigue loading stress-life curves. The investigational questions which were considered in Task II concerning the nature of laminated composite energy states and changes in state are listed in Table 1 along with the experiments conducted to infer the answers. The questions summarized in Table 1 constitute the key inquiries made during Task II and form the basis of the experimental program discussed in this section.

The first question concerns ascertaining the dependence of state change on the amount, rate, and form of application of energy input. The experimental probes employed were monotonic tension and compression load at different

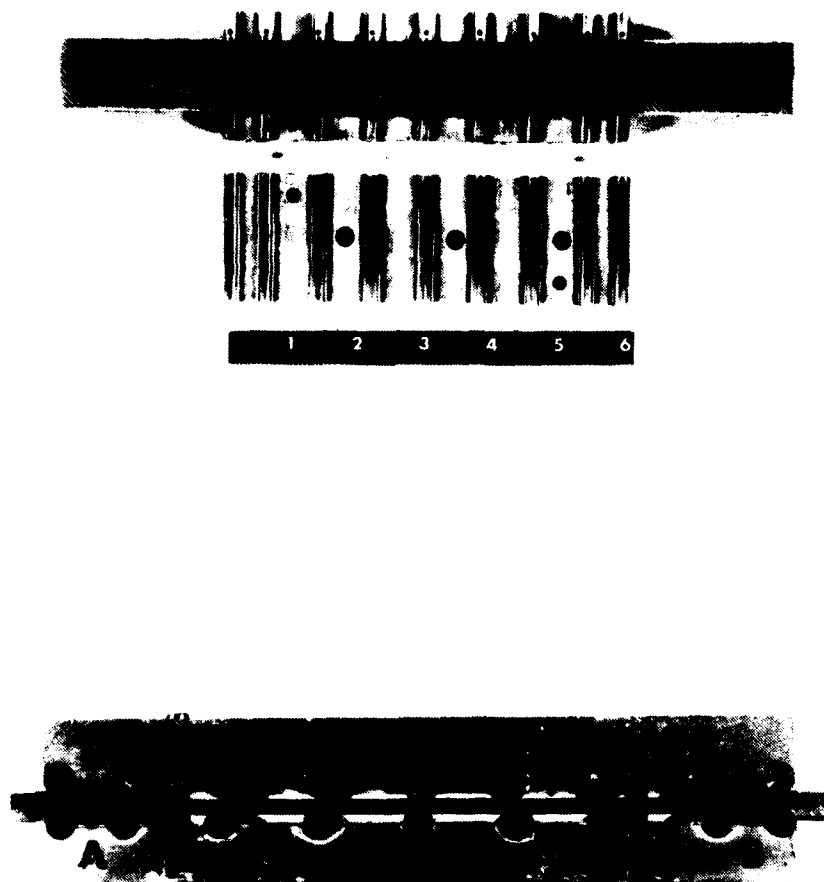


FIGURE 1: Fixture Used for Compression-Compression Fatigue Loading

TABLE 1
INVESTIGATIVE QUESTIONS CONCERNING
NATURE OF DYNAMIC ENERGY STATES

<u>QUESTION</u>	<u>PRIMARY EXPERIMENTAL PROBE</u>
Are the material/structure state and rate and sequence of change dependent on: energy magnitude, rate of energy input, form of application?	Monotonic tension (T) and compression (C) loading at different strain rates, constant amplitude fatigue (T-T, T-C, C-C)
Are the material/structure state, rate and sequence of change dependent on: repeated input of energy, energy storage time?	Progressive loading, Constant amplitude trapezoidal wave shape loading
Does the magnitude of previous energy input alter the state change process?	Preload, block loading
Based on the knowledge of the material/structure state change process, what are the implications for understanding the effects of complex input?	Overload

strain rates, and constant amplitude fatigue loading in the three forms of tension-tension (T-T), tension-compression (T-C), and compression-compression (C-C). The dependence of state on energy magnitude was determined using the monotonic experiments at one strain rate while the dependence on rate was examined using the results of the monotonic load experiments conducted at various strain rates. Comparison of the monotonic and constant amplitude loadings (both tension and compression type) allowed the determination of state (and the process of change) dependence on the form of energy application. Since the states reached under monotonic and fatigue loading are known to be different^{4,9}, the second question of Table 1 was asked in order to ascertain the reason. Progressive cyclic loading and constant amplitude trapezoidal wave loading were used to ascertain whether the difference is more due to repeated energy input or to the amount of time the energy is forced to be stored.

The third question of Table 1 has to do with the fundamental manner in which the state change process is dependent on the magnitude of prior energy input. In a strong sense, a fundamental understanding of laminated graphite/-epoxy composites lies in the answer to this third question. The state change process (or damage accumulation, if you like) is usually expected (if not always clearly demonstrated) to be dependent on amount, rate, and form of energy input. Also, the dependence on repeated input of energy is well known. All of these properties are qualitatively true of all materials. The key question is ascertaining the fundamental nature of the state change process dependence on the magnitude of prior energy input. This dependence is believed to be based upon the intrinsic structural nature of the material.

The dependence of the functional nature of the rate and process of state change on the magnitude of prior energy input can be observed in the response of metallic materials. If a sufficiently high magnitude energy level (for example, a high load) is inputted to a metal, a state is reached globally (in an unnotched coupon) or locally (in a notched coupon) of a type which cannot be reached at a lower level of energy input. This state, well

known as plastic deformation, is usually characterized by the presence of a dominant crack⁵⁶. If one coupon is subjected to the sufficiently high energy level and a second to a lower level, the first is now in a state of a type quite different than the state of the second. The difference is such that repeated application of the low energy level to the second coupon never results in a state similar to that which occurs in the first coupon (at least over the same volumes of material). Further, if the high energy level induced state of the first coupon is followed by repeated application of the low energy input, the sequence of state change events are often sufficiently altered as to be associated with much shorter cyclic lives in unnotched coupons⁵⁵ or longer lives in notched coupons⁵⁷. This plasticity/retardation phenomenon of metals can be (and often is) important enough to be a dominant theme for understanding the effects of spectrum loading on the state change process or for the development of damage tolerance procedures. The appearance of the phenomenon is a manifestation of the fact that the functional relation between the state change process and energy input is dependent on the magnitude of prior energy input. In other words during the state change process, a specific form of energy storage and dissipation occurs because of the nature of the relatively isotropic and crystalline metallic state. This specific form is dependent on the absolute magnitude of energy input during any one application in addition to a dependence on sum amount of repeated energy input.

The simple dependence of state on energy input magnitude is as true for laminated graphite/epoxy composite materials as for metals. Increase the level of energy input (as by a monotonic tension load) and a new state is reached as evidenced by increased matrix cracking and/or delamination^{1,15}. However, there is evidence from monotonic and fatigue loading data^{1,15} to suspect that the functional dependence of the state change process on prior energy input may be quite different for graphite/epoxy laminated composites than that for metals. This difference is believed to be an intrinsic manifestation of the structural nature (anisotropic with polymeric and fibrous phases) of laminated graphite/epoxy materials.

The third experimental question of Table 1 was therefore to determine, for laminated graphite/epoxy composites, whether the dependence of state change on the magnitude of prior energy input was similar to or different than that of metals. The experiments previously discussed were used to infer the answer, but the preload and block loading experiments were necessary for confirmation and clarification. The overload experiments were used as an exploration of a partial answer to the fourth question of Table 1. Based on the understanding gained from the previous experiments as to the nature of the state change process, the significance of that nature was examined for the case of more complex forms of energy input. The overload study thus laid part of the firm basis required for understanding what are called cumulative damage and damage tolerance concepts for laminated graphite/epoxy composites under spectrum loading.

2.1 REFERENCE DATA, MONOTONIC AND CYCLIC LOADING

2.1.1 Monotonic Loading

The results of the Task I monotonic tension and fully supported compression tests are summarized in Tables 2 to 5. Included in Table 2 are the results of Task II tension tests conducted in the machines used for fatigue testing. The high values of the Weibull exponent for the tension experiments were expected because no tape edges in the 0° or 90° plies were allowed during manufacture to fall within the coupon gage lengths. Under tension load, an approximately 8 percent drop in average strength was associated with the higher strain rate experiments compared to the lower strain rate results. The significance of the small strain rate effect observed under compression load is not clear, but will be discussed later in this section.

Under low strain rates in monotonic tension, matrix cracks were found by edge replication, acoustic emission and photomicrography to first appear in the 90° plies at approximately the 0.005 to 0.006 strain level followed by

TABLE 2: SUMMARY OF QUASI-ISOTROPIC STATIC TENSION TEST RESULTS AT ROOM TEMPERATURE

Strain Rate, mm/mm/min	No. of Coupons Tested	Failure Stress, σ_{ult} MPa ksi	Average Strain, at Failure ϵ_{ult} , mm/mm	Initial Apparent Modulus of Elasticity, E_{1A} GPa psi x 10 ⁶	Final Apparent Modulus of Elasticity, E_{2A} GPa psi x 10 ⁶
0.01	20	547 ^a 79.3 19.1 2.77 3.49	0.0105 0.00042 4.03	53.8 ^a 7.81 1.03 0.15 1.96	47.4 6.88 1.72 0.25 3.57
0.01 Tested in Fatigue Machine	10	536 77.8 39.3 5.7 7.3	--- ^c	--- ^c	--- ^c
6.0 Tested in Fatigue Machine	13	507 73.6 17.9 2.60 3.53	0.0098 0.00055 6.66	51.8 7.52 2.96 0.43 5.68	--- ^b

a = Average, standard deviation, and % coefficient of variability, respectively.

b = The stiffness of coupons at 6.0 strain rate did not significantly deviate from a straight line.

c = Strain to failure and stiffness data was not measured for these coupons.

TABLE 3: SUMMARY OF WEIBULL PARAMETERS FOR QUASI-ISOTROPIC STATIC TENSION RESULTS AT ROOM TEMPERATURE

Strain Rate, mm/mm/min	Average Failure Stress, σ_{ult} MPa ksi	Weibull Coefficients k e v	Correlation Coefficient, R
0.01	547 79.3	33.87 -0.061 80.30	0.99958
6.0	507 73.6	30.10 -0.040 74.64	0.99972

TABLE 4: SUMMARY OF QUASI-ISOTROPIC STATIC COMPRESSION TEST RESULTS AT ROOM TEMPERATURE

Strain Rate, mm/mm/mm	Stress At Failure		Average Strain At Failure mm/mm	Secant Modulus of Elasticity At Failure, $E_{SF}^{1/6}$	
	MPa	ksi		GPa	psi
0.01	562 ^a	81.5	0.0115	48.2 ^a	6.99
	22.3	3.23	0.00075	1.65	0.24
	3.96		6.47	3.48	
6.0	546	79.2	0.0121	46.8	6.79
	51.6	7.48	0.0012	1.65	0.24
	9.44		10.5	3.5	

a = Average, standard deviation, and percent coefficient of variation, respectively.

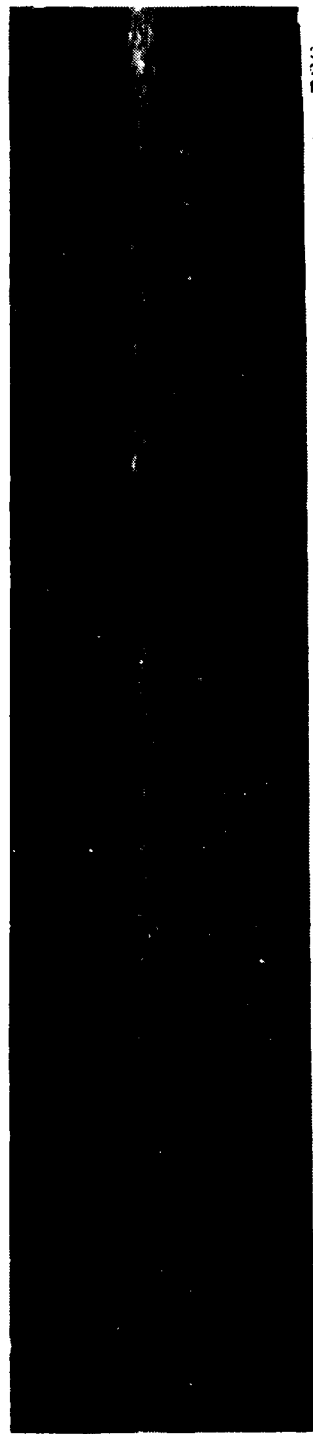
TABLE 5: SUMMARY OF WEIBULL PARAMETERS FOR QUASI-ISOTROPIC STATIC COMPRESSION RESULTS AT ROOM TEMPERATURE

Strain Rate, mm/mm/min	Average Failure Stress,		Weibull Coefficients			Correlation Coefficient, R
	MPa	ksi	k	e	v	
0.01	562	81.5	27.75	-0.076	82.6	0.99950
6.0	546	79.2	11.96	-0.235	81.7	0.99884

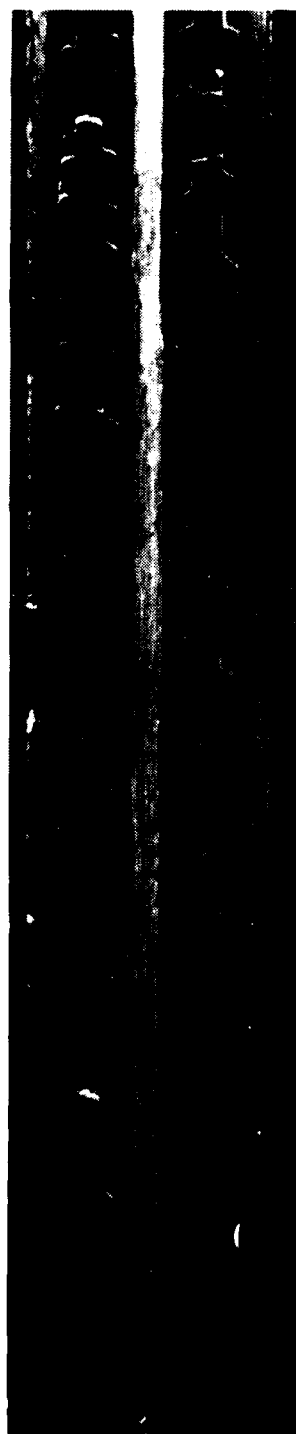
their appearance in the -45° plies near a 0.0075 strain value. Acoustic emission data showed occasional low level activity before the 0.005 strain level¹, but matrix cracks were not found by edge replication or photomicrographs of cross sections. The low energy level acoustic emission data may represent: rare 90° ply crack formation missed by the other techniques because of their large spacing; possibly internal fiber slippage; small perturbations in the acoustic transducer coupling; or extraneous mechanical or acoustic system noise. At approximately the same strain value as the -45° ply cracks appeared, the moduli of the coupons decreased by approximately 10 percent as indicated in Table 2. Cracks appeared in the $+45^\circ$ plies above 0.008 strain. Figure 2 shows typical matrix cracks obtained at various load levels using the edge replication technique. The matrix cracks are essentially perpendicular to the loading direction since they are tensile fractures. They do exhibit a slight angle to the loading direction and short delaminations at their ends due to the local shear stress flow.

Short delaminations were found by edge replication between all of the 90° and 45° plies, but were predominant between the inner 90° and $+45^\circ$ plies and outer 90° and -45° plies. However, delamination was not observed, by enhanced x-ray, to extend significantly into the coupon interior, see Figure 3. Fracture of a tensile loaded coupon was hypothesized to occur when delamination, confined to the coupon edges, began to occur between the outer 0° and $+45^\circ$ plies, Figure 4. When the latter event occurred, 0° fibers fractured locally in the 0° and $+45^\circ$ ply delamination region. This fracture progressed along a $+45^\circ$ ply direction, sometimes on both sides of the coupon (see Figure 5) until of sufficient magnitude to result in rupture across the coupon perpendicular to the load direction. No delaminations in the coupon interiors outside of the fracture region were observed in the enhanced x-ray photographs.

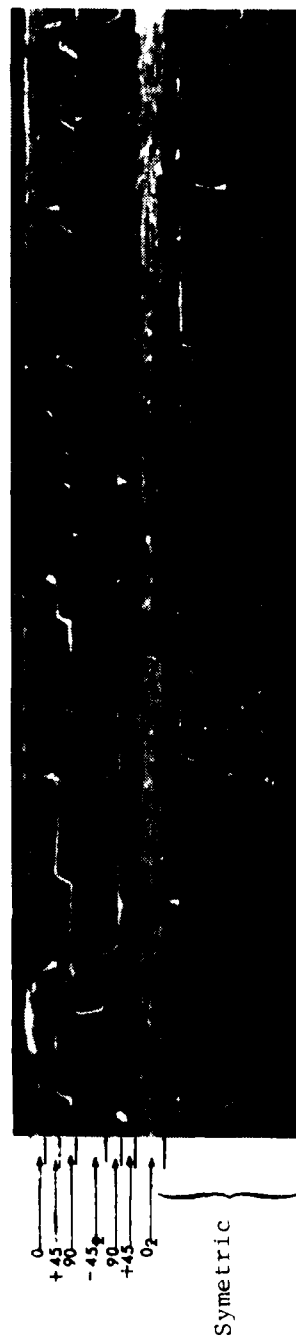
Whether or not the number of cracks per inch in the plies saturated prior to fracture, see Table 6, was not entirely clear. The lack of matrix cracks



Coupon 2VX1403-D17 at 60% of the Average Ultimate Strength 143 079K

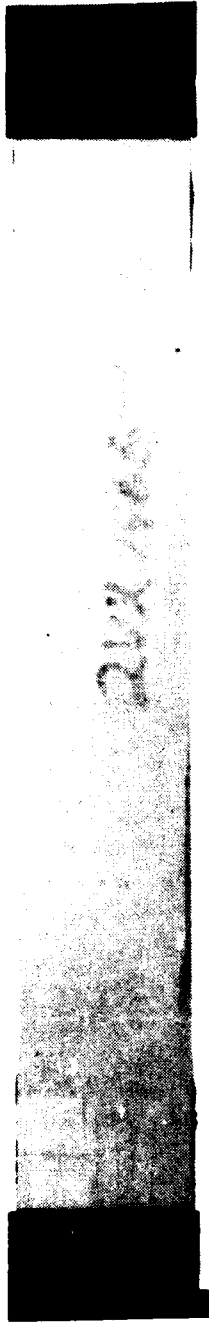


Coupon 2VX1403-D27 at 80% of the Average Ultimate Strength 143 083K

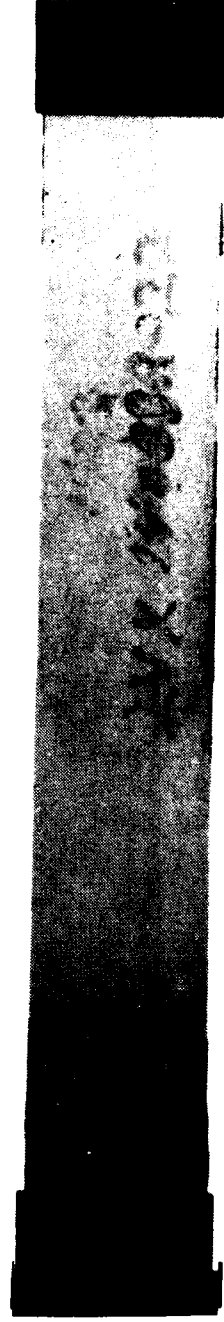


Coupon 2VX1403-D29 at 95% of the Average Ultimate Strength 117K

FIGURE 2: Matrix Cracks at Various Monotonic Load Levels



2VX1403-B15



1VX1403-B22

FIGURE 3: Enhanced X-Ray Photographs of Monotonic Tension Coupons Just Prior to Fracture,
2VX1403-B15 and 1VX1403-B22 at Approximately 97.5% Of Their Ultimate Strength

0° , $+45^{\circ}$ Delamination

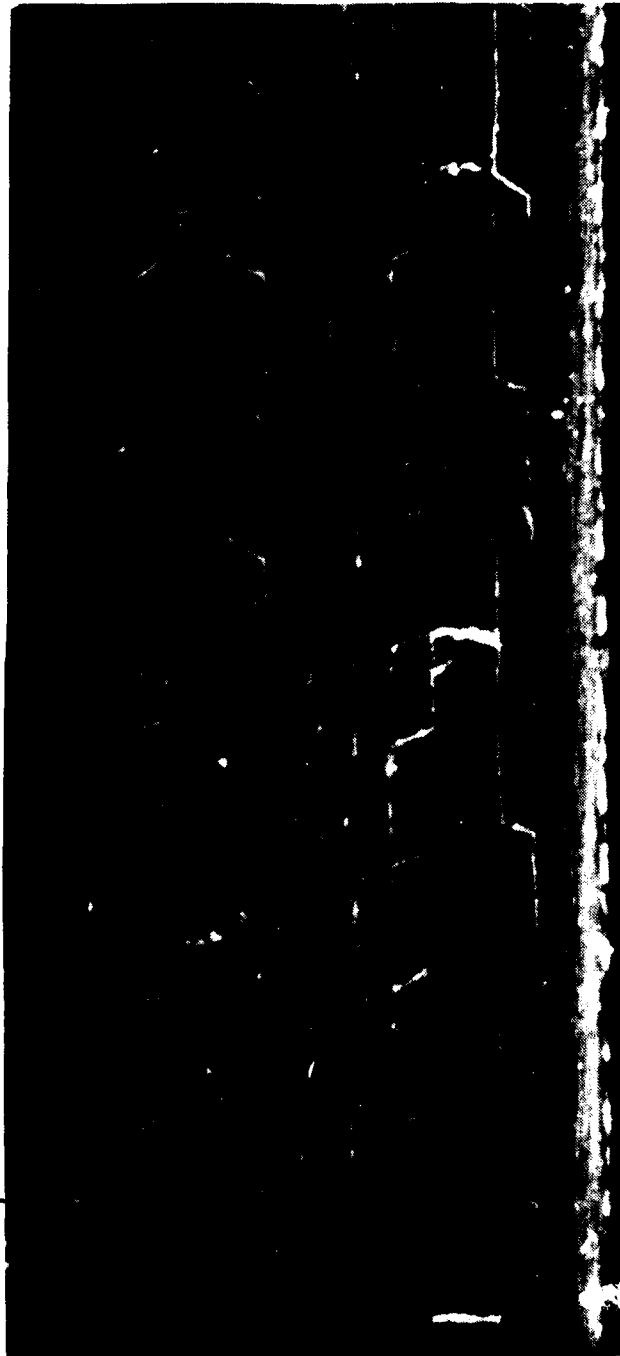
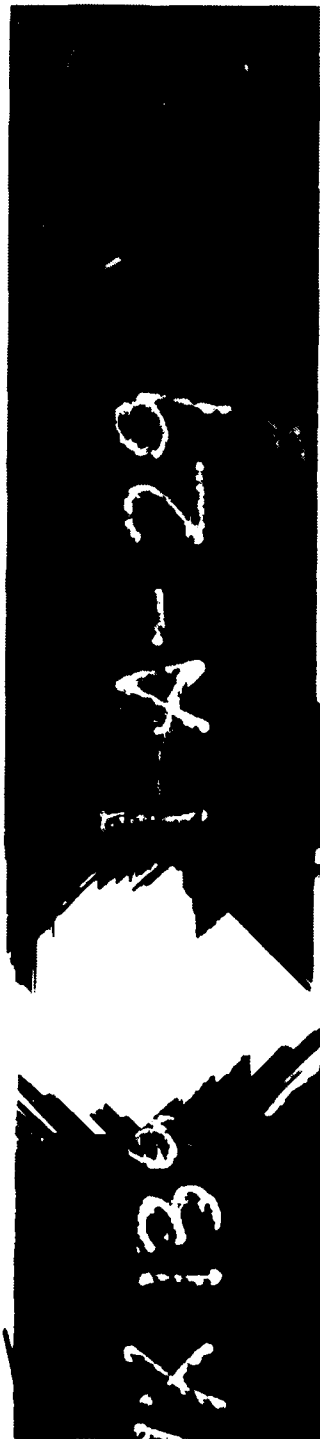


FIGURE 4: Appearance of Matrix Cracking and Delamination of a Coupon Under Monotonic Tension at Approximately 97.5% of the Average Ultimate Strength Showing Delamination Between the Outer 0° and $+45^{\circ}$ Plies.

FRONT



144091

BACK



144090

FIGURE 5: External Appearance of Failed Coupon 2VX1391-A29
Subjected to Monotonic Tension Loading Showing
+45° Delamination Fracture Region.
(NOTE: +45° Fracture Growth in Unfailed Region
on Both Faces).

TABLE 6
MONOTONIC TENSION TEST, NDI DATA MATRIX CRACKING
AS DETECTED BY EDGE REPLICATION

% Average Ultimate Strength	Average Number of Cracks Per Inch ^a		
	90°	-45°	+45°
20	--b	--	--
40	--	--	--
60	18	--	--
80	45	5	2
90	48	12	8
92.5	50	12	6
95	51	15	11
97.5	54	16	8

a = Each data point is an average of six readings per each of three coupons.

b = Matrix cracking not detected by edge replication.

prior to a strain level of about 0.005 (mentioned previously) as indicated in Table 6 was confirmed using photomicrographs. Six 25 mm (1 in.) sections were taken (three down the center, three approximately 2.5 mm (0.1 in.) from the edge) from the coupons which had been loaded to the various levels indicated in Table 6. These sections were examined at 25, 100, and 500X magnifications. In those coupons loaded to approximately 20 and 40% of the average ultimate strength (0.002 and 0.004 strain levels) no matrix cracks or delaminations were detected. Representative photomicrographs are presented in Appendix D.

At high strain rates, a similar detailed description of the manifestation of state changes was not obtained. However, the facts that the modulus to fracture did not change at high strain rate (unlike at low strain rate), that the average strength and strain to failure both decreased, and that a larger number of secondary compression failures occurred at low strain rate than at high strain rate, indicated at least some state and state change sequence differences between the low strain rate and high strain rate experiments. Table 2 shows that the strain rate effect was not simply a result of test machine type since the experimental results at the low strain rate were essentially the same in different test machines. This conclusion was supported by comparisons of the two sets of 0.01 strain rate data using two non-parametric statistical procedures¹⁶). The two procedures showed no significant difference between the two low strain rate populations.

To obtain a more pertinent data base for later comparison to fatigue experiments containing compression load excursions, monotonic compression experiments were conducted in the compression fatigue fixture. Results are shown in Table 7. Coupons failed by local inelastic column buckling at approximately 0.0075 to 0.0080 mm/mm strain when loaded at a standard strain rate. A possible effect of strain rate can be seen by comparing the results for specimens loaded to failure in 60 sec to those in 0.1 sec.

TABLE 7
COMPARISON OF COMPRESSION FAILURE STRENGTHS OF
COUPONS WHICH FAILED IN THE COMPRESSION FATIGUE FIXTURE
AT VARIOUS LOADING RATES

Approximate Failure Time (Seconds)	Stress at Failure	
	MPa	ksi
60	370	53.6
	392	56.9
	415	60.2
	419	60.8
	425	61.7
Average	404	58.6
1	386	56.0
	405	58.8
	423	61.4
	425	61.7
	432	62.6
Average	414	60.1
0.1	435	63.1
	436	63.3
	441	64.0
	480	69.6
Average	448	65.0

The locally buckled failure region exhibited both delamination and matrix cracking. Enhanced x-ray photographs revealed no cracking outside of the failure regions, see Figure 6. The appearance of the high strain rate coupons at failure was found to be indistinguishable, by enhanced x-ray, from that of those loaded at low strain rate. The outer 0° ply fibers on one surface were fractured essentially perpendicular to the loading direction while those on the other surface usually displayed a $+45^\circ$ fracture of the 0° fibers starting at the edge of the coupon. Matrix cracks were observed to be at a shallow angle to the delaminations unlike those under tensile load which were more perpendicular. The reason for the shallow angle is that the matrix cracks are apparently induced by local shear stresses. Outside of the failure region, small delaminations and a few matrix cracks were occasionally found by using photomicrographs of coupon sections (see Figure 7 for typical photographs). The delaminations also occurred predominantly between the outer 90° and $+45^\circ$ plies with lesser amounts between the outer and inner 90° and -45° plies. These delaminations did not extend more than approximately 2.5 mm (0.1 in.) into the coupon interior as confirmed by photomicrograph sections of the coupons. The few matrix cracks observed outside of the failure region were again found to be along 45° angles to the load direction (see Figure 7B) on an angle compatible with the shear stress flow within the coupon. Usually the matrix cracks were found in the 90° plies, but occasionally they occurred in the outer $+45^\circ$ plies.

The monotonic tension and compression experiments allowed inference of a partial answer to the energy state dependence questions posed in Table 1. An integration of the non-destructive and destructive inspection results and the mechanical response data was used to infer several conclusions. The material/structure state is dependent on both the level and the rate of energy input. Energy state is also dependent on the manner in which that

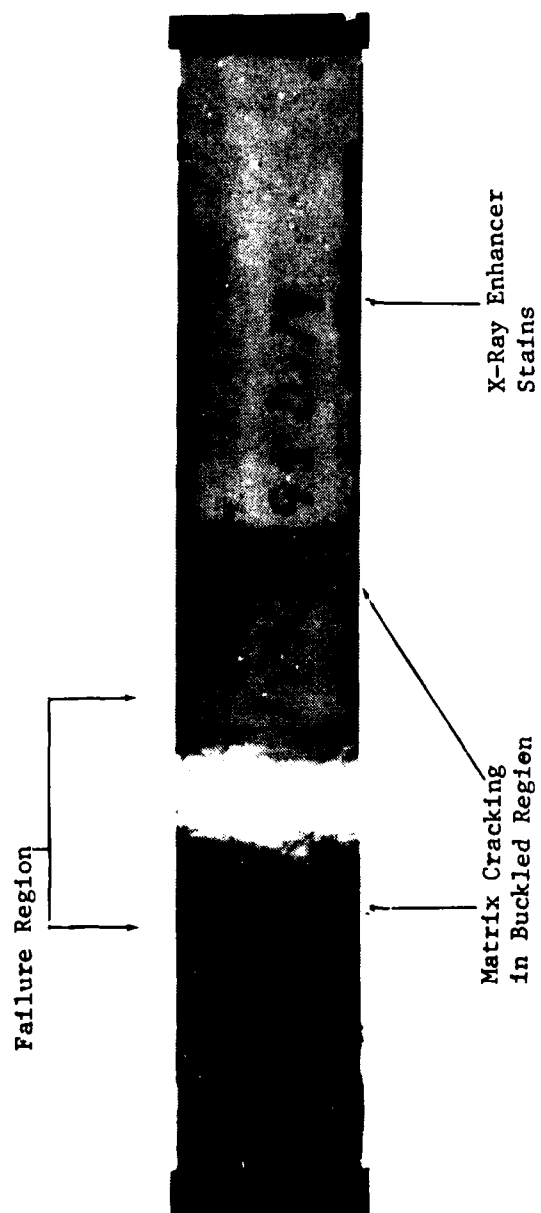
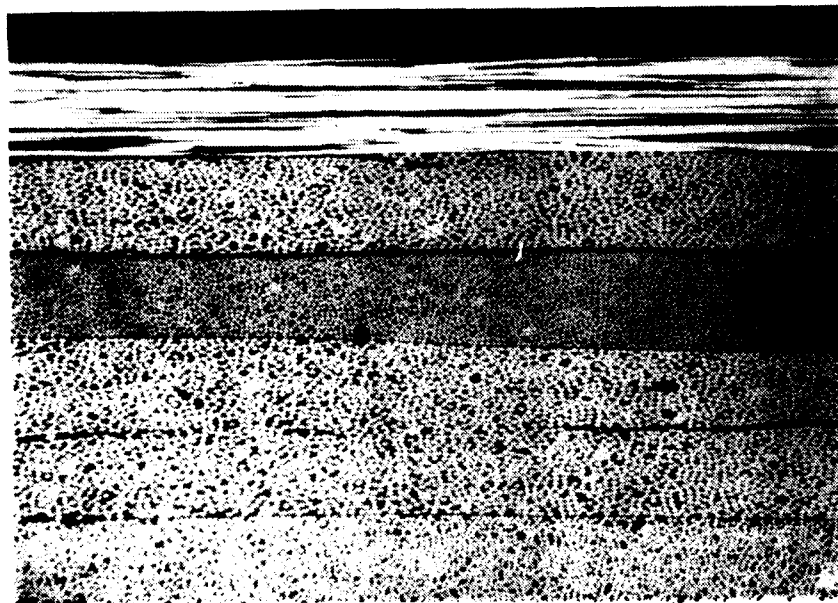
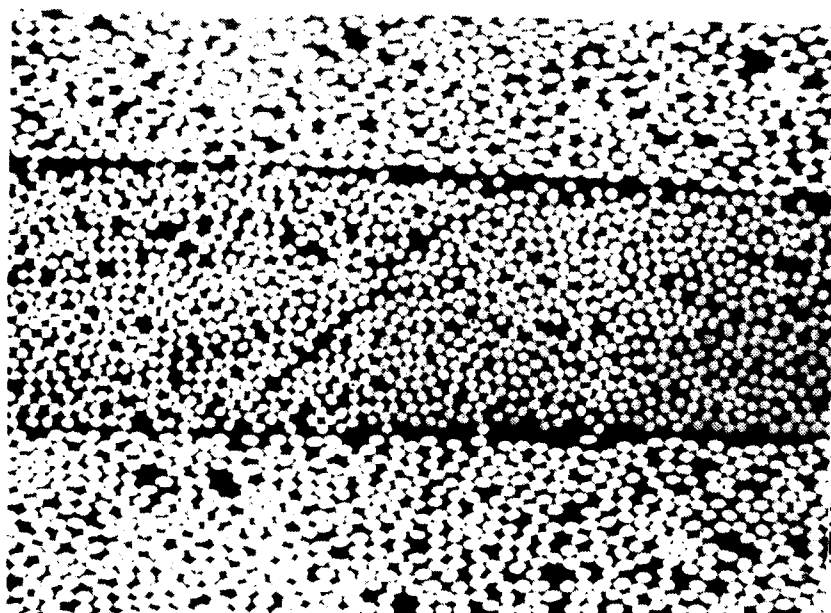


FIGURE 6: Enhanced X-Ray Photograph of Failed Coupon Monotonically Loaded in Compression Fatigue Fixture. NOTE: No Delamination and No Matrix Cracking Outside of Failure Region.



A. Delamination Between the Outer 90° and $+45^\circ$ Plies



B. Matrix Crack in the Inner 90° Ply

FIGURE 7: Typical Photomicrographs of Sections Taken Near the Edge (Approximately 0.25 mm (0.01 in.) away) of Coupons Loaded To Failure in Monotonic Compression.

energy is applied as a comparison between the NDI data for the tension and the compression experiments clearly shows. In general, the state change process can be said to be significantly different under tension and compression load. These results are, of course, not surprising since similar data are available in the technical literature for tension loading^{15,17-19}. However, the conclusions are stated in a form believed to be of value when combined later with other conclusions.

2.1.2 Cyclic Long

In Task I, the basic shape of the $R = 0$, constant amplitude, stress-life (S-N) curve was established using a sine wave loading and five coupons per stress level. In Task II, the extent of scatter in fatigue life was estimated at four selected stress levels: 276, 310, 345, and 414 MPa (40, 45, 50, and 60 ksi). Enough coupons were cycled to failure to establish at least the 90% probability of survival life at each stress level. Detailed test results are tabulated in Appendix D while the data are plotted in Figure 8. Fatigue failure was defined to be coupon fracture. At $R = 0$, the S-N curve for this laminate made of T300/5208 material was found in Task I¹ to be essentially the same as when made of T300/934 material, see Figure 9. The comparison between materials was made to indicate that the general nature of state change and the states themselves are laminate dependent and essentially independent of the matrix (for similar types of matrix materials) under ambient conditions.

Based on the limited number of monotonic compression experiments which were conducted in the compression fatigue fixture, Table 7, the minimum compression stress under fatigue load was restricted to -345 MPa (-50 ksi). Compression fatigue experiments consisted of obtaining the shape of the stress-life curve at $R = -1.0$ and the shape and scatter at $R = -\infty$. The experiments at $R = -1.0$ were conducted to evaluate the selected restraint fixture

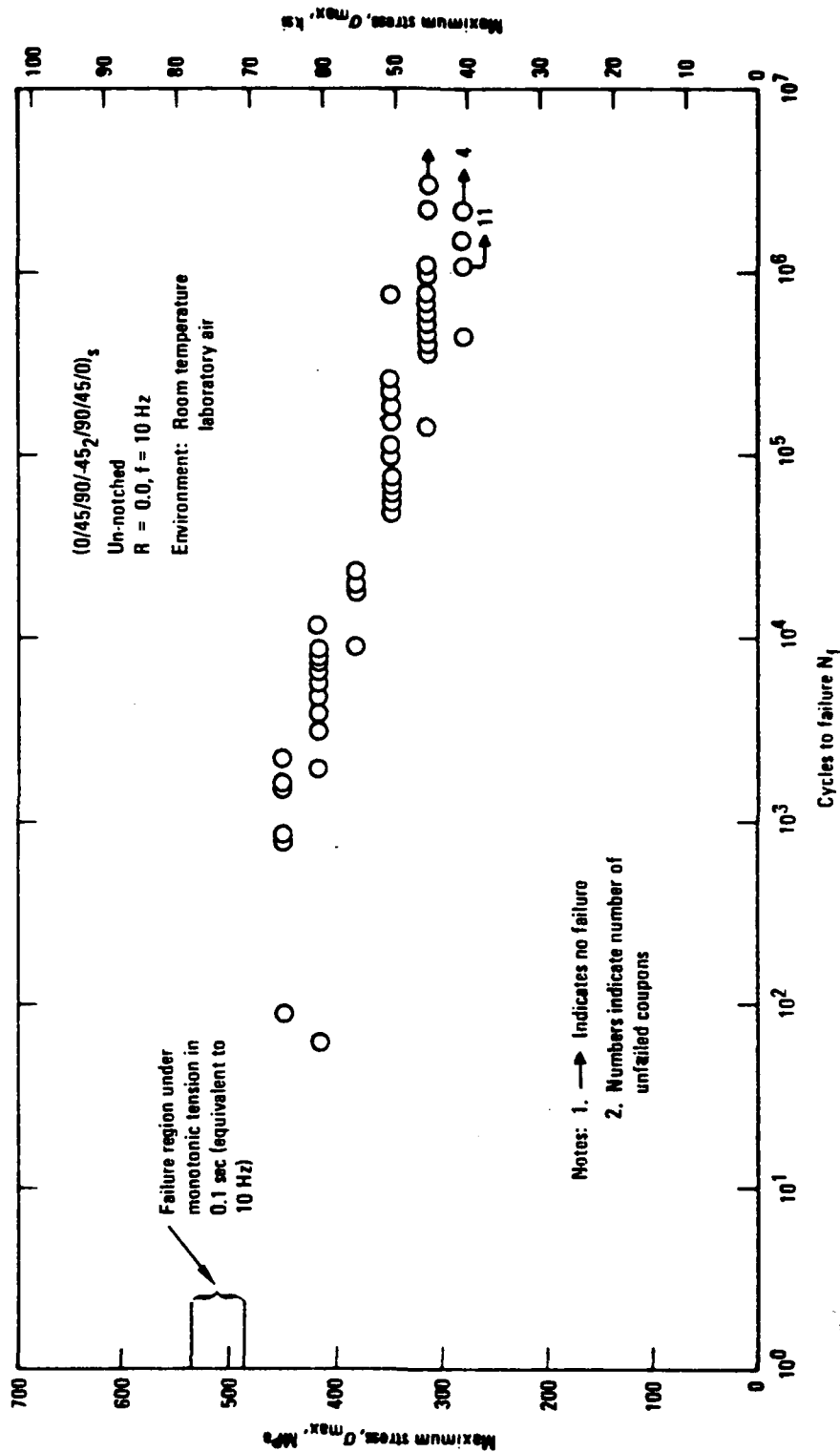


Figure 8. Constant Amplitude Fatigue, Stress-Life Results at $R = 0.0$
 Showing Extent of Data Scatter

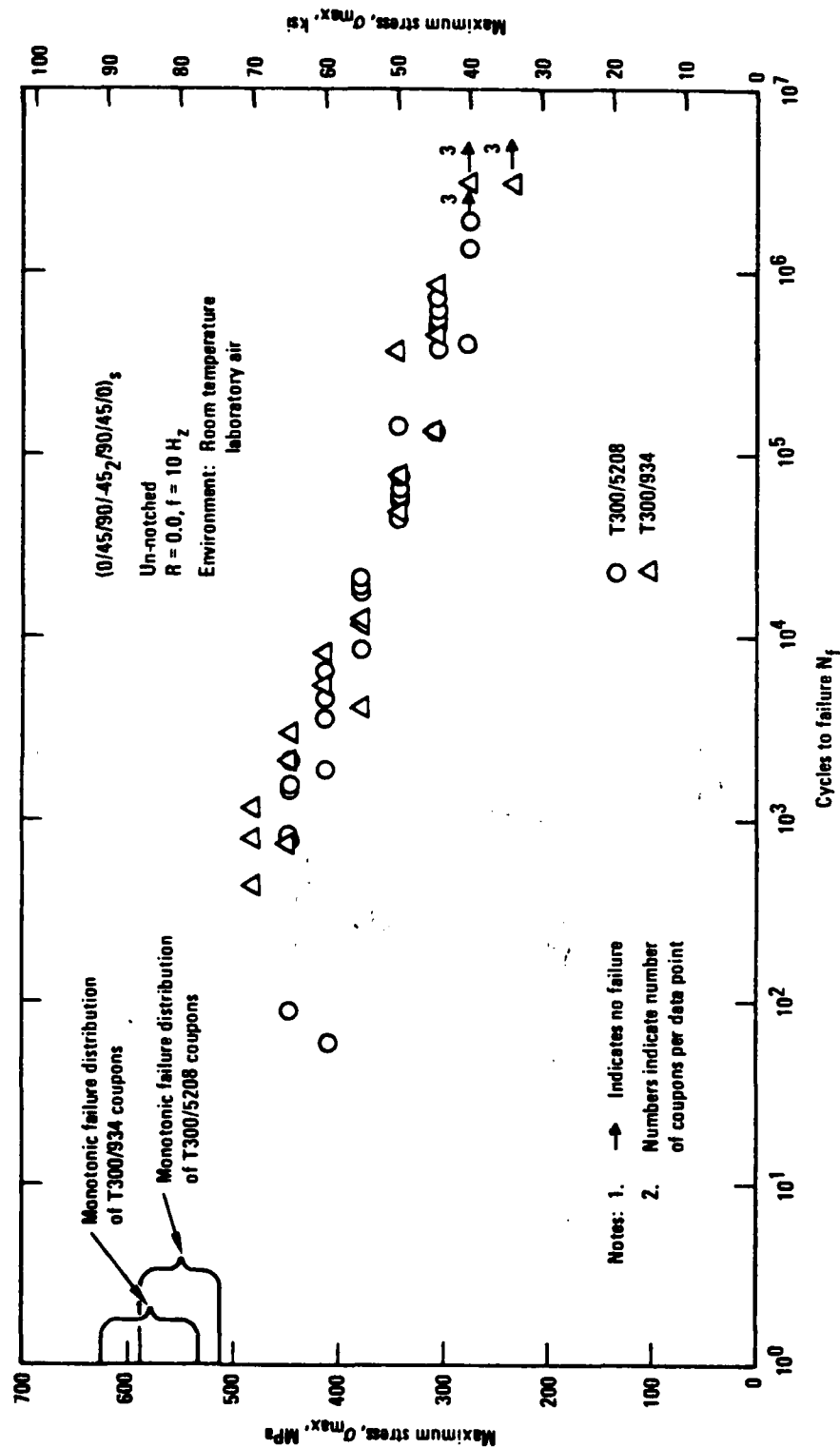


Figure 9. Comparison of Constant Amplitude Fatigue Data of T300/5208 and T300/934 Laminated Composites in Room Temperature, Laboratory Air at $R = 0.0$

while those at $R = -\infty$ provided the baseline data for the load history studies. Experimental results are plotted in Figures 10 and 11. Failure in fatigue was defined to be the inability of the coupon to sustain further compressive load. This occurred due to local buckling. Compression fatigue experiments were conducted at $R = -\infty$ because load history effects under pure compression need to be distinctly understood before considering the complexities which occur under tension-compression load conditions (such as at $R = -1$). As shown by the monotonic load experiments, state changes which occur under tension load are quite different than those which occur under compression load. Further, all coupon tests conducted under tension-compression (T-C) or compression-compression (C-C) fatigue load failed in buckling at a local delamination region which is a quite different failure mode than that which occurs under tension-tension (T-T) loading.

The state changes which occurred under constant amplitude fatigue loading at $R = 0$ manifested in a manner similar to that which was observed under monotonic tension load. The only significant difference was in the observed extent of delamination. That state changes were occurring was evidenced by the appearance of matrix cracks in the 90° plies followed by their appearance in the -45° plies and finally in the $+45^\circ$ plies, see Figures 12 and 13. The order of appearance was identical to that which occurred under monotonic tension load. A slight angle of the matrix cracks relative to the load direction seen in Figure 12 is believed to be due to the shear flow between plies. Matrix cracks found by edge replication appeared to saturate in the 90° plies, see Table 8, with the number of load cycles to saturation dependent on stress level. However, the number of matrix cracks in the $\pm 45^\circ$ plies increased beyond that observed in monotonic tension coupons. These observations are consistent with those made by other investigators^{15,18,19}. Delamination occurred in the same planes as under monotonic tension, especially between the outer 90° and -45° plies, but also significantly between the inner 90° and $+45^\circ$ plies, see Figures 12 and 13. The outer delamination plane often shifted to the outer 90° and $+45^\circ$ ply interface as

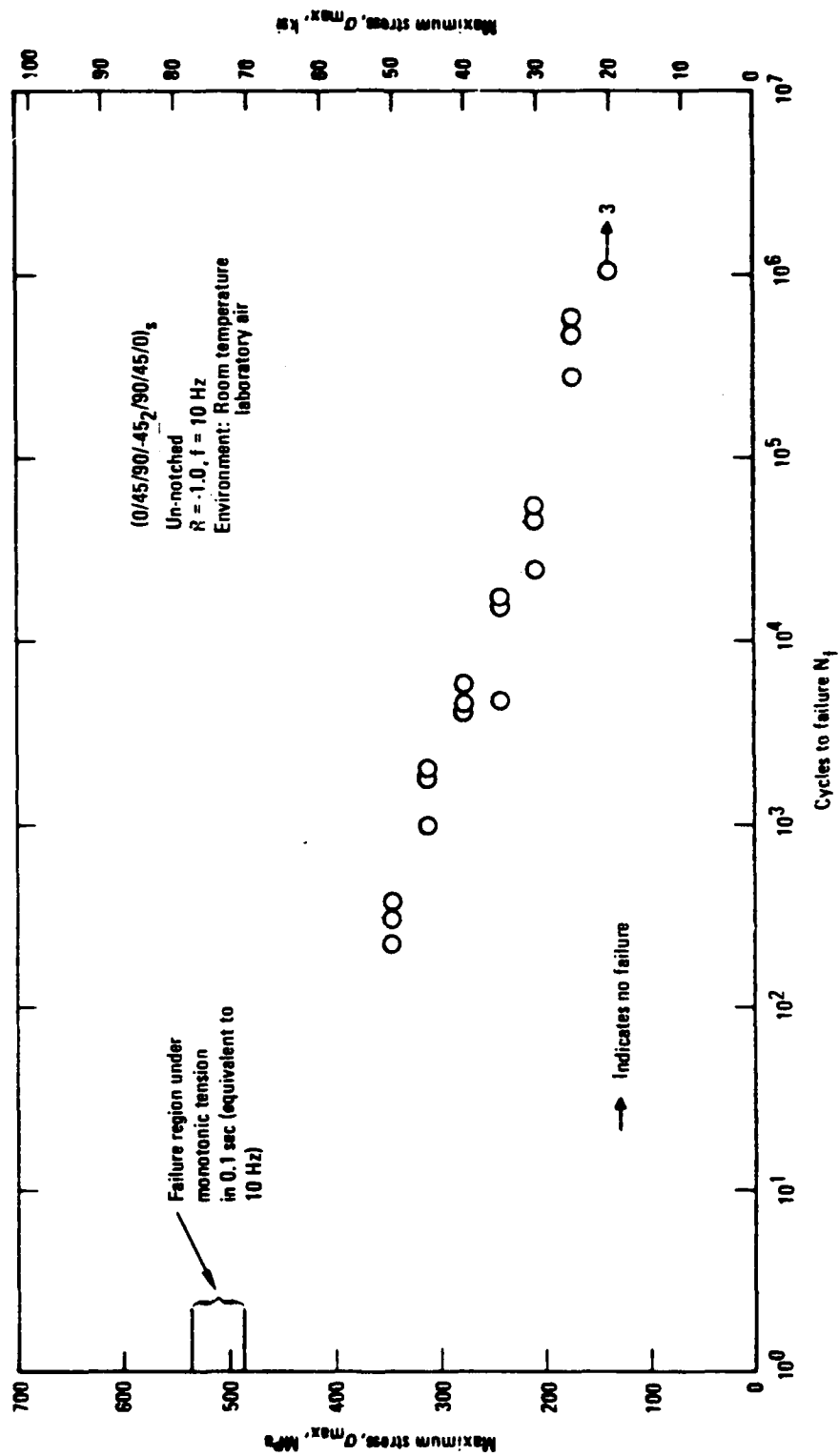


Figure 10. Constant Amplitude Fatigue, Stress-Life Results at $R = -1.0$
Showing Extent of Data Scatter

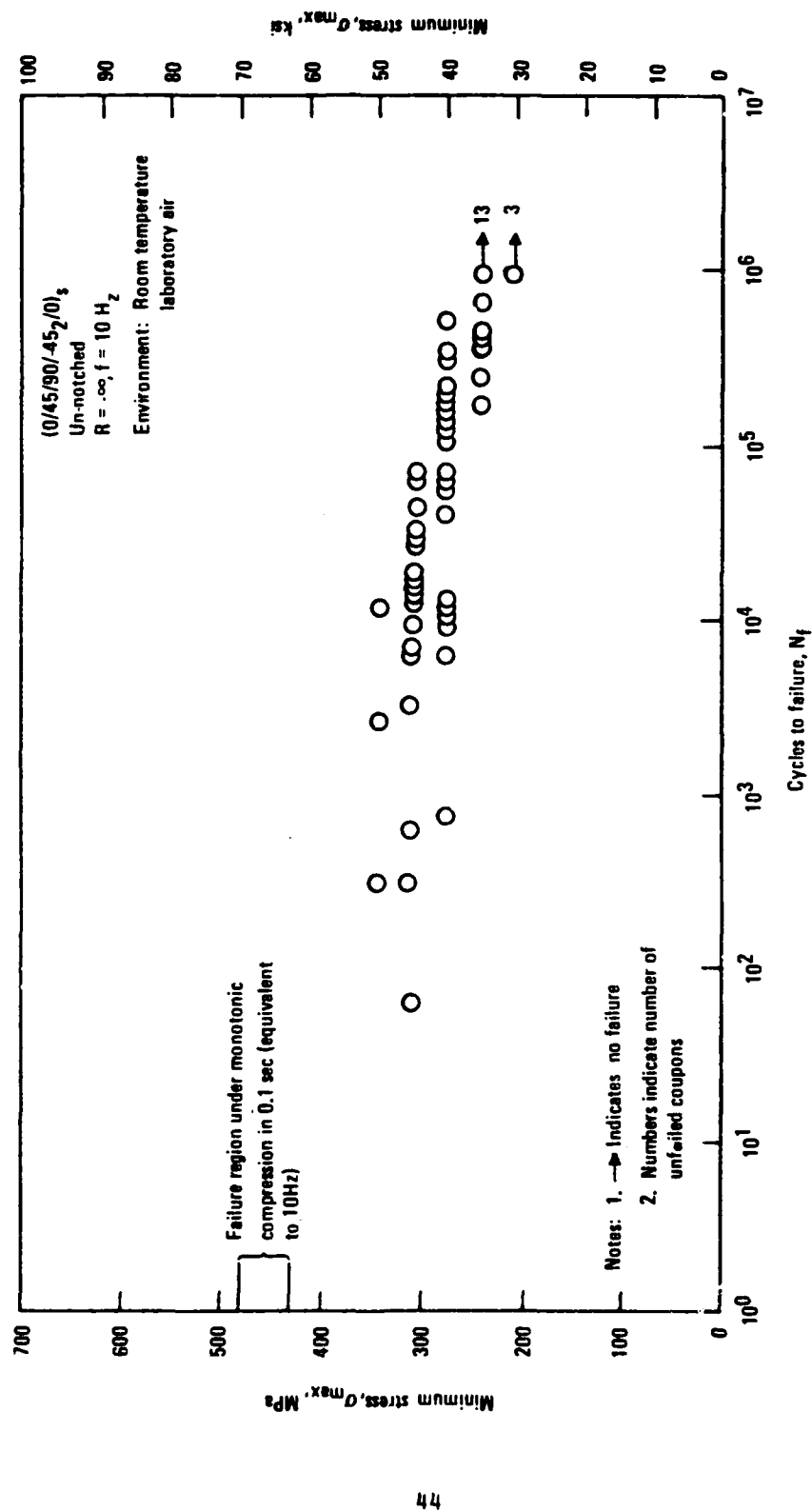
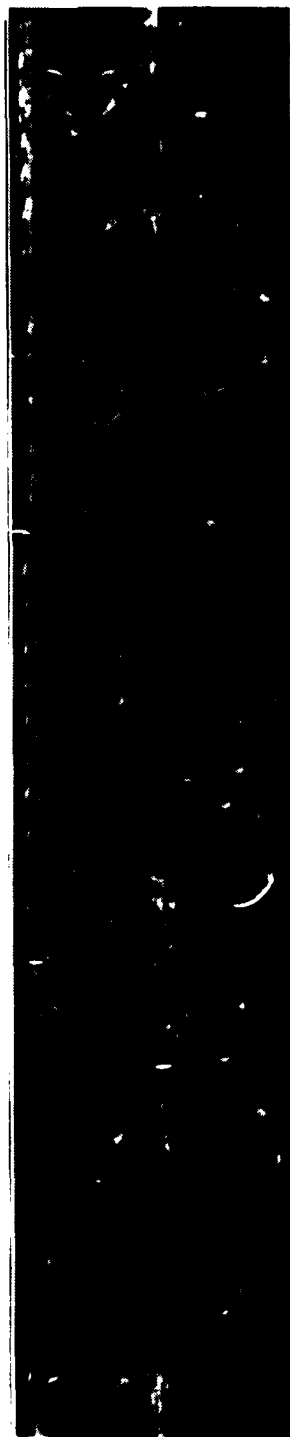


Figure 11. Constant Amplitude Stress-Life Results at $R = -\infty$ Showing Extent of Data Scatter



FIGURE 12: Edge Replication of Matrix Cracks and Delamination Due to Fatigue Loading at a Maximum Stress of 310 MPa (45 ksi) at $R = 0.0$.



100N

143 235K



500N

143 673R



1 800N

143 265K

FIGURE 13: Edge Replication of Matrix Cracks and Delamination Due to Fatigue Loading at a Maximum Stress of 414 MPa (50 ksi) at $R = 0.0$.

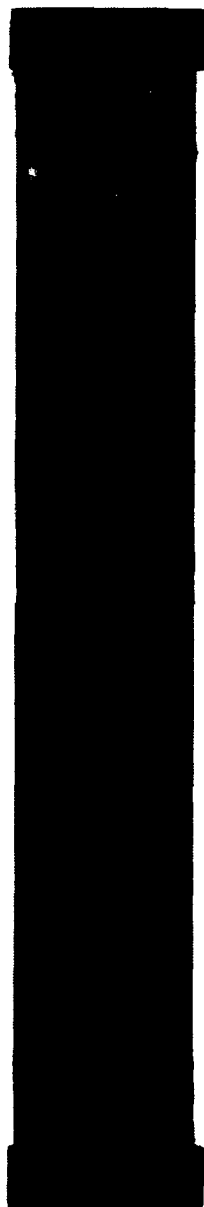
TABLE 8
MATRIX CRACKING AND DELAMINATION UNDER T-T FATIGUE LOADING (R=0.0)

Loading Condition	Average Number Cracks Per 25mm (Inch) ^a			Observed Extent of Delamination into Coupon Interior
	90°	-45°	+45°	
310 MPa (45 ksi), 100 Cycles	12	0	0	None
310 MPa (45 ksi), 1 000 Cycles	33	4	2	None
310 MPa (45 ksi), 200 000 Cycles	54	25	50	Extensive
414 MPa (60 ksi), 100 Cycles	54	15	18	None
414 MPa (60 ksi), 500 Cycles	54	19	31	Slight
414 MPa (60 ksi), 1 800 Cycles	60	21	39	Moderate
Tension at 97.5% of Average σ_{ult}	54	16	8	None

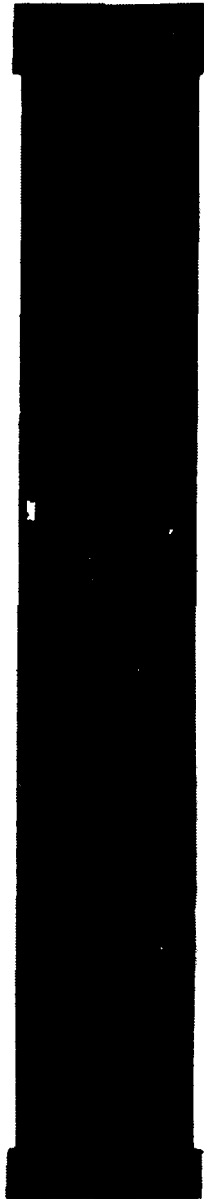
a = Calculated values are the averages of counts of edge cracks within six 25mm (1 in.) long observation regions for each of three coupons for a total of eighteen data points.

apparent in Figures 12 and 13. These delaminations extended in both the length and width directions as load cycling continued, Figure 14. Eventually delamination occurred in rare locations between the outer 0° and $+45^\circ$ plies (see Figure 15) similar to the monotonic tension case. This results in a local region where all load must flow only through the inner and outer 0° plies as diagramed in Figure 16. The outer 0° plies eventually fracture in these regions starting at the coupon edge and proceeding stepwise (as tow bundles) along the $+45^\circ$ ply direction of the outer delamination, see Figure 17. This is similar to that which was observed under monotonic tension load. After some progress of the $+45^\circ$ direction fracture, coupon failure occurs, see Figure 18.

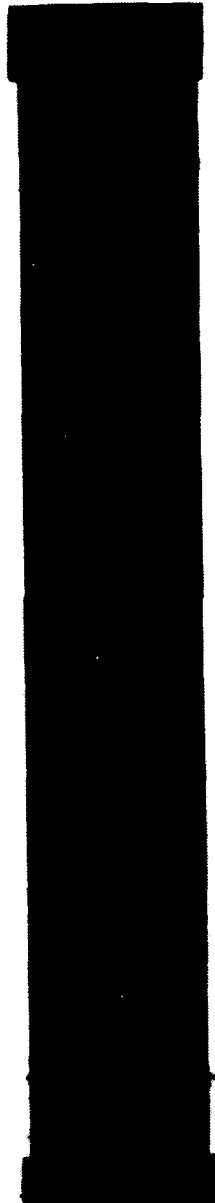
There are two key observations to be emphasized which were made concerning those coupons subjected to constant amplitude, T-T, fatigue loading. The first observation was that the state which occurred just prior to fracture under only monotonic load appeared to also occur early in the cyclic life of a fatigue loaded coupon. The second observation was that the states which occurred under a high magnitude of energy input per cycle appeared to essentially manifest under a lower magnitude of energy input per cycle, but after a much greater number of loading cycles. Because of this phenomenon, the state just prior to failure under, for example, a 414 MPa (60 ksi) constant amplitude fatigue load (after approximately 5 500 cycles) was observed to essentially occur in a coupon subjected to a 310 MPa (45 ksi) fatigue load but after approximately 30 000 to 100 000 cycles (which is however, well before failure). These two observations formed the basis of the inference that the dependence of the functional nature of the state change process on the magnitude of prior energy input is significantly different than that which occurs in metallic materials. This property concerns the third of the four questions formulated for this experimental investigation (see Table 1) and is specifically addressed in the discussion of the preload and block load experimental results.



310 MPa (45 ksi)
200 000N



310 MPa (45 ksi)
200 000N



414 MPa (60 ksi)
1 800N

FIGURE 14: Enhanced X-Ray Photographs of Delamination Extension Due to Fatigue Loading



FIGURE 15: Edge Replication of Coupon Fatigue Loaded at 414 MPa (60 ksi) Maximum Stress at $R = 0.0$ Showing Delamination Between the Outer 0° and $+45^\circ$ Plies.

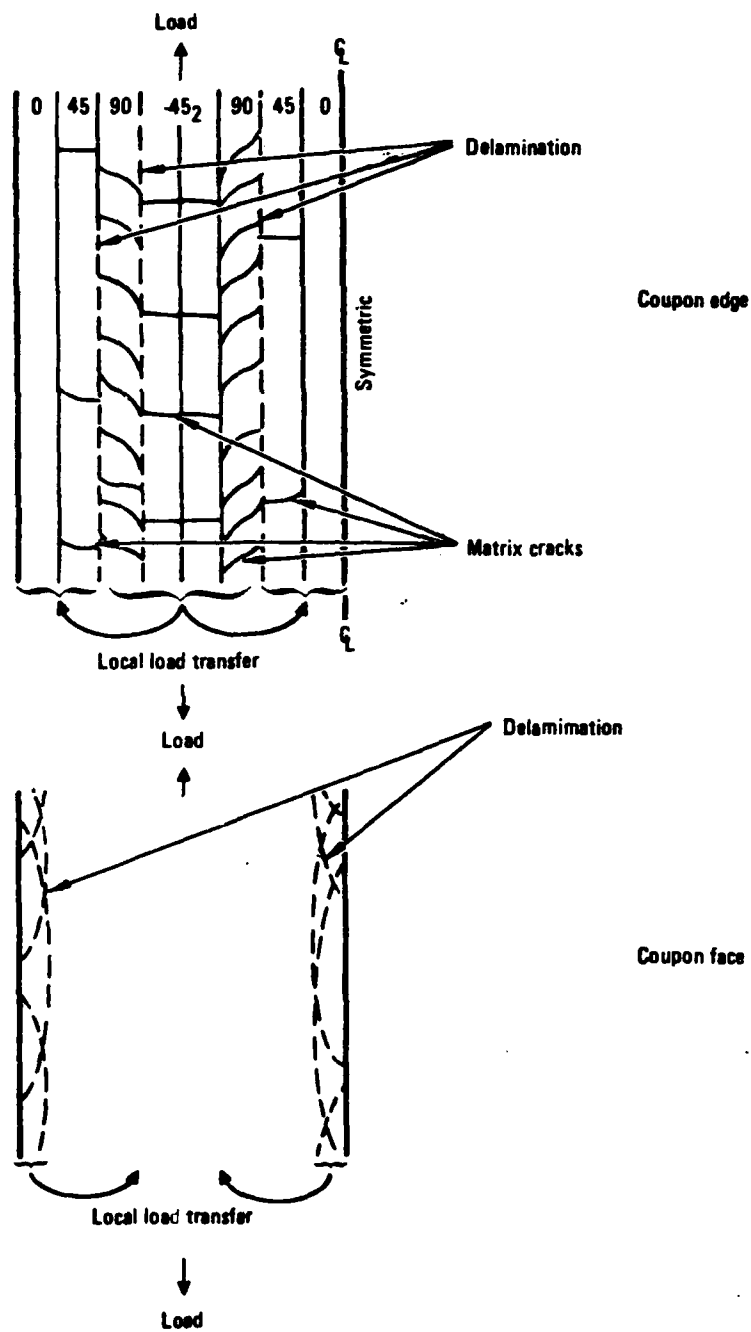


Figure 16. Diagram of Delamination and Matrix Cracking

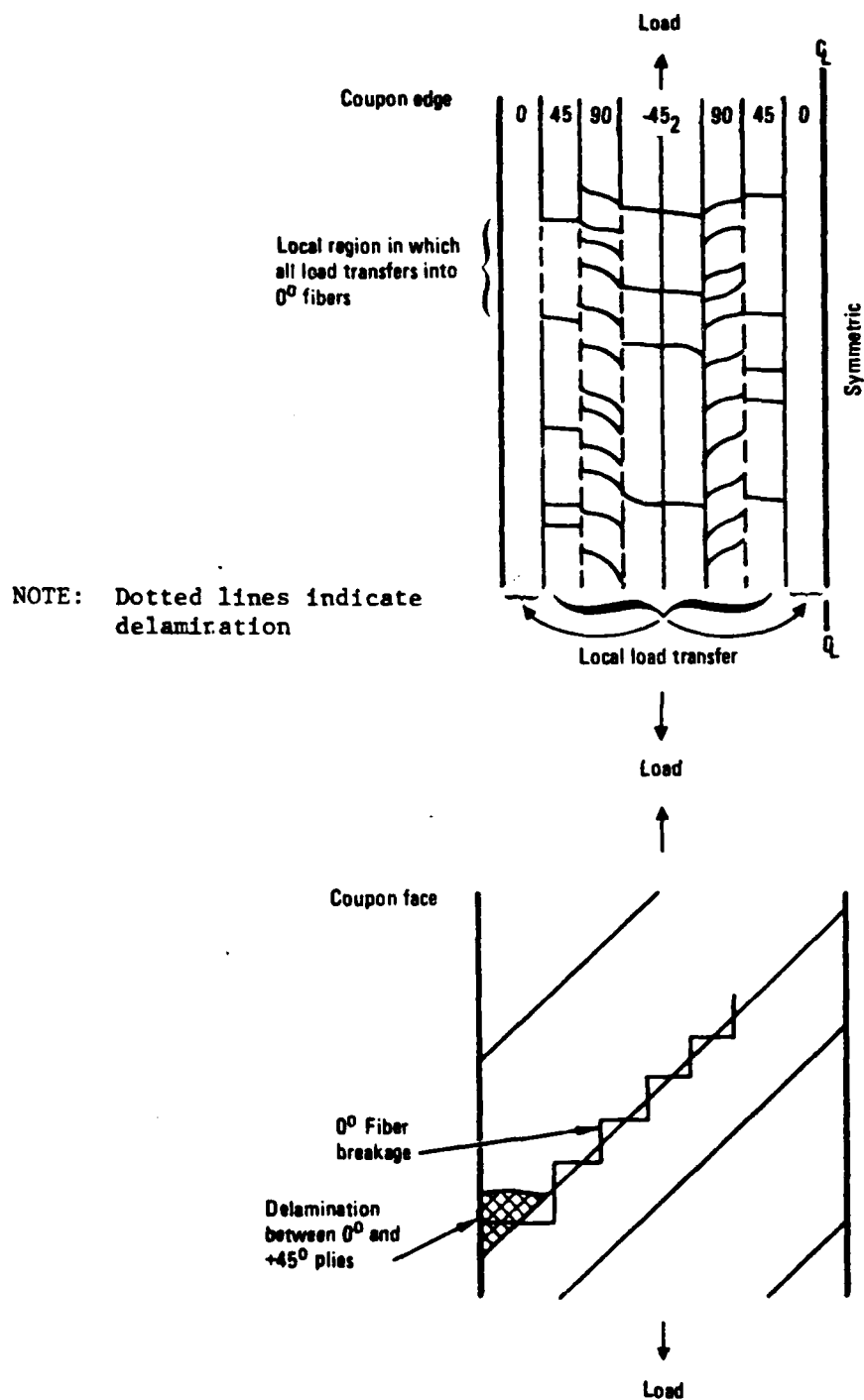


Figure 17. Diagram of Outer 0° Ply Fracture at $+45^\circ$ Angle

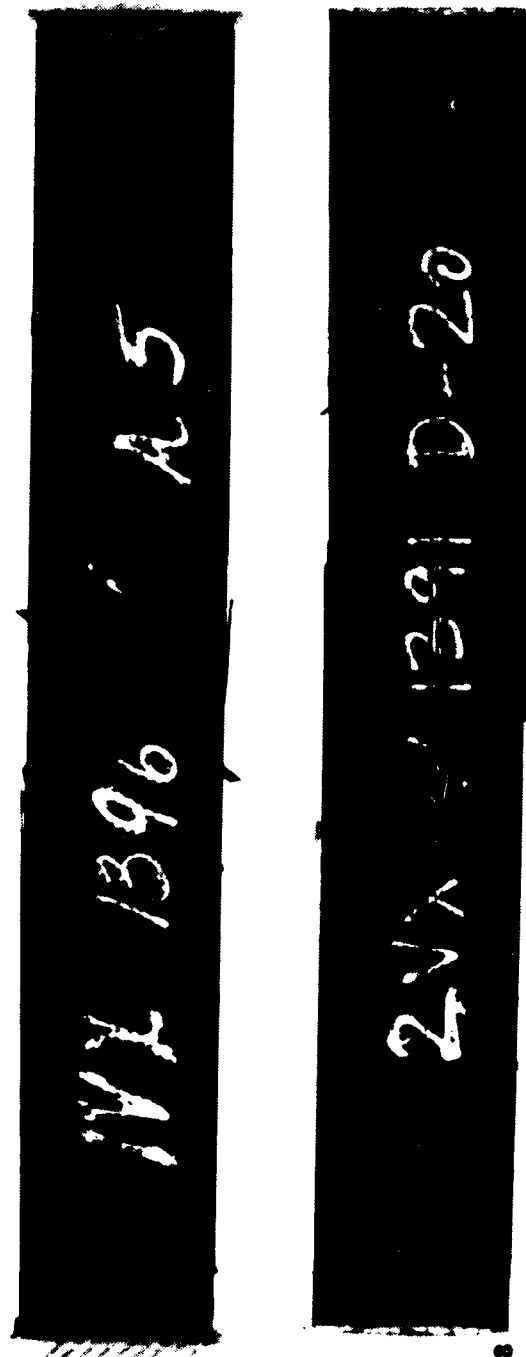


FIGURE 18: Photographs of Failed Fatigue Loaded Coupons Showing +45° Fracture of Outer 0° Plies (Maximum Stress 310 MPa (45 ksi), $R = 0.0$).

The manifestation of states and state changes under cyclic compression loading could not be as well documented as for tension load. However, visual and low power microscopic observations were made, enhanced x-ray photographs obtained and photomicrographs taken (up to 500X) of failed coupons. In addition edge replications outside of the failure regions were obtained on a few coupons. The observations revealed that the state changes which occurred under monotonic or cyclic load were again quite similar, Figure 19. Notice in Figure 19C the typical $+45^\circ$ fracture of the outer 0° ply on one side of a coupon and the 90° fracture on the other side. The extent of delamination at failure was not obviously different under fatigue load as compared to monotonic load. The restriction of delamination extent under compression fatigue load was, of course, due to the buckling of the coupon soon after delamination eventuated. Delamination within the buckled region occurred on many planes, but near the ends of the region was essentially restricted to the interface of the outer 90° and $+45^\circ$ plies. This is in contrast to the tension fatigue case where delamination was predominately between the outer 90° and -45° plies and the inner 90° and $+45^\circ$ plies. Occasional $+45^\circ$ angle matrix cracks occurred in the adjacent plies. Photomicrographs of the cross sections of failed coupons revealed no matrix cracks or delaminations outside of the region of buckling failure. However, edge replications of several more coupons revealed the occasional appearance of delamination, again primarily between the outer 90° and $+45^\circ$ plies, outside of the failure region, and accompanied, although rarely, by $+45^\circ$ angle intraply matrix cracking.

A consideration of both the monotonic and constant amplitude fatigue data allows further conclusions to be drawn as to the nature of material/structure state dependence on energy input. State and rate of change are dependent on the magnitude, rate and form of energy input. There is some evidence that the sequence of events is also dependent on rate of energy input. The dependence of state change on form of energy input is clear by comparing the tension data to the compression data. Not only were there no matrix

2VX 1395 A-29



1VX 1395 D-19

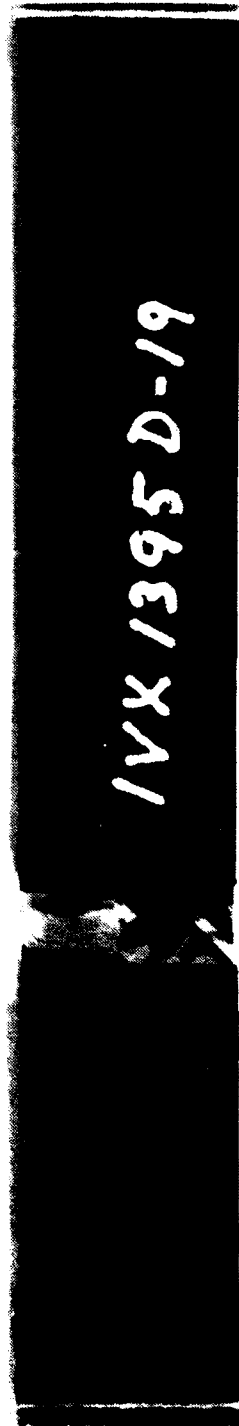


FIGURE 19a: Appearance of Coupons Which Failed Under Compression Load (Monotonic Load)

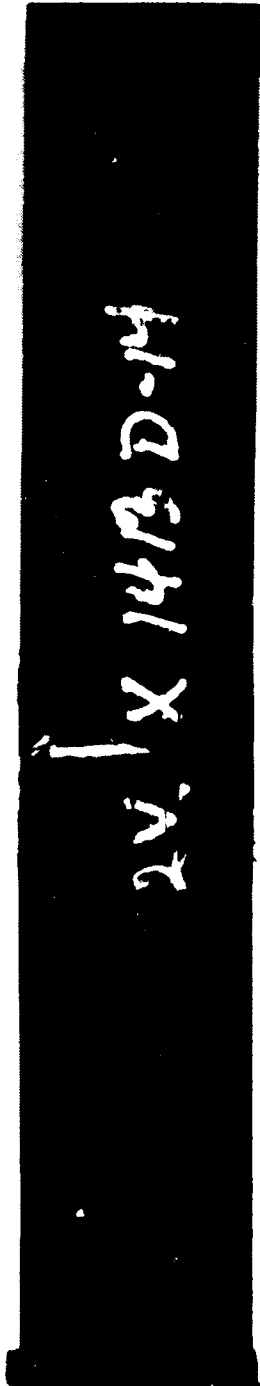
1VX 1395 D-19



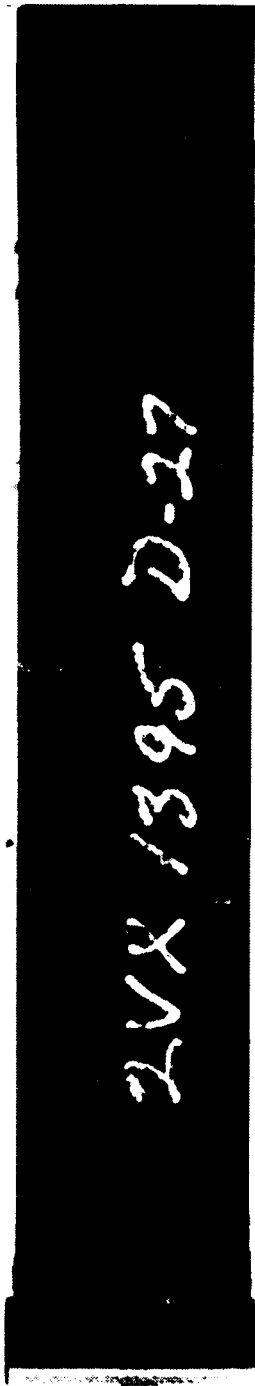
2VX 1395 A-29



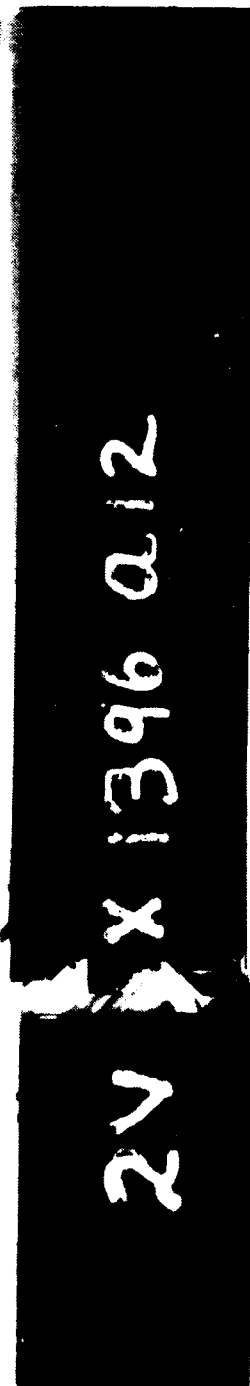
FIGURE 19b: Appearance of Coupons Which Failed Under Compression Load (Monotonic Load)



2VX 1413 - D-14



2VX 1395 - D-27



2VX 1396 - A-12

FIGURE 19c: Appearance of Coupons Which Failed Under Compression Load (Fatigue Load, $R = -\infty$, $\sigma_{\min} = -310 \text{ MPa } (-45 \text{ ksi})$).



FIGURE 19d: Appearance of Coupons Which Failed Under Compression Load (Fatigue Load, $R = -\infty$, $\sigma_{min} = -310 \text{ MPa}$ ($-45,000 \text{ psi}$)).

cracks outside of the fracture region for compression loading , but delamination tended to occur only between the outer 90° and $+45^{\circ}$ plies, an entirely different plane than under tension load. The complete difference in the nature of state change under tension and compression provided good support for the decision to keep the two forms of energy input separated for this program.

If the energy input is restricted to one form, either tension or compression, two further conclusions can be drawn. First, the difference between the nature of state change, exclusive of a small possible rate effect, under monotonic or fatigue loading appears to be one of degree as evidenced by the extent of delamination. Second, the functional nature of the state change process appears to be essentially independent of the magnitude of prior energy input. This second conclusion was a significant, although tentative, inference since it implies that the nature of energy dissipation in laminated graphite/epoxy composites is quite different than that for metals. The possible meaning and significance of the difference is discussed in subsequent sections on the preload, block load, and overload experiments.

2.2 LOAD HISTORY EXPERIMENTAL RESULTS

This subsection summarizes the results of the load history experiments conducted in Task II to determine the effect of energy input on state and changes in state of the selected quasi-isotropic, graphite/epoxy laminate. The progressive load and trapezoidal wave loadings were used to determine if the difference observed between monotonic and cyclic induced states at fracture was due to the repeated input of energy or because of the length of time that the energy was stored (time at load). The preload and block loading experimental results were used as a means to ascertain the validity of the second conclusion discussed at the end of the previous subsection.

That tentative conclusion was that the nature of the dependence of rate of state change on magnitude of energy input is significantly different than that of metals. If the conclusion is confirmed, the manner in which complex energy input affects state change is greatly altered as are the procedures by which that effect is represented. The extent to which those procedures might have to be altered was partially evaluated using both the block loading and overload data.

2.2.1 Relationship Between Monotonic and Fatigue Load Results

Progressive cyclic loading and constant amplitude trapezoidal waveform loading were used to ascertain the dependence of state change on repeated energy input and on enforced energy storage (by time at load). This allowed discernment of the reason for the difference between the states reached during monotonic and fatigue load.

2.2.1.1 Progressive Loading experiments

The progressive cyclic loading experiments were conducted in such a manner as to answer the question of whether the difference between the states reached at fracture under monotonic and cyclic loads was due to the repeated input of energy on each load cycle (beyond that simply due to the application of a monotonically applied load). The question arises because the fact that the material state is dependent on the magnitude of energy input is, and correctly, not doubted within the technical community. However, as mentioned in Section 1, certain approaches or models for understanding composite materials (such as that which we called the stress/brittle material concept) do not consider that the repeated input of energy up to the magnitude previously reached can cause any additional state change (usually termed damage) of significance. The fact, therefore, that failures do occur under repeated input of energy at a constant magnitude (for example, fatigue loading) has been hypothesized to be a reflection of the amount of time that

the load remains at a high level^{12,20}. In essence, the hypothesis has been that the phenomenon of change which occurs under fatigue loading is the same as a creep phenomenon. Therefore, in the attitude of this report, state change under fatigue loading is often considered to be due to the inability of the material to store energy without permanent significant change and not to the repeated input of energy. The progressive load experiments were designed, therefore, to evaluate the effect of repeated input of energy on state change independent of other effects.

Progressive load cycling consisted of applying a sinusoidal waveform of constant load ratio, R , consisting of a stress amplitude increasing linearly with time to failure, see Figure 20. Fifteen (15) coupons were loaded to failure at 10 Hz frequency and at an increasing tensile or compressive load versus time rate approximately equal to that of a standard monotonic tensile test (approximately one minute). The experiment was repeated using a second set of coupons which were loaded to failure in about one hour at a slower rate of increase. Both sets of tests were conducted at the two selected R ratios of 0 and $-\infty$. The first loading rate allowed approximately 600 fatigue cycles to be applied before failure and the second approximately 36 000 cycles. During the experimentation, coupon fracture was observed to occur at a load level slightly below that recorded on the previous to last cycle.

If the failure strength distributions of the progressive load populations were found to be the same as their respective initial monotonic strength distributions, a logical conclusion would be that the repeated input of energy during each load cycle does not significantly affect the state reached at fracture or the change in state sequence. The entire state change process would thus be due to the energy input of the increasing monotonic load. On the other hand, if the failure distributions of the progression loadings are significantly different from the monotonic strength distributions, as they proved to be, a reasonable conclusion is that the energy

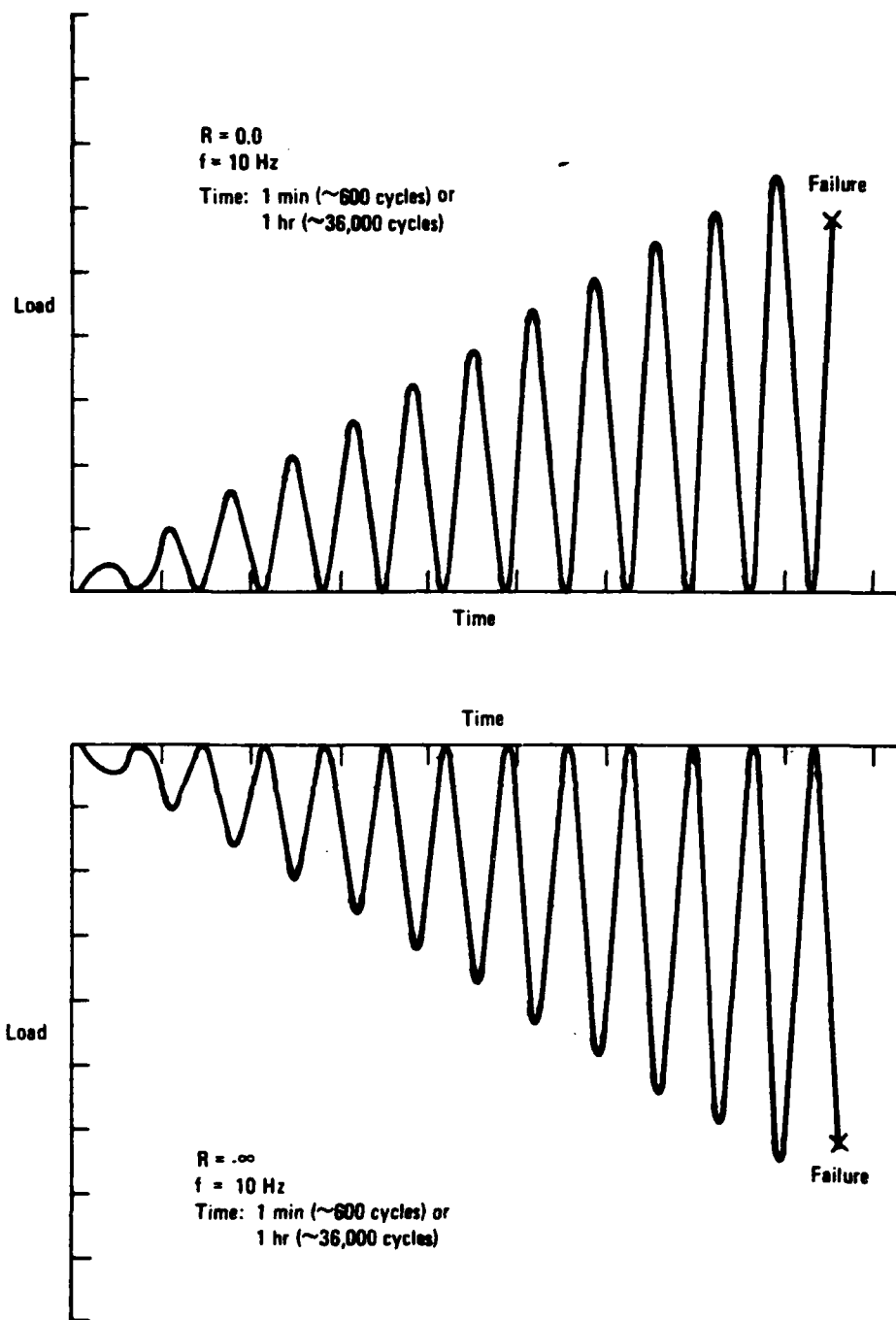


Figure 20. Loading Waveforms Used in Progressive Load Experiments

states reached, and thus fatigue life, are dependent on the repeated input of energy and not just on the magnitude of input energy.

A comparison of the progressive load experimental results at $R = 0$ is given in Table 9. The first two rows of the table, those for monotonic tension, show that there was essentially an insignificant effect of test machine type on the experimental results, as previously discussed. This is an important observation since the progressive load experiments were conducted in fatigue type loading machines.

Comparison of the second and third rows of Table 9 indicates the previously mentioned strain rate effect on state change and the associated strength distribution change of approximately 8 percent. The value of this comparison is to eliminate the possibility that any observed effects of load variation could be simply due to strain rate. This possibility is apparent when comparing the data of rows two and four and three and four. The first comparison indicates a possible effect of repeated input of energy on the state reached at fracture or on the rate of state change as shown by the difference in tensile strength, but the second comparison shows that the effect could equally be attributed to a difference in the rate of energy input (here achieved by varying the loading rate). The latter conclusion was supported by low power, visual observations and by enhanced x-ray photographs of the fractured coupons. None of the coupons from rows one to four showed any significant delamination extending into the interior of the coupons, see Figure 21.

A limited edge replication study of the one minute progressively loaded coupons indicated that the order of appearance of matrix cracks and the strain levels at which they occurred in the different plies were similar to those which occurred under monotonic load. Therefore, the inference was made that the coupon states at fracture and the nature of state change due to a one minute progressive loading cycle were essentially the same as that which

TABLE 9
SUMMARY OF THE EFFECT OF PROGRESSIVE LOAD (R=0)
ON TENSILE STRENGTH

Test Type	Number of Test Coupons	Approximate Failure Time, Min.	Average Stress At Failure		Weibull Exponent Parameter
			MPa	ksi	
Monotonic Tension in Static Machine	20	1.3	547 ^a	79.3	33.9
			19 ^b	2.8	
			3.5% ^c		
Monotonic Tension in Fatigue Machine	10	1	536	77.8	-
			39	5.7	
			7.3%		
Monotonic Tension in Fatigue Machine	13	0.0167 ^d	507	73.6	30.1
			17.9	2.6	
			3.5%		
Progressive Load	15	1	506	73.4	35.0
			17	2.5	
			3.4%		
Progressive Load	15	60	434	62.9	67.5
			7.7	1.1	
			1.8%		

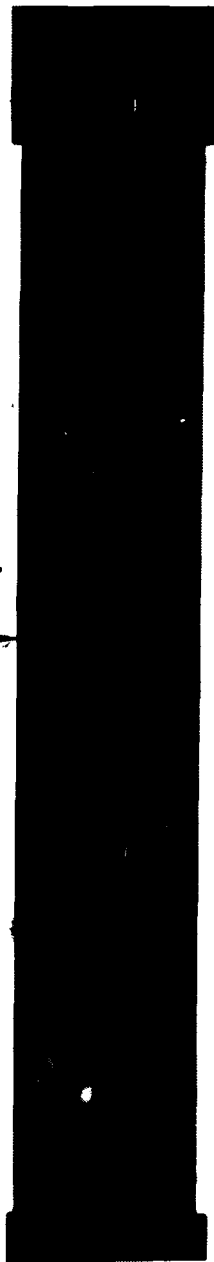
a = Average

b = Standard Deviation

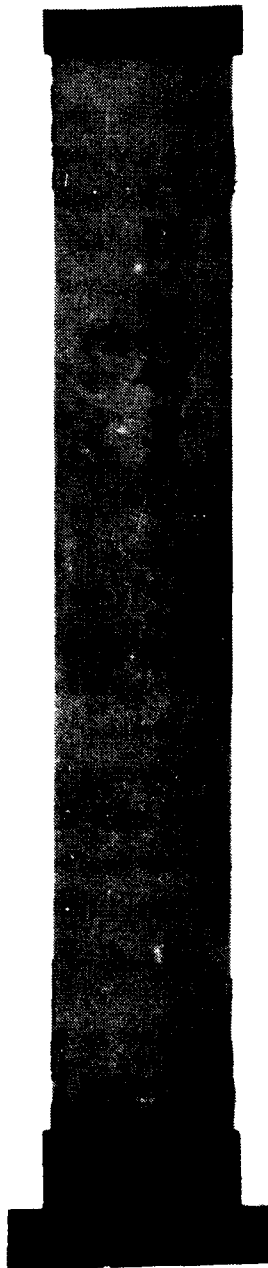
c = Coefficient of Variation

d = Loading rate equivalent to 10 Hz fatigue test

Enhancer Stains on
Coupon Surface



Coupon 1VX1413-D25, Progressively Loaded to Approximately one minute to 98% of Failure Load



Coupon 2VX1403-B22, Monotonically Loaded at Low Strain Rate to Approximately 97.5% of Failure Load

FIGURE 21: Enhanced X-Ray Photographs of Monotonic and Progressively Tensile Loaded Coupons Showing Absence of Delamination Prior to Failure

occurred under a high strain rate monotonic load. Non-parametric statistical tests also supported the observation that the data of rows three and four are essentially the same just as rows one and two are the same as previously mentioned, see Table 10.

In contrast, if the data of Table 9 row five are compared to those of rows one to four, a significant change in average failure strength can be clearly seen. This is also apparent in the non-parametric statistical comparison of Table 10. NDI observations revealed extensive delamination just before failure, see Figure 22, for the coupons progressively loaded to failure in one hour. Note also in Table 9 that the data scatter for the one hour progressively loaded coupons was much smaller than that for the other experimental conditions as indicated by the lower percent coefficient of variation and the high Weibull exponent. This comparison of mechanical and NDI data of row five to those of rows one to four shows that there is an effect on the material/structure state reached due to the fact that energy has been repeatedly inputted. A large number of repeated cycles of energy input is required for the effect to be apparent (36 000 versus 600), but the state change process is clearly dependent on the repeated input of energy and not just on the magnitude. Whether or not the effect of repeated energy input is a manifestation of the events occurring during the cycle itself or just near the maximum level of each cycle (and thus a creep phenomenon) cannot be determined from the progressive load data. The data obtained from the preload and time at load experiments were used to evaluate these two possibilities.

The effect of repeated energy input on the state change process was further explored under compression-compression fatigue loading. The results of the experiments conducted at $R = -\infty$ are shown in Table 11. A possible strain rate effect is apparent by comparing the results shown in rows one and two. Comparison of rows two and three reveals that the effect of a repeated input of energy on state change for progressive cycling to failure in one minute

TABLE 10
NON-PARAMETRIC STATISTICAL
STUDY ⁽¹⁶⁾ OF T-T PROGRESSIVE LOADING DATA

HYPOTHESIS: THESE DISTRIBUTIONS ARE THE SAME	HYPOTHESIS CAN BE ACCEPTED (A) OR REJECTED (R)	
	MANN-WHITNEY STATISTIC	WALD-WOLFOWITZ TEST
Monotonic Tension in Static and in Fatigue Machine (Rows 1 and 2 of Table 9)	0.175 A	A
One Minute Prog. Load and High Strain Rate Monotonic Tension	0.483 A	A
One Hour Prog. Load and High Strain Rate Monotonic Tension	4.49 R	R



FIGURE 22: Enhanced X-Ray Photographs of Coupons Progressively Loaded to Failure in One Hour Showing Extensive Delamination at 98% or Greater of their Failure Load.

TABLE 11
SUMMARY OF THE EFFECT OF PROGRESSIVE LOAD ($R=-\infty$)
ON COMPRESSIVE BUCKLING STRENGTH

Test Type	Number of Test Coupons	Approximate Failure Time, Min.	Average Compressive Stress At Failure	Weibull Exponent Parameter
Monotonic	5	1	58.6	-
Monotonic	5	0.0167 ^a	65.0	-
Progressive Loading	15	1	61.8	27.9
Progressive Loading	13	60	56.1	37.5

a = Loading Rate Equivalent to a 10 Hz Fatigue Load Frequency.

was not large as evidenced by similar strength distributions. However, the data of row four when compared to the data of rows two or three can be used to infer that a significant effect occurs if sufficient cycles are applied. Unlike the $R = 0$ results, the reason for the difference is not obvious. Both visual observations (see Figure 23) and enhanced x-ray photographs (see Figure 24) showed no significant differences in the appearance of the failure regions. Due to early program truncation, because of Air Force funding limitations, a definitive NDI study of the state change process was not undertaken. However, it was logically inferred that the greater number of cycles in the one hour progressive load experiment allowed significant delamination to develop earlier than under either a monotonic load or a one minute progressive loading such that buckling instability occurred at a lower maximum compressive load.

The results of the progressive load experiments, both at $R = 0$ and $-\infty$, were used to conclude that the repeated input of energy due to load cycling is a major reason that the states at fracture are different under monotonic and cyclic load. The effect was inferred because: 1) the average strength at failure decreased if the number of cycles was large; and 2) after a large number of cycles, extensive delamination was observed (under tension load) which did not significantly occur under monotonic load or after a relatively small number of progressive load cycles.

2.2.1.2 Trapezoidal Wave Loading (Time at Load)

Part of the question posed in the beginning of Section 2, namely, what is the reason for the difference in the material state at fracture under monotonic and fatigue load, was answered by the progressive load experiments. That difference is, at least in major part, due to the repeated input of energy. The question remained as to whether, at least at room temperature, any significant portion of the difference could be related to the time over which the material was forced to store energy. This is a similar, although

2VX 1396 - A-28



2VX 1396 - A-28

FIGURE 23a: Coupons Monotonically and Progressively Loaded to Failure in Compression (Failure in One Minute Progressive Load).

2VX 1413 - A-8

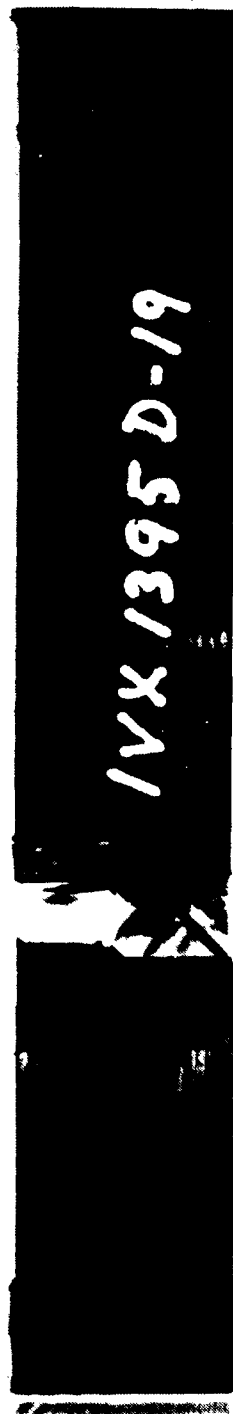


2VX 1413 A-8

2VX 1413 - A-8

FIGURE 23b: Coupons Monotonically and Progressively Loaded to Failure in Compression (Failure in One Hour Progressive Load).

1VX 1395 D-19



1VX 1395 D-19

FIGURE 23c: Coupons Monotonically and Progressively Loaded to Failure in Compression (Failure in Monotonic Load in One Minute).

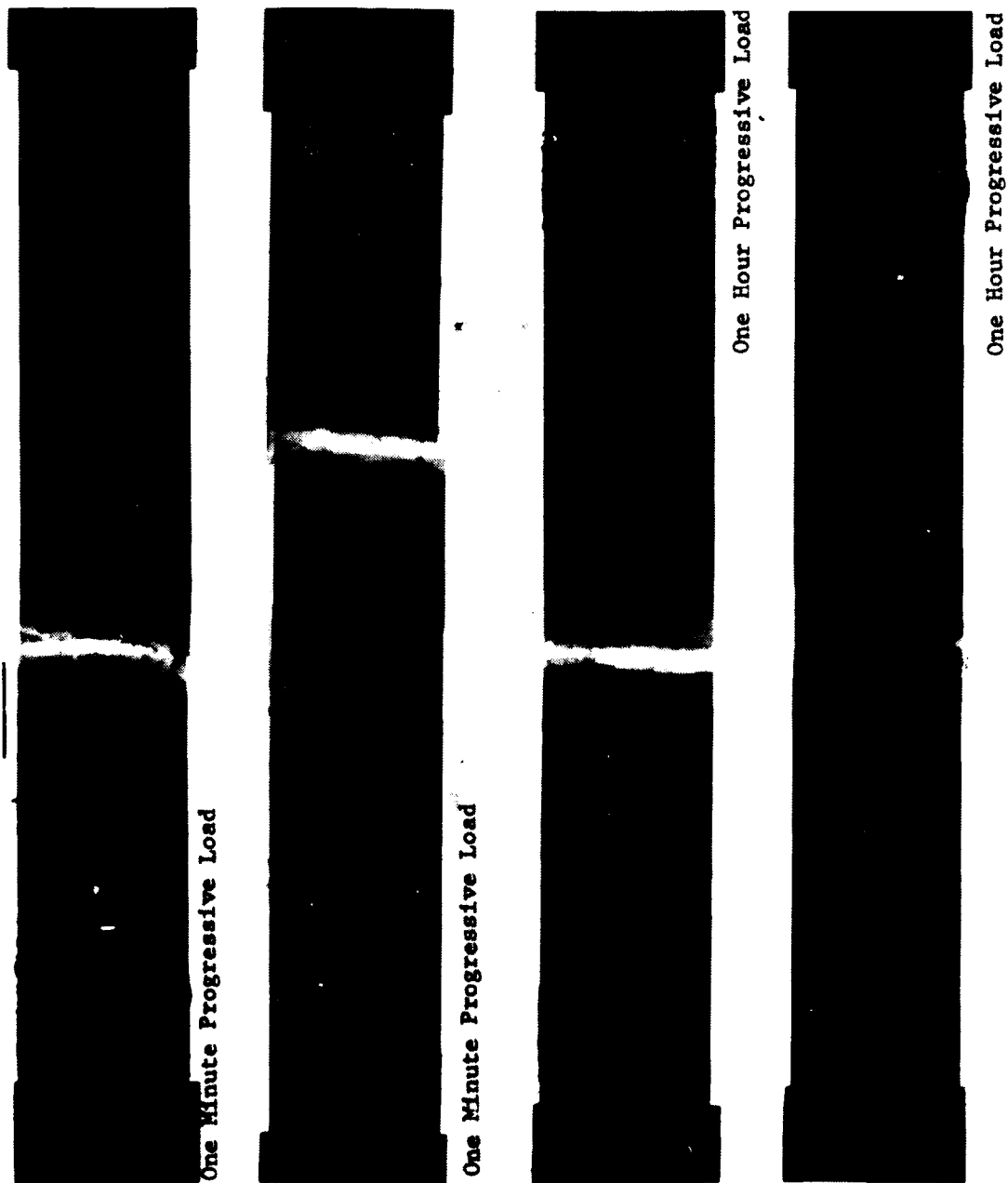


FIGURE 24: Enhanced X-Ray Photographs of Failed Coupons Progressively Loaded in Compression

(NOTE: Darkness Along Coupon Edges are enhancer stains on the coupon surface not delamination).

more basic, question to that previously asked as to whether the difference between monotonic and fatigue load generated states is related to a creep phenomenon of the material when held at high load. At high temperatures, such an effect might not be unexpected since matrix properties are altered and viscoelastic phenomena eventuate²¹. Under ambient environmental conditions the answer is less clear. However, time at load has been hypothesized as a major if not principal cause of fatigue load induced state change in laminated, graphite/epoxy composites^{12,20}.

Trapezoidal waveform loading experiments were used to probe the importance of time at load. Experiments were only conducted at $R = 0$ because those at $R = -\infty$ were eliminated due to imposed financial restrictions. Coupons were load cycled to failure at constant amplitude using a trapezoidal waveform. The time at the peak load of each cycle was either 60 seconds or 1 second and the maximum stress either 310 MPa (45 ksi) or 414 MPa (60 ksi). These two stress levels were selected because a higher stress led to such short cyclic lives as to make comparison of results difficult, and at lower stress levels cyclic lives would be in excess of 10^6 cycles. The load rise and fall times were adjusted to match the rise and fall times of the sinusoidal waveform used to obtain the baseline fatigue data of Section 2.1. Therefore, a comparison of the trapezoidal waveform data to the baseline sinusoidal waveform data allowed a direct evaluation of the effect of energy storage (time at load) on laminate state change and associated fatigue life. Because of the long test times associated with the 60 sec time at load experiments, these tests were terminated after 10 000 cycles which was sufficient for experimental evaluation of the time at load effect.

Experimental results are graphically summarized in Figure 25. At 414 MPa (60 ksi), the time at load clearly had no significant effect. Non-parametric statistical tests,¹⁶ both Mann-Whitney and Wald-Wolfowitz, showed that the two populations were essentially identical. Similarly, the inference from the data at 310 MPa (45 ksi) was that time at load had no significant effect

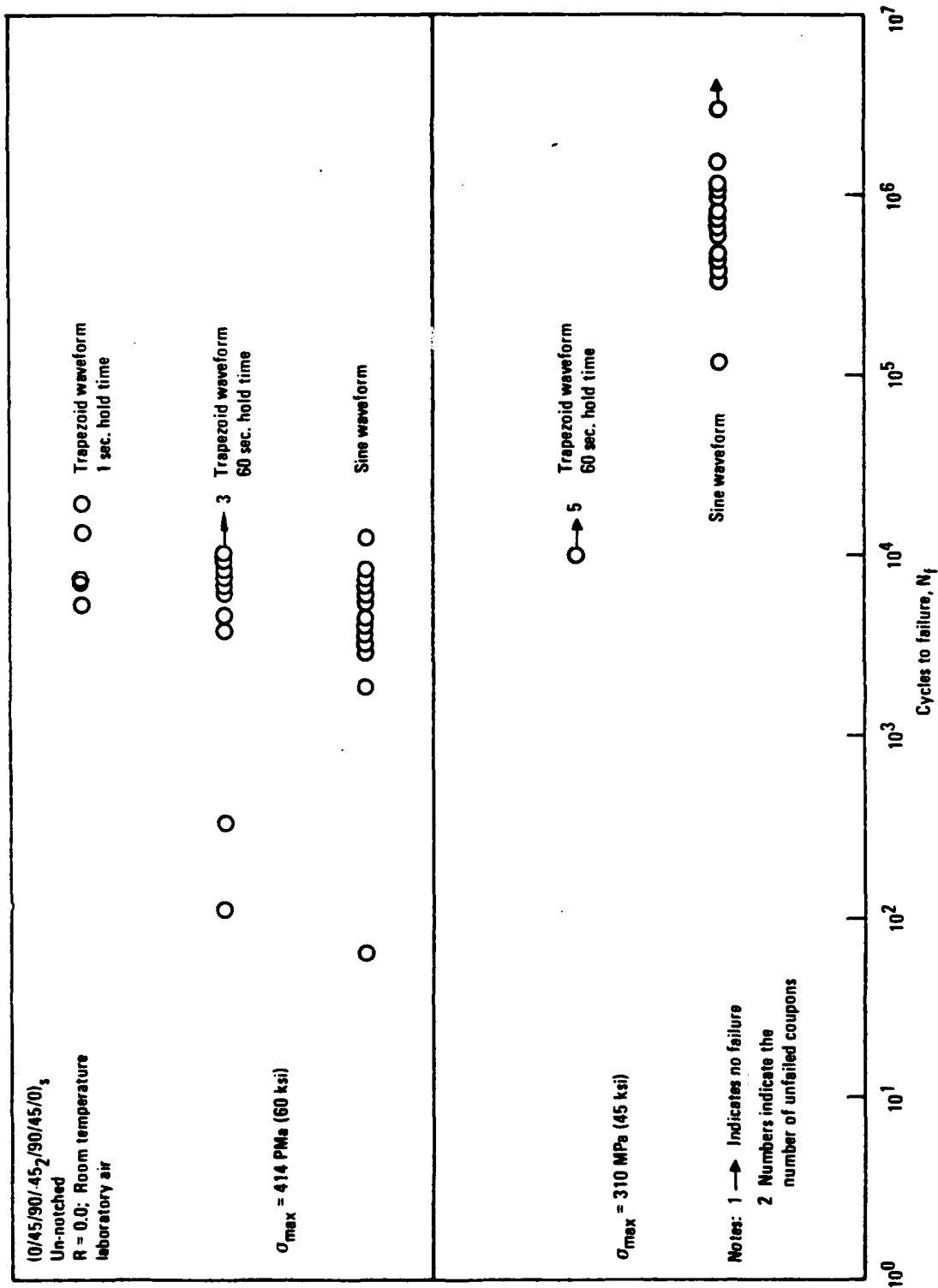


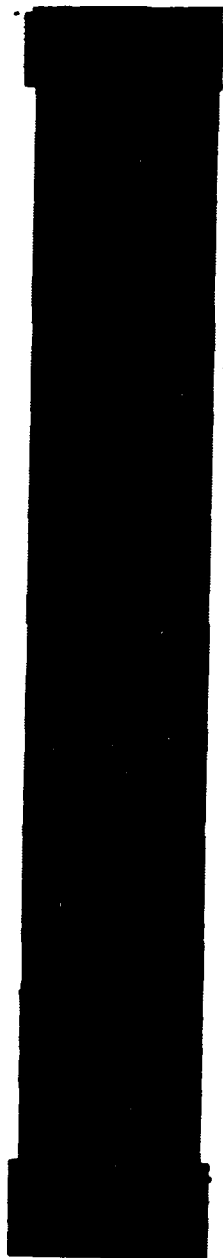
Figure 25. Results of Time at Load Experiments

at this load level otherwise some fatigue failures would have occurred. Unfailed coupons subjected to trapezoidal waveform loading were examined by enhanced x-ray, Figure 26. For those coupons tested at 414 MPa (60 ksi) delamination was found to extend into the interior and to be similar to that observed for coupons subjected to sinusoidal waveform loading. Coupons tested at 310 MPa (45 ksi) were observed to be undelaminated as were coupons under sinusoidal loading after only 10 000 load cycles.

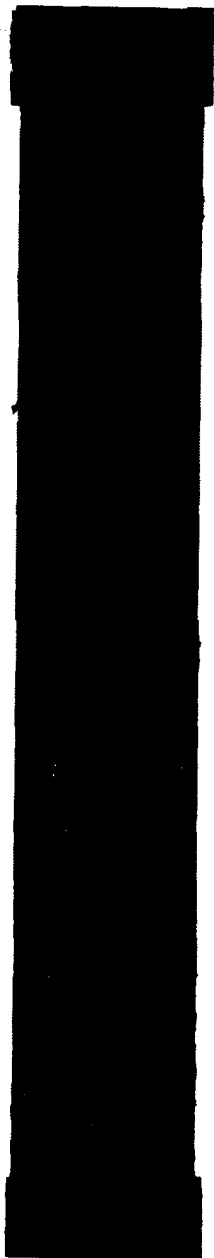
The fatigue life distribution data and the NDI data were combined to infer the conclusion that energy storage (time at load) does not significantly effect state change under ambient conditions. A further conclusion was made by considering both the progressive cycling and time at load experiments. The difference between the nature of material state change under monotonic and fatigue load was due to the repeated input of energy without any significant effect of energy storage (time at load). These NDI data supported the conclusion that time at load does not significantly change the state reached at a particular time nor the rate or nature of state change and thus the associated fatigue life is not altered.

2.2.2 Structural Dependence of the State Change Process

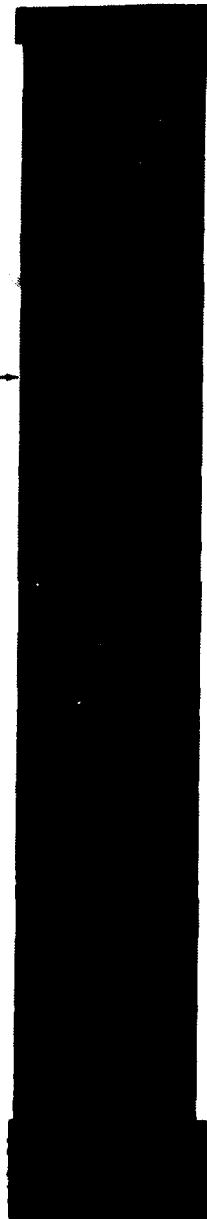
The previously discussed experiments showed that the state reached and state change process are dependent on the magnitude, rate, and form of energy input and also on the repeated input of energy. No effect of time at load was observed in these room temperature experiments. The manner in which these effects of energy input manifest macroscopically was determined using the mechanical data generated during the experiments. The qualitative nature of the dependence of state and the state change process for laminated, graphite/epoxy composites on energy input has, up to this point, been shown to be similar to that of metals. The reason for this similarity is that none of these types of dependency reflect intrinsic manifestations of the structural nature (highly anisotropic with polymeric and fibrous



Coupons Cycled at 414 MPa (60 ksi) Showing Delamination



Stains Due To Enhancer on Surface



Coupon Cycled at 310 MPa (45 ksi) Showing No Delamination
(NOTE: -45° Matrix Cracks)

FIGURE 26: Enhanced X-Ray Photographs of Time At Load Coupons Unfailed After 10 000 Cycles.

phases) of laminated composites. Instead they reflect qualitatively the dynamic, continuously changing nature of all materials. However, examination of the constant amplitude fatigue data led to the inference that there is a fundamental difference between laminated graphite/epoxy composites and metals in the nature of state change dependence on the magnitude of prior energy input.

The difference between these composites and metals was inferred for two reasons. First, the state near fracture under monotonic load was similar to that which occurred early in the cyclic life of fatigue loaded coupons. Second, the states reached under a high constant amplitude fatigue load in the laminated composite coupons (even one very near to the monotonic ultimate strength) did not appear to be significantly different than those attained under a lower amplitude, but at a much greater number of cycles. For metals, as previously mentioned, there are high magnitudes of repeated energy which can induce states which cannot be reached at lower magnitudes (one appearance of this phenomenon is called strain hardening or softening and another is called crack growth retardation). The reason for the difference was hypothesized to be due to a sharp distinction between laminated graphite/epoxy composites and metals in the manner in which the state change process is dependent on the magnitude of previous energy input. This distinction is believed to reflect a fundamental difference in the nature of energy dissipation which is, in turn, a manifestation of the structural difference between the materials.

The material/structure state continuously changes during the complex, variational rate and magnitude of energy input which often occurs (such as during spectrum fatigue loading). The rate of state change varies because the energy input is variable. There is, in essence, a particular state change function associated with any particular constant level of repeated energy input. In metals, the magnitude of prior energy input alters not only "where you are" on the state change function of a subsequent level of

energy input (at the beginning, middle, or near the end of the "damage accumulation curve"), but also alters the very functional nature of the process itself. For laminated graphite/epoxy composites, the hypothesis was made that the magnitude of prior energy input altered "where you are" for a subsequent level of energy input (similar to metals), but due to the structure of the material the functional nature of the process itself is not altered. Thus, the time (or cycle) based functional nature of the state change process was hypothesized to be essentially independent of prior energy input magnitude in these laminated graphite/epoxy composite coupons in contrast to the dependent nature which occurs in metals. The reason for the difference, recall, is believed to be a principal manifestation of the inherent distinctions between the structural natures of the two materials.

This section of the discussion of experimental results is divided into two parts because of the hypothesis mentioned above concerning the nature of the state change process. The preload experimental results were used to evaluate the hypothesis when the state induced by the prior high magnitude energy input primarily manifested as matrix cracking. The block load experiments allowed a further evaluation for the case where the induced state was also, in the case of T-T fatigue loading, accompanied by extensive delamination. Subsequent to the discussion on the preload and block load results, the overload experimental data are presented for the purpose of examining part of the significance of the conclusions inferred in this section.

2.2.2.1 Preload Experimental Results

The significance of the fact that the state which occurred near fracture under a monotonic tension load was observed to be essentially the same as that which occurred relatively early in the cyclic life of a coupon subjected to tension-tension fatigue load was evaluated using the preload experiments. If the states are indeed not significantly different, the

fatigue life distribution of monotonically preloaded coupons would not be expected to be measurably different from that of unpreloaded coupons. To test this hypothesis, coupons were loaded (in approximately one minute) to either 90 or 95 percent of the average monotonic strength followed by constant amplitude fatigue cycling at 414 MPa or 310 Mpa (60 ksi or 45 ksi). Experimental results are summarized in Tables 12 and 13. Coupons did fail during preload because the preload levels were within the monotonic failure load distribution. Despite the loss of coupons during preload, the nature of the fatigue life distributions for coupons with or without preload were essentially the same as evidenced by the similarity of the average lives, the Weibull parameters, and the results of the various statistical tests. Enhanced x-ray photographs of representative failed coupons showed no obvious difference between coupons cycled to failure with and without preload, Figures 27 and 28.

The results of the preload experiments were interpreted as confirmation of the hypothesis that the functional nature of the state change process is essentially independent of the magnitude of previous energy input. This conclusion is supported by the fact that essentially the same state as that reached under a high monotonic load (up to 95 to 98 percent of the average ultimate strength) was rapidly reached early in cyclic life and passed beyond by a coupon subjected to subsequent constant amplitude fatigue load. The fact that preload did not significantly affect the subsequent fatigue life distribution provided additional support for the conclusion.

2.2.2.2 Block Load Experiments

The generality of the conclusion that the functional nature of the state change process is essentially independent of the prior magnitude of energy input was evaluated using the block load experiments. The preload experiments provided strong support for the hypothesis developed based on the monotonic and constant amplitude fatigue data. However, the preload

TABLE 12
SUMMARY OF TENSION PRELOAD EXPERIMENTAL RESULTS
R = 0.0, f = 10Hz

Preload Stress, MPa	ksi	Constant Amplitude Fatigue Stress Level,		No. of Coupons	No. Failed During Preload	Average Life, Cycles	Weibull Parameters		
		MPa	ksi				k	e	v
-	-	414	60	17	-	5 675	3.36	-761.3	6 026
497	72	414	60	14	2	5 352	3.66	-183.6	5 852
-	-	310	45	16	-	643 702	2.97	-101792	678 906
497	72	310	45	20	3	607 560	2.39	-81386	712 492
625	76	310	45	14	4	482 568	2.95	-27044	520 354

TABLE 13
SUMMARY OF THE RESULTS OF STATISTICAL COMPARISON
OF PRELOAD AND UNPRELOADED POPULATIONS
R = 0.0, f = 10Hz

Constant Amplitude Fatigue Stress Level of Compared Populations,		Preload Stress		Statistical Test Results, Are These Properties Different?		
MPa	ksi	MPa	ksi	Mean	Std. Dev.	Dist. Func.
414	60	497	72	No	No	No
310	45	497	72	No	No	No
310	45	625	76	No	No	No

a - Mann-Whitney and Wald-Wolfowitz non-parametric statistical test results ¹⁶



Not Preloaded, IVX1396-B3



Preloaded, IVX1395-A15



Preloaded, IVX1395-B5

FIGURE 27: Enhanced X-Ray Photographs of Coupons Fatigue Cycled to Failure at 414 MPa (60 ksi) With and Without Preload at 497 MPa (72 ksi)

AD-A118 084

LOCKHEED-CALIFORNIA CO BURBANK RYE CANYON RESEARCH LAB

F/G 11/4

EFFECT OF LOAD HISTORY ON FATIGUE LIFE.(U)

DEC 81 J T RYDER, K N LAURAITIS

F33615-78-C-5090

UNCLASSIFIED

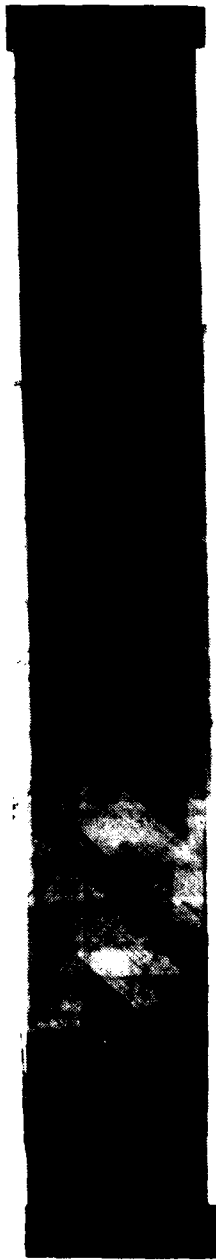
LR-29586-1

AFWL-TR-81-4155

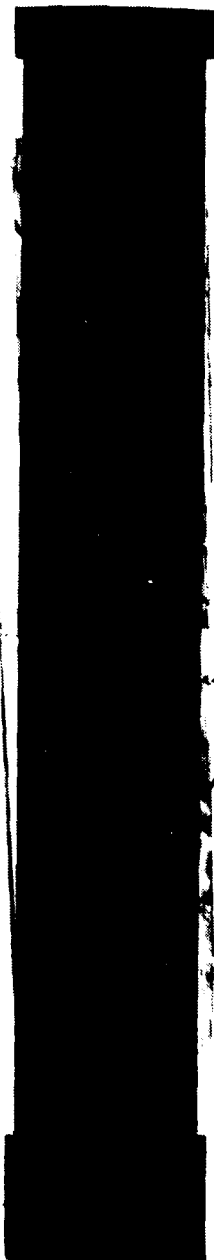
NL

2-11
AC
AD-8084

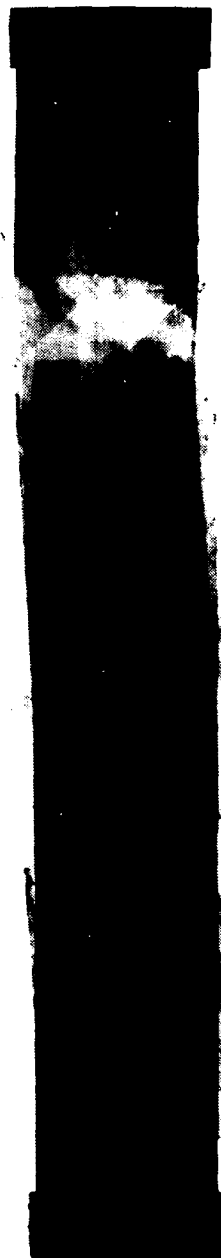




Not Preloaded 2VX1319-D16



Preloaded to 523 MPa (76 ksi), 1VX1395-A22



Preloaded to 497 MPa (72 ksi), 1VX1395-B7

FIGURE 28: Enhanced X-Ray Photographs of Coupons Fatigue Cycled to Failure at 310 MPa (45 ksi) With and Without Preload at 497 MPa (72 ksi) or 523 MPa (76 ksi).

data could only be used to infer the validity of the hypothesis for the case where the state induced by the prior high magnitude energy input did not exhibit any significant delamination extension in the coupon width direction. The block load experiments allowed a further evaluation of the hypothesis when the induced state exhibits significant delamination.

In a metal, the nature of state change is such that if a block of constant amplitude fatigue load cycles of high enough load magnitude is applied to a coupon, subsequent fatigue life at a much lower load amplitude can be greatly decreased⁵⁵. This state change property is due to the presence of a dominant crack initiated during the high load block. Also, in metals, if a high load magnitude block of cycles follows a low load amplitude block, the nature of state change is such that the fatigue life at the high load would be essentially unchanged⁵⁵. For laminated graphite/epoxy composites, the conclusion was inferred, as previously discussed, that the functional dependence of the state change process on the magnitude of prior energy input is significantly different from that of metals. If the nature of the difference is properly understood, the qualitative results of fatigue block loading can be anticipated. The validity of that anticipation was evaluated by selecting the experimental conditions in such a manner as to greatly enhance the difference.

The postulate is that the state reached near failure under a high magnitude, constant amplitude fatigue load is essentially the same as that reached under a low magnitude load after a sufficient number of cycles usually corresponding to a relatively small probability of failure. If the postulate is correct, the application of a high magnitude tension-tension (T-T) fatigue load for a number of cycles sufficient to induce delamination should not significantly affect fatigue life at a subsequent low fatigue load amplitude. This would result because the state reached under the high amplitude would have been reached under a low load amplitude, but would only represent a small percentage of the expected life at the low load amplitude.

If, however, the nature of state change was similar to that of many metals, a significant change (usually a decrease) in fatigue life at the low load amplitude would be expected. Similarly, if a high load amplitude block of cycles follows a small number of cycles of a low load amplitude block, fatigue life should be greatly reduced if the fatigue loading is tension-tension. This would result because the load cycles at the low amplitude, although a small percentage of life at the low amplitude, would represent a state which would occur after a relatively large percentage of life at the high amplitude. Therefore, under tension-tension fatigue load, block loading of the types described should manifest as effects exactly opposite to that of many metals; a high block should have no significant effect on, rather than decrease, the life at the subsequent low block, and a low block should decrease life at, rather than have no effect on, the subsequent high block.

Under compression-compression (C-C) fatigue loading, similar effects were anticipated for the same reason as the T-T loading. However, the life reduction effect of the low amplitude block on the subsequent high amplitude (greater compression load) block was expected to be less than under T-T loading. This follows from the fact that matrix cracks do not develop under compression load and that buckling failure must result soon after delamination develops. Therefore, since delamination is not likely to have developed after a small percentage of the life at low amplitude, the state developed can only be associated with a small percentage of the fatigue life at the high load amplitude.

In order to establish the validity of the above ideas, groups of coupons were subjected to the types of block loading shown in Figure 29. The number of cycles applied at the first load levels were equivalent to fatigue life percent probability of survival levels of greater than 90 percent at those stress levels as determined by the baseline fatigue tests of Section 2.1. The cycles equivalent to these small percentages of fatigue life were applied for the reasons just discussed.

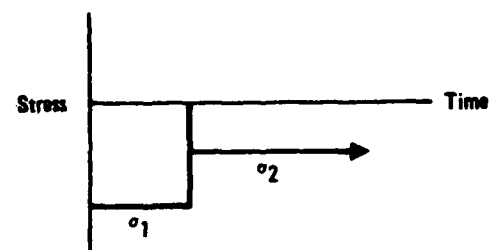
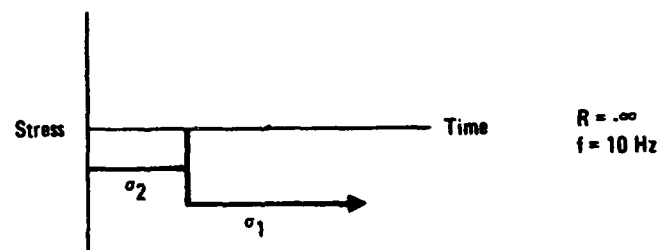
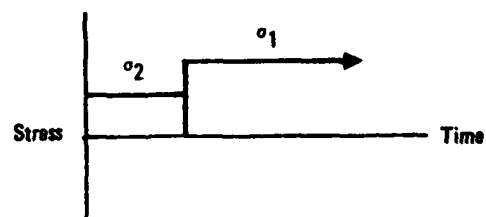
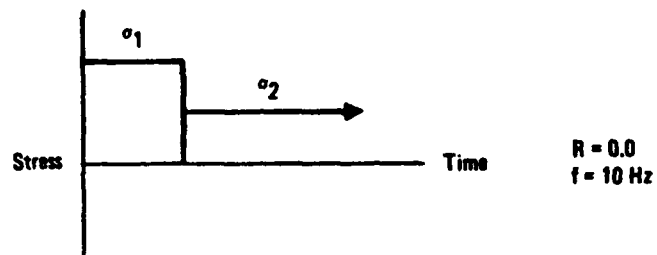


Figure 29. Loading Waveforms Used in Block Load Experiments

At least fifteen coupons were tested in each block fatigue loading group. The load levels were selected so that the baseline fatigue life at the high level was between 1 000 and 10 000 cycles and that at the low level was above 10^5 , but below 10^6 cycles. The large differences in cyclic lives do not represent large differences in stress levels, but this is not considered of great importance in these experiments because: 1) the average cyclic lives differed by two orders of magnitude, and 2) the effect of a much larger difference in energy input magnitude was evaluated during the preload and the overload experimentation. For T-T fatigue loading, the number of cycles applied, if the high load block were applied first, was either 1 360 or 1 800 while for the low load block the total cycle count was 108 000 or 200 000. These corresponded to approximately 98 and 95 percent probability of survival levels, respectively. For the C-C fatigue study, 5 000 or 15 000 cycles were applied for the high load block and 200 000 for the low load block. These corresponded to approximately the 96, 91 and 98 percent probability of survival levels for their respective load levels.

Results of the block load experiments are summarized in Tables 14 and 15. The data show that under high to low block fatigue loading (for both T-T and C-C), life distributions at the low load level did not significantly change. This result indicated that the state reached under a high load level is not significantly different than that which is attained under a low magnitude of fatigue load. If the states were greatly different, a significantly increased or decreased average life would be expected at the low load level compared to the baseline data set. Instead, the state at approximately the 95 percent probability of survival level (1 800 cycles) at 414 MPa (60 ksi) appears to correspond to a state reached at 310 MPa (45 ksi) equivalent to approximately the 98 or 99 percent probability of survival level (50 000 to 150 000 cycles).

The low to high block results under T-T fatigue loading displayed the anticipated effect. Both the average fatigue life and the distribution of

TABLE 14
SUMMARY OF BLOCK LOADING DATA
TENSION: LOW AMP. = 310 MPa (45 ksi), HIGH AMP. = 414 MPa (60 ksi)
COMPRESSION: LOW AMP. = -241 MPa (-35 ksi), HIGH AMP. = -310 MPa (-45 ksi)

Test Type	Block Type	Percent Probability of Survival at First Level,	Number of Cycles At First Level	Expected Life At Second Level If No Effect, Cycles	Average Cyclic Life At Second Level
T-T	H-L	98	1 360	644 000 ^a	513 000 ^b
		95	1 800		671 000 ^c
T-T	L-H	98	108 000	5 675	4 502
		95	200 000		2 739
C-C	H-L	96	5 000	800 000 ^d	659 000 ^e
		91	15 000		735 000 ^f
C-c	L-H	98	200 000	27 407	45 287

a = 3 out of 17 coupons did not fail after 10^6 cycles.

b = 1 out of 14 coupons did not fail after 10^6 cycles.

c = 4 out of 15 coupons did not fail after 10^6 cycles.

d = 13 out of 20 coupons did not fail after 10^6 cycles.

e = 6 out of 14 coupons did not fail after 10^6 cycles.

f = 9 out of 14 coupons did not fail after 10^6 cycles.

TABLE 15
SUMMARY OF CONCLUSIONS CONCERNING BLOCK LOADING

Test Type	Block Type	Percent Probability of Survival First Level	Non-Parametric ^a Statistical Tests, A-Accept, R-Reject	Conclusion As To Effect of First Level on Second
T-T	H-L	98 95	A A	None
T-T	L-H	98 95	A R	Reduction as Cycles at First Level Increase
C-C	H-L	96 91	A A	None
C-C	L-H	98	A	None

^a = Hypothesis is that the fatigue life distribution at second level is the same as the baseline distribution, see Appendix D data and Reference for Procedure.

cyclic levels at the high load level were significantly altered because of the prior application of cycles (equivalent to a 95 percent probability of survival) at the low amplitude level. The reduction in average fatigue life was inferred to be due to the fact that the state at the end of the low level block constituted a significant percentage of life at the high level block, see Figure 30. The limited results of the low to high block loading under C-C fatigue showed no significant effect of the low level block on subsequent life distribution. This was expected as previously discussed, because of the nature of state change under compression load. However, the results are not definitive due to the lack of experimental results at the 95 percent probability of survival level for C-C fatigue loading caused by the early program termination due to governmental funding restrictions.

The results of the block load experiments were in agreement with those anticipated based upon the present understanding of the difference between laminated composites and metals. The block loading experiments can be summarized as providing support for the concept that the nature of state change and associated energy storage and dissipation properties of laminated graphite/epoxy composites are significantly different than those of metals. The change of state process in the composite material evaluated is essentially independent of the magnitude of the prior energy input. That prior input appears to only determine where you are in the process and not the functional nature of the process itself.

2.2.3. Overload Experiments

The overload experiments were used to explore the significance of the understanding developed from the previous experiments as to the nature of the state change process in laminated graphite/epoxy composites. The specific interest was to provide a basis for understanding the effects of more complex types of energy input on state change. The previous experiments established the difference between the nature of the state

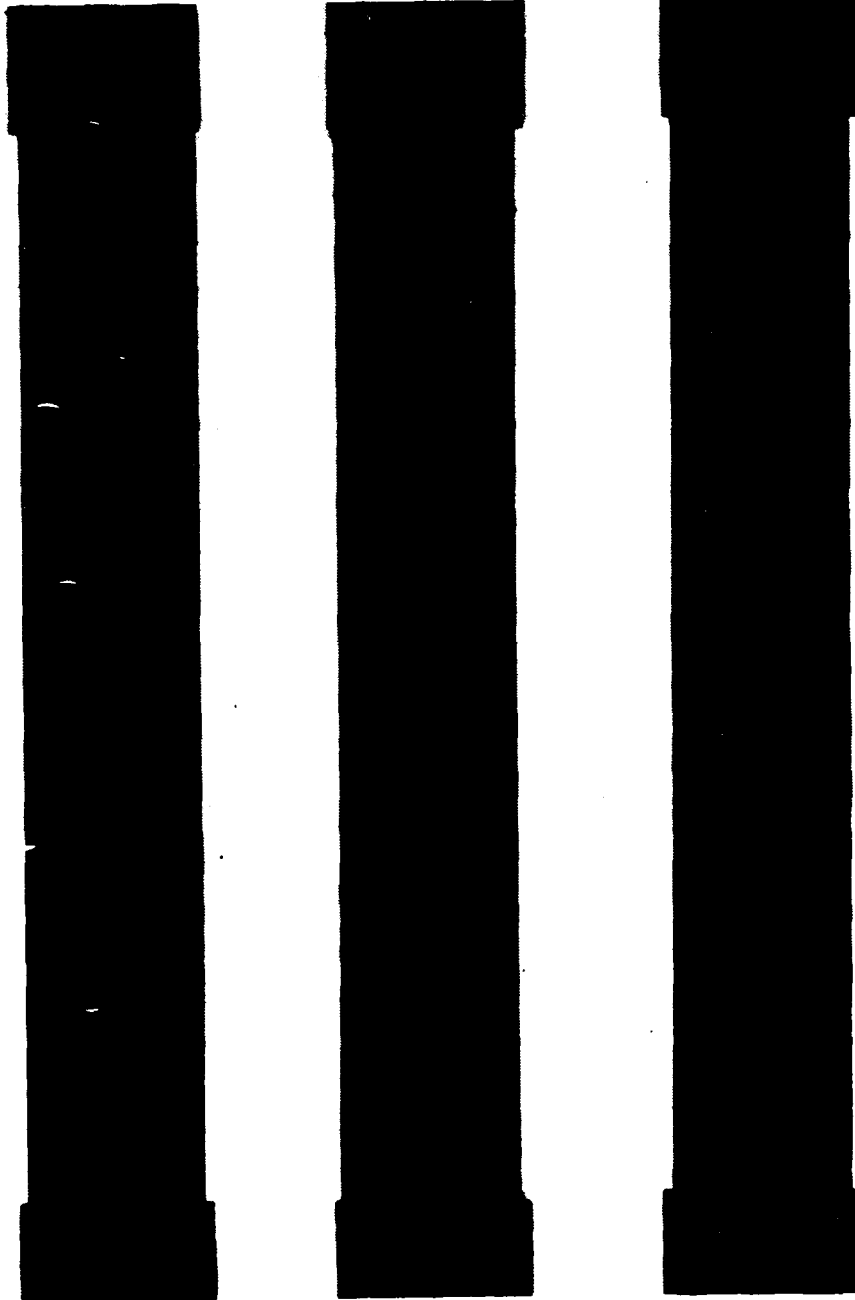
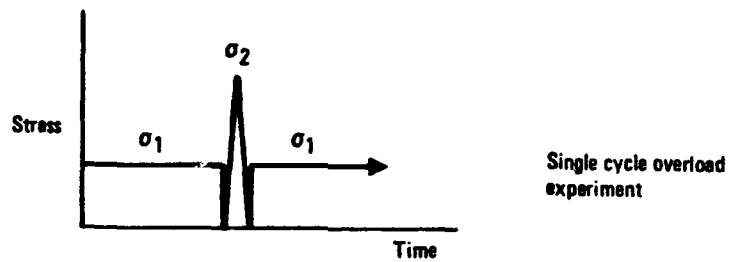


FIGURE 30: Enhanced X-Ray Photographs of Coupons Cycled at 310 MPa (45 ksi) to Approximately the 95% Probability of Survival Level (200 000 Cycles) Prior to Cycling at 414 MPa (60 ksi).

change process in the selected laminated composite and that which occurs in metals. Two questions were addressed using the overload experiments. The first concerned further evaluation of the significance of the apparent independence of the state change process with respect to the prior magnitude of energy input. If the state change process was understood correctly, the results of overload type fatigue loading experiments could be, at least qualitatively, anticipated. The second question was concerned with determining whether a state change induced by a high energy input could be further changed by the repeated input of an amount of energy which would not normally lead to states of significantly different properties. This question was partially answered by the preload experiments which showed that if that state manifested primarily as matrix cracking, no significant change in the subsequent state change process or fatigue life distribution would occur. However, if the repeated input of a high amount of energy caused states manifesting as delamination, in addition to matrix cracking, the question remained as to whether the state could now be further changed by the repeated input of a much lower amount of energy which would not otherwise even induce matrix cracking.

Two types of T-T fatigue overload experiments were conducted as diagrammed in Figure 31. No C-C fatigue loading experiments were conducted because of the early program termination due to the funding limitations previously discussed. One type of experiment consisted of applying a single overload cycle within a constant amplitude fatigue spectrum while the second was periodic application of an overload. The overload cycles were applied at essentially the same loading rate as the baseline cycles were applied.

For the single cycle overload experiments, two overload levels were used (414 MPa and 483 MPa (60 ksi and 70 ksi), and a single baseline fatigue stress level of 310 MPa (45 ksi). The baseline stress level was chosen, based on the previously developed understanding of the state change process, such that the overload would be expected to reduce fatigue life if a signi-



$R = 0.0$
 $f = 10 \text{ Hz}$

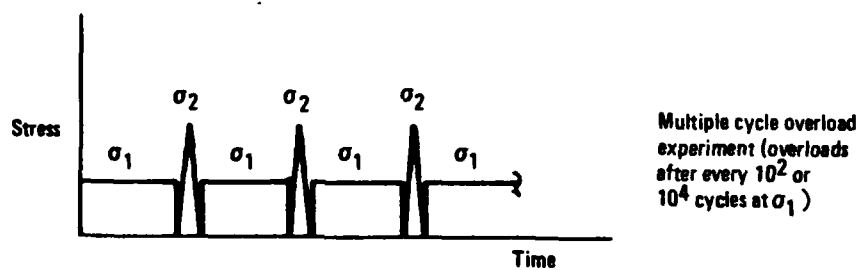


Figure 31. Loading Waveforms Used in Overload Experiments

ficant effect occurred. This would result because the state would be changed during the overload in a detrimental manner relative to the expected coupon fatigue life. However, no significant effect of a single cycle overload was expected if it occurred early in the baseline fatigue life since the amount of state change would be small. Therefore, if some coupons failed during the overload, the average life of the unfailed coupons would be slightly increased because those coupons whose states had changed the most would be eliminated. To test the validity of this expectation, single cycle overloads were applied after completion of a block of cycles equivalent to approximately a 98 percent probability of survival for the baseline level (108 000 cycles).

The results of the single cycle overload experiments are given in Table 16. The 414 MPa (60 ksi) overload was found to have no significant effect upon the fatigue life distribution of the coupons when compared to the 310 MPa (45 ksi) baseline life distribution. This result is clear since the average life was found to be essentially the same; the number of coupons which survived 10^6 cycles was similar; and a difference in the population distributions could not be discerned using the non-parametric statistical tests. In contrast the high overload level of 483 MPa (70 ksi) clearly resulted in a change in life distribution. This was interpreted to be due to the fracture during the overload of those coupons whose state had changed the most, as anticipated.

For the multiple overload experiments, data were obtained using three different overload ratios. The first ratio of 1.33 was achieved, in this program, by using a 310 MPa (45 ksi) baseline fatigue level and a 414 MPa (60 ksi) overload level applied either once every 100 or once every 1 000 cycles of the baseline level. This type of overload experiment was distinguished by the fact that both the baseline and the overload fatigue level, if applied separately to different coupons, would induce state change manifesting as delamination. Coupons were anticipated to fail during an

TABLE 16
SUMMARY OF SINGLE CYCLE OVERLOAD EXPERIMENTAL RESULTS
BASELINE FATIGUE STRESS LEVEL: 310 MPa (45 ksi)
SINGLE CYCLE OVERLOAD APPLIED AT: 108 000 CYCLES (98 percent probability of survival)
R = 0.0, f = 10Hz

Overload Level, MPa	No. of Coupons Tested	No. of Failed In Overload	Baseline Average Life, Cycles	Overload Experiment, Average Life, Cycles	Non-Parametric ^d Statistical Test Results
414	60	15	>640 000 ^a	>722 000 ^b	A
483	70	13	>640 000 ^a	>888 000 ^c	R

a = 3 of 17 Coupons Did Not Fail After 10⁶ Cycles

b = 3 of 14 Coupons Did Not Fail After 10⁶ Cycles

c = 5 of 8 Coupons Did Not Fail After 10⁶ Cycles

d = Hypothesis: Baseline and Overload Population are the Same Fatigue Life Distributions;
A - Accept Hypothesis, R-Reject Hypothesis.

overload cycle. Further the number of overload cycles prior to failure was expected to be less for the 1 per 1 000 cycles experiment than for the 1 per 100 cycles. This was anticipated because the state change occurring during the repeated energy input baseline cycling would dominate the state change process. In contrast, for the 1 overload cycle per 100 baseline cycles, the overload cycle would dominate the state change process. This must result in a larger number of overload cycles before failure, compared to the 1 per 1 000 experiment, but result in a shorter fatigue life when comparing the total number of cycles.

In the second type of multiple overload experiments, the overload ratio was either 2.0 or 3.0. In these experiments, the baseline fatigue stress level was known to be unable to induce failure, delamination, or significant matrix cracking after even 10^7 cycles⁹. The data were obtained from a Lockheed supported internal research program²². The overload stress level was again 414 MPa (60 ksi), but the baseline level was either 207 MPa (30 ksi) or 138 MPa (20 ksi). One overload cycle was applied for every 100 baseline cycles. The loading rates were the same in the overload and baseline cycles to eliminate any possible effect of strain rate. The 2.0 and 3.0 overload ratios were used to determine if the state induced by the high energy input level would be further changed by the lower energy input per cycle baseline level.

The results of the multiple cycle overload experiments are summarized in Table 17. All of the data obtained at an overload ratio of 1.33 were in accordance with those anticipated. This result indicates that the nature of the state change process is reasonably well understood. First, the number of cycles to failure at the overload stress level was significantly reduced relative to a constant amplitude fatigue life. Second, a slightly longer total life was obtained for the 1 overload cycle per 1 000 baseline cycles. Third, the number of overload cycles for the 1 per 1 000 was less than that

TABLE 17
SUMMARY OF MULTIPLE CYCLE OVERLOAD EXPERIMENTS
R = 0.0, f = 10Hz, Room Temperature, Laboratory Air
Overload Stress: 414 MPa (60 ksi)
Average Fatigue Life at Overload Stress: 5675 Cycles

Baseline Stress Level, MPa ksi		No. of Baseline Cycles Per Overload Cycle	Avg. No. of Blocks or Overload Cycles to Failure	Avg. No. of Total Cycles To Failure
310	45	1 000	175	174 559
310	45	100	1 500	149 985
207	30	100	1 174	117 400
138	20	100	1 557	155 700

for the 1 per 100 cycles, Fourth, all of the coupons subjected to 1 overload cycle per 1 000 failed during the overload.

The results obtained for the overload ratios of 2.0 and 3.0 are interesting. The average life at the overload stress level was reduced by a factor of approximately five when the baseline level was 207 MPa (30 ksi) and by approximately 3.5 for the 138 MPa (20 ksi) baseline level. In fact, the average fatigue life for the 414/138 MPa (60/20 ksi) spectrum was the same as that which occurred under the 414/310 MPa (60/45 ksi) spectrum. The considerable reduction in fatigue life at 414 MPa (60 ksi) was inferred to be due to the fact that the fatigue cycles applied at the baseline level induced the state to significantly change. This result is important in that it strongly suggests that levels of repeated energy input exist which cannot by themselves induce significant changes in some states (for example, the initial unloaded state), but can induce significant changes in certain other kinds of states. In the case at hand, the 207 MPa (30 ksi) loading level cannot induce significant delamination in the laminate used in this program even after 10^7 cycles. However, if the state characterized by delamination already exists, that state can apparently be induced to change further by a low fatigue stress level. Whether or not the induced state change is simply one characterized by additional delamination growth has not been determined partially due to funding limitations on this contract. Perhaps the induced state changes manifest in a more complex manner than simply as delamination growth. In either case, the possible implications for spectrum truncation and complex loading can be of major concern.

The coupons used for the 2.0 and 3.0 overload ratio experiments were from different panels than those from which coupons were obtained for the previous T-T, 414 MPa (60 ksi) constant amplitude fatigue experiments. Therefore, baseline 414 MPa (60 ksi) amplitude data were also obtained using coupons from the same panels as used for the 2.0 and 3.0 overload experiments. The results of the new 414 MPa (60 ksi) baseline data had an

average life of 5 222 cycles as compared to that of 5 675 for the previous baseline data set. Based on non-parametric statistical tests, the life distributions were found to be identical. Therefore the effect of the fatigue cycles applied at either 207 or 138 MPa (30 or 20 ksi) on the life at 414 MPa (60 ksi) is not an illusionary artifact.

SECTION 3

DISCUSSION

The extended purpose of this program is the same as many other such programs, namely to aid in the ensurance of structural integrity of those components fashioned from graphite/epoxy composites. Program objectives were viewed as specific actional forms designed to meet that purpose. Such forms consisted of determining those externally influencing parameters which primarily cause material/structure changes, characterizing the nature of the changes, and defining associated mechanical response. The results of any such experiments would have no significance unless their meaning in terms of the purpose could be established. Therefore, in order to relate the program purpose to the selected program experimental forms, a plan was evolved which consisted of employing the concept that the interaction of the material/structure with the surrounding environment (mechanical, chemical, and thermal) could be considered as a dynamic process of energy exchange. This plan was developed out of the experience of several externally and internally funded research programs and was applied in this investigation. The plan is thought of as an attitude which, if maintained, results in a specific way of organizing experiments and interpreting their results which is closely in line to the program purpose. The attitude is not a quantification procedure or a mathematical one, but instead allows determination of that which should be quantified or mathematically modeled for a particular case.

Specifically, the concept consists of the idea that a material/structure can be thought of as an energy state existing in an open system, external energy field. This external field is commonly called the environment and is in this report thought of as including the loads, chemical species, tempera-

ture, electrical potential and like phenomena. Measurements of the material/structure such as chemical/atomic species, density, temperature, geometry, and discontinuities (cracks) are thought of as various ways of describing the corporal manifestation of the energy field. Because of the input of the external field energy and due to initial imbalances in the material/structure energy state itself, that state tends to change as shown by such micro phenomena as the stretching and breaking (often with reformation) of atomic and chemical bonds or such macro phenomena as variations in temperature or geometric shape.

If inputted energy cannot be dissipated fast enough or if the amount of energy concentrating locally or globally is large enough, permanent state change must occur. The fact that a significant change in state has occurred is registered by quantifying the extent of cracking or changes in mechanical response such as global stiffness. In this energy state concept, such phenomena as cracks or stiffness change are considered simply manifestations that non-recoverable state changes have or are occurring. The engineering phenomena called failure and/or fracture are thus considered as terms for describing a condition in which cumulative state changes have occurred during the energy exchange and one in which mechanical response is no longer within the desired range. Since the nature of energy exchange (usually recorded as changes in mechanical response) of a particular energy state (material/structure) is required by engineering design to remain within a preset range, an understanding of energy exchange and the nature of associated state change under different types of external energy inputs (loading histories) is required. The understanding is believed to provide a framework in which our choice of material/ structure and selection of external environment can be balanced such that mechanical response varies within an acceptable range and structural integrity is maintained.

In the following subsection, some of the implications of the energy state concept for experimental research are reviewed. The subsequent subsection

summarizes how the energy state concept was used to interpret the experimental results of this program. This discussion thus gives an initial example (this research program) of the use of the concept. In subsection 3.3, some implications of the concept for relating laboratory data to structural response are discussed.

3.1 CONCEPTUAL IMPLICATIONS

In this subsection, some of the implications of using the experimental approach of this research investigation are addressed. These implications fall principally into three categories: 1) the role of the cause and effect relation in the experimental process; 2) experimental design and interpretation; and 3) the use of modeling procedures to represent relationships among experimental parameters.

The understanding of the relationship between cause and effect is of importance for interpretation of experimental results. Our investigational habit is to observe that a component of interest has failed (by whatever definition we choose) and subsequently to search for the cause of failure. We begin this search by describing the material/structure changes which have occurred, labeling ("pigeon holeing") the description (as, for example, creep, fatigue, etc.) and usually, though unconsciously, end the search by calling the description the cause of failure. For example, we say the cause of failure (but one event in a series of events) is creep, the label for the entire state change process. Finally we investigate the mechanism (means by which) of the creep or fatigue (or other such descriptions) which cause the failure. This investigative habit has been used in metallic research efforts for many years and has led to a disturbing position in the research of metals as evidenced by the following quotation of Dr. Coffin:

"A tremendous effort has been devoted to the study of crack propagation, both in a highly formalized sense by analysis and by experimental information. In addition, we have carried out

studies to extend our knowledge of the environment and at high temperature.

Many new tools and techniques have been introduced, including the scanning electron microscope, Auger spectroscopy methods, and closed-loop testing.

One wonders, though, whether our basic understanding over this period has really made tremendous strides. My feeling is that it really has not,"

When the focus of attention is upon the failure event and its prevention, the mind rationally leads to determining the cause. But, this has led to great confusion and disappointment concerning our understanding of metals and the current seems to be flowing the same way in composite research. Fundamentally, focus upon the failure events leads to the common conclusion, often unrecognized, that the description or name of a dynamic process "causes" failure. For example, the cause of failure is creep, followed by the question, what is the mechanism of creep. The research investigation invariably results in a micro or macroscale description of the process which although well documented is still accompanied by various levels of frustration at not having found the mechanism. The search then continues for this thing (mechanism) which "causes" the events which makeup the process.

The reason for this frustration is suggested to be due to the fact that we are in the habit of focusing upon the failure event and the initial state of the material. This leads to essentially a static viewpoint of the effect of energy input on material changes. Although the effect of fatigue loading on material state is known to be a highly dynamic process of change, this fact is unfortunately not emphasized. Professor J. Morrow commented at the end of a recent major international symposium on fatigue mechanisms in metals that "All I've seen this week [at the conference] are snapshots of horses [in the horse race]. Nobody has mentioned or showed evidence of the dynamic process responsible for fatigue damage which I feel is very important."⁷ The problem of a static view becomes clear when searching for mechanisms. For example, in the creep phenomenon of metals, the combination of thermal

and mechanical energy input is known to be inadequate to explain the creep deformation of the initial material state. Therefore, an internal mechanism has been searched for and several suggested.²⁴ If, however, creep is seen as a label for a dynamic change process, the input of thermal and mechanical forms of energy are adequate, knowing the initial state, to explain the series of events which occur. The "thing" called a mechanism is but one in a series of events, an inherent manifestation of the dynamic energy field. The "mechanism" can not cause failure. Instead, failure is the final event in the interactive energy exchange process between the material energy field and the external environmental energy field.

When investigative focus is upon the dynamically changing energy state, the cause of failure is viewed as being due to the excessive input of external energy or storage of that energy for too long. The need for a "thing" is removed and the process itself, the events and their sequence, then becomes important. Creep becomes a label for the interaction of events which manifests as physical changes reflecting the changing energy state. Effort can then be directed without guilt towards the documentation and quantification of the events in the interest of understanding the details of the energy exchange process. The need to study the micro and macro structure of the material is not eliminated, but emphasized, since the process is now the focus of attention.

There is a tendency, which might be called a corollary, associated with the unconscious ignoring of the dynamic state change process. This is the tendency to look not only for the "things" that caused the undesired condition (failure or even change itself), but to search for a single thing. In the introduction to the conference on fatigue mechanisms in metals is the quotation: "By fatigue mechanism, we mean the* underlying principle which explains the microstructural changes at a laboratory time scale . . ."²⁵ When the focus of attention is on the dynamic process of change itself, a single "mechanism" or single principle becomes inadequate. To understand

* Underline added by the authors.

the process requires an integration of all the events occurring and not just the focus on some one separated piece. This problem of integration is beginning to be recognized for metals: "What then is the reason for our lack of precision in predicting fatigue life when we appear to have all the facts at hand? . . . nor are we yet able to separate and integrate the individual aspects of the process."⁶ The individual aspects of the process of change constitute various static slices of the whole and cannot give, by themselves, a sense of the whole process. These aspects are indeed like the "snapshots" that Professor Morrow mentioned. The integration of the various quantified, experimentally obtained "snapshots" (at separated times and spaces) is required to allow the development of the necessary intuitive appreciation of the dynamic state change process.

The dynamic energy exchange process results in energy states whose associated mechanical response is eventually deemed undesirable. The cause of reaching the undesirable state (failure) is due to the input of energy (mechanically, chemically, or thermally). Use of a static mechanistic point of view has led to much difficulty in understanding the process of change which leads to that undesirable state. This has occurred in fields of endeavor as apparently diverse as research on materials and the function of the brain. Roger Walsh in his recent book on brain research said: "Strictly speaking, the mechanism is the total change -- everything is involved and constitutes the mechanism, and no one subsystem or its alteration can be isolated, set apart and looked to as it."⁸

Instead, therefore, of a search for mechanisms, emphasis must be subtly transferred to achieving awareness of state change at whatever macro or micro level is dictated by the purpose at hand. This subtle transference of attention allows focus upon the entire energy exchange dynamic process and not just the restricted one of describing the state changes and calling them the cause. The experimental field of view is thereby expanded to include the material/structure and surrounding use environment as a whole system.

Without this view, cause and effect are confused, and a deeper and more desperate search for mechanisms ensues without the realization that they are simply more detailed descriptions of energy state manifestation.

In the application of the energy state concept, therefore, emphasis is removed from "mechanisms" and kept on the energy state change process. This shift in emphasis changes the nature of experimental design and interpretation of results. Recall that the pragmatic purpose of experimental efforts is to ensure structural integrity. This purpose can be achieved when there is an intuitive feel or sense of the manner in which a material changes under the input of energy. The achievement of this feel is related to the often mentioned research goal of desiring to understand "what is going on". For this reason, both the "applied" and "basic or fundamental" research goals do not significantly differ. To meet the purpose, experimental actions are undertaken, the results of which are either used directly and applied to the structural situation or indirectly by inferring ideas for general understanding. The problem is that the experiment must be designed and results related to the purpose.

Experimental design and interpretation is either based consciously upon a previously held hypothesis or unconsciously upon a bias derived from our research experience. If a hypothesis is held consciously, the risk exists of interpreting the results as confirming or denying the hypothesis, when in fact they may be unrelated to the hypothesis. If no hypothesis is made, a search is made for meaning which is likely to be wide of the mark due to the unconscious bias which drives our interpretation. In either case, the likelihood is that the experimental interpretation will be only inefficiently related to the original purpose. It is to avoid this problem or, at least, to reduce the likelihood that a plan is needed. A plan is not how to do the experiments nor a way to model, but a means by which to gain an insight into what experiments to perform and what to model or represent for the case of interest.

The material/structure and surrounding environment form an energy exchange field undergoing a continuous dynamic process of change. An experiment "freezes" a slice of that process and hence is essentially static. Therefore, to reduce the entrance of personal bias and to relate form (experiments) to purpose, the plan must itself be dynamic and thereby is, itself, the implementation of the concept of a dynamic energy exchange process. The continued development of that dynamic intuitive feel for materials and structures, which is fed by experimentation, analysis, and the study of various micro and macro "snapshots" (states) of the state change process, is in a very real sense the plan itself.

In the light of the energy state concept experimental emphasis is removed from attempting to quantify such things as monotonic strength or fatigue life distributions. Nor is there an emphasis on attempting to find "the" most important event in the process. This is not to say that quantification or observation of mechanical response or such phenomenon as cracking or material structural detail is unimportant. The concept is far from a black box approach and an ignoring of micro and macro phenomena. However, experimental design is aimed towards understanding the process of change itself. This is also not to say that research investigators do not already aim for this understanding. However, the thought is strongly brought forward that that understanding is greatly hindered because of our unconscious tendency to emphasize only particular events of the process thereby resulting in a static viewpoint.

The application of the energy state concept is the idea that at the start of an experiment (or structural life), the material/structure and environment exist in an initial state. Observation of this is the first slice of the dynamic process. As the experiment is conducted, that initial state changes (as does the associated mechanical response). Observations of state change manifestations (cracks, deformations, mechanical response) are later slices of the process. The sum total of all slices is integrated to gain an

awareness of the entire process. Experimental design is thus focused by obtaining those slices or snapshots of the state change process which best lend themselves to development of the intuitive holistic feel. The extent to which we have developed that feel determines where our attention is focused in a particular situation. Formulation of hypothesis, the choice of what variable relationships require mathematical representation, and the development of mathematical descriptions are guided by our empirically based intuitive appreciation rather than by a direct use of deductive logic and mathematical representation.

The problem of analyzing what is observed for the purposes of mathematical representation is one of many subtleties. When investigational emphasis is upon failure, and upon research for several levels of "mechanism", an attempt is usually made to model what is observed or to suggest changes in the material. This procedure has, as is well known, led to much success, but it also has often led to changes which improve one material property, but detrimentally affect others. For example, investigations conducted to improve impact properties emphasize improvements in matrix properties, specifically strength. While such improvements may help, they often do not because they ignore the role of fiber elongation and matrix stiffness in energy absorption. The focus is on a part of the system which not only reduces the chance of improving the property of interest (always a system or entire state property), but also increases the probability of detrimentally changing other properties such as moisture and temperature sensitivity and resistance to fatigue load. Often, mathematical representations of material property changes due to external energy input are developed which approximate some narrow range of laboratory data, but have little significance towards meeting the purpose of ensuring structural integrity. Often, other models lead to great misunderstandings because they ignore certain "boundary conditions" or key events in the process.

Use of the energy state concept places consideration upon the entire material/environment system allowing a development of an intuitive grasp of the entire process. Emphasis is placed on state, change in state, and amount and rate of change. This intuitive grasp and emphasis on energy state is believed to better help in determining what might be altered to obtain a desired material/structural behavior.

3.2 EXPERIMENTAL DESIGN AND INTERPRETATION

With regards to the experimental objectives of this program, use of the energy state concept led to the idea of considering the various experiments as probes to discern the nature of the dynamic state change process. This required observation of the initial energy state, changes in state, rate of change and state at fracture. The energy state concept was used in this program to guide quantification of the experimental loading variables and to interpret results. A summary of that interpretation is given in this subsection.

The NDI data were used as a means for assessing whether permanent state changes had occurred and the mechanical response data as a means of assessing their significance. The combination of the two sets of experimental data allowed interpretation of what kinds of energy inputs result in significant state changes. Thus, fundamental to the use of the energy state concept is the assumption that energy states and changes in state can be indirectly, but usually adequately, represented by quantifying such phenomena as crack manifestation and mechanical response. By the term adequate is meant that measurement of such phenomena is sufficient to know; 1) that permanent change in state has occurred; 2) the significance of the change; and 3) what options must be exercised in a particular structure where response is expected or been proven to be undesirable.

To say that a material/structure is an energy state is to bring to mind the concept of an energy field with a variable intensity. The variations in density are reflected in the local differences in stress state or in strength and stiffness of what, for example, are called matrix and fiber in a composite. External applied energy, for example by mechanical load application, is stored non-uniformly both because of the mode of application and the variation in the material/structure energy state. The initial energy state is changed (though not necessarily in a manner of engineering significance) by the input of energy because the additional energy is partially stored which is reflected as variations in deformation and stress. Since some of the inputted energy is dissipated (for example, in what we call heat and sound), the stored energy is not exactly equal to the input. From an engineering point of view, the questions concerning the initial energy state are of two types. First, is the manifested mechanical response, associated with a particular energy state, of the type desired. Second, under what circumstances of energy input will the material/structure energy state permanently change by an amount such that the altered mechanical response is significant for the application of concern. The latter question was addressed by using the experiments of this program.

If the amount of energy added to any one region of the energy state is greater than the amount which can be stored, a crack appears. A crack is a term for a region in which the local energy flow path is permanently altered due to the energy density field having exceeded the local storage capacity. The energy which is released is in part dissipated (for example, as heat and sound), and in part flows to adjacent regions. If this storage problem occurs over a large enough region, global scale dissipation and flow of energy eventuates; the appearance of that condition is called fracture. If equal amounts of external energy are applied to the energy state, but over different time increments, the details of local energy storage will change, by however small or large extent, and thus the states reached, cracking

pattern and type, and mechanical response will be different. If the dissipation and rearrangement of a specific amount of energy is occurring in a manner called cracking and the amount of initial input energy is not increased, and local storage capacities are exceeded sequentially, the phenomenon is termed creep. When ultimately significant state changes occur during repeated energy inputs, the associated changes in mechanical response are considered as fatigue loading induced.

Permanent energy state changes and the associated changes in mechanical response can, therefore, be seen to be, at least, potentially dependent on the amount of input energy, the time rate of energy application (i.e., flux), the length of storage time, and repeated input of energy. The experimental results of this program were interpreted in the light of these four energy state change dependencies. In the experiments described in Section 2, external energy inputs exclusive of mechanical load were relatively benign, thus, the selected experiments allowed determination of the nature of state change due to mechanical load without severe complication.

The application of a monotonic load allowed determination of whether the state change process and the energy states reached are dependent on amount and rate of energy input. Application of a variable load (fatigue cycling) allowed inquiry as to their dependence on repeated energy input and energy storage time. The monotonic load experiments clearly showed that the energy state of a material/structure is dependent on the amount of energy input. This dependence was revealed by the ordered pattern of matrix crack appearance (constituting one manner in which the state change process manifested) as applied load increased. Other experimental investigations have revealed the same type of dependence^{15,17-19}. The monotonic experiments performed at different strain rates and resulting in different strength distributions indicated a possible dependence of energy state and process of change on the rate of energy input. This inference was supported by the different states

observed at failure, as noted in Task I¹, for the two monotonic strain rate experiments under tension load.

The monotonic and fatigue load experiments revealed that the state change process is dependent on the form of energy input. Change in state manifested under tension load first as a specific matrix cracking pattern, followed by the appearance of delamination and subsequent growth, and culminated by fiber breakage along a $+45^\circ$ angle in the outer 0° plies. In contrast, compression loading first resulted primarily in the appearance of delamination (in different locations than for tension loading) followed by subsequent growth and some matrix cracking at 45° angles to the delamination. The delaminated region which formed under compression loading buckled outward and experienced outer 0° ply fiber breakage along a $+45^\circ$ angle because of the tension stresses occurring during the buckle; eventually a buckling failure mode occurred. Noteworthy, matrix cracking and delamination rarely appeared outside of the final failure region. The differences between state change manifestation under tension and compression were thus clearly obvious.

Comparison of the monotonic and fatigue experimental NDI data clearly showed that the states reached at fracture were different, not necessarily in kind, but in degree. The same pattern of state change manifested under fatigue loading as that which occurred near fracture under monotonic loading, but that state was quickly passed early in cyclic life as shown by the extensive delamination which occurred under fatigue loading. Thus, the state change process under fatigue loading could be said to have been the same as that which occurs under monotonic load up to the onset of delamination. At that point, the progress of change differed. The reason for the difference could be attributed to change in state being dependent on the time rate of energy application, length of time energy is stored, or on the repeated input of energy. However, since the states reached at fatigue failure under tension load were significantly different than those reached under monotonic load at

the same strain rate, the difference must be primarily due to either the effect of time of energy storage or of repeated energy input.

The progressive load experiments were used to infer that the difference in the process of state change and the different states reached under monotonic and fatigue load were at least due to a dependence of permanent state change on repeated input of energy. This dependence was indicated by both the extent of delamination and by the mechanical response distribution. Trapezoidal wave form loading experiments showed no effect of time at load on fatigue life or state reached. These experiments were interpreted to mean that energy state is not dependent on energy storage time under ambient conditions. Thus differences between states reached under monotonic and cyclic loading were attributed to a dependence on repeated energy input. Each repeated input of energy is primarily stored, partially dissipated as heat and sound, and recovered with a small loss. Small, but permanent, state changes occur during each cyclic input of energy with the state ultimately reached having quite different mechanical response properties than the original.

The results of the monotonic and the constant amplitude fatigue experiments were used to conclude that for laminated graphite/epoxy composites the state reached and process of state change is dependent on the magnitude, rate, form, and repetition of energy input. No significant dependence on time of energy storage (time at load) was observed. These effects of external energy input on the energy state field are qualitatively the same as that which occur in metallic materials. The reason is that (as mentioned in Section 1 and 2) they are reflective of the general nature of all things, namely, there is ceaseless change. They are not qualitatively properties of the materials structure. The specific manner in which the state change manifests, the various states themselves, and the quantity of mechanical response are, of course, due to the specific anisotropic, polymeric and

fibrous phase structure of the material itself and of the laminate experimentally examined.

The preload and block loading experiments were used to investigate a state change property whose qualitative, not just quantitative, response was hypothesized to be uniquely reflective of the structure of the material. This un-named property primarily appears as the manner in which the functional relationship between state change and repeated energy input depends on the magnitude (and most likely the form) of prior energy input. The reason that even the qualitative nature of the state change process dependence on prior energy input magnitude is relective of the structural nature is because it is a property of the specific manner in which energy flows through, is stored, and is dissipated within the material. That manner inherently rests upon the particular material structure and not just on the fact that an energy field is being acted upon by external force and energy. The preload experiments were used to investigate the dependence of the state change process on prior energy magnitude when that previous input induced a change in state primarily manifesting as matrix cracking. Block loading experiments were employed to extend the investigation to states exhibiting significant delamination (under T-T fatigue loading) in addition to matrix cracking.

Preload experiments indicated no significant difference between the cyclic life distribution functions or matrix cracking and delamination conditions of the preloaded and the unpreloaded fatigue population. This result can be anticipated from observations of the states achieved under fatigue and monotonic loading. Coupons of this laminate subjected to alternating load attained a state early in their cyclic life similar to that reached under monotonic load near failure and progressed quickly beyond this condition to an entirely different state characterized by extensive delamination.

Because the state characteristic of failure under monotonic loading can be attained in a relatively short time under fatigue loading, a preload cannot be expected to shorten the process by more than the few hundred to thousand cycles it may otherwise take to reach that state, thus having little effect on the distribution. Nor can a few coupons that fracture under the high monotonic preload affect the distribution by truncation of the tail of the distribution since the initial static distribution for such coupons is a smooth function without a long "tail" indicative of major manufacturing induced alterations such as large areas of porosity or delamination. Consequently, specimens which may potentially develop rapidly to a fatal state under fatigue loading are not removed by preload application. This is due in great part because the state change process under fatigue loading is dominated by the manifestation of delamination and not by matrix cracking. The changing energy state manifests as events occurring throughout the coupon which are not highly localized. The life of the coupon depends on the path (location and interaction) of these events. A dominant flaw condition does not exist; thus "weakest" specimens are not eliminated nor are remaining "flaws" blunted by the preload and so no beneficial shift of the distribution function can occur.

Unlike metals⁵⁵, no detrimental shift in the life distribution occurs due to the aforementioned observation that the monotonic damage was a small percentage of that which developed under the fatigue load levels studied. However, if the alternating loads were lower, the preload damage may constitute a more significant portion of the total damage with a resultant shift of the distribution towards shorter lives. Nevertheless, the experimental results which displayed no significant difference between the distribution functions or states at failure of the preloaded and unpreloaded fatigue populations and the inferred path dependence indicate that the rank order of coupons changes under cyclic load because that order is now a reflection of an entirely new state with different mechanical response characteristics. Thus

the often hypothesized direct relationship between the strength of a coupon under monotonic load and its potential fatigue life does not appear to represent the situation; "strong" coupons are not believed to necessarily have long fatigue lives and "weak" coupons short lives.

The conclusion was drawn from the preload experiments that a high mechanical energy input does not create a significantly new material/structure state or subsequent sequence of change events which are uniquely due to that prior magnitude of energy input. This is quite different than that which occurs in metals. A high overload into the inelastic regions of an unnotched metallic coupon can result in a much shorter fatigue life at a subsequent, lower constant amplitude fatigue load because of the induced plastic field and the introduction of a crack⁵⁵. The reversed phenomenon is usually observed for notched coupons. The well known reason is that the high load creates a state which cannot be reached even after repeated application of a low load and one in which the nature of subsequent energy storage and dissipation is greatly changed. In unnotched coupons, the phenomenon is called strain hardening (or softening) and in notched coupons, crack growth retardation. This state change property of metals is significantly different than that inferred from these preload experiments on graphite/epoxy coupons where the energy state which can be reached at the high preload is not unique to that magnitude of energy input. Instead, essentially the same state can be reached after repeated input of a lower amount of inputted energy.

There appears to be, based on the monotonic, fatigue, and preload experiments, a fundamental difference between metals and laminated composites in the nature of the state change process. That difference lies in the manner in which energy is stored and dissipated within the material and is clearly evident in laminated composites in the preload experimental results. The difference manifests in metals in the appearance of strain hardening or softening and in crack growth retardation. The nature of the state change

process in metals is such that states can be reached under energy input conditions which cannot be achieved under any amount of repeated input of a lower level of energy. In contrast, the process of state change in laminated graphite/epoxy composites seems to be such that states achieved at high energy inputs can always be essentially attained after repeated input of a lower amount of energy. In both metals and laminated composites, a new input of energy during each cycle of spectrum loading must result in an alteration in the state. But, the rate of change itself is apparently not significantly altered in laminated composites by the magnitude of prior energy input. This is the reverse of the situation in metals.

The block loading experiments were designed to further explore the state change process for laminated graphite/epoxy composites and the nature of the states which occur. Especially emphasized was the dependence of that process on the magnitude of prior energy input. Stress levels were selected which were known to produce significant state changes, consisting of both matrix cracking and delamination for T-T load, in "virgin undamaged" coupons. The number of cycles applied in the first loading block of the experiments corresponded to extremely high probability of survival levels for that stress amplitude. The experimental procedure was designed to evaluate whether or not the state change process under the first block of loading was significantly different than that which can occur under the second block. At the beginning of the second load level block of cycles, the coupon state was naturally expected to be in a different "position" on the state change versus energy input curve, for that load level, than it would have been if only the second level had been applied from the start of cyclic life. The question was to determine whether or not there had been a shift not only in position, but also an alteration in the functional relationship between the state change process and subsequent energy input.

Caution is suggested, however, when interpreting the significance of the block load experimental results. The possibility exists that a state can be

produced under a high magnitude of energy input per cycle (in this case, high load) which can be induced to change further under a subsequent much lower level of energy input which could not itself produce significant change in a "virgin undamaged" coupon. The overload experiments, to be discussed shortly, strongly indicated that this situation can occur.

A block of fatigue cycles, corresponding to a high probability of survival at a high load amplitude, was not found, in contrast to metals, to significantly affect the distribution of fatigue lives at a subsequent low amplitude. This lack of an effect was found for both T-T and C-C fatigue loading conditions. In the case of T-T loading, an effect was not observed despite the presence of obvious macroscale delamination after the high amplitude block of cycles. The reason was simply that the state reached at the high load amplitude can also be essentially reached at a low amplitude (as anticipated from the preload constant amplitude fatigue experiments), but this occurs at an insignificant percentage of the total life. Based on the lack of an effect of high to low block loading, the inference was again drawn that the state induced at the high load did not prevent states from developing at the lower load typical of such a lower energy level input per cycle. This is equivalent to concluding that the state reached after the high amplitude block is essentially the same as that reached after a greater number of cycles at a lower amplitude. In addition, the high amplitude induced state did not influence the rate of state change at the subsequent low amplitude fatigue load.

In contrast to the high-low block loading results, the average life distribution of coupons cycled at a high amplitude, after a prior lower amplitude block of cycles, was reduced under T-T loading, but not under C-C loading. These expected results were due, in the case of T-T loading, to the fact that the state reached after the low amplitude cycle block was similar to that which is normally reached after a fewer number of cycles at a high amplitude fatigue loading. Thus the fatigue life of the coupon at

the subsequent high amplitude is significantly reduced since the state has already changed greatly towards the final state at failure. For the C-C fatigue loading, no low-to-high block loading effect was anticipated because significant state change does not usually manifest until near the final failure event. The lack of an effect of the low block on fatigue life at the high block was, again, exactly the reverse of that of metals⁵⁶.

The block loading experimental results were combined with those of the preload experiments to conclude that the nature of the possible energy states and the state change process is quite different in laminated graphite/epoxy composites as compared to metals. This difference appears to be in the nature of the energy storage and dissipative properties of the materials and is a primary manifestation of the structural nature of the materials. This difference between laminated graphite/epoxy composites and metals is qualitative in nature and thus of great potential significance for anticipating and understanding the effects of complex energy input (such as that which occurs in spectrum loading).

The overload experimental results can be understood based on the results of the previously discussed load histories. These experiments constitute an attempt to clearly delineate some of the effects of complex energy input. Most of the overload experiments were conducted using load levels which induce significant state changes in initially "undamaged" coupons. The inference was drawn for these experiments that a single cycle overload could not affect fatigue life distribution unless the overload level was high enough to fracture some coupons in the sample set. In that case, those coupons where the state changes induced by the fatigue loading are progressing the fastest would be eliminated. The fatigue life distribution of unfailed coupons would thus be increased relative to a baseline distribution. These expected results were observed as discussed in Section 2. The state of coupons remaining unfailed after a single cycle overload was inferred to be insignificantly changed by the overload since the

monotonic load does not result in appreciable changes in state or in subsequent rates of state change as inferred from the previous experimental results. In other layups, there could possibly be a single cycle overload effect due to the inducement of a state change during the overload manifesting as large delamination extension of a size greater than that already induced by the fatigue load.

Multiple overloads naturally result in a shift of the life distribution of the entire initial sample set towards shorter lives commensurate with frequency of overload. At each successive overload, failure is more and more likely and thus the life for the whole sample set is reduced or that of the remaining unfailed coupons increased. These results occur because the state is altered during the baseline load level in a manner not dissimilar to that in which it changes at the higher load level. However, the rate of change is different under each constant level of repeated input of energy.

The T-T overload experiments conducted with baseline stress levels of 138 or 207 MPa (20 or 30 ksi) and an overload level of 414 MPa (60 ksi) revealed another property of the state change process. The energy input of the baseline stress levels is not sufficient to induce significant state change by itself in initially "undamaged" coupons⁹. However, the fatigue life of coupons at a stress level of 414 MPa (60 ksi) was significantly reduced by the added input of energy of a lower magnitude. This result was inferred to mean that once a state of a particular type was induced by the high energy input, then the lower input can produce further state changes which could not be induced in an "undamaged" coupon. The effect appears to be due to the concentration of energy in the many regions of matrix cracking and delamination. Therefore, this reduction in fatigue life at 414 MPa (60 ksi) due to the low amplitude loading is a further reflection of the materials structural nature. The significance of this result is not yet fully clear. A baseline stress level insufficient to normally induce even matrix cracking may have a large effect on state change after, for example, the inducing of

a state typical of impact load. Therefore, the truncation from a fatigue spectrum of load levels below that sufficient to induce matrix cracking may not be wise if a component will be in a state significantly different than the "undamaged" state.

3.3 THOUGHTS ON IMPLICATIONS

Use of the energy state concept appears to have wide implications in the realm of relating laboratory data to structure. Successful representation, mathematically, of the relationship between laboratory coupon data and structural response requires transfer functions which eliminate the influence of geometry. For metals two such functions have been derived: notch acuity analysis and linear elastic or elasto-plastic fracture mechanics analysis of a dominant, self-similar, crack-like defect. These two procedures often have an applicability for metals precisely because the structure of the material of interest is usually small relative to geometric dimensions and is relatively isotropic. The reverse conditions are true for laminated composites because of the very nature of their structure. Therefore, neither of the two transfer functions used for metals can normally be applied to composites on a macroscale.

Experiments on laminated graphite/epoxy coupons with holes show notch acuity decreasing with fatigue cycles³⁻⁵ and those on notches show that they must be large relative to the microstructure to use linear elastic fracture mechanics on a macroscale²⁶⁻³⁵. This is not to say that concepts of stress concentration and fracture cannot be used for laminated composites, but only that their application cannot be free of considerations which focus on the specific geometry and structure of the composite material. Unlike metals, we cannot, in general, analyze a laminated composite independent of its microstructure.

Another problem in this regard is that of developing cumulative damage theory and associated mathematical representation. The entire question is heavily, though often unconsciously, colored by past experience with metals. One consequence of this is the effort to record "damage" accumulation in some laboratory geometry, an attempt to represent the relationships among the variables, and the hope that the representation can be applied to design. This approach usually ignores the tremendous differences in state change behavior between laminated composites and metals and especially ignores the structural nature of the materials. The influence of geometry on the state change process is often not fully appreciated. For example, there are many differences in the state change process among finite width coupons versus torsion tubes versus flat plate edge delamination restricted structure. Also, as has often been observed, composites do not usually exhibit state change as growth of a single dominant flaw though a region of greatest interest may exist.

The cumulative damage problem can be partially relieved by using the energy state concept to focus upon how the state will change in a particular application. This allows selection of what details in the process could or should be mathematically represented. For example, the block, preload, and overload data can be used to anticipate certain fatigue spectrum loading effects. A single overload cycle applied early in cyclic life is not likely to seriously affect the state change process within the laminate used in this program and thus, from a spectrum standpoint, can be essentially ignored. However, the same single overload cycle becomes progressively more important if applied later in fatigue life. Overloads cannot, apparently, increase fatigue life, and low amplitude loads can, perhaps, only be truncated in specific situations.

In essence, the entire attitude towards such problems as life prediction, cumulative damage, fatigue spectrum load truncation, or damage tolerance

is altered in the light of the energy state concept. Emphasis is placed on the state change process and not on a specific event in that process such as a defined failure condition. Present concepts of life prediction, for example, appear to be based on rather a static viewpoint despite the acknowledgement of the presence of a dynamic process. The problem of relating laboratory coupon results to the response of structural components remains, at present, acute. This is not to say that the problems of precise life prediction or developing cumulative damage theory are unsolvable. However, the suggestion is offered that they can best be quantified by focusing on the nature of the state of a material and the process of state change. Especially important is an awareness of that process in different geometries and under different energy input conditions. Until that awareness is more highly developed, ensurance of structural integrity can more likely be achieved by the development of damage tolerance concepts.

An example of using the energy state concept in formulation of damage tolerance approaches lies in the observation that the presence of delamination appears to be highly important. Without the development of delamination, material/structure states associated with failure in fatigue do not appear to be attainable except at extremely high percentages (perhaps greater than 80 percent) of the ultimate strength. If this inference is experimentally substantiated, as already appears to be true from preliminary results,⁴ attention must be focused upon delamination. Most likely the development of delamination can be prevented or rate of expansion delayed in many practical applications. If this is true, ensurance of structural integrity may often be a case of "static" strength and stiffness design combined with delamination delay or prevention.

SECTION 4

CONCLUSIONS AND RECOMMENDATIONS

Throughout the program, the major emphasis was placed on developing a means to relate the experimental results to the overall purpose of ensuring structural integrity. The plan suggested to achieve the relationship was developed during the course of this program and during several other research investigations. Use of the plan consisted of applying the concept that the material/structure constitutes an energy state immersed within an open energy field. The whole of the two energy fields were considered as a single energy system within which a continuous dynamic energy exchange process is ongoing. The energy state concept was used both to select the magnitude of experimental variables and to interpret results.

The principal conclusions were:

- The material/structure state which develops and the energy state process of change is dependent on the magnitude, rate, form, and repeated application of energy input. No dependence on constant storage of energy (time at load) was found in these room temperature experiments.
- The functional nature of the state change process was essentially independent of the magnitude of prior input of energy.

The first of these two conclusions is reflective of the basic property of all materials, namely, to change. The specific manner and type of state

change and the reasons for the observed state appearances were explained based upon the structural nature of the material. That structural nature was also found to be responsible for the appearance of the property mentioned in the second primary conclusion. The second conclusion is important precisely because the property is directly related to the material's structural nature. Because the material structure is well known to be greatly different than that of metals, a significant difference in response to energy input is not unexpected. However, structural difference is apparently responsible not only for distinctions in quantity of response and form of appearance, but also in the very quality of response. The difference in response quality is such as to require significant distinctions in the approach used to analyze and anticipate the effects of complex energy input. The nature of the response to energy input also requires that the interaction between the structure of the material and the geometry of the component of interest be carefully considered.

A final point concerns the generality of these two principal conclusions for laminated graphite/epoxy composites. Because the first conclusion is true qualitatively, due to the nature of all materials, and the second is based on the structure of the material, both must apply to other laminate configurations. The specific quantity of response and appearance of state change must naturally depend on component geometry, layup and form and direction of applied forces and energies. These, however, would probably not negate the qualitative nature of the conclusions.

4.1 DETAILED CONCLUSIONS

This subsection details several conclusions of this research investigation which were both of a general and of a specific nature. They were general in the sense that there are implications inferred from the results which apply

to the general application of laminated graphite/epoxy materials in structures. The conclusions are also specific in that certain detailed experimental results may not apply to all possible laminates and environment/load conditions. Some of the conclusions are rather obvious and well known within the technical community, but they need to be emphasized since they appear to be often overlooked.

4.1.1 General Concept

A series of conclusions were made which constitute general concepts believed to be fundamental to laminated graphite/epoxy composites.

1. Our attention must be refocused on the macroscale, anisotropic nature of the composite. Like wood, the awareness must ever center on the inherent structural nature of the material.
2. Emphasis must be placed on the fact that the material/-structure, energy state is continuously changing. There is no "static" state condition, but only a continuous dynamic process of change.
3. The macroscale structural nature of laminated composites relative to their geometric size is well known to be greatly different than that of metals. This nature results in:
 - a. A state change process with properties distinctly different than metals (this greatly influences, for example, such concepts as load truncation under spectrum fatigue load);
 - b. The state change process within a laminate not being a

simple sum of the processes which occur in separately loaded lamina;

- c. A state change process which cannot generally be understood by using concepts of a single dominant flaw;
 - d. A state change process which can be understood by placing attention on the general region in which that process is occurring;
 - e. The changes which take place in the material being intimately entwined with the geometry such that the geometry effects cannot be isolated as they can be in many metallic applications.
- 4. The nature of the material state structure relative to the geometry and the fact that state change process is occurring requires an emphasis on the development of an intuitive feel of the materials' nature and process of change. This is accomplished by measurement and observation of an initial state, sequence of change under external energy input, rate of state change, and, most importantly, the integration of all such data.
 - 5. The focus of research should be on the dynamic process of state change and not on a particular "static snapshot" manifestation of that process such as monotonic tensile fracture, fatigue failure, appearance of matrix cracking, or initial modulus.
 - 6. The nature of the dynamic state change process and associated mechanical properties may be qualitatively anticipated by de-

fining the initial state, the geometry of application, and the external energy field.

7. Mathematical models deemed necessary to quantify and represent the relationship among variables should be derived in the light of an intuitive understanding of the state change process. This is in contrast to a more usual practice of, in effect, deriving the nature of the state change process from the model.

4.1.2 Nature of the State Change Process

Describing quantitatively the state change process or any particular aspect is essentially a non-ending task. However, the nature of the process can be understood to any level desired. The conclusions reached in this report concern the qualitative manner in which the state change process depends on energy inputted as mechanical load.

1. The state change process and the state reached is dependent on:
 - a. Amount of energy input (shown by increasing the magnitude of load).
 - b. Repeated input of energy (as shown by progressive load cycling).
 - c. Form of energy input (shown by the differences between tension and compression loading).
 - d. Rate of energy input (shown by changing the rate of loading).

2. The state change process is not significantly dependent on the length of energy storage time at room temperature (as shown by the lack of an effect of hold time).
3. The state reached at some defined failure criteria is dependent on the history of energy input. (For example, the state at fracture or failure is different under monotonic, fatigue, or fatigue and residual strength loading).
4. The functional nature of the state change process (under the same time rate of energy application) is essentially independent of the prior magnitude of energy input. This is in direct contrast to that which occurs in metals where the state change process can be greatly altered if the magnitude of prior energy input is high enough (this manifests, for example, as retardation or macroscale plasticity).
5. A repeated input of energy can induce significant state change from some initial states and not from others. (For example, a $R = 0$, 207 or 138 MPa (30 or 20 ksi)) constant amplitude fatigue load cannot induce significant state change in an "undamaged" coupon, but can do so if the state is altered by a high overload).
6. The nature of the state change process is probably similar for all laminated graphite/epoxy composites, but the pattern is probably characteristic of each laminate a (dynamic counterpart to the hypothesis of a characteristic damage state (CDS))⁵⁸.
7. Similar mechanical properties are not necessarily reflective of the same initial state or state change history, but a

particular initial state and history of energy input must be associated with unique mechanical properties.

4.1.3 State Change Manifestation Characteristics

The energy state change process manifests in many different ways. The principal ways that the process was characterized in this investigation was by observing matrix cracking and delamination and by quantifying strength and fatigue life distributions.

1. Manifestation of the state change process depends on the form of energy input.
 - a. Under tension load, the process is principally characterized by: Matrix cracking (first in the 90° plies, followed by the -45° and then the $+45^\circ$ plies); subsequent delamination (primarily between the outer 90° and -45° plies and the inner 90° and $+45^\circ$ plies); and final fracture of the coupon (with 0° fibers fracturing along the $+45^\circ$ direction).
 - b. Under compression load, the process is characterized by: delamination (between the outer 90° and $+45^\circ$ plies) with no significant prior matrix cracking, subsequent buckling, a growing fracture along a $+45^\circ$ direction of the outer 0° ply fibers on the tensile surface (because of buckling); and final buckling failure.
2. Differences in the states which develop in the same laminate under different energy inputs primarily manifest as differences in delamination extent.

3. The mechanical responses which can be associated with the state change process are:

a. Monotonic tensile strength can be dependent on rate of energy input (loading rate effect).

b. Fatigue life distribution is dependent on:

i. Magnitude of energy input per cycle;

ii. Form of energy input (tension or compression),

but not on the length of time that the coupon is near maximum load.

c. A preload does not significantly affect subsequent fatigue life distribution if the amplitude of the fatigue load can cause significant state change from an initial "undamaged" state.

4.1.4 Thoughts on Implications

The approach taken in this investigation and the inferences drawn from the experimental results have led to a few thoughts on possible implications of the work.

1. Development of delamination is a key phenomenon in the state change process. That development is highly geometry dependent. Therefore:

a. Delay of onset, prevention of development, or stoppage of ongoing delamination are likely to be valuable in ensuring safe structural components.

- b. The understanding of the interaction between a geometric configuration and the state change process is highly important.
- 2. Mechanical response under more complex energy input (such as that which occurs in block loading, overload sequences, or random loading) can be qualitatively understood using the energy state concept.
- 3. A fatigue loading amplitude may possibly be truncated from a fatigue spectrum if delamination does not initially exist, but if delamination is developed or introduced (for example, by impact), such truncation may be unwise.
- 4. For laminate geometrical configurations in which delamination can easily develop under fatigue loading:
 - a. The breakage of 0^0 fibers cannot be used to monitor state change in a significant way because the fracture of 0^0 fibers occurs primarily near failure;
 - b. The manifestation of significant state change can be observed by monitoring delamination initiation and growth.
- 5. For laminate geometrical configurations in which delamination cannot easily develop under fatigue loading:
 - a. Failure does not appear to be possible except at extremely high loads;

- b. The detection of significant state change may possibly be achieved by monitoring fiber breakage since this should often occur significantly prior to failure (as has been observed experimentally^{4,36}).

4.2 RECOMMENDATIONS

Based on the awareness developed during this investigation, the following recommendations for future research endeavors are suggested.

1. The focus of investigational attention should be on the nature of the material/structure, continuous state change process.
2. The relationship between laboratory experiment and structural application should be sought through the development of an intuitive feel for material states and changes in state. This intuitive feel allows development of an understanding as to how a specific geometry influences state change in particular applications.
3. Life assurance of structures made of composites should at present be gained by a focus on damage tolerance and not specifically on developing cumulative damage or life prediction models.
4. The strong possibility that a low amplitude fatigue load not normally considered important, can induce significant further state change if delamination is initially present should be investigated.

5. The effect of energy input due to both mechanical load and chemical/thermal environment on the state change process should be studied under more extreme environmental conditions.
6. The relative importance of various mechanical and environmental energy inputs on the state change process should be evaluated on notched components.

REFERENCES

1. Ryder, J. T., "Effect of Load History on Fatigue Life," AFML-TR-80-4044, June 1980.
2. Gordon, J. E., Structures or Why Things Don't Fall Down, Penguin Books Ltd., N.Y., N.Y., 1979, p.30.
3. Lauraitis, K. N., Ryder, J. T., and Pettit, D. E., "Advanced Residual Strength Degradation Rate Modeling for Advanced Composite Structures, Volume II - Task II and III", AFWAL-TR-79-3095, July 1981.
4. Ryder, J. T., and Walker, E. K., "The Effect of Compressive Loading on the Fatigue Lifetime of Graphite/Epoxy Laminates," AFML-TR-79-4128, October 1979.
5. Reifsnider, K. L., Stinchcomb, W. W. and O'Brien, T. K., "Frequency Effects on a Stiffness Based Fatigue Failure Criterion in Flawed Composite Specimens," ASTM STP 636, K.L. Reifsnider and K.N. Lauraitis, Eds., American Society for Testing and Materials, 1977, pp. 171-184.
6. LeMay, I, "Symposium Summary and an Assessment of Research Progress in Fatigue Mechanisms," Fatigue Mechanisms, Proceedings of an ASTM-NBS-NSF Symposium, Kansas City, Mo., May 1978, J.T. Fong, ed., ASTM-STP 675, American Society for Testing and Materials, 1979, pp. 873-888.
7. Morrow, J. in "General Discussion and Concluding Remarks", Fatigue Mechanisms, Proceedings of an ASTM-NBS-NSF Symposium, Kansas City, Mo., May 1978, J. T. Fong, Ed., ASTM STP 675, American Society for Testing and Materials, 1979, p. 890.
8. Walsh, R., Towards an Ecology of Brain, S. P. Medical and Scientific Books, Jamaica, New York, 1981.
9. Ryder, J. T., and Walker, E. K., "Ascertainment of the Effect of Compressive Loading on the Fatigue Lifetime of Graphite Epoxy Laminates for Structural Applications," AFML-TR-76-241, December 1976.
10. Gordon, J. E., Structures or Why Things Don't Fall Down, Penguin Books Ltd., N.Y., N.Y., 1979, p. 63.

11. Gordon, J. E., Structures or Why Things Don't Fall Down, Penguin Books Ltd., N.Y., N.Y., 1979, p. 21.
12. Hahn, H. T., and Kim, R. Y., "Proof Testing of Composite Materials," J. Composite Materials, Vol. 9, (July 1975), p. 297.
13. Yang, J. N., and Jones, D. L., "Load Sequence Effects on Fatigue of Unnotched Composite Materials," Fatigue of Fibrous Composite Materials, ASTM STP 723, American Society for Testing and Materials, 1981, pp. 213 - 232.
14. Rhines, F. N., "Quantative Microscopy and Fatigue Mechanisms," Fatigue Mechanisms, Proceedings of an ASTM-NBS-NSF Symposium, Kansas City, Mo., May 1978, J.T. Fong, ed., ASTM-STP 675, American Society for Testing and Materials, 1979, pp. 23 - 46.
15. Kim, R. Y., "Experimental Assessment of Static and Fatigue Damage of Graphite/Epoxy Laminates," Advances in Composite Materials, ICCM3, Vol. 2, Proceedings of the 3rd International Conference on Composite Materials, Paris, France, 26 - 29 August, 1980, pp. 1015 - 1028.
16. Burington, R. S., and May, J., Handbook of Probability and Statistics with Tables, McGraw-Hill Book Company, 1970, pp. 265 and 268.
17. Henneke, E. G., II, Reifsnider, K. L., and Stinchcomb, W. W., "Defect Property Relationships in Composite Materials," presented at AFML, AFOSR, and AFFDL Mechanics of Composites Review, Bergamo Center, Dayton, Ohio, 25 - 27 October, 1977, pp. 150 - 162.
18. Stalnaker, D. O., and Stinchcomb, W. W., "An Investigation of Edge Damage Development in Quasi-Isotropic Graphite Epoxy Laminates," Interim Report, AFML Contract F33615-75-C-5119, Virginia Polytechnic Institute and State University Report VPI-E-77-24, September 1977.
19. Reifsnider, K. L., Henneke, E. G., II, and Stinchcomb, W. W., "Delamination in Quasi-Isotropic Graphite-Epoxy Laminates," Composite Materials: Testing and Design (Fourth Conference), ASTM STP 617, American Society for Testing and Materials, 1977, pp. 93 - 105.
20. Sendekyj, G. P., and Stalmaker, H. D., "Effect of Time at Load on Fatigue Response of [(0/+45/90)₃]₂ T300/5208 Graphite/Epoxy Laminate," Composite Materials: Testing and Design (Fourth Conference), ASTM STP 617, American Society for Testing and Materials, 1977, pp. 39 - 52.

21. Crossman, F. W., Mauri, R. E., and Warren, W. J., "Moisture Altered Viscoelastic Response of Graphite/Epoxy Composites," Advanced Composite Materials - Environmental Effects, ASTM STP 658, J. R. Vinson, Ed., American Society for Testing and Materials, 1978, pp. 205 - 220.
22. Lauraitis, K. N. and Ryder, J. T., "Mechanics of Composites", Lockheed-California Company report to be published in 1982.
23. Coffin, L. F., Jr., "Fatigue Mechanism - An Historical Perspective," Fatigue Mechanisms, Proceedings of an ASTM-NBS-NSF Symposium, Kansas City, Mo., May 1978, J.T. Fong, ed., ASTM-STP 675, American Society for Testing and Materials, 1979, pp. 9 - 20.
24. Reed-Hill, R. E., Physical Metallurgy Principles, D. Van Nostrand Company, Inc., Princeton, New Jersey, 1964, pp. 577 - 593.
25. Fong, J. T., "Fatigue Mechanism - Key to the Solution of the Engineer's Second Fundamental Problem," Fatigue Mechanisms, Proceedings of an ASTM-NBS-NSF Symposium, Kansas City, Mo., May 1978, J.T. Fong, ed., ASTM-STP 675, American Society for Testing and Materials, 1979, pp. 3 - 8.
26. Morris, D. H., and Hahn, H. T., "Fracture Resistance Characterization of Graphite/Epoxy Composites", Composite Materials: Testing and Design (Fourth Conference), ASTM STP 617, American Society for Testing and Materials, 1977, pp. 5 - 17.
27. Adsit, N. R., and Waszczak, J. P., "Fracture Mechanics of Boron/Aluminum Coupons Containing Stress Risers," Fracture Mechanics of Composites, ASTM STP 593, American Society for Testing and Materials, 1975, pp. 163 - 176.
28. Slepetz, J. M., and Carlson, L., "Fracture of Composite Compact Tension Specimens," Fracture Mechanics of Composites, ASTM STP 593, American Society of Testing and Materials, 1975, pp. 143 - 162.
29. Konish, H. J., Jr., "Mode I Stress Intensity Factors for Symmetrically-Cracked Orthotropic Strips," Fracture Mechanics of Composites, ASTM STP 593, American Society for Testing and Materials, 1975, pp. 99 - 116.
30. Zimmer, J. E., "Fracture Mechanics of a Fiber Composite," J. Composite Materials, Vol. 6, April, 1972, p. 312.
31. Konish, H. J., Jr. and Swedlow, J. L., "On Fracture Phenomena in Advanced Fiber Composite Materials," Presented at the 13th Structures, Structural Dynamics, and Materials Conference, sponsored by AIAA/ASME/SAE, San Antonio, Texas, April 10 - 12, 1972.

32. Beaumont, P. W. R., and Phillips, D. C., "Tensile Strengths of Notched Composites," J. Composite Materials, Vol. 6, January, 1972, p. 32.
33. Hancock, J. R., and Swanson, G. D., "Toughness of Filamentary Boron/Aluminum Composites," Composite Materials: Testing and Design (Second Conference), ASTM STP 497, American Society for Testing and Materials, 1971, p. 299.
34. Cooper, C. A., "The Fracture Toughness of Composites Reinforced with Weakened Fibers," J. Material Science, Vol. 5, 1970, p. 645.
35. Beaumont, P. W. R., and Tetelman, A. S., "The Fracture Strength and Toughness of Fibrous Composites," Reports Group, School of Engineering and Applied Science, University of California, Los Angeles, August, 1972.
36. Ryder, J. T., and Crossman, F. W., "A Study of Stiffness, Residual Strength, and Fatigue Life Relationships for Composite Laminates," NASA Contract NAS1-16406, Monthly Reports.
37. Pipes, R. B., and Pagano, N. J., "Interlaminar Stresses in Composite Laminates Under Uniform Axial Extension," J. Comp. Materials, Vol. 4, 1970.
38. Wang, A. S. D., and Crossman, F. W., "Some New Results on Edge Effect in Symmetric Composite Laminates," J. Comp. Materials, Vol. 11, 1977, p. 92.
39. Pettit, D. E., Ryder, J. T. and Lauraitis, K. N., "Effects of Line Discontinuity in Composite Laminates on Static and Fatigue Strength Distribution," Presented at the 24th National SAMPE Symposium, San Francisco, California, May 8 - 10, 1979, published in the Conference Proceedings.
40. Sandorff, P. E., Ryder, J. T. and Lauraitis, K. N., "Experimental Evaluation of Column Compression Properties of Graphite/Epoxy Composites," Composites Technology Review, Vol. 3, No. 1, spring 1981, pp. 6 - 16.
41. Bowie, G. E., Pettit, D. E., Ryder, J. T., and Krupp, W. E., "NDI Life Analysis Interface," Lockheed-California Company Report LR 27013, September 1974.
42. Gumbell, E. J., Statistics of Extremes, Columbia University Press, New York, 1958.

43. Talreja, R., "Estimation of Weibull Parameters for Composite Material Strength and Fatigue Life Data," Fatigue of Fibrous Composite Materials, ASTM STP 723, American society for Testing and Materials, 1981, pp. 291 - 311.
44. Weibull, W., and Weibull, G. W., "New Aspects and Methods of Statistical Analysis of Test Data with Special Reference to the Normal, the Log Normal and the Weibull Distributions," Part I and II, FOA Report D20045-DB. Defense Research Institute, Stockholm, Denmark, June, 1977.
45. Antle, C. E., and Klimko, L. A., "Choice of Model for Reliability Studies and Related Topics II," ARL-73-0121, AD 772775, 1973.
46. Harter, H. L. and Moore, A. H., "Maximum Likelihood Estimation of the Parameters of Gamma and Weibull Populations from Complete and Censored Data," Technometrics, Vol. 1, No. 4, 1965, pp. 639 - 643.
47. Bowie, G. E., Besari, M. S. and Trapp, W. J., "Experimental Mechanics: Development of Methods for Numerical Analysis of Composite Fatigue Data," Lockheed-California Company Report LR 27981, January, 1977.
48. Lieblein, J., "On Moments of Order Statistics from the Weibull Distribution," Annals of Math. Statistics, Vol. 26, 1955, pp. 330 - 333.
49. Stalnaker, D. O., and Stinchcomb, W. W., "An Investigation of Edge Damage Development in Quasi-Isotropic Graphite Epoxy Laminates," Interim Report, AFML Contract F33615-75-C-5119, Virginia Polytechnic Institute and State University Report VPI-E-77-24, September 1977.
50. Sandifer, J. P., "Fracture of Engineering Materials", Lockheed-California Company Report, LR 28974, December, 1980.
51. Sandorff, P. E., and Tajima, Y. A., "A Practical Method for Determination of Moisture Distribution, Solubility, and Diffusion Coefficient for Composite Laminate," Lockheed-California Company Report, LR 28047, April 28, 1978.
52. Lauraitis, K. N., and Sandorff, P. E., "The Effect of Environment on the Compressive Strengths of Laminated Epoxy Matrix composites," AFML-TR-79-4179, December 1979.
53. Van Dreumel, W.H.M., and Kamp, John L. M., "Non Hookeon Behavior in the Fibre Direction of Carbon-Fibre Composites and the Influence of Fibre Waviness on the Tensile Properties," J. Comp. Matls., Vol. 11, October 1977, pp. 461 - 469.

54. Curtis, G. J., Milne, "Non-Hookean Behavior of Strong Carbbon Fibres," Nature, Vol. 220, December 1968.
55. Topper, T. H., and Sandor, B. I., "Effects of Mean Stress and Prestrain on Fatigue Damage Summation", University of Illinois, Department of Theoretical and Applied Mechanics, T. & A. M. Report No. 318, August 1968.
56. Dowling, N. E., "Fatigue Failure Prediction for Complicated Stress-Strain Histories", University of Illinois, Department of Theoretical and Applied Mechanics, T. & A.M. Report No. 337, January, 1971.
57. Gemma, A. E., and Snow, D. W., "Prediction of Fatigue Crack Growth Under Spectrum Loads", Fracture Mechanics, ASTM STP 677, C. W. Smith, Ed., American Society for Testing and Materials, 1979, pp. 320 - 338.
58. Stinchcomb, W. W., Reifsnider, K. L., Yeung, P., and Masters, J., "Effect of Ply Constraint on Fatigue Damage Development in Composite Material Laminates", Fatigue of Fibrous Composite Materials, ASTM STP 723, American Society for Testing and Materials, 1981, pp 64 - 84.

APPENDIX A
MATERIAL SELECTION AND QUALITY ASSURANCE

This appendix presents a discussion of the rationale for the material and laminate selected in Task I and used in Task II, the manufacturing procedures used and the coupon geometry, and presents the quality assurance plan employed.

A.1 MATERIAL AND LAMINATE SELECTION

The selected fiber/resin system was Narmco's Rigidite T300/5208. The reasons for selection of this material were:

- The quality of the T300 fiber was highly consistent.
- There was an extensive data base at Lockheed-California Company and at other companies on this material. Much of the data were directly related to those which were to be obtained in this program. The most pertinent data was from AFFDL Contract F33615-77-3084, "Advanced Residual Strength Degradation Rate Modeling for Advanced Composite Structures;" AFML Contract F33615-77-C-5140, "Effect of Environment on Compressive Strengths of Laminated Epoxy Matrix Composites;" and NASA/Langley Contract NAS1-14000, "Flight Service Evaluation of an Advanced Composite Empennage Component on a Commercial Transport aircraft." All three of these contracts used the T300/5208 system.
- The Air Force had a greater interest in this material than other materials at the time of contract award.

The laminates used in this program were a unidirectional 0° layup, $(0)_{16}$, designated U1 from which 0° and 90° unidirectional coupons were obtained; a $\pm 45^\circ$ layup, $(\pm 45^\circ)_{4S}$, designated U2, and a quasi-isotropic layup, $(0/45/90/-45_2/90/45/0)_S$, designated L1. The U1 and U2 unidirectional laminates were used in Task I to obtain lamina properties. Only one laminate, L1, was

selected for evaluating load history effects as per the original Air Force request. The selection of Laminate L1 for Tasks I, II, and III was based on the following considerations:

- a. The laminate must be representative of those commonly used in aircraft structures.
- b. Interlaminar shear and tensile normal stresses should be minimized to prevent premature edge delamination.
- c. Symmetry about the mid-plane should be maintained to avoid warping under load or due to fabrication stresses.
- d. Laminate thickness must be such that adequate bond strength can be obtained.

Laminates for aircraft structures are typically selected from the $0_i/\pm 45_j/90_k$ or $0_i/\pm 45_j$ orientation families. The 0° direction is generally oriented parallel to the principal axial loading direction; $\pm 45^\circ$ plies provide shear strength and stiffness or buckling resistance, and when needed, 90° plies provide additional strength in the transverse direction, reduce the Poisson's ratio, and can be used to mitigate some of the free-edge stresses.

The selection of laminate stacking sequence was governed by three considerations: symmetry, tab bond strength requirements, and free-edge effects. Laminates of sixteen or more plies impose severe strength requirements on the tab bond, so surface plies were oriented at 0° . This choice was selected although many laminate designs for aircraft skin covers have 45° fiber orientations on the outside surface. Angle plies terminating at a free edge induce interlaminar shear and normal stresses due to differences in Poisson ratios. The magnitude and sign of these stresses are functions of the lamina orientations, thicknesses, stacking sequence, and external and thermal stresses. Interlaminar normal tension stresses of sufficient magnitude can cause edge delamination that reduces both static and fatigue strengths. Stacking the laminate so that the normal stresses

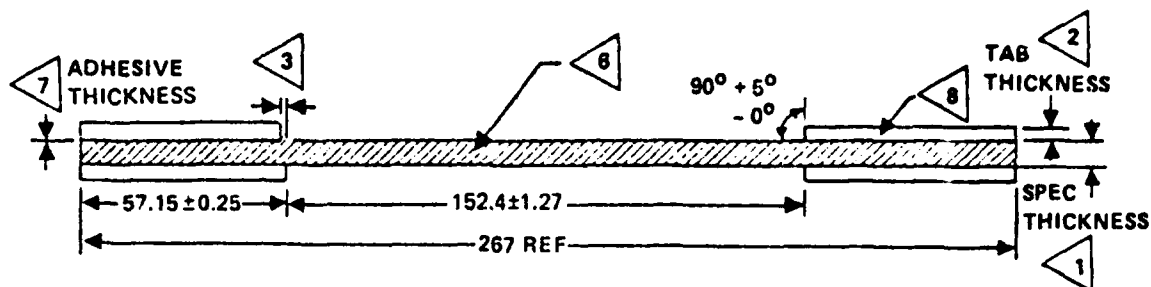
are compressive generally increases the fatigue strength over that of a laminate with tensile normal stresses. However, cyclically applied loading with reversing direction, as in this program, results in reversal of the sign of the normal stress. Consequently, for fatigue coupons subjected to compressive loading, laminae must be stacked to minimize normal stresses and thus their effects on fatigue strength. Another point of consideration was that matrix dominated layups (low number of 0° plies) would be generally expected to be more susceptible to load history effects than fiber dominated layups (high number of 0° plies). This conclusion is supported by the literature^{4,9}. The above considerations were combined with the objectives of the RFP, (restriction to one laminate configuration) and used to arrive at the selected laminate, L1. This type of laminate is often said to have matrix dominated failure modes.

A.2 FABRICATION AND QUALITY ASSURANCE

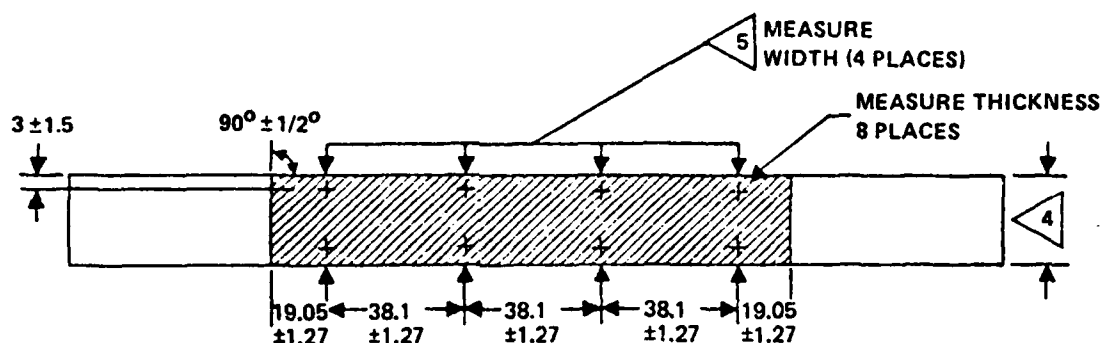
Essentially, fabrication and quality assurance procedures followed those used previously in Contract F33615-77-C-5045⁴. A single batch of 305 mm (12 in.) wide prepreg tape was used for all test laminates thus preventing the possibility of the data being affected by batch-to-batch variations. The assumption was made (and was supported by previously obtained results^(2,14)) that after coupons have been manufactured, no significant change in their properties would occur during shelf storage at room temperature, $40 \pm 10\%$ R.H. Although this assumption was not expected to be perfectly true over the three year testing period of this contract, the variation in properties due to long-term storage was expected to be less than that due to batch-to-batch variations. For laminate U1, two panels were fabricated of approximate dimensions, 610 by 1219 mm (24 by 48 in.); for laminate U2, two panels of approximate dimensions, 610 by 635 mm (24 by 25 in.), and for laminate L1, 19 panels of approximate dimensions 914 by 1219 mm (36 by 48 in.)

Figure A1 shows the specimen design for the coupons machined from laminates U1, U2, and L1 used in Task I and for the L1 panels of Task II. Features considered in the selection of this configuration are outlined below:

- The geometry can be used for static tension and compression tests as well as for either tension-tension or tension-compression fatigue tests.
- Adequate specimen length is important in composite specimens in order to obtain uniform stress conditions within the test section. Load introduction through the tabs must be transferred to the central plies by shear; the low shear modulus results in appreciable shear lag within the tabbed area. The resultant relative displacement of surface and centerline fibers must be accommodated within the specimen test length.
- Longer test specimens accommodate much more easily to small test misalignment and eccentricity. The 152 mm (6 in.) gage length selected here is considered important in minimizing stress variations which may be introduced by practical limitations in fabrication tolerances and test installation and thus in reducing test scatter.
- The relatively long length aids in minimizing end effects which could affect damage propagation behavior from a hole.
- The specimen size is sufficient or provide a good probability of including point--to-point variations in material and layup properties, as well as large enough to be more representative of aircraft structures.
- Variations in test results due to the discontinuity at the specimen edge will vary with laminate, material, and fabrication practice, but in general will diminish as width is increased. The 25 mm (1 in.) width was chosen to minimize the free edge effects which are usually on the order of a laminate thickness^{37,38} so that these do not unduly influence the damage propagation behavior.



ALL DIMENSIONS IN MILLIMETERS



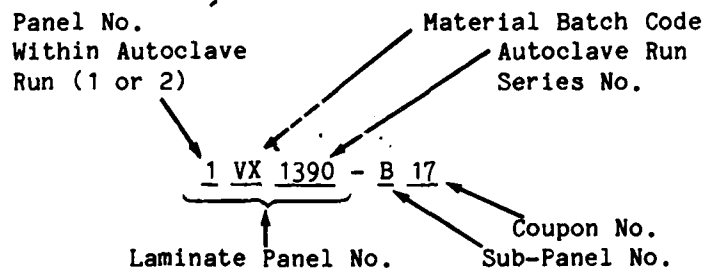
- ④ SPECIMENS TO BE FLAT OVER THE ENTIRE 267 mm (10.5 in.) LENGTH WITHIN 0.25 mm (0.01 in.)
- ⑧ TAB EDGES TO BE PARALLEL TO SIDES OF SPECIMEN WITHIN 0.025 mm (0.001 in.) OVERHANG NOT TO EXCEED 3.8 mm (0.003 in.)
- ⑦ THE TAB AND SPECIMEN BONDING SURFACES TO BE THOROUGHLY SOLVENT CLEANED USING METHYL-ETHYL-KETONE PRIOR TO BONDING. A 177°C (350°F) CURING ADHESIVE IS TO BE USED AND MUST COVER ENTIRE SURFACE UNIFORMLY.
- ⑥ SPECIMENS TO BE CUT DRY. MACHINED SURFACES TO BE rms 50 OR BETTER. NO EDGE DAMAGE OR FIBER SEPARATION SHOULD BE VISIBLE UNDER 10X MAGNIFICATION.
- ⑤ MEASURE SPECIMEN WIDTH 4 PLACES. WIDTH MUST NOT VARY BY MORE THAN 0.102 mm (0.004 in.)
- ④ SPECIMEN WIDTH TO BE 22.225 ± 0.127 mm (0.875 ± 0.005 in.)
- ③ MISMATCH OF TABS FROM SIDE TO SIDE NOT TO EXCEED 0.25 mm (0.01 in.)
- ② TABS TO BE CUT FROM AN 6 PLY LAMINATE FABRICATED FROM PREPREG OF 1581 GLASS FABRIC IN A 177°C (350°F) CURING EPOXY.
- ① SPECIMEN THICKNESS TO BE WITHIN ± 0.08 mm (± 0.003 in.) OF THE AVERAGE OF 8 THICKNESS MEASUREMENTS.

Figure A1: - Unnotched composite test specimen

- Dimensions are convenient for fabrication and machining; tolerances required to obtain the necessary precision in test results are achievable without extraordinary measures.

After fabrication and prior to testing, the thickness of all coupons was measured in eight places and the width in four places (see Figure A2 for these locations). The width of any one coupon varied at most ± 0.0127 mm (± 0.0005 in.), $\pm 0.06\%$, within the gage length. The width of all coupons varied by less than ± 0.10 mm (± 0.004 in.) within the gage lengths. The area of any one coupon was found to vary by less than $\pm 1.5\%$ from the average area of all coupons.

All coupons were identified by the following system:



Autoclave and panel numbers are consecutive at Lockheed and are an internal reference number unique to each panel. The test panels were cut into sub-panels, and numbered as A, B, C, and D. This system of coupon identification allowed for traceability of each coupon to previous panel location and of each panel to fabrication history.

Panel layout was designed such that adjacent 90° and 0° direction tapes within a ply had their edges (line discontinuity) aligned with those of other plies of the same orientation. Thus, all 0° line discontinuities of one ply were directly lined up above those of other 0° plies within a total error of 0.1 mm (0.004 in.). The same alignment error occurred for the 90°

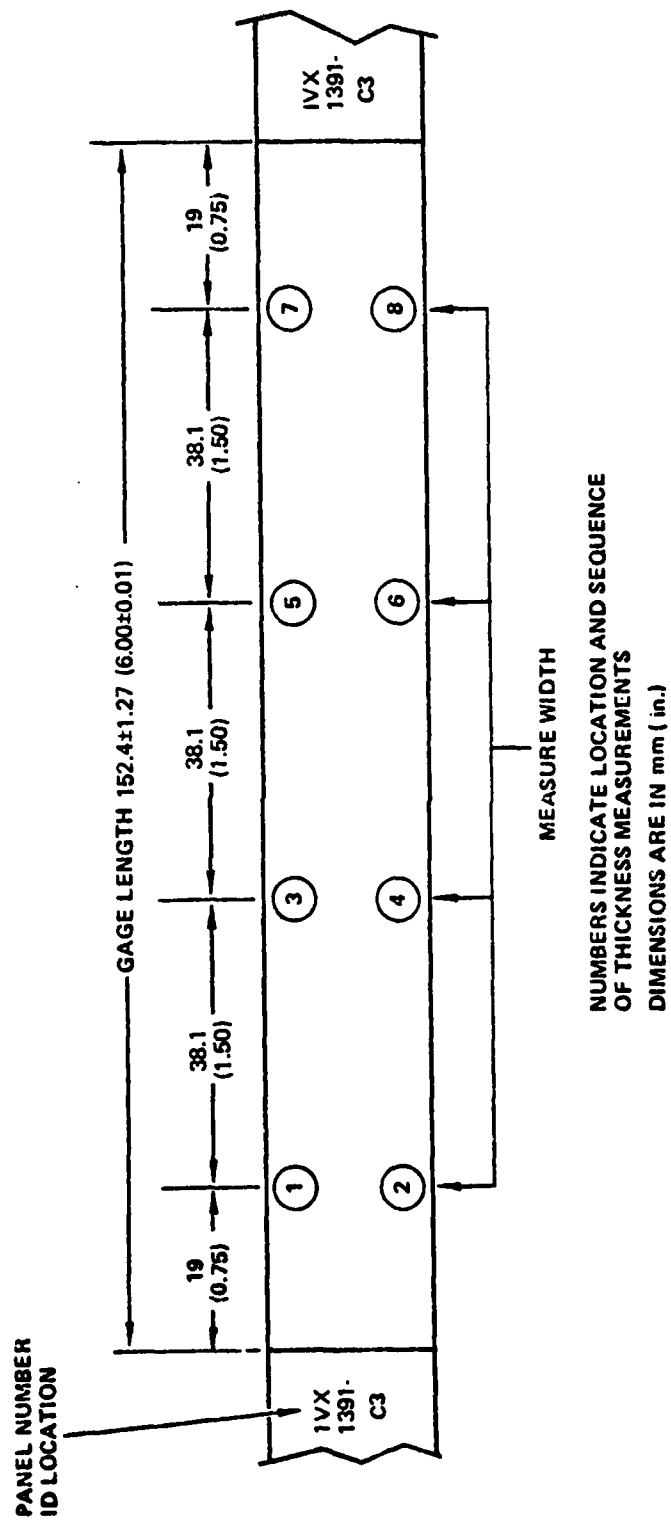


Figure A2: Location of thickness and width measurements

line discontinuities. However, none of the line discontinuities of a $+45^\circ$ or -45° ply aligned with those of another ply of the same orientation. The layup pattern is shown in Section A3, Figures A3 to A5.

This choice of line discontinuity pattern combined with the pattern of coupon location within a panel insured that 90° line discontinuities would lie within the coupon tabs, that all 0° line discontinuities would fall within two coupons of each subpanel (numbers 11 and 22) and that each coupon would be similarly influenced by $+45^\circ$ and -45° line discontinuities. Coupons 11 and 22 from each subpanel were eliminated from the experimental program. The care in panel and coupon manufacture resulted in coupons without 0° or 90° line discontinuities and similarly influenced by $+45^\circ$ and -45° line discontinuities. Thus the results of test program would not be influenced by line discontinuities. This influence was of concern since previous investigations have shown a significant effect of such discontinuities on distributions of static strength and fatigue life^{4,39}.

A.3 QUALITY CONTROL PLAN

Manufacturing and quality assurance procedures will be applied to material and laminates, as described below, to ensure quality, uniformity and traceability of test specimens.

A.3.1 Material Acquisition

Narmco T300/5208 graphite/epoxy prepreg material conforming to Lockheed Material Specification C-22-1032/111 will be acquired for this program in one procurement. Other materials required for the fabrication of test laminates will be purchased to the requirements given in the Lockheed Engineering Purchasing Specification (EPS) Manual, to the extent indicated in section 3. Fiberglass for the specimen tabs will be acquired to Lockheed Material Specification LCM C-22-1032/141.

A.3.2 Material Acceptance

The prepreg material supplier will be required to provide a certificate of conformance, including test data, resin/catalyst age, and date of mixing with each delivery. Lockheed Quality Assurance laboratories will then conduct acceptance tests on the delivered material in confirmation of supplier data. These tests will include:

- **Uncured Properties**
 - Fiber orientation
 - Resin content
 - Volatiles content
 - Resin flow
 - Gel time
 - Infrared Analysis
 - Areal Weight

- Mechanical and Physical Properties of Cured Material

- Void Content
- Specific Gravity
- Cured Resin Content or Fiber Volume
- Interlaminar Shear
- Longitudinal Tensile Strength and Modulus
- Longitudinal Flexural Strength and Modulus
- Cured Ply Thickness

The test methods and acceptance limits shall be as specified in the applicable material specifications, C-22-1379/111 and C-22-1379A. Materials not conforming to the requirements of the Specifications will be rejected.

Material specifications further stipulate preparation-for-delivery provisions covering date of shipment, allowable time and temperature in transit, and vapor-tight packaging required for supplier and transporter conformance. Materials requiring refrigerated storage will be placed in Quality Assurance approved refrigerators immediately upon receipt. Pending acceptance by the Quality Assurance laboratory, all materials will be kept segregated and withheld from use. After acceptance, each container, roll, or spool of material will be stamped or otherwise approved by Quality Assurance and controlling labels will be attached.

A.3.3 Material Processing

This section establishes the requirements and procedures for the lamination of graphite/epoxy (T300/5208) test panels, fabrication of glass/epoxy tab stock and bonding of tabs to coupons.

A.3.3.1 Applicable Documents and Materials

A.3.3.1.1 Lockheed Materials Specifications

The following documents form a part of this procedure to the extent specified herein.

Lockheed Material Specification, C-22-1379A Graphite Fiber Non-Woven Tape and Sheet, Resin Impregnated, General Specification for.

Lockheed Material Specification C-22-1379/111 Graphite Fiber Non-Woven Tape and Sheet, 2410 MPa (350 ksi) Strength, 228 GPa (33 Msi Modulus, 177°C (350°F) Curing, Epoxy Preimpregnated.

Lockheed Material Specification LCM C-22-1032/141 Glass Fabric/Epoxy Preimpregnated, 177°C (350°F) Cure.

A.3.3.1.2 Commercial Materials

The following commercial materials, covered by the Lockheed Engineering Purchasing Specification (EPS) Manual, form a part of this procedure to the extent specified herein.

<u>Material</u>	<u>EPS Item No.</u>
Vacuum Bag Nylon Film	22.9001
Parting Agent Film	22.9004
Porous Release Cloth	22.9030
Peel Ply	25.5910
Stick Contact Adhesive	30.0650

The following commercial materials not covered by the Engineering Purchasing Specification Manual are required for use in this procedure.

American Cyanamid Co.	FM-400 Epoxy Adhesive Film, 3.35 Pa (0.07 lb/ft ²), 177°C (350°F) Cure
Air Tech International Inc.	Flashbreaker 5 Pressure Sensitive Tape

A.3.3.2 Material Control

All materials shall conform to the applicable specifications.

Storage and control requirements shall be as specified in Table A1. Refrigerated material shall be stored in sealed, moisture vapor proof containers.

Refrigerated materials shall be thawed until moisture no longer condenses on the moisture-proof containers.

All perishable materials shall have had validation tests performed within 30 days of use, if initial storage time limit has been exceeded. Validation tests are the same as those shown in Table A1.

A manufacturer's identified defects (MID's) record is furnished with each roll of Gr/Ep by the material supplier. This record shall be furnished to the Composites Laboratory with each roll of Gr/Ep.

Stored perishable material in which visible water is observed in the bag shall be rejected.

TABLE A1: MATERIAL CONTROL

Material	Max. Storage Temp.	Maximum Storage Time Before Retesting, Days		Minimum Required Tests	Max. Allowed Out Time During Proc. @ 23°C (75°F) & 55% R.H.
		Initial	Subsequent		
Gr/ep Prepreg	18°C (0°F)	180	60	△ △	14 days
Adhesive Film	18°C (0°F)	180	90	---	10 days
△ Flow and gel time, room temp, flexural and short beam shear, specific gravity and resin content.					
△ See applicable Material Specifications for test methods and requirements.					

A.3.3.3 Environmental Control

All work shall be done in controlled areas to avoid degradation of the materials and laminates. Temperature shall be between 18-27°C (65-80°F) and relative humidity shall not exceed 55%.

All incoming air into controlled areas shall be filtered by at least a 3.7 cm (1-1/2 in.) thick throw-away type or permanent washable type filter or by an equivalent method. Inspect and clean filters monthly.

A.3.3.4 Tooling

All tools shall be designed and coordinated to produce parts that meet all requirements of this specification and the Engineering drawing. Tools shall have the minimum mass necessary for dimensional and thermal control.

All tool plates used for curing laminates shall be aluminum. Thickness of the caul plate shall be 12.7 mm (0.500 in.) with a tolerance of ± 0.08 mm (± 0.003 in.), flat and parallel. Caul plates used on top surface of laminate under the vacuum bag shall be aluminum sheet 1.62 mm (0.064 in.) standard thickness.

Tooling parting agents and cleaners shall not contaminate the laminates or interfere with subsequent bonding, finishing and inspection.

A.3.3.5 Material Preparation

Templates or patterns shall be placed on the prepreg in such a way as to ensure that the fiber direction is in accordance with Engineering drawing requirements and does not include any MID's flagged by the supplier.

Panels will be laid-up such that the edges of tape are parallel or perpendicular to the required fiber direction within 1°.

All areas from which material will be cut shall be checked prior to cutting for the defects defined in C-22-1379, Quality and Condition Requirements, which may not have been flagged by the manufacturer. Material containing unacceptable defects will not be used. Patch plies are not permitted.

Plies shall be cut with sufficient care so as not to disorient fibers. Cutting tools shall be cleaned prior to use on preregs.

No ply end butt splices are permitted in the laminate assembly.

A.3.3.6 Tool Preparation

The tool molding surfaces shall be solvent wiped and all resin removed prior to layup.

A.3.3.7 Panel Lay-up

The preimpregnated graphite tape shall be placed on the tool in the sequence and orientation specified on the Engineering drawing or Engineering Test Request. As each ply is placed on the assembly, it shall be checked for the defects defined in C-22-1379 prior to applying the ply firmly in place. A check-off system shall be used to assure proper orientation and stacking sequence of each ply.

The surface of each ply shall be wiped with a teflon, polyethylene or equivalent device to give maximum adhesion to the previous ply. Wiping shall be done only in the direction of the fibers to prevent fiber separation and distortion. Wiping the surface should be done only when the orientation of the tape edge has been verified to be within $\pm 1^\circ$ of the drawing requirement. Excessive pressure shall not be applied during wiping and wiping shall be kept to a minimum.

Panels shall be layed up as shown in figures A3 to A5. Parallel $+45^\circ$ or -45° plies shall be laid up so that edge splices are staggered a minimum of 5.08 cm (2.0 in.) in adjacent plies and shall not coincide from one to the next.

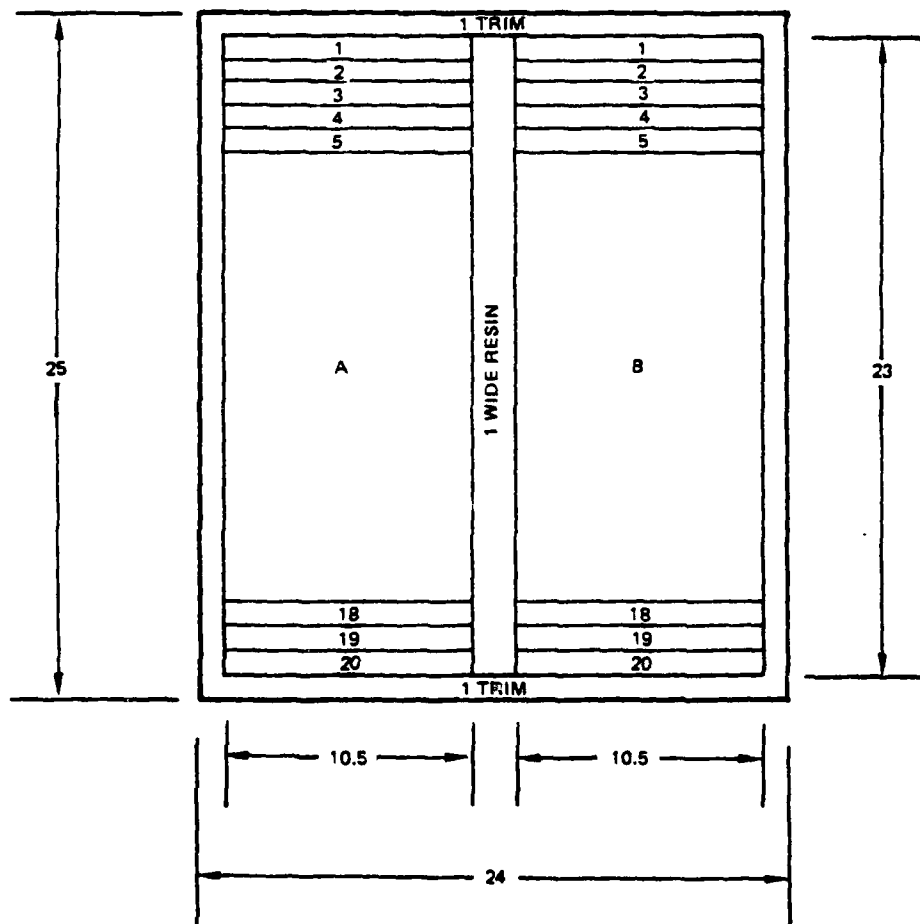
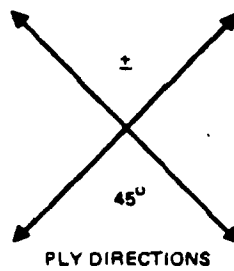
The diagram illustrates the cross-section of a composite laminate with the following layers and dimensions:

- Top Layer (A):** 1 WIDE X 10.5 LONG, 90° COUPONS. Dimensions: 10.5 (height), 1 TRIM (width).
- Second Layer (B):** 90° COUPONS. Dimensions: 10.5 (height), 1 TRIM (width).
- Third Layer (C):** 3 WIDE RESIN. Dimensions: 3 (height), 1 TRIM (width).
- Bottom Layer (D):** 1 WIDE X 10.5 LONG, 0° COUPONS. Dimensions: 22 (height), 1 TRIM (width).

Dimensions and ply counts are indicated on the left and right sides of the diagram:

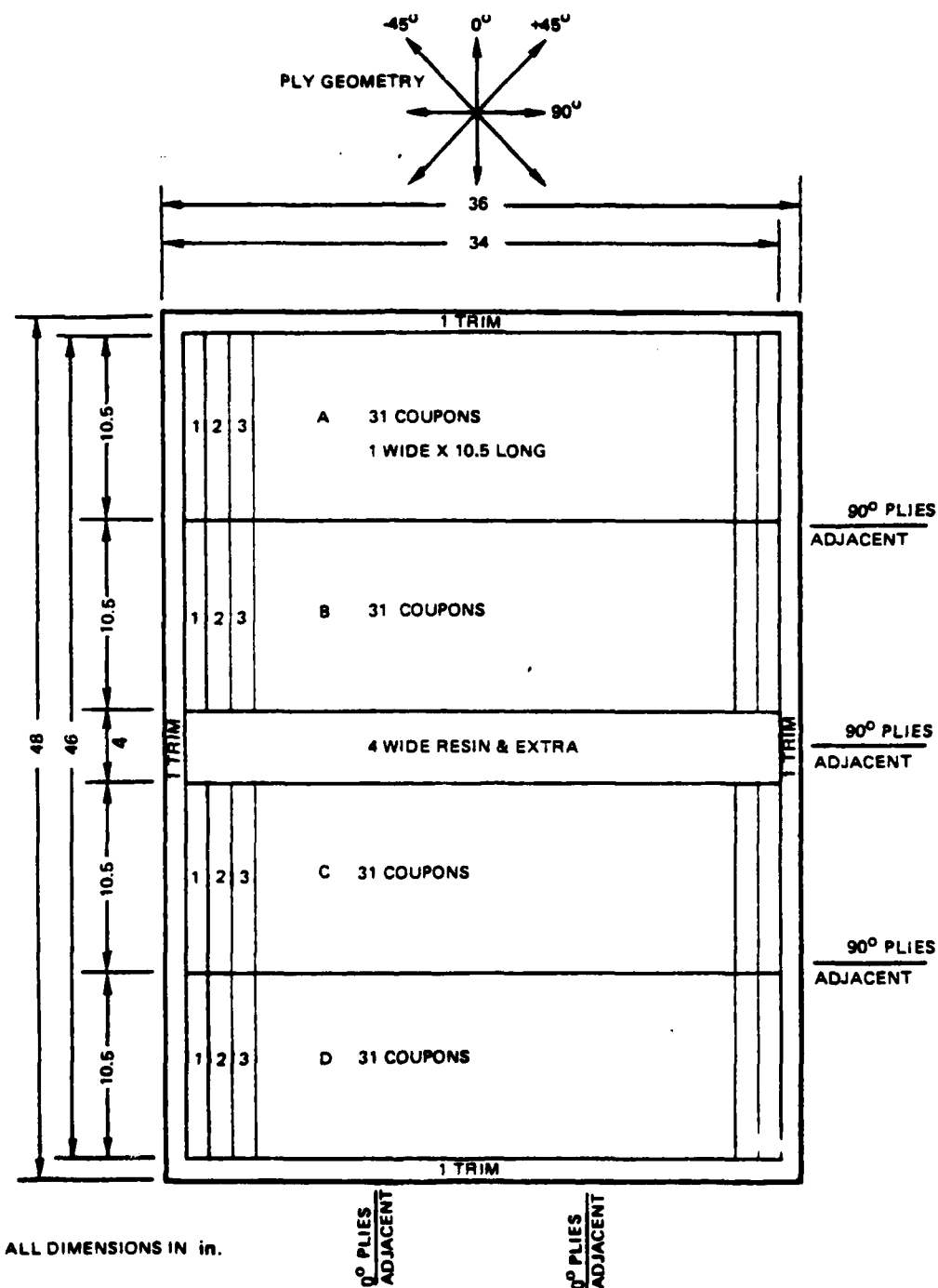
- Left Side Dimensions:** 48 (total height), 46 (height of A and B), 3 (height of C), 22 (height of D).
- Right Side Dimensions:** 18, 19, 20 (ply counts for A and B), 18, 19, 20 (ply counts for C and D).
- Bottom Dimensions:** 11" (width of A and B), 22" (width of C), 24" (width of D).

Figure A3 - Layup of Laminate U1 16 Ply $(0^\circ)_{16}$



NOTE: NO TAPE JOINTS ARE LINED UP THROUGH THE PANEL THICKNESS.
ALL DIMENSIONS IN in.

Figure A4 - Layup of Laminuate U2 16 Ply ($\pm 45^\circ$)_{4S}.



NOTE: 0° AND 90° TAPE JOINTS ARE LINED UP THROUGH PANEL THICKNESS.
45° JOINTS ARE NOT LINED UP

Figure A5 - Layup of Laminuate L1 16 Ply (0/45/90/-45₂/90/45/0)_S.

Edge splices shall be butted flush ± 0.8 mm (± 0.03 in.).

Entrapped air in blisters that cannot be wiped out without distorting fibers shall be removed by puncturing the blister with a needle or pointed sharp blade as often as needed and wiping in the direction of the fibers toward the puncture. Care shall be taken not to damage the under ply fibers.

Where permanent edge steps or dams are not incorporated in the tool for edge thickness control, an edge dam shall be built around the perimeter of the laminate. The dam shall not be more than 1.52 mm (0.06 in.) from the laminate edge and shall be of sufficient height to enclose the laminate. The bleeder may not extend over the dam surface. Joints in the dam shall be kept to a minimum. Dam joint gaps shall not exceed 0.8 mm (0.03 in.).

A dry peel ply of fabric (EPS 25.5910) or equivalent shall be placed on both sides of the layup and wiped smooth.

A bleeding and bagging system of the following construction shall be used.

- (a) Cure plate
- (b) Separator film - perforated parting agent film or porous release cloth.
- (c) Mochburg CW1850 bleeder paper (1 ply for 4 plies of prepreg.)
- (d) One ply of porous Teflon-coated glass cloth (DuPont Armalon)
- (e) Nylon peel ply
- (f) Graphite/epoxy laminate
- (g) Nylon peel ply
- (h) One ply Armalon
- (i) Mochburg CW1850 bleeder paper (4:1 ratio)
- (j) Release film
- (k) Caul plate (aluminum)

- (l) One ply Mochburg CW1850
- (m) Release film
- (n) Glass breather
- (o) Nylon film vacuum bag placed over the laminate and sealed to the tool face.

Curing - Pressure and cure cycle should be within the limits given in Table A2.

A.3.3.8 Laminate Control Specimens

Each panel will be laid up to contain an excess strip at least 2.5 cm (1.0 in.) wide and running either the width of the panel.

Laminate control coupons will be cut from this strip for the determination of resin content, specific gravity and average ply thickness. Test requirements are given in Table A3.

Void volume fraction will be obtained from laminate control coupons from selected panels using standard metallographic techniques. This method will be used to confirm results calculated from the acid digestion and density measurement values for each panel. Void content shall not exceed 1.0% maximum by volume.

TABLE A2 CURE CYCLE

1.	Apply full vacuum.
2.	Heat to $135^{\circ} \pm 3^{\circ}\text{C}$ ($275^{\circ} \pm 5^{\circ}\text{F}$) @ $1 - 2^{\circ}\text{C}$ ($2 - 3^{\circ}\text{F}$)/min.
*3.	Dwell @ 135°C ($275^{\circ} \pm 5^{\circ}\text{F}$) for 30 ± 1 minutes.
4.	Apply 0.69 ± 0.04 M Pa (100 ± 5 psi) vent vacuum to air @ 0.14 M Pa (20 psi).
5.	Heat to $177^{\circ} \pm 3^{\circ}\text{C}$ ($350 \pm 5^{\circ}\text{F}$) @ $1 - 2^{\circ}\text{C}$ ($2 - 3^{\circ}\text{F}$)/min.
6.	Cure for 120 ± 10 min. @ $177^{\circ} \pm 3^{\circ}\text{C}$ ($350 \pm 5^{\circ}\text{F}$).
7.	Cool to $60^{\circ} \pm 3^{\circ}\text{C}$ ($140 \pm 5^{\circ}\text{F}$) under pressure @ less than 2.5°C (4°F)/min.
8.	Cool to room temperature.
*NOTE: Dwell time started when temperature reaches 130°C (265°F).	

TABLE A3: TEST REQUIREMENTS

Test	Requirements
Fiber Volume	66 ± 2%
Specific Gravity	1.56 - 1.60
Thickness/Ply	0.117 - 0.135 mm (.0046 - .0053 in.) (Report for information only)

A.3.3.9 Workmanship

All laminated details and bonded assemblies shall be of highest quality. Conditions in excess of the following shall be cause for rejection.

There shall be no evidence of surface cracking, uncoated fibers, excess resin, pits, tackiness or other indications of defective resin characteristics or distribution.

No visual delaminations are allowed.

No wrinkles containing graphite fibers are permitted. Resin wrinkles caused by peel ply gathering or by the bleeder system shall not be cause for rejection if the resin ridge can be removed without damaging the graphite fibers using 320 grit or finer sandpaper.

The presence of foreign material, e.g., separator film, masking tape, etc., in the part is not acceptable.

There shall be no sharp or frayed edges, nor edge delaminations resulting from trimming and routing operations.

A.3.3.10 Cleanup

Chemical strippers shall not be used in any way to remove excess resin or adhesive. If removal is necessary, it shall be done with an abrasive, and shall not damage any surface graphite fibers.

A.3.3.11 Records

The following records are required for permanent retention and traceability.

1. Temperature-pressure-vent-time profile record for each cure cycle.
2. Thermocouple locations.
3. Material batch and roll number, acceptance laboratory report number and cumulative out-time up to the time of vacuum application.
4. A completed autoclave record sheet as shown in Figure A6.

A.3.3.12 Machining of Test Specimens

Specimens are to be machined to the dimension shown in Figures A7 and A8. Specimen cuts will be made parallel to the panel edge to ± 1 degree. Cutting rates will be chosen to minimize edge damage.

A.3.3.13 Fabrication and Bonding of Glass Fabric/Epoxy Grip Tabs

Grip tab sheet material shall be fabricated by laminating the required number of plies of Style 181, 1581, or 7581 glass fabric/epoxy prepreg. For most standard coupons, the laminate consists of 6 plies or 3 plies in thickness depending on the type of coupon. Thicknesses and other dimensions shall be in accordance with Figures A7 and A8. Tab dimensions shall be as specified on specimen drawing.

The material used for grip tab stock shall be glass/epoxy prepreg conforming to Lockheed Material Spec. LCM C-22-1032/141. This material shall be cured at 177°C (350°F) for one hour under a pressure of 0.24 M Pa (35 psi) plus vacuum. A caul sheet shall be used under a vacuum bag for pressure application.

The adhesive used for bonding tabs to coupons shall be American Cyanamid Co. FM-400, 3.35 Pa (0.07 lbs/ft^2). Aluminum caul plates 0.63 to 1.27 mm (0.25 to 0.5 in.) thick shall be used to apply bonding pressure on tabs.

Run # _____

ETR/Dwg.# _____ Panel I.D. _____ Matl. Code _____

Q.A. Lab. Report # _____ Made for _____ Date _____

I. Description of Materials

Designation _____ Batch# _____ Roll# _____ Date Mfd. _____

No. of Plies _____ Orientation _____

CURE CYCLE (NARMCO)

II. Cure Press. _____ psi

Cure Temp _____ °F

Cure Time _____ min.

Vac. Bag _____ inch-Hg

1. Apply fuel vacuum

2. Heat to $275^{\circ} \pm 5^{\circ}\text{F}$ @ $2-3^{\circ}\text{F}/\text{min}$.*3. Dwell @ $275^{\circ} \pm 5^{\circ}\text{F}$ for 30 ± 1 min.4. Apply 100 ± 5 psi & vent vac to air @ 20 ± 5 psi.5. Heat to $355 \pm 5^{\circ}\text{F}$ @ $2-3^{\circ}\text{F}/\text{min}$.6. Cure 120 ± 10 min. @ $355 \pm 5^{\circ}\text{F}$ 7. Cool to $140 \pm 5^{\circ}\text{F}$ under press. @ $<4^{\circ}\text{F}/\text{min}$.

8. Cool to R.T.

III. Autoclave Pressurization

Time @ start _____

Time @ press. _____

Delta Time min. _____

IV. Temp _____ °

* NOTE: dwell time starts when temp reaches 265°F .

V. Temp _____ °F @ lay-up

V. %R.H. _____ @ lay-up

VI. TIME RECORD

	1	2	3	4	5
Temp Time	Temp Time	Temp Time	Temp Time	Temp Time	Temp Time
Start heat					
At temp.					
Time to temp min.					
Time @ temp min.					OFF _____
Heat-up rate °F/min.					
Cool-down rate °F/min.					

VI. Panels

I.D.	Size(in.) x	No. Plies	Meas. Thick

IX. Comments

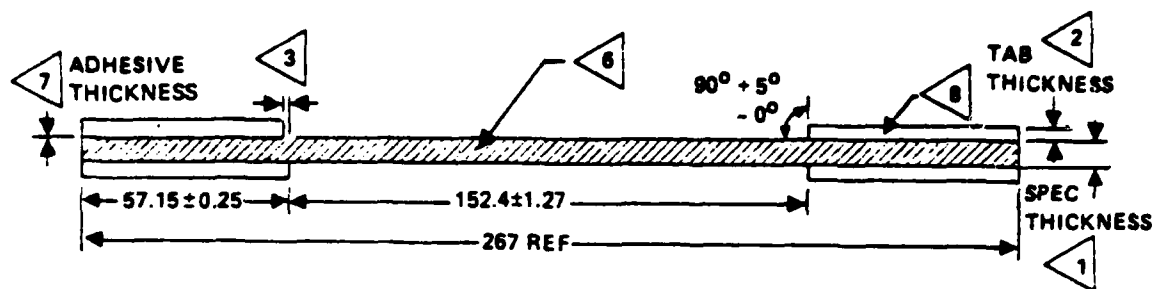
VIII. Bleeding & Bagging

_____	nylon bag
_____	18l glass breather
_____	vac pac
_____	Mochburg (1 ply)
_____	caul plate
_____	vac pac
_____	Mochburg (4:1 ratio)
_____	armalon
_____	nylon peel ply
_____	LAMINATE
_____	nylon peel ply
_____	armalon
_____	Mochburg
_____	vac pac
_____	cure plate

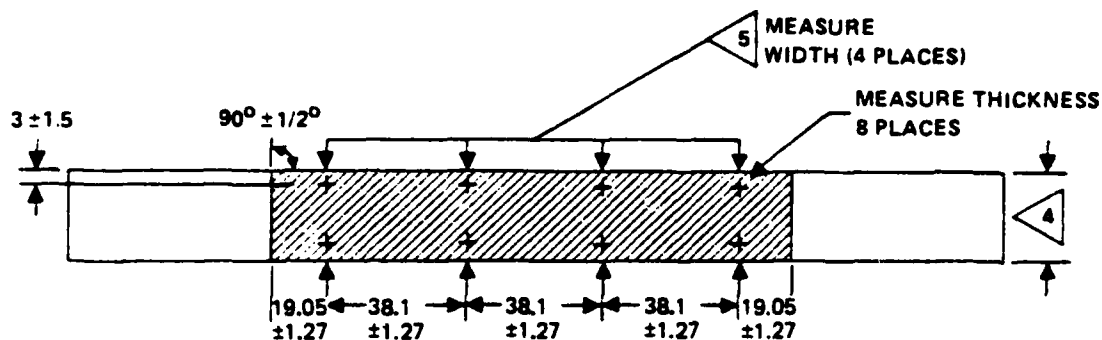
Signature of Inspecting Engineer _____

NOTE: Laminate completely damaged
perforated vac pac taped to dam.

Figure A6 - Sample Autoclave Record.

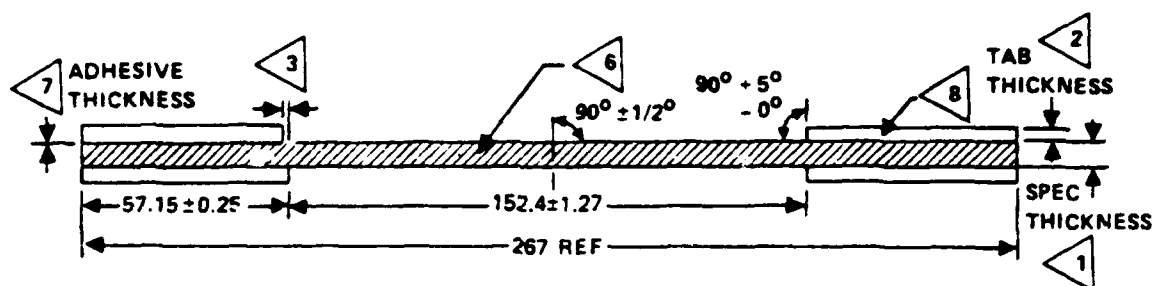


ALL DIMENSIONS IN MILLIMETERS

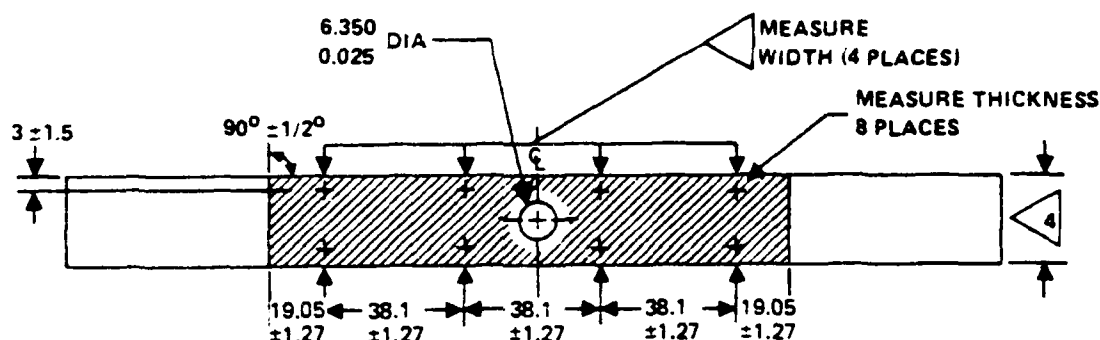


- <9> SPECIMENS TO BE FLAT OVER THE ENTIRE 267 mm (10.5 in.) LENGTH WITHIN 0.25 mm (0.01 in.)
- <8> TAB EDGES TO BE PARALLEL TO SIDES OF SPECIMEN WITHIN 0.025 mm (0.001 in.) OVERHANG NOT TO EXCEED 3.8 mm (0.003 in.)
- <7> THE TAB AND SPECIMEN BONDING SURFACES TO BE THOROUGHLY SOLVENT CLEANED USING METHYL-ETHYL-KETONE PRIOR TO BONDING. A 177°C (350°F) CURING ADHESIVE IS TO BE USED AND MUST COVER ENTIRE SURFACE UNIFORMLY.
- <6> SPECIMENS TO BE CUT DRY MACHINED SURFACES TO BE rms 50 OR BETTER. NO EDGE DAMAGE OR FIBER SEPARATION SHOULD BE VISIBLE UNDER 10X MAGNIFICATION.
- <5> MEASURE SPECIMEN WIDTH 4 PLACES. WIDTH MUST NOT VARY BY MORE THAN 0.102 mm (0.004 in.)
- <4> SPECIMEN WIDTH TO BE 22.225 ± 0.127 mm (0.875 ± 0.005 in.)
- <3> MISMATCH OF TABS FROM SIDE TO SIDE NOT TO EXCEED 0.25 mm (0.01 in.)
- <2> TABS TO BE CUT FROM AN 6 PLY LAMINATE FABRICATED FROM PREPREG OF 1581 GLASS FABRIC IN A 177°C (350°F) CURING EPOXY.
- <1> SPECIMEN THICKNESS TO BE WITHIN ± 0.08 mm (± 0.003 in.) OF THE AVERAGE OF 8 THICKNESS MEASUREMENTS.

Figure A7 - Unnotched Composite Test Specimen



ALL DIMENSIONS IN MILLIMETERS



- 9 SPECIMENS TO BE FLAT OVER THE ENTIRE 267 mm (10.5 in.) LENGTH WITHIN 0.25 mm (0.01 in.)
- 8 TAB EDGES TO BE PARALLEL TO SIDES OF SPECIMEN WITHIN 0.025 mm (0.001 in.) OVERHANG NOT TO EXCEED 3.8 mm (0.003 in.)
- 7 THE TAB AND SPECIMEN BONDING SURFACES TO BE THOROUGHLY SOLVENT CLEANED USING METHYL-ETHYL-KETONE PRIOR TO BONDING. A 177°C (350°F) CURING ADHESIVE IS TO BE USED AND MUST COVER ENTIRE SURFACE UNIFORMLY.
- 6 SPECIMENS TO BE CUT DRY. MACHINED SURFACES TO BE rms 50 OR BETTER. NO EDGE DAMAGE OR FIBER SEPARATION SHOULD BE VISIBLE UNDER 10X MAGNIFICATION.
- 5 MEASURE SPECIMEN WIDTH 4 PLACES. WIDTH MUST NOT VARY BY MORE THAN 0.102 mm (0.004 in.)
- 4 SPECIMEN WIDTH TO BE 22.225 ± 0.127 mm (0.875 ± 0.005 in.)
- 3 MISMATCH OF TABS FROM SIDE TO SIDE NOT TO EXCEED 0.25 mm (0.01 in.)
- 2 TABS TO BE CUT FROM AN 6 PLY LAMINATE FABRICATED FROM PREPREG OF 1581 GLASS FABRIC IN A 177°C (350°F) CURING EPOXY
- 1 SPECIMEN THICKNESS TO BE WITHIN ± 0.08 mm (± 0.003 in.) OF THE AVERAGE OF 8 THICKNESS MEASUREMENTS.

Figure A8 - Notched Composite Test Specimen.

Cure adhesive at $177^{\circ} \pm 3^{\circ}\text{C}$ ($350^{\circ}\text{F} \pm 5^{\circ}\text{F}$) for 60 to 70 minutes using 0.10 ± 0.01 M Pa (15 ± 1 psi) positive pressure on bondline (no vacuum). Cool to 77°C (170°F) under pressure.

A.3.4 Quality Assurance Provisions

To produce test panels of consistent quality, strict adherence to all the minimum Engineering requirements of Section A.3.3 is vital. The requirements of Section A.3.4 are intended to outline the minimum amount of inspection and surveillance before, during, and after processing testing to confirm that adherence has been achieved.

A.3.4.1 Material

Verification shall be made that only adhesives and prepreg materials are used that are approved to the material specifications specified.

Adhesive or prepreg material which is stored below room temperature shall be wrapped in a closed impermeable bag at all times. Evidence of material cracking or moisture condensation on the material is cause for rejection. Exposure to ambient temperature shall be minimized.

Adhesive or prepreg material which is withdrawn from storage and left out 30 minutes or more before returning to the box, shall have the out-time marked on an appropriate tag attached to the roll. Material for which accumulated out-time at ambient temperature exceeds the allowable out-time given in table A, shall not be used.

All adhesive and prepreg materials shall be controlled as to batch, lot, and roll numbers for traceability.

Material which has exceeded the allowable storage shall not be used unless tested within one week prior to use.

All refrigerated materials shall be checked for compliance to Section A.3.3.2 prior to use.

A.3.4.2 Identification

Panels and coupons shall be clearly marked before and after application of tabs to indicate the bag side of the graphite/epoxy laminate as originally cured. Panels shall be identified with a number including material code and autoclave run number. Coupons shall be identified with panel number from which cut and a dash number indicating location.

Example: 1VX1391-A7

Coupons shall be numbered consecutively as they are cut from panels to indicate relative location of the panel (see Figures A3, A4 and A5).

Equipment and facilities used for materials storage, processing, and inspection shall be controlled in accordance with LCP79-1053.

A.3.4.3 Quality Control System

An effective quality control system shall be provided to ensure compliance with the requirements of this procedure as specified in the following sections.

Material Acceptance testing will be performed by Lockheed Quality Assurance Laboratories.

Panel and tab fabricating and tab bonding will be accomplished by personnel of the Composites Laboratory at Rye Canyon Research Laboratories. Layup and cure of each panel will be witnessed and inspected by Engineering.

Dimensional inspection of specimens will be the responsibility of the machining company.

The principal investigator will have final acceptance/rejection authority for material, panels and specimens.

An engineering approved autoclave record will be maintained for each panel.

A.3.3.4 Non-Destructive Inspection

All test panels shall be non-destructively inspected for internal defects by ultrasonic "C" Scan procedure. Standard reference 0.005 mm (0.002 in.) thick teflon pads of 3.175 and 12.37 mm (0.125 and 0.500 in.) diameter will be placed at one corner of each panel. A permanent record of the C-Scan results shall be retained with the records required in A.3.3.11.

Specimens will not be cut from areas in the panels which show indications comparable to the standards.

APPENDIX B
EXPERIMENTAL PROCEDURES

B1.0 MONOTONIC TENSION AND COMPRESSION

For both monotonic tension and compression tests, load and deflection were continuously read out on an X-Y recorder so that stress-strain curves could be constructed. For the laminate tests, strain gauges were used to record strain, and stress-strain curves were displayed on a CRT screen by a computer after which hard copies were made. Ultimate strength, strain to failure, and the apparent modulus of elasticity were calculated. Stress was calculated using the coupon average area based on four locations equally spaced within the gauge length. An enclosure (metal or acrylic) surrounded the test equipment for the lamina, elevated temperature testing. The internal space was supplied with heated air. The arrangement provided specimen temperatures which were uniform throughout the gauge length and controlled to $\pm 1^{\circ}\text{C}$ ($\pm 2^{\circ}\text{F}$); the use of a convection heating or cooling ensured against local variations in specimen temperature such as may go undetected when radiant heating is used.

Monotonic tension tests of laminates U1 and U2 were conducted in a 534 kN (120 kip) Baldwin test machine while those for L1 were conducted in a 440 kN (100 kip) MTS machine. All testing was conducted similar to the procedures of ASTM D3039-74. Tests were conducted using MTS hydraulic self-aligning grips. Coupon alignment was assured by using a special exterior fixture attached to the grip assembly. Because coupon width varied only within ± 0.012 mm (± 0.005 in.), the alignment procedure assured end-to-end coupon alignment within ± 0.076 mm (± 0.003 in.). A 50.8 mm (2 in.) extensometer was used to record deflection. Testing was conducted at a standard rate of approximately 0.01 mm/mm/min.

The experimental procedures selected for monotonic compression testing were of two types: one a fully constrained mode²¹ and one a column buckling mode using the compression fatigue fixture. These procedures enabled the same coupon geometry used for monotonic tension and for fatigue testing to be used for monotonic compression. The test results of fully constrained coupons should be thought of in terms of column buckling under compression load in that the test condition consists of the state where the unsupported column length is zero. Thus the test results correspond to an inelastic (fully constrained) failure mode while the results of the coupons tested in the compression fatigue fixture correspond to an inelastic short column length failure mode.

In graphite/epoxy composite, compression failure is often assumed to be elastic and brittle, to correspond to the true compression strength, and to be essentially equivalent to the tensile strength. In practice, the composite responds inelastically in a manner not dissimilar to the macroscopic behavior of metals loaded in compression. Compression properties are dependent on test constraint and thus reflect the inelastic properties of the laminated structure formed of matrix and fibers which tend to buckle locally. Final fracture has a brittle-like appearance, but should be thought of as an inelastic phenomena. In this sense, an ultimate compression strength does not exist for composites similar to the situation for metals. These considerations are more fully discussed elsewhere⁴⁰. Monotonic, fully supported, compression tests were conducted using the same 534 kN (120 kip) Baldwin and 440 kN (100 kip) MTS test machines used for the tension tests. Lamina tests were run at a strain rate of approximately 0.01 mm/mm/min.

B2.0 FATIGUE TEST PROCEDURES

Fatigue testing was accomplished using closed-loop, electro-hydraulic, servo controlled, testing machines of 89 kN (20 kip) maximum allowable load. Each

machine was equipped with a peak and valley load monitoring system which allowed continuous monitoring of the load signal maximum peak, maximum valley, and minimum peak and minimum valley such that load accuracy was maintained within $\pm 1.0\%$ of the full-scale reading. Fatigue grips were of the friction bolt type with integral alignment fixtures, see Figure B1. Coupon alignment was maintained within ± 0.0762 mm (± 0.003 in.) in any direction. All tests were conducted at 10 Hz. Figure B2 shows a typical tension-tension (T-T) fatigue test set up and coupon failure. Minimum load in tension-tension (T-T) fatigue tests was approximately 200 N (50 lb.)

Tension-compression (T-C) and compression-compression (C-C) fatigue tests were conducted using the fixture shown in Figure B3. The fixture is a six-bay, column buckling restraint type selected because the buckling of coupons in monotonic compression in such fixtures is well understood⁴⁰. The two end bays are of a shorter length than the six interior bays, this was planned so that the end bay grip fixture simulated the fully unstrained condition.

Preliminary experiments were conducted, to evaluate the fixture, by subjecting coupons to increasing load up to 345 MPa (50 ksi) and measuring out of plane deflection. Such deflection was found not to exceed 0.0254 mm (0.001 in.) in one bay for repeated loadings of one coupon and to be at least less than 0.0025 mm (0.0001 in.) in the other bays. The experiment was repeated with two other coupons and again out of plane deflection at 345 MPa (50 ksi) was 0.0254 mm (0.001 in.) and in the other 0.0125 mm (0.0005 in.). These experiments verified that the fixture restraint met the prior expected constraint of out of plane deflection being limited to 0.0254 mm (0.001 in.). In addition, the bay in which such a maximum deflection value was recorded varied from coupon to coupon.

The amount of out of plane deflection in the six bay fixture was identical to that previously found using a different fixture type⁴, thus allowing

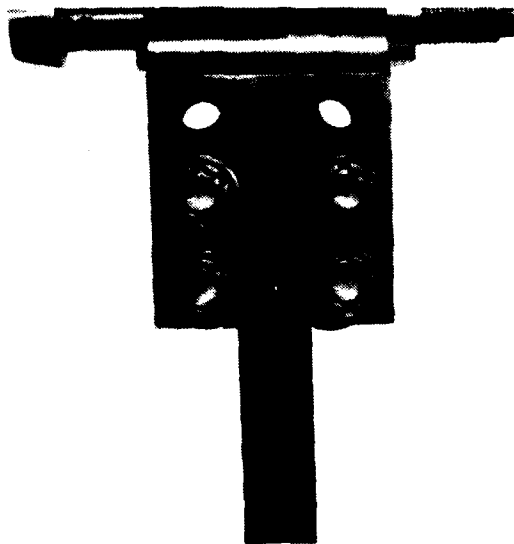


Figure B1: Fatigue Grip

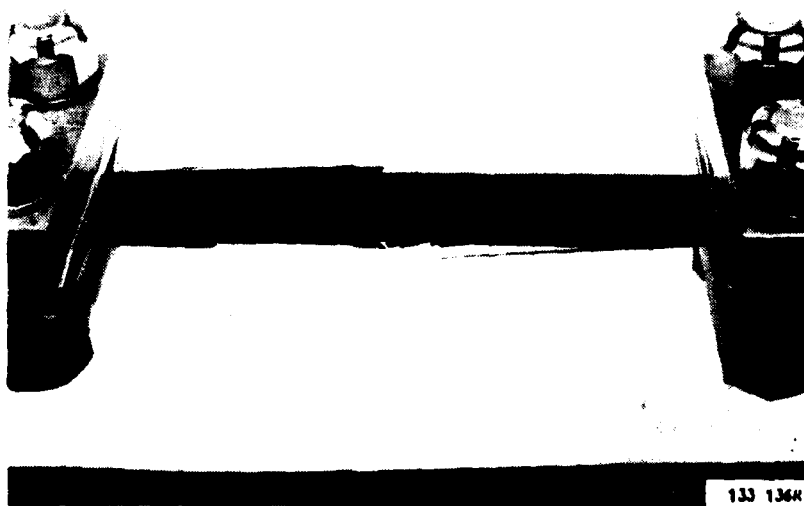


Figure B2: Tension-Tention Fatigue Test Showing Failed Quasi-Isotropic Laminate Coupon.



Figure B3: Compression Fatigue Fixture

direct comparisons of the data. On the basis of stress range, the results at 207 and 138 MPa (30 and 20 ksi) maximum stress (414 and 276 MPa (60 and 40 ksi stress range)) were similar to those found previously^{4,9} for this material using a three bay, two stiffener constraint system. In the previous case, our of plane buckling also was restricted to 0.0254mm (0.001 in.). The similarity of the fatigue loading results shown in Table B1, even for the higher stress ranges, strongly supports the hypothesis that buckling instability controls fatigue life when compression loads are present. The constraint fixture used in this program was designed based on that hypothesis.

Fatigue tests were conducted by first dialing to the calculated mean load and setting the amplitude control such that the maximum load was approximately equal to 95% of the desired maximum load. Five or less cycles were then applied and the load time history recorded on high speed visicorders. This eliminated any possibility of a first cycle load overshoot and allowed the load at failure to be recorded for any first cycle failure coupon. The span control was subsequently increased such that minimum and maximum load were those desired. The peak and valley controls shutdown the fatigue loading and returned the load to the mean value if any load deviations beyond 0.5% were detected.

B3.0 DATA ANALYSIS

For fatigue resistant design, one of the major questions concerning application of damage tolerance concepts is specification of percent levels of probability of survival. This question arises because of the need to translate reliability and confidence measures of data to parallel ones for design requirements⁴¹. In fatigue, reliability can often be successfully defined in terms of the Weibull survivorship function. In Task IV of this program, all of the test data results were statistically analyzed and compared using a Weibull⁴² distribution.

TABLE B1

EFFECT OF CONSTRAINT TYPE AND STRESS RANGE ON
FATIGUE LIFE OF QUASI-ISOTROPIC LAMINATE OF T300/5208

Environment: Room Temperature, Laboratory Air

Fixture Type	Stress Range,		Average Cycles to Failure, N_f
	MPa	ksi	
a	503	86	508
b	639	100	301
a	558	81	1742
b	552	80	4597
a	421	61	32030
b	414	60	42772
a	290	42 ^c	$>1 \times 10^6$
b	270	40	$>1 \times 10^6$

a - Two stiffener, three bay constraint of the type previously reported ¹

b - Six bay, pin supported fixture of the type used in this program.

c - T300/934 material.

B.3.1 General Discussion of Weibull Function

In Weibull's representation of the statistics of fatigue, there are two random variates at each stress test condition. The first of these variates is the ordered sequence of the numbers of cycles to failure for each test result, n_i :

$$n_i: (n_1, n_2, n_3 \dots n_N)$$

The second random variate, x , is continuous and is the argument of the Weibull survivorship function, or probability of survival, expressed as

$$P(x) = \exp [-((x-e)/(v-e))^k], \quad (B1)$$

where

$$x \geq e, v \geq e, k > 0, P(e) = 1, P(v) = 1/\exp(1).$$

The connection between the random variates, n_i and x , is entirely empirical. In practice, numerical procedures are used to derive the three Weibull parameters k , e , and v by means of the approximation:

$$P(x) = 1 - i/N \text{ when } x = n_i, \quad (B2)$$

or

$$P(x) = 1 - 1/(N + 1).$$

For equation (B1), the mean of the sample set is given by ⁴²:

$$\bar{x} = e + (v-e) \Gamma(1 + 1/k) \quad (B3)$$

the median by:

$$x = e + (v-e)(\log_e 2)^{1/k} \quad (B4)$$

and the mode by:

$$x = e + (v-e)(1 - 1/k)^{1/k} \quad (B5)$$

where $\Gamma(\)$ indicates the incomplete Gamma function.

During the past twenty-five years, a number of names have been applied to the parameters. In general, parameters e and v are considered as scale parameters or factors and the exponent k as a sharp parameter. The term threshold parameter is usually applied to parameter e and the term characteristic value to v . In analysis of composite data, k is frequently denoted by β and v by F . The scale parameter, e , is often referred to as the minimum life estimate. With this choice of words, e is suggested on physical grounds to be $e \geq 0$. Many authors have reasoned further that since $e \ll n_i$, $i = 1, 2, 3, \dots, N$, the Weibull survivorship function can be appropriately reduced to dependence on two parameters, k and v , with $e = 0$ arbitrarily. An argument against this practice will be described in this section.

The influence of the shape parameter k can be explained as follows. Define a reduced variate Z as:

$$Z = (x-e)/(v-e), \quad Z \geq 0, \text{ dimensionless}, \quad (B6)$$

and express the probability of survival function as:

$$P(x) = \exp \left[-Z^k \right], \quad k > 0, \quad (B7)$$

where $P(Z) = 1/\exp(1)$ when $Z = 1$,

and $P(Z) = 1$ when $Z = 0$, for all k ,

If $k < 1$, this is sometimes interpreted as implying that the material develops resistance to fatigue as the number of load cycles is increased. If $k = 1$, the Weibull survivorship function reduces to the constant failure rate relation commonly used in reliability studies. If $k > 1$, one can inquire whether the test material experiences progressive damage as numbers of load cycles are increased.

Figure B4 illustrates the manner in which $P(Z)$ is dependent on the shape parameter k for the range of the reduced variate Z from zero to two. Empirical evidence does not support the interpretation that k might be a smoothly increasing function of stress amplitude. For practical purposes, in the case of structural fatigue, the region of Figure B4 of most interest to designers is bounded as follows:

- (a) Above by the limit $P(Z) = 1.0$
- (b) Below by the median $P(Z) = 0.5$
- (c) On the left by the curve $P(Z) = \exp [-Z]$
- (d) On the right by the curve $P(Z) = \exp [-Z^{-10}]$.

B.3.2 Weibull Analysis Procedures

There are three principal procedures which have been used to determine the Weibull parameters (k , e , and v) for a given data set. These are: the moment estimation (ME) method; the maximum likelihood estimation (MLE) procedure; and some form of the linear regression (LR) procedure. All three methods are also used to determine the unknown parameters of other types of fitting functions. The ME method principally consists of equating several

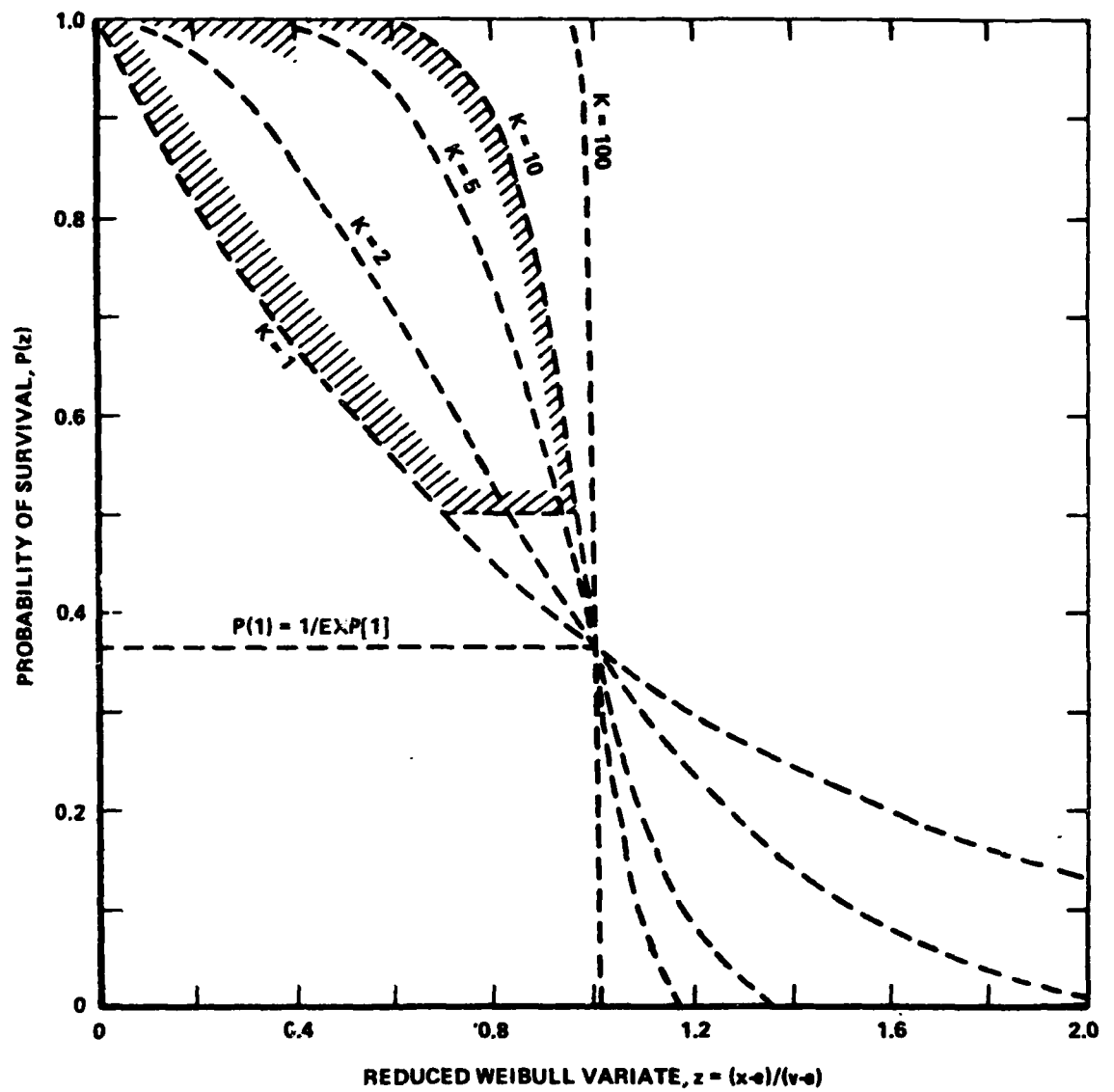


Figure B4: Influence of Shape Parameter k on Probability of Survival

AD-A118 084

LOCKHEED-CALIFORNIA CO BURBANK RYE CANYON RESEARCH LAB

F/G 11/4

EFFECT OF LOAD HISTORY ON FATIGUE LIFE.(U)

DEC 81 J T RYDER, K N LAURAITIS

F33615-78-C-5090

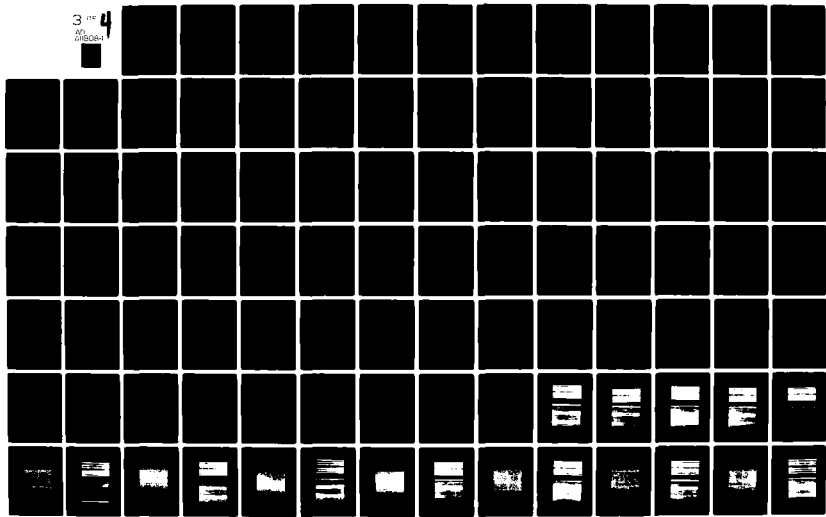
UNCLASSIFIED

LR-29586-1

AFWAL-TR-81-4155

NL

3 4
AT
000001



population moments (equal to the number of unknown parameters) to the sample moments. The MLE method consists of setting the partial derivatives of the logarithm of $P(X)$, with respect to the parameters sought, equal to zero. In the LR procedure, the Weibull survivorship function is reduced to a linear equation. For the LR method, the solution for a two-parameter Weibull function is straightforward, but in the three-parameter case the solution is found by optimization of the correlation coefficient or by matching the sample skewness coefficient.

When one of the above described procedures was originally selected⁹ for analyzing graphite/epoxy composite strength and fatigue data, consideration was given to two thoughts. First, how well does the resultant Weibull survivorship function represent the original data set? Second, what, if any, extrapolative potential exists for the resultant function? Consideration of these two questions led to the selection of the LR procedure. The reasons for this selection will be described in detail along with references to recent work which supports the original choice.

Both the ME and MLE methods require homogeneous samples. The reason for this requirement is that in the ME procedure the Weibull density function is integrated while in the MLE procedure, partial derivatives of the function are obtained. In this program, requirement of homogeneity was not assumed, a priori, to be necessarily met by sample information obtained from fracture data of composites. A procedure was desired which would be sensitive to the possible existence of multicomponent strength and fatigue life data. Such a requirement appears to be met by a LR procedure⁴³. The ME method can result in significant errors in estimation of k , e , and v ⁴³ and such errors increase as k increases. In the case of two-parameters, errors in estimation of k and v increase linearly with the true value of e (assumed to be zero) and can be greater than 100% when $e \geq v$ ⁴³. For the MLE procedure, three difficulties are encountered. First, the MLE solution of a data set is often a local maximum, but is not necessarily the maximum likelihood

estimate⁴³⁻⁴⁷. Weibull and Weibull⁴⁴ found in a study of 300 random samples of 10 and 20 points each that approximately half of the estimates were not the maximum likelihood estimate, but were local maximums. Second, valid data sets can occur for which convergent solutions are not forthcoming, particularly for three parameter solutions⁴⁷. Third, if a given data set which actually belongs to a three-parameter Weibull population is assumed to be a two-parameter population ($e = 0$), the estimates of k and v can be significantly higher than their true values⁴³.

As previously alluded in the analysis of graphite/epoxy composite data, the parameter e is often set equal zero. This practice greatly simplifies the mathematics especially for MLE procedures; however, there are strong objections against such a practice^{42,43,47}. These have already been discussed with reference to the ME and MLE procedures and are based upon the statistical error induced by the practice of setting $e = 0$. In summary, the three-parameter Weibull fit can be shown to fit the actual data set better than the two-parameter^{42,43,47}. However, objections against the three-parameter Weibull fitting procedure are often raised upon the grounds that the parameter e may be found to have a negative value, particularly for a fatigue data set. The objection is thus raised that actual coupons can not have a finite probability of failure when the applied load is zero. Setting e equal to zero solves this problem. Setting e equal to zero is principally related to the question of the extrapolative capability of the Weibull function for graphite/epoxy composite fracture data.

Setting $e = 0$ results in the probability of survival, P_s , being equal to 1 when no load is applied to a coupon. While this is a reasonable expectation, the accuracy of fit in the range of the data is often sacrificed. At the same time, the resultant extrapolative estimates of strength and fatigue life at $P_s > 0.90$ may still be intolerably conservative. Therefore, in many cases by setting $e = 0$ little may be gained, and much lost. This problem is most critical for fatigue life data.

The problem of correctly extrapolating composite fatigue data is presently one of conjecture. This is due to three deficiencies: 1) large laboratory data sets for evaluating extrapolation from small subsets; 2) experimental data which correlates laboratory coupon results with structural test results; 3) field service experience. Therefore, while e should be greater than or equal to zero if it is truly a threshold parameter, correct values can not be determined at this time. Thus, setting $e = 0$ reduces the accuracy of our calculated fit to the data set but most likely results in extrapolative predictions being too conservative.

A possible solution to these problems has been suggested by Bowie, Besari, and Trapp⁴⁷ and will be discussed below. For the present, a three-parameter Weibull analysis procedure has been used throughout this report. The resultant analytical solutions closely fit the data and avoid the problems of ME and MLE solution procedures. The resultant functions are not of extrapolative value, but this is not considered to be pertinent for comparison of data sets. Significant statistical analysis effort combined with extensive experimental investigations are needed before any extrapolative procedure can be developed and used with confidence. Hence, using a procedure which does not allow for extrapolation is not considered at the present time to be detrimental.

B3.3 Description of Selected Analysis Procedure

The particular form of Weibull analysis used in this report has been discussed in detail elsewhere^{41,47}. Essentially, this procedure which consists of linear regression analysis in Z variate space, is similar to that used by Talreja⁴³. The analysis procedure used is described in this section.

In the analytic procedure used in this program, an initial estimate was made of the probability of survival based directly on the test results, in a staircase manner, $P(n_i)$, $i = 1, 2, 3, \dots, N$.

where

$$P(n_1) = 1 - 1/N$$

$$P(n_2) = 1 - 2/N$$

$$P(n_3) = 1 - 3/N$$

$$\cdot \quad \cdot$$

$$\cdot \quad \cdot$$

$$\cdot \quad \cdot$$

$$P(n_N) = 1 - N/N = 0.$$

The function $P(n_i) = 1 - i/N$ was selected instead of the alternate function, $P'(n_i) = 1 - i/(N+1)$. The difference $(P'(n_i) - P(n_i))$ diminishes as N increases. Thus for N equal to or greater than approximately 15, as in this investigation, the difference is undetectable. However, if extrapolations to probability of survival in the range above 90% are to be attempted, the choice of $P(n_i)$ rather than $P'(n_i)$ as initial distribution is the more conservative approach⁴¹. This is especially true for N less than 15.

With the above approach, the initial distribution is defined as:

$$P(n_i) = 1 - i/N$$

and

$$P(n_{i+1}) = 1 - i/N \text{ if } n_{i+1} = n_i$$

otherwise

$$P(n_{i+1}) = 1 - (i+1)/N$$

In most other analysis procedures, $P'(n_i) = 1 - i/(N+1)$ is selected as the initial description without regard to replication of the type: $n_{i+1} = n_i$. The choice of assigning the same initial probability to different coupons with the same n_i was considered appropriate because they do actually form a local mode, within the limits of testing accuracy, of the sample distribution obtained by experiment.

The appropriate variables of Equation B1 are found by forming $N-1$ relations:

$$P(n_i) = 1 - i/N = \exp [-((n_i - e)/(v - e))^k]$$

$$\begin{array}{c}
 P(n_2) = 1-2/N = \exp [-((n_2-e)/(v-e))^k] \\
 \cdot \quad \quad \cdot \quad \quad \cdot \\
 \cdot \quad \quad \cdot \quad \quad \cdot \\
 \cdot \quad \quad \cdot \quad \quad \cdot
 \end{array}
 \tag{B8}$$

$$P(n_N) = 1-(n-1)/N = \exp [-((n_{N-1}-e)/(v-e))^k]$$

The last relation for N is not used since $P(N) = 0$.

The parameters of Equation B1 were found by reducing the relationships of Equation B8 to the linear equation:

$$Y = bX + a \tag{B9}$$

The three-parameter Weibull linear equation is:

$$[-\ln P(X)]^{1/k} = bX + a,$$

where

$$e = -a/b$$

(B10)

and

$$v = (1+be)/b.$$

For the two-parameter Weibull function ($e = 0$), the linear equation is:

$$\ln(-\ln(p(X))) = b \ln(x) + a, \tag{B11}$$

where

$$k = b$$

and

$$v = \exp(-a/b).$$

A linear regression method is used to determine k , e , and v . The initial order distribution is:

$$P(X_i) = 1-i/N_p, \quad i = 1, 2, 3 \dots N_p \tag{B12}$$

Regression coefficients are found by least square analysis of $N_p - 1$ equations such as:

$$-\ln(1-i/N_p)^{1/k} = bX_i + a, \quad i = 1, 2, 3 \dots N_p-1. \tag{B13}$$

The sample correlation coefficient, R, is calculated as:

$$R = \frac{M \sum_{i=1}^M Y_i (aX_i - b) - \sum_{i=1}^M Y_i \sum_{i=1}^M (aX_i + b)}{\left[\left(M \sum_{i=1}^M Y_i^2 - \left(\sum_{i=1}^M Y_i \right)^2 \right) \left(M \sum_{i=1}^M (aX_i + b)^2 - \left(\sum_{i=1}^M (aX_i + b) \right)^2 \right) \right]^{1/2}} \quad (B14)$$

where $M = N_p - 1$

The coefficients of linear regression and alternative correlation coefficient r are calculated by means of the following steps:

$$S_x = \frac{\left[M \sum_{i=1}^M X_i^2 - \left(\sum_{i=1}^M X_i \right)^2 \right]^{1/2}}{M (M-1)}$$

$$S_y = \frac{\left[M \sum_{i=1}^M Y_i^2 - \left(\sum_{i=1}^M Y_i \right)^2 \right]^{1/2}}{M (M-1)}$$

$$b = \frac{M \sum_{i=1}^M X_i Y_i - \left(\sum_{i=1}^M X_i \right) \left(\sum_{i=1}^M Y_i \right)}{M \sum_{i=1}^M X_i^2 - \left(\sum_{i=1}^M X_i \right)^2}$$

$$a = \frac{\left(\sum_{i=1}^M Y_i - b \sum_{i=1}^M X_i \right)}{M}$$

$$r = b (S_x/S_y).$$

The standard deviation of the linear regression is calculated by means of the expression:

$$s = \left[\frac{(M-1)}{(M-2)} S_y^2 + (1 - r^2) \right]^{1/2}$$

The values of k , e , and v are found by iterating on $1/k$ in Equation 13 and maximizing R in Equation B4. An alternative procedure would be to match the sample skewness to the Weibull function skewness by iteration of $1/k$. The coefficient of skewness is given by:

$$c.o.s = \frac{\Gamma(1+3/k) - 3\Gamma(1+1/k)\Gamma(1+2/k) + 2\Gamma^3(1+1/k)}{(\Gamma(1+2/k) - \Gamma^2(1+1/k))^{3/2}} \quad (B15)$$

and recalling that $\Gamma(\)$ denotes the incomplete gamma function.

There are two primary difficulties with the method employed. First, the resultant Weibull functions could be used to imply that in some three-parameter cases and at a given extrapolation, high probability of survival ($P_S > 0.95$), fatigue life decreases as applied stress amplitude decreases. Second, in the case of two-parameter analysis, probability of survival functions tend to predict overly conservative extrapolated fatigue lives, particularly at low applied stress amplitudes. Both of these difficulties refer to the extrapolative capability of the resultant functions. This is not considered a problem for comparing the data sets, and as discussed in Section B3.2, extrapolation of the data does not appear to be presently feasible.

B3.4 Alternative Procedures

Two other procedures are available for analyzing fracture data. They are

the Standardized Variable Estimation (SVE) method⁴³ and the Modified Double Exponential Function (MDEF) method⁴⁷.

In the SVE method⁴³ the standardized variable Z is defined as in Equation B6 for a Weibull survivorship function or as:

$$Z = \frac{X-e}{v} \quad (B16)$$

for a Weibull probability of failure function. Thus, as mentioned in Section B3.1, the order statistics Z_i are independent of e and v and depend only on the shape parameter k . The expected value, EZ_i , median, MZ_i , and variance, VZ_i , of the order statistic Z_i depend only on the sample size, N , and the shape parameter, k ⁴³. From Equation B16, we obtain⁴³:

$$X_i = e + v EZ_i \quad (B17)$$

or

$$X_i = e + v MA_i. \quad (B18)$$

Equations B17 and B18 can be solved by linear regression. The shape parameter k is the value for which the correlation coefficient is a maximum⁴³. The parameters e and v are found as the X_i - intercept and slope of the best fit line⁴³. If the sample data belong to different populations, this will result in the (X_i, EZ_i) and (X_i, MZ_i) scattering about different straight lines⁴³.

Talreja⁴³ found that the SVE method provided accurate estimates of k , e , and v , for low values of k . At higher k values, the method often gives negative estimates of e . The procedure gave more accurate estimates of the parameters than the ME and MLE methods⁴³.

The MDEF is based upon the double exponential function of Gumbel⁴². In this procedure⁴⁷, for a set of sample fatigue lines, N_p , the initial distribution is defined by:

$$P(X_1) = 1 - 1/(N_p + 1) \quad (B19)$$

and

$P(x)$ by:

$$P(X) = 1 - \text{Exp} [-\text{Exp} [-\alpha_0 (X-u)]]. \quad (B20)$$

For lives greater than u , the above function is used as described by Gumbel²³. For lives less than u , is a function of the life, X , where:

$$\alpha(X) = \alpha_0 \left[\frac{\ln u - \ln X_0}{\ln X - \ln X_0} \right] \quad (B21)$$

The parameter X_0 is defined as the threshold fatigue life. For $X \leq X_0$, P_S is defined as equal to unity. The modified double exponential function (MDEF) can be solved by ME, MLE, or LR procedures. The best procedure appeared to be linear regression⁴⁷. The MDEF function was found to not only fit the sample data with high correlations, but to provide procedures for exploration of data extrapolation accuracy⁴⁷.

B4.0 NDI PROCEDURES

A major effort of Task I was to select NDI procedures to document load induced matrix cracking and delamination during Task II and III. During Task I¹ several nondestructive investigational techniques were evaluated as to their usefulness for providing reproducible and clear detection of indications of state change in the graphite/epoxy coupons used in this program. The ease of use, time required, and cost of each technique were considered. The technique evaluation process began with a survey of those NDI techniques available at the inception of the program. Several techniques were selected from the survey for further investigation and evaluation. The selected techniques were used to detect manifestations of state change subjected to monotonic and fatigue load.

B4.1 NDI SELECTION PROCESS

At the inception of this program, the methods most commonly used for the inspection of composites were ultrasonic C-scan, x-ray, Moire, brittle lacquer, acoustic imaging, photoelastic casting, penetrant, thermography, acoustic emission, and laser holography. In addition, some methods were being used to measure specific parameters, such as ultrasonics to measure moisture level, eddy current to monitor fiber volume, and radiography and thermal neutron mass adsorption to determine resin content. A review of the literature showed that of the variety of NDI methods available, few provided detailed information on the type of damage present.

Based upon the literature survey of the state-of-the-art of NDI techniques as applied to composites, the following procedures were selected for further evaluation in Task I of this program:

- 1) Enhanced x-ray radiography
- 2) Ultrasonic pulse-echo using a Holosonic unit
- 3) Acoustic emission
- 4) Plastic-cast edge replication
- 5) Monitoring of stiffness change
- 6) Monitoring of thermal temperature rise

Both the enhanced x-ray radiography and the ultrasonic pulse-echo techniques had the potential to detect internal composite coupon damage, such as matrix cracking and ply delamination. The acoustic emission method was a real-time monitoring technique which had the potential of detecting damage location and differentiating among damage types. However, the level of ply damage at a particular location would not be identifiable. Plastic-cast edge replication enabled the making of permanent records of the matrix cracking and delamination that had occurred along coupon edges. The recording of changes in coupon temperature and stiffness was undertaken as per the

requirements of the RFP. Coupon temperature monitoring was retained mainly to ensure that overall coupon temperature change was not excessive. Coupon stiffness is related to the damage state, but the sensitivity of the procedure is dependent on layup configuration. Layups with a high percentage of 0° fibers (>50%) in the loading direction can withstand severe damage without significant tensile stiffness changes¹⁴. This fact reduces the general efficiency of stiffness monitoring.

Thermography was not included because of the large effort which remained to make the technique available for general use on graphite/epoxy laminates. Acoustic imaging was not selected because no system was available, at the time of the program inception, in the form required and similar information could be obtained using the Holosonics ultrasonic system. Other possible ultrasonic systems were also not included for they did not seem to add any different or additional information to that obtainable from the selected NDI techniques. Simple penetrant inspection was eliminated because of the lack of definitiveness of damage detection and lack of knowledge as to the potential damage to the graphite/epoxy composite material.

The NDI studies were conducted on laminate coupons loaded in monotonic tension to selected load levels and in tension-tension fatigue to selected cycle intervals. The state-of-the-art of some of the procedures was found to be less adequate than expected and thus development studies were undertaken. Since the objective was to select NDI procedures for Tasks II and III, more emphasis was placed upon developing sound techniques than simply on obtaining test data. Difficulties encountered with the NDI procedures during the selection process necessitated restricting experimentation to tension load excursions.

The capabilities of the NDI techniques as found by the evaluation conducted in Task I are summarized in Table B3. The DIB enhanced x-ray radiography technique was selected for use in Tasks II and III of this program. With

this technique, matrix cracking in the 90° , -45° , and 0° plies as well as interply delamination could be detected. The edge replication technique was selected because the procedure compliments the radiography procedure by allowing observation of the level of delamination. The damage that is detectable by either of these techniques is limited to only that which intersects the edges of the coupon. Pulse-echo ultrasonic inspection could distinguish ply delamination isolated from the specimen edges, but the technique was not selected for further use because of the geometric scanning restriction and insensitivity to intraply matrix cracking. The NDI techniques of acoustic emission, "go, no-go" ultrasonic inspection, temperature and stiffness monitoring were not selected for further use because these techniques were not able to reliably and reproducibly indicate the composite damage of interest in this program. However, the temperature monitoring did show that temperature rise during fatigue cycling was small, (8°C). The NDI selection process conducted in this task is outlined in Table B3.

B4.2 Selected NDI Experimental Procedures

Enhanced X-Ray Radiography

A Norelco MG 150 constant potential radiographic x-ray system with a 150 kV Beryllium window tube was used in conjunction with the radio-opaque penetrant DIB (1,4, diiodobutane). The DIB was applied to the specimen edges, and the surface residue was removed after soaking for 15 minutes. A microfocus x-ray tube with a 0.7 mm focal spot was used to produce the x-rays on Kodak type M film. The exposures were made at 25 kVp, 5 ma for 70 seconds (350 Mas), and focal distance of 183 cm (72 inches).

Edge Replication

The plastic-cast edge replication technique primarily used in this program

was developed and modified from the original method of Stalnaaker and Stinchbom⁴⁹. A strip of acetate tape, 5 mil thick was softened by acetone and placed on the edge of a specimen being held under load. A fresh acetate strip was placed over the first tape and pressed firmly to ensure good contact of the tape with the specimen edge and to remove air bubbles from between the two tapes. After drying for fifteen minutes, the replica was removed from the specimen edge and placed between two glass slides to keep it flat. To make photographs of selected portions of a replica, the replica were first used as a negative in a photographic enlarger. A microfisch reader was used to determine areas of the replicas for photography. For many coupons, the extent of matrix cracking was recorded by photographing coupon edges which had been rubbed with chalk. This technique has also been shown to be a viable procedure⁵⁰.

APPENDIX C

MATERIAL CHARACTERIZATION

The characteristics of the graphite/epoxy material used in this program are described in this section. These properties include the prepreg and panel properties and a summary from the Task I report¹ of the baseline monotonic and cyclic load induced coupon properties.

C.1 PREPREG PROPERTIES

A single batch of Rigidite T300/5208 mm (12 in.) wide graphite/epoxy tape was received the second week of November, 1978, from Narmco Materials Inc. This batch was numbered 1283 and consisted of 11 rolls weighing a total of 1222 N (274.8 lb.) with a 40 to 44% resin content. The fiber tensile strength and modulus of this batch was higher than previous batches received at Lockheed as shown in Table C1. The continuing change in fiber properties shown in Table C1 implies that any historical comparison of laminate properties is, at best, difficult to draw upon for determining future properties.

The required quality control tests on the material were conducted. The material was found to meet all requirements of the Quality Control Plan, see Section A3, and, therefore, was accepted. Material qualification tests were conducted by the Lockheed-California Company Quality Control Division and Narmco Materials, Inc. to assure material quality. The results of both sets of tests are presented in Tables C2 and C3.

C.2 PANEL PROPERTIES

From the received graphite/epoxy prepreg, two panels of 0° unidirectional laminate, two $\pm 45^\circ$ panels, and nineteen quasi-isotropic panels were manufactured. The panel numbers are listed in Table C4. Of the nineteen quasi-isotropic panels, only seventeen full panels and part of 1VX1392 could be

TABLE C-1
PROPERTIES OF T300 FIBERS USED IN VARIOUS LOCKHEED PROGRAMS

Manufacturer/ Batch No.	Date of Manufacture	Lockheed ID No.	Air Force Contract No. on which Material Used	Fiber Density g/cc	Fiber Tensile Strength MPa (ksi)	Fiber Modulus GPa (psi x 10 ⁶)
Fiberite/80-2 ^a	April, 1975	MJ	F33615-75-C-5118	1.76	2654 (385)	227.5 (33.0)
Fiberite/112-2 ^a	Oct. 1975	NH	F33615-75-C-5118	1.75	2537 (368)	233.0 (33.8)
Fiberite/6-C-73 ^b	July, 1977	SF	F33615-77-C-5045	1.76	2840 (412)	223.4 (32.4)
Narmco/1015 ^c	Nov. 1977	SY	F33615-77-C-5140	1.72	2840 (412)	226.2 (32.8)
Narmco/1079 ^c	Jan. 1978	TY	F33615-77-C-5140	1.74	3043 (441)	229.8 (33.3)
Narmco/1283 ^d	Oct. 1978	VX	F33615-78-C-5090	1.75	3284 (476)	237.4 (34.4)
Narmco/1295 ^e	Nov. 1978	WI	F33615-77-C-3084	1.75	3271 (474)	236.7 (34.3)

^a - data reported in AFML-TR-76-241

^b - data reported in AFML-TR-79-4128

^c - data reported in AFML-TR-79-4179

^d - material used on present contract

^e - data reported in AFFDL-TR-79-3095

TABLE C2
SUMMARY OF LOCKHEED QUALITY CONTROL TESTS FOR NARMCO
RIGIDITE 5208-T300 MATERIAL BATCH #1283

Material Property	Specification Requirements C-22-1379A/111 (9/13/77)	Measured Property	Accepted
UNCURED PROPERTIES			
1. Areal Fiber Weight (4 req)	139 - 149 g/m ²	143 145 146 <u>141</u> Avg. 144 g/m ²	x ^a x x x
2. Infrared Spectrophotometric Anal. (1 req)	Conformance to file spectrogram	-	x
3. Volatiles (2 req) 60 ± 5 min at 350°F	3% Maximum	0.4% edge 0.35% center	x x
4. Dry resin content (4 req) (Soxhlet)	38 - 44%	43.3% left 41.8% left center 41.9% right center <u>41.3% right</u> Avg. 41.0%	x x x x
5. Resin Flow at 350°F and 85 psi (2 req)	15 - 29%	19.2% 19.4%	x x
6. Gel Time at 350°F (2 req)	For information only	19.0 minutes 19.5 minutes	- -
7. Fiber Orientation	0°	-	x
CURED LAMINATES			
1. Cured Fiber Volume, 16 ply panel (3 req)	60 - 68%	66.4 66.2 <u>66.0</u> Avg. 66.2%	x x x
2. Cured Fiber Volume, 8 ply panel (3 req)	60 - 68%	67.3 67.2 <u>67.5</u> Avg. 67.3%	x x x
3. Specific Gravity, 16 ply panel (3 req)	1.55 - 1.62	1.586 1.584 <u>1.588</u> Avg. 1.586	x x x
4. Specific Gravity, 16 ply panel (3 req)	1.55 - 1.62	1.592 1.590 <u>1.594</u> Avg. 1.592	x x x
5. Tensile Strength, longitudinal at 75°F (3 req)	170 ksi min.	242 235 <u>220</u> Avg. 232 ksi	x x x
6. Elastic Modulus, longitudinal at 75°F (3 req)	20·10 ⁶ psi min.	21.2·10 ⁶ 22.6·10 ⁶ <u>22.2·10⁶</u> Avg. 22.0·10 ⁶	x x x

TABLE C2 (Cont.)

SUMMARY OF LOCKHEED QUALITY CONTROL TESTS FOR NARMCO
RIGIDITE 5208-T300 MATERIAL BATCH #1283 (Continued)

Material Property	Specification Requirements C-22-1378A/111 (9/13/77)	Measured Property	Accepted
7. Flexural Strength at 75°F (3 req)	210 ksi min.	289 280 <u>286</u> Avg. 285 ksi	x x x
8. Flexural Modulus at 75°F (3 req)	18-10 ⁶ psi min.	22.6 22.5 <u>22.7</u> Avg. 22.6-10 ⁶ psi	x x x
9. Flexural Strength at +180°F (3 req)	200 ksi min.	254 268 <u>261</u> Avg. 261 ksi	x x x
10. Flexural Modulus at +180°F (3 req)	16-10 ⁶ psi min.	21.8-10 ⁶ 22.8-10 ⁶ <u>22.5-10⁶</u> Avg. 22.4-10 ⁶ psi	x x x
11. Short Beam Shear Strength at 75° (3 req)	13 ksi min.	18.7 17.8 <u>18.4</u> Avg. 18.3 ksi	x x x
12. Short Beam Shear Strength at +180°F (3 req)	12 ksi min.	15.8 16.6 <u>14.8</u> Avg. 15.7 ksi	x x x
13. Thickness per ply, 16 ply panel (5 req)	0.0046 - 0.0056 inch	0.0049 0.0049 0.0048 0.0048 <u>0.0048</u> Avg. 0.0048 inch	x x x x x
14. Thickness per ply, 8 ply panel (5 req)	0.0046 - 0.0056 inch	0.0049 0.0046 0.0046 0.0049 <u>0.0049</u> Avg. 0.0048 inch	x x x x x
15. Ingestion: Acid, Temperature, Time		H ₂ SO ₄ /350°F/1.5 hrs.	
16. Resin Content	Information Only	8 Ply 26.4% Avg. 16 Ply 27.4% Avg.	
17. Water Absorption (24 hrs D.I.H ₂ O)	0.2% max.	8 Ply 0.15 16 Ply 0.17	
18. Liquid Chromatography		On file at Lockheed, Rye Canyon Research Laboratory	

a - an x indicates that the material passed this requirement

TABLE C3

SUMMARY OF NARMCO QUALITY CONTROL TESTS FOR RIGIDITE
5208/T300, NARMCO CERTIFIED TEST REPORT NO. 35990

MATERIAL: Rigidite 5208-T300-12" Batch No. 1283					
Roll	Amount	Resin Content	Areal Fiber Weight	Mfg. Date	Test Date
1	25.4 lb	42%	143 g/m ²	10-31-78	11-2-78
2	25.0	41	143		
3	21.1	41	144		
4	25.0	41	144		
5	25.6	42	144		
6	25.0	41	144		
7	24.8	40	144		
8	26.0	42	144		
9	25.2	41	144		
10	25.7	42	144		
11	26.0	44	143		
Volatiles:		0.6%			
Flow:		25%			
Gel Time:		27-25" min. @ 350°F.			
Tack:		Acceptable			
Specific Gravity:		1.58/1.58/1.58: 1.58 g/cc average (8 plies)			
		1.58/1.58/1.58: 1.58 g/cc average (16 plies)			
Fiber Volume:		65/65/65: 65% average (8 plies)			
		65/65/65: 65% average (16 plies)			
Cured Ply Thickness:		0.0051" (8 plies, Tensile panel)			
		0.0050" (16 plies, Flex and Shear panel)			
RT, 0° Flex:		261,550/307,120/329,390: 299,353 psi average			
RT, 0° Flex Modulus:		20.51/20.91/19.38: 19.38 x 10 ⁶ psi average			
RT, 0° Tensile:		237,530/257,280/212,470: 235,760 psi average			
RT, 0° Tensile Modulus:		20.99/20.62/20.28: 20.63 x 10 ⁶ psi average			
180°F., 0° Flex:		243,460/308,630/230,200: 260,760 psi average			
180°F., 0° Flex Modulus:		18.15/20.30/19.78: 19.41 x 10 ⁶ psi average			
RT Short Beam Shear:		18,820/20,200/19,710: 19,580 psi average			
180°F. Short Beam Shear:		17,520/18,150/17,400: 17,690 psi average			
Batch No. 1283					
RAW FIBER DATA					
Lot No.	Tensile Modulus	Tensile Strength	Yarn Density		
575-2	34.6 psi x 10 ⁶	471 psi x 10 ³	1.75 g/cm ³		
571-2	34.0	489	1.74		
577-2	34.3	457	1.78		
574-2	34.6	485	1.76		

used in the experimental program due to damage to two panels during manufacture into coupons.

Resin, fiber, and void analysis results for the panels used in all three tasks are given in Table C5. The fiber volume testing was conducted by Delsen Testing Laboratories, Inc., Glendale, California, in accordance with ANSI/ASTM B3171-73, Procedure A, entitled "Fiber Content of Reinforced Resin Composites" except as noted below:

- (a) Determinations for each strip of material were carried out in triplicate (see Figure C1 for location of test specimens).
- (b) Specimen size was approximately 1 gm rather than 0.3 gm.
- (c) The volume of Nitric Acid used for digestion was increased from 30 cm³ to 100 cm³ because of the larger specimen size.

The specific gravity testing was conducted in accordance with ANSI/ASTM D-792-66, procedure A-1: "Specific Gravity and Density of Plastics by Displacement."

Void content was determined in accordance with ANSI/ASTM D2734-70 (Reapproved 1976). The void content results have an inherent error of $\pm 1.6\%$ in void content; i.e., a result of 2% voids can be between 0.4 and 3.6% voids. The error is due to uncertainty in original fiber and matrix density properties and in the amount of absorbed moisture which also affects density. This level of inherent error can result in physically impossible negative void content determinations. The chemical analysis void content determinations combined with the lack of any C-scan indications do imply that the void content of all panels is extremely low, $<<1\%$. Because no C-scan indications were observed in any part of the panels, photographs of the C-scans are not included.

TABLE C4
IDENTIFICATION NUMBERS OF PANELS USED
IN EXPERIMENTAL PROGRAM

Laminate U1 (0°) ₁₆ Unidirectional	Laminate U2 (±45°) ₄₅	Laminate L1 Quasi-isotropic (0/45/90/-45/90/45/0) ₅
2VX1394 1VX1453	1VX1386 1VX1471	2VX1390 1VX1391 2VX1391 1VX1392 2VX1392 1VX1395 2VX1395 1VX1396 2VX1396 1VX1403 2VX1403 1VX1413 2VX1413 1VX1414 2VX1414 1VX1425 2VX1425 1VX1442 2VX1442 1VX1458

TABLE C5
RESIN, FIBER, AND VOID ANALYSIS RESULTS

Panel Production No.	Resin Content wt. %	Fiber Content vo. %	Void ^a Content, V _c %	Density gm/cc
2VX1394	26.0	67.1	0.34	1.578
1VX1453	25.8	67.5	-0.12	1.590
1VX1386	27.3	65.5	0.44	1.579
1VX1471	28.0	65.0	-0.05 ^b	1.579
1VX1394	26.2	66.7	0.45	1.585
2VX1390	27.9	64.8	0.42	1.576
1VX1391	26.8	66.2	0.36	1.583
2VX1391	26.4	66.5	0.42	1.584
1VX1392	26.8	66.0	0.49	1.581
2VX1392	27.3	65.6	0.39	1.580
1VX1395	26.4	66.5	0.43	1.584
2VX1395	26.4	66.5	0.44	1.584
1VX1396	26.5	66.3	0.52	1.582
2VX1396	26.6	66.2	0.48	1.582
1VX1403	26.5	66.4	0.33	1.585
2VX1403	26.1	66.8	0.47	1.585
1VX1413	26.5	66.4	0.34	1.585
2VX1413	26.4	66.6	0.30	1.586
1VX1414	26.9	66.0	0.26	1.584
2VX1414	26.6	66.3	0.30	1.585
1VX1425	27.3	65.6	0.26	1.582
2VX1425	26.8	66.1	0.37	1.583
1VX1442	27.6	65.3	0.22	1.584
2VX1442	27.2	65.8	0.16	1.584
1VX1458	27.3	65.7	0.14	1.584
Avg.	26.8	66.1	-	1.583
Std. Dev.	0.57	0.63	-	0.0037
Coeff. of Var. %	2.14	0.95	-	0.23
^a - V _c void content determined by standard chemical analysis procedures, accuracy is $\pm 1.6\%$ ^b - Artifact of chemical analysis procedure				

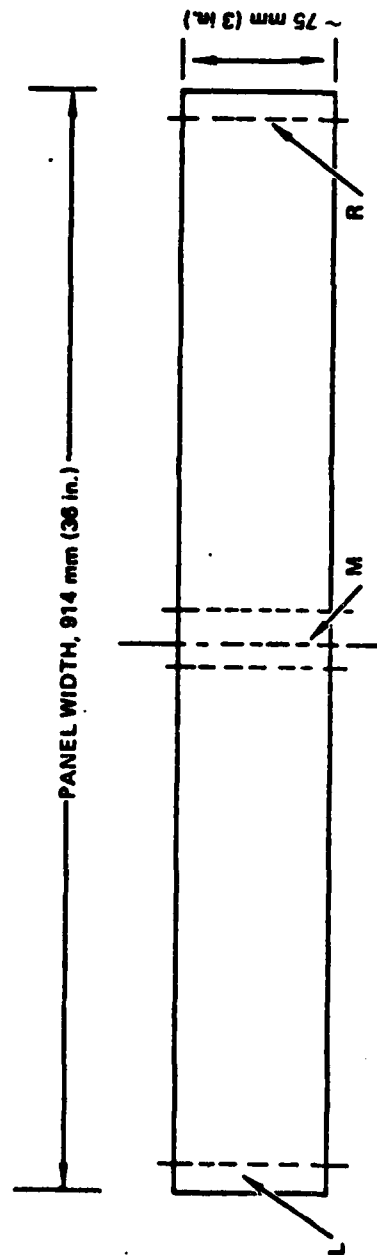


Figure C1 - Locations of three specimens from each panel used for specific gravity and acid digestion tests.

Micrographs were taken of longitudinal and transverse cross-sections of panels representative of each different layup. Typical photomicrographic sections were shown in the Task I final report¹. These photographs confirmed the low void content of the panels and showed that no ply cracks existed after panel manufacture.

C.3 ENVIRONMENTAL CONDITIONING

Some coupons, used to determine lamina properties, were conditioned at 82.2°C (180°F), 90 ±3% R.H. until an essentially equilibrium moisture content was obtained. These coupons were monotonically load tested at 82.2°C (180°F). All other coupons were held at room temperature in laboratory air, 22°C (72°F), 40% R.H. Moisture distribution and weight gain was measured using 127 mm (5 in.) long by 25.4 mm (1.0 in.) wide traveler coupons cut from the gage section of typical test coupons. Traveler and moisture distribution coupons taken from the various laminates were used in four different groupings, they were:

- Group 1: Coupons used for determining initial moisture content and distribution prior to testing or to conditioning at 82.2°C (180°F), 90% R.H.
- Group 2: Coupons used to measure weight gain changes while being held in the room temperature, 45% R.H. holding chambers.
- Group 3: Coupons used for measuring weight gain during conditioning at 82.2°C (180°F) and 90% R.H. and for determining moisture distribution just prior to static and fatigue tests.
- Group 4: Coupons used for determining weight loss and moisture distribution changes which occurred during static testing.

The results of each of these four groups were discussed in detail in the Task I final report¹. They will only be summarized in this report. Moisture distributions given in the following figures were experimentally

determined using the procedure of Sandorff and Tajima⁵¹. Three samples cut from the traveler test coupon under investigation were used to determine each moisture distribution. The average weight loss values determined were those recorded during the dry out process used to determine the moisture distribution. The procedure used to determine the moisture distribution was conducted in such a way to ensure that only moisture loss was being recorded during the drying process⁵¹. However, the weight loss obtained by any drying process is only that due to the release of unbound water. Thus, the amount of weight loss due to drying is not necessarily the same as the total weight gain from a zero condition since some of the water may be bound at the drying temperature.

The initial average moisture content within the traveler coupons was found to range from 0.3% to 0.6%. Conditioning of the lamina at 82.2°C (180°F), 90% R.H. for 90 days led to an essentially equilibrium moisture content of approximately 1.5% within the 0° and 90° unidirectional traveler coupons and approximately 1.7% in the $\pm 45^\circ$ coupons. The tests conducted and corresponding estimated average moisture levels are summarized in Table C6.

C.3 MONOTONIC TENSION AND COMPRESSION PROPERTIES

Monotonic load testing included determination of both unidirectional and quasi-isotropic laminate properties. Lamina testing was conducted at three different environmental conditions: room temperature (RT), dry (as received); 82.2°C (180°F), dry (as received); and 82.2°C (180°F), wet. All laminate tests were conducted at the RT, dry condition. The detailed static test data is tabulated in Appendix B of the Task I final report¹.

C.3.1 Lamina Properties

Ten lamina coupons were tested at each of twelve conditions. The unidirec-

TABLE C6
ESTIMATED PERCENT MOISTURE CONTENT WITHIN

Lamina or Laminate Type	Test Type	Test Environment	Estimated Average Moisture Content %
0°, 90°	Static	R.T. ^b , L.A. ^c	0.4
		82.2°C, Dry ^d	0.4
		82.2°C, Wet ^d	1.5
±45°	Static	R.T., L.A.	0.5
		82.2°C, Dry	0.5
		82.2°C, Wet	1.7
Q-1. ^a	Static & Fatigue	R.T., L.A.	0.6

- a Q-1 - Quasi-Isotropic
- b R.T. - Room Temperature
- c L.A. - Laboratory Air
- d Dry - as received moisture content
- e Wet - moisture content after conditioning at 82.2°C (180°F), 90% R.H. for 109 days

tional lamina properties of this material are summarized in Tables C7 to C11. The compression results are for the fully-constrained column buckling mode described in detail in Reference 40. The stress-strain curve of the 0° unidirectional tension tests had a slightly increasing curvature while that of the compression tests was slightly decreasing. Thus the moduli are really secant values. These slight nonlinear properties are consistent with other experimental observations.^{52,53} The nonlinear, increasing curvature properties under tension load are due to the non-Hookean, increasing curvature of fibers⁵³ as reported by Curtis.⁵⁴ Van Druemel and Kamp⁵³ hypothesized that the increasing modulus effect of the fibers would result in heavily stressed regions behaving stiffer, thus absorbing more load than would be expected. Possibly this would explain unexpected experimental results in cases where large stress variations occur in small volumes.⁵³ For the 90° unidirectional coupons, tension stress-strain curves were linear while the compression curves slightly decreases. The $\pm 45^\circ$ curves were continuous decreasing curves as expected.

The unidirectional coupons exhibited a large amount of splintering when failed under static tension loading. The amount of splintering appeared to be unaffected by the high humidity and temperature environment. Similarly, the 0° coupons which failed under static compression suffered severe splintering but this was significantly reduced at the 82.2°C (180°F), 95% R.H., wet condition. Under tension loading, the 90° coupons failed straight across at or near the tabs without apparent variation due to environment. In contrast, these 90° coupons exhibited a 45° to the loading plane failure region within the gage length when under compression load, however environment again did not affect the degree of fracture severity. Lastly, the \pm coupons, exhibited a fracture region whose damage state became worse as the severity of the environment was increased.

TABLE C7: COMPARISON OF 0° UNIDIRECTIONAL LAMINA STATIC TEST RESULTS

Test Type	Test Environment	Average Ultimate Stress, σ_{ult}		Average Strain to Failure, ϵ_f	Average Secant Modulus at Failure, E_{sf}		Average Secant Modulus at 70 ksi, E_{S70}	
		MPa	ksi		mm/mm	GPa	psi x 10 ⁶	GPa
Tension	RT, LA ^a	1645	238.6	0.0095	170.3	24.7	156.5	22.7
	82.2°C (180°F) Dry ^b	1736	251.8	0.0109	159.3	23.1	153.8	22.3
	82.2°C (180°F) Wet ^c	1629	236.3	0.0101	161.3	23.4	151.7	22.0
Compression	RT, LA	847	122.8	0.0066	128.2	18.6	140.0	20.3
	82.2°C (180°F), Dry	885	128.3	0.0067	132.4	19.2	142.7	20.7
	82.2°C (180°F), Wet	669	97.1	0.0070	95.8	13.9	103.4	15.0

^aRT – Room Temperature, LA – Laboratory Air^bDry – Coupons contains ~ 0.4% moisture by weight^cWet – Coupons contained ~ 1.7% moisture by weight

TABLE C8: SUMMARY OF WEIBULL PARAMETERS FOR 0° UNIDIRECTIONAL LAMINA STATIC TEST DATA

Test Type	Test Environment	Average Ultimate Stress, σ_{ult}		Weibull Coefficients			Correlation Coefficient, R
		MPa	ksi	k	σ	v	
Tension	RT, LA ^a	1645	238.6	17.92	-0.330	243.3	0.99931
	82.2°C (180°F), Dry ^b	1736	251.8	18.44	-0.300	255.3	0.99931
	82.2°C (180°F), Wet ^c	1629	236.3	24.42	-0.289	236.8	0.99929
Compression	RT, LA ^a	847	122.8	14.82	-0.107	128.9	0.99957
	82.2°C (180°F), Dry ^b	885	128.3	8.34	-0.816	132.5	0.99637
	82.2°C (180°F), Wet	669	97.1	7.98	-0.448	98.5	0.99733

^aRT – Room Temperature, LA – Laboratory Air^bDry – Coupons contained ~ 0.4% moisture by weight^cWet – Coupons contained ~ 1.7% moisture by weight

TABLE C9: COMPARISON OF 90° UNIDIRECTIONAL LAMINA STATIC TEST RESULTS

Test Type	Test Environment	Average Ultimate Stress, σ_{ult}		Average Strain to Failure, ϵ_{sf}	Average Secant Modulus at Failure, E_{sf}		Average Secant Modulus at 70 ksi, E_{S70}	
		MPa	ksi		GPa	psi x 10 ⁶	GPa	psi x 10 ⁶
Tension	RT, LA ^a	34.1	4.95	0.0033	10.2	1.48	—	—
	82.2°C (180°F), Dry ^b	39.0	5.66	0.0047	8.3	1.21	—	—
	82.2°C (180°F), Wet ^c	15.5	2.25	0.0018	8.5	1.24	—	—
Compression	RT, LA	203	29.4	0.0232	8.8	1.28	9.7	1.40
	82.2°C (180°F), Dry	177	25.6	0.0243	7.5	1.09	8.8	1.27
	82.2°C (180°F), Wet	172	25.0	0.0471	3.7	0.54	4.6	0.67

^aRT — Room Temperature, LA — Laboratory Air

^bDry — Coupons contained ~0.4% moisture by weight

^cWet — Coupons contained ~1.5% moisture by weight

TABLE C10: SUMMARY OF WEIBULL PARAMETERS FOR 90° UNIDIRECTIONAL LAMINA STATIC TEST DATA

Test Type	Test Environment	Average Ultimate Stress, σ		Weibull Coefficients			Correlation Coefficient, R
		MPa	ksi	k	m	v	
Tension	RT, LA ^a	34.1	4.95	—	—	—	—
	82.2°C (180°F), Dry ^b	39.0	5.66	4.53	-0.229	5.63	0.98926
	82.2°C (180°F), Wet ^c	15.5	2.25	8.04	-0.026	2.32	0.99488
Compression	RT, LA ^a	203	29.4	8.06	-0.302	30.36	0.99569
	82.2°C (180°F), Dry ^b	177	25.6	8.74	-0.056	26.28	0.99897
	82.2°C (180°F), Wet ^c	172	25.0	19.89	-0.022	25.07	0.99946

^aRT — Room Temperature, LA — Laboratory Air

^bDry — Coupons contained ~0.4% moisture by weight

^cWet — Coupons contained ~1.7% moisture by weight

TABLE C11: COMPARISON OF $\pm 45^\circ$ UNIDIRECTIONAL LAMINA STATIC TENSION TEST RESULTS

Test Environment	Shear Stress at Failure, τ_{xy}		Shear Secant Modulus at 4 ksi, GS_4	
	MPa	ksi	GPa	psi x 10^6
RT, LA ^a	89.6	13.0	5.3	0.77
82.2°C (180°F), Dry ^b	78.6	11.4	5.4	0.78
82.2°C (180°F), Wet ^c	73.1	10.6	4.5	0.65

^aRT - Room Temperature, LA - Laboratory Air

^bDry - Coupons contained ~ 0.4% moisture by weight

^cWet - Coupons contained ~1.7% moisture by weight

C.3.2 Laminate Properties

C.3.2.1 Monotonic Tension

Monotonic loading tests on laminate coupons were conducted at two different strain rates, 0.01 mm/mm/min and 6.0 mm/mm/min. This allowed a comparison to be made between normal tension test results and those conducted at rates equivalent to the 10 Hz sequencing used in the experimentation. The tension failures at both strain rates were brittle-like with a discernible inelastic like flow at the end of the high strain rate stress-strain curves. The stress-strain curves of the low-strain rate tensile coupons exhibited an initial linear, elastic portion with an apparent modulus of elasticity designated at E_1 . This straight portion was followed by a short, gradual, change to a second, inelastic, linear curve to failure with an apparent modulus designated E_2 . In contrast, stress-strain curves of high-strain rate coupons were linear without the dual slope characteristic at low rates. The stress-strain curves were similar to those previously observed for this layup^{4,9}.

All tensile failures were within the gage length. Fracture regions were often within the region of 25 to 50 mm (1 to 2 in.) from a tab, but these did not differ in their failure strengths from those which failed near the center. The fracture region of high strain rate coupons was similar though apparently less extensive than those observed for the low strain rate coupons. Only minor amounts of delamination occurred which was confined to the fracture region. Fibers in the outer 0° plies often failed along a $+45^\circ$ direction indicating a strong influence of the $+45^\circ$ plies on the fracture process. A secondary damage region due to compressive rebound usually occurred in the low strain rate coupons, but less often in the high strain rate specimens.

Tables C12 and C13 give summaries and comparisons of the laminate tension results. The detailed data are tabulated in the Task I Final Report¹. Twenty coupons were tested at the low strain rate and thirteen at the high. To avoid the influence of line discontinuities (adjoining tape edges) which are known to increase the scatter in static and fatigue properties,^{4,39} panel layups were designed so that test coupons did not contain such discontinuities, see Section A3. This was expected to result in a coefficient of variation of less than 4 percent and a Weibull parameter, k , greater than 30 for the static tension results. This expectation was confirmed as shown in Table C13. Strain gauges were placed, on half of the coupons tested at each strain rate, at the 1/3 gauge length point and on the other half at the center. The strain gauge data at the two locations were compared and found to differ by less than 2 percent and thus to be statistically insignificant. This confirmed that at least the center 100 to 125 mm (4 to 5 inches) of the coupon gauge length experienced the same strain field.

C.3.2.2 Monotonic Compression

Twenty compression tests were conducted at both 0.01 and 6.0 mm/mm/min. Quasi-Isotropic coupons which failed in static compression, exhibited no obvious damage prior to fracture although the stress-strain curve often was flat just prior to fracture indicating internal damage. Coupons usually failed at one location with the outer plies in the fracture region buckled out of plane. Extensive delamination usually occurred, but was limited over approximately 25 to 50 mm (1 to 2 in.) of the gage length in the vicinity of the fracture region. Fractures appeared on the outer plies along an irregular line along either a $\pm 45^\circ$ or 90° angle to the loading direction. Failure modes did not appear to be affected by the strain rate. Compression test results are summarized in Tables C14 and C15. The quasi-isotropic laminate showed essentially the same compression strength using this test method as in tension. Table C14 shows that strain rate had no significant

TABLE C14: SUMMARY OF QUASI-ISOTROPIC STATIC COMPRESSION TEST RESULTS AT ROOM TEMPERATURE

Strain Rate, mm/mm/min	Stress at Failure		Average Strain at Failure mm/mm	Secant Modulus of Elasticity at Failure, E _{sf} ,	
	MPa	ksi		GPa	psi x 10 ⁶
0.01	562 ^a	81.5	0.0115	48.2 ^a	6.99
	22.3	3.23	0.00075	1.65	0.24
		3.96	6.47		3.48
6.0	546	79.2	0.0121	46.8	6.79
	51.6	7.48	0.0012	1.65	0.24
		9.44	10.5		3.5

a - Average, standard deviation, and percent coefficient of variation, respectively.

TABLE C15: SUMMARY OF WEIBULL PARAMETERS FOR QUASI-ISOTROPIC STATIC COMPRESSION RESULTS AT ROOM TEMPERATURE

Strain Rate, mm/mm/min	Average Failure Stress,		Weibull Coefficients			Correlation Coefficient, R
	MPa	ksi	k	σ	v	
0.01	562	81.5	27.75	-0.076	82.6	0.99950
6.0	546	79.2	11.96	-0.235	81.7	0.99884

TABLE C12: SUMMARY OF QUASI-ISOTROPIC STATIC TENSION TEST RESULTS AT ROOM TEMPERATURE

Strain Rate, mm/mm/min	Failure Stress, σ_{ult}		Average Strain at Failure, ϵ_{ult} , mm/mm	Initial, Apparent Modulus of Elasticity, E_A	
	MPa	ksi		GPa	psi x 10 ⁶
0.01	547 ^a	79.3	0.0105	53.8 ^a	7.81
	19.1	2.77	0.00042	1.03	0.15
		3.49	4.03		1.96
6.0	507	73.6	0.0098	51.8	7.52
	17.9	2.60	0.00055	2.96	0.43
		3.53	6.66		5.68

^a Average, standard deviation, and % coefficient of variability, respectively.

TABLE C13: SUMMARY OF WEIBULL PARAMETERS FOR QUASI-ISOTROPIC STATIC TENSION RESULTS AT ROOM TEMPERATURE

Strain Rate, mm/mm/min	Average Failure Stress, σ_{ult}		Weibull Coefficients			Correlation Coefficient, R
	MPa	ksi	k	s	v	
0.01	547	79.3	33.87	-0.061	80.30	0.99958
6.0	507	73.6	30.10	-0.040	74.64	0.99972

effect on the quasi-isotropic compression properties, as expected, since the coupons were fully supported.

APPENDIX D
SUMMARY OF TEST DATA

PRECEDING PAGE BLANK-NOT FILMED

TABLE D1
FATIGUE SCATTER STUDY
TENSION-TENSION FATIGUE RESULTS OF COUPONS CYCLED AT A MAXIMUM
STRESS OF 276 MPa (40 ksi) AT ROOM TEMPERATURE IN LABORATORY AIR

$f = 10 \text{ Hz}$, $\sigma_{\min} = 0 \text{ MPa (ksi)}$, Average Moisture Content Approx. 0.6%

Coupon ID	Average Area		Cycles to Failure, N_f
	mm ²	in. ²	
1VX1391-B12	52.7	0.0817	NF ^a
-C2	53.0	0.0822	NF
-C31	52.7	0.0817	NF
2VX1391-D9	51.9	0.0805	NF ^b
-D19	52.2	0.0810	NF ^b
-D23	52.2	0.0810	408 900
1VX1392-A12	52.4	0.0812	1 435 755
2VX1392-B10	53.4	0.0827	NF
-B25	53.4	0.0827	NF
-C4	52.6	0.0816	NF
-C17	53.4	0.0827	NF
-C26	52.2	0.0809	NF
1VX1396-A4	51.7	0.0802	NF ^b
-A24	52.1	0.0808	NF ^b
-C1	52.0	0.0806	NF
-C13	52.4	0.0812	NF
-C16	52.6	0.0815	NF
-D9	53.0	0.0821	NF

a = NF indicates no failure at 1×10^6 cycles

b = This coupon was cycled to 2×10^6 cycles without failure

TABLE D2

FATIGUE SCATTER STUDY
TENSION-TENSION FATIGUE RESULTS OF COUPONS CYCLED AT A MAXIMUM
STRESS OF 310 MPa (45 ksi) AT ROOM TEMPERATURE IN LABORATORY AIR

$f = 10 \text{ Hz}$, $\sigma_{\min} = 0 \text{ MPa (ksi)}$, Average Moisture Content Approx. 0.6%

Coupon ID	Average Area		Cycles to Failure, N_f
	mm^2	in.^2	
1VX1391-A20	52.6	0.0816	695 000
-B7	53.4	0.0827	331 420
-C12	51.8	0.0803	650 535
-C26	52.6	0.0816	100 178
-C28	52.4	0.0812	337 646
-D28	52.0	0.0806	910 811
-D31	51.8	0.0803	548 370
2VX1391-D16	51.7	0.0802	708 917
-D22	51.9	0.0804	132 677
2VX1392-B31	52.0	0.0806	890 290
-C6	52.8	0.0818	380 267
-D20	52.7	0.0817	616 025
-D23	52.8	0.0818	NF ^a
1VX1396-C23	52.0	0.0806	1 514 720
-C29	51.9	0.0804	672 850
-D8	52.4	0.0812	433 511

^a = NF indicates no failure at 2.9×10^6 cycles

TABLE D3
FATIGUE SCATTER STUDY
TENSION-TENSION FATIGUE RESULTS OF COUPONS CYCLED AT A MAXIMUM
STRESS OF 345 MPa (50 ks') AT ROOM TEMPERATURE IN LABORATORY AIR

$f = 10 \text{ Hz}$, $\sigma_{\min} = 0 \text{ MPa}$, Average Moisture Content Approx. 0.6%

Coupon ID	Average Area		Cycles to Failure, N_f
	mm ²	in. ²	
1VX1391-B6	52.7	0.0817	51 202
-B31	52.6	0.0816	62 240
-C8	52.2	0.0809	95 333
-D5	51.9	0.0804	107 914
-D12	52.0	0.0806	51 440
-D13	52.1	0.0808	62 226
2VX1391-C5	52.2	0.0809	68 028
1VX1392-A20	52.7	0.0817	58 364
2VX1392-A5	52.2	0.0809	252 122
-A26	53.4	0.0827	58 300
-B15	54.0	0.0837	46 900
-B24	52.9	0.0820	701 699
-C15	52.6	0.0815	104 481
-C25	52.8	0.0818	61 965
-D28	52.2	0.0809	63 983
1VX1396-A10	52.5	0.0813	140 013
-C17	52.4	0.0812	177 275
-C19	52.5	0.0813	220 659

TABLE D4
FATIGUE SCATTER STUDY
TENSION-TENSION FATIGUE RESULTS OF COUPONS CYCLED AT A MAXIMUM
STRESS OF 414 MPa (60 ksi) AT ROOM TEMPERATURE IN LABORATORY AIR

$f = 10 \text{ Hz}$, $\sigma_{\min} = 0 \text{ MPa}$, Average Moisture Content Approx. 0.6%

Coupon ID	Average Area		Cycles to Failure, N_f
	mm ²	in. ²	
1VX1391-A23	52.0	0.0806	7 635
-A25	53.0	0.0821	4 620
-C15	51.9	0.0804	7 232
-D3	51.6	0.0800	5 450
2VX1391-D2	51.9	0.0805	6 200
1VX1392-B3	52.1	0.0807	4 420
2VX1392-A10	51.9	0.0805	3 768
-A13	53.4	0.0827	6 579
-A29	52.3	0.0811	2 949
-B13	53.7	0.0832	1 820
-B16	52.5	0.0814	3 450
-C3	53.4	0.0827	3 580
-C30	52.5	0.0814	4 602
1VX1396-A25	51.5	0.0798	8 169
-C15	52.1	0.0807	12 046
-C21	52.4	0.0812	6 312
-D13	51.8	0.0803	7 639

TABLE D4 - Continued
 FATIGUE SCATTER STUDY
 TENSION-TENSION FATIGUE RESULTS OF COUPONS CYCLED AT A MAXIMUM
 STRESS OF 414 MPa (60 ksi) AT ROOM TEMPERATURE IN LABORATORY AIR

$F = 10 \text{ Hz}$, $\sigma_{\min} = 0 \text{ MPa}$, Average Moisture Content Approx. 0.6%

Coupon ID	Average Area		Cycles to Failure, N_f
	mm^2	in.^2	
1VX1413-D2	53.5	0.0829	6 000
-D3	52.7	0.0817	3 610
-D6	52.8	0.0818	6 670
2VX1414-C12	52.5	0.0814	5 120
-C20	52.5	0.0814	4 670
-D3	52.4	0.0812	3 050
-D4	52.4	0.0812	6 700
-D5	52.1	0.0807	7 160
-D6	52.6	0.0815	5 870
-D9	53.0	0.0822	5 750
2VX1425-B27	53.0	0.0821	4 250
-C18	52.3	0.0811	3 820

TABLE D5
TENSION TEST RESULTS AT A 27.9 kN/MIN (6270 lb/min) RAMP RATE
IN FATIGUE MACHINE WITHOUT CYCLING

Room Temperature, Laboratory Air, Average Moisture Content Approximately 0.6%

NOTE: Test Ramp Rate equivalent to failure in approximately one minute

Coupon ID	Average Area		Stress at Failure	
	mm ²	in. ²	MPa	ksi
1VX1391-A30	53.3	0.0826	551	79.9
-B25	53.2	0.0825	474	68.7
-C17	53.1	0.0823	585	84.8
-D9	53.0	0.0822	496	72.0
-D10	51.9	0.0804	555	80.5
2VX1392-A17	53.7	0.0832	567	82.3
-A19	53.4	0.0828	485	70.4
-B18	53.6	0.0831	553	80.2
-D5	52.3	0.0811	523	75.9
-D7	52.4	0.0813	575	83.4
Average			536	77.8
Standard Deviation			39	5.7
Coefficient of Variation (%)				7.3

TABLE D6
PROGRESSIVE LOADING RESULTS AT 27.6 kN/MIN (6200 lb/min)
RAMP RATE AND AT A 10Hz CYCLING FREQUENCY

Room Temperature, Laboratory Air, Average Moisture Content Approximately 0.6%

NOTE: Test ramp rate equivalent to failure in approximately one minute

Coupon ID	Average Area ₂		Number of Cycles to Failure	Percent of 600 Cycles	Stress at Failure	
	mm ²	in. ²			MPa	ksi
IVX1391-B2	51.9	0.0805	548	91.3	514	74.6
-B5	52.3	0.0810	542	90.3	485	70.4
-B24	53.5	0.0829	600	100.0	536	77.7
-C4	52.0	0.0806	592	98.7	523	75.9
-C7	53.0	0.0822	562	93.7	512	74.3
-C19	52.3	0.0811	566	94.3	501	72.7
-C23	52.4	0.0813	556	92.7	512	74.2
-D18	52.5	0.0814	558	93.0	490	71.1
-D20	52.3	0.0810	540	90.0	477	69.2
2VX1392-A20	52.4	0.0812	540	90.0	506	73.4
-A30	52.5	0.0814	588	98.0	517	75.0
-B9	52.8	0.0818	546	91.0	478	69.3
-B23	52.9	0.0820	598	99.7	520	75.4
-C23	53.2	0.0824	576	96.0	505	73.3
-D15	53.4	0.0827	594	99.0	513	74.4
Average		0.0816			506	73.4
Standard Deviation					17	2.5
Coefficient of Variation (%)						3.4

TABLE D7
PROGRESSIVE LOADING RESULTS AT 423 kN/MIN (95 lb/min)
RAMP RATE AND AT A 10Hz CYCLING FREQUENCY

Room Temperature, Laboratory Air, Average Moisture Content Approximately 0.6%

NOTE: Test ramp rate equivalent to failure in approximately one hour

Coupon ID	Average Area		Number of Cycles to Failure	Percent of 36,000 Cycles	Stress at Failure	
	mm ²	in. ²			MPa	ksi
1VX1391-A27	52.4	0.0813	34276	95.2	430	62.4
-B17	53.4	0.0827	34200	95.0	441	63.9
-B26	52.4	0.0813	33212	92.3	430	62.3
-B29	52.1	0.0808	33592	93.3	438	63.5
-C13	52.2	0.0810	34428	95.6	419	60.8
-D4	52.2	0.0810	33516	93.1	433	62.8
-D15	52.8	0.0818	34960	97.1	444	64.4
2VX1392-A3	52.2	0.0810	33212	92.3	432	62.6
-A12	52.1	0.0807	35112	97.5	428	62.1
-A23	52.6	0.0816	34352	95.4	449	65.1
-B7	52.6	0.0816	34276	95.2	439	63.6
-B20	52.4	0.0813	34276	95.2	423	61.3
-C29	52.8	0.0819	34048	94.6	434	63.0
-D1	52.8	0.0818	33820	93.9	434	63.0
-D3	52.2	0.0810	34884	96.9	436	63.2
Average					434	62.9
Standard Deviation					7.7	1.1
Coefficient of Variation (%)						1.8

TABLE D8
TIME AT LOAD FATIGUE STUDY
RESULTS OF COUPONS CYCLED AT A MAXIMUM STRESS OF 414 MPa (60 KSI)
WITH A ONE MINUTE HOLD TIME

R = 0.0, f = 10 Hz, Room Temperature , Laboratory Air,
Average Moisture Content Approximately 0.6%

Coupon ID	Average Area		Cycles to Failure, N _f
	mm ²	in. ²	
1VX1391-B19	52.3	0.0811	10 ⁴ NF ^a
-D6	52.3	0.0811	3 868
-D25	52.3	0.0810	106
2VX1392-A4	51.9	0.0804	4 656
-A15	52.5	0.0813	336
-D8	52.6	0.0815	7 493
1VX1395-C14	52.1	0.0807	9 946
-D27	52.1	0.0807	7 708
2VX1395-A6	52.1	0.0807	10 ⁴ NF
-B5	52.8	0.0819	6 964
-C27	51.7	0.0801	7 208
2VX1396-B5	52.4	0.0812	10 ⁴ NF
2VX1403-D7	52.2	0.0809	8 167
2VX1413-C26	52.8	0.0818	8 991
-C27	52.5	0.0814	7 162

a = NF Indicates No Failure

TABLE D9
TIME AT LOAD FATIGUE STUDY
RESULTS OF COUPONS CYCLED AT A MAXIMUM STRESS OF 414 MPa (60 KSI)
WITH A ONE SECOND HOLD TIME

R = 0.0, f = 10 Hz, Room Temperature , Laboratory Air,
Average Moisture Content Approximately 0.6%

Coupon ID	Average Area		Cycles to Failure, N_f
	mm ²	in. ²	
1VX1395-C3	52.4	0.0812	6 864
2VX1395-A7	52.4	0.0812	4 995
-B24	52.7	0.0817	14 867
-D13	52.7	0.0817	7 194
2VX1413-A16	53.0	0.0821	18 892

TABLE D10.
FATIGUE RESULTS UNDER TRAPEZOIDAL WAVE AND SINOSIDAL WAVE
LOADING AT 10 Hz

$R = 0.0, \sigma_{\max} = 414 \text{ MPa (60 ksi)}$, Room Temperature, Laboratory Air,
Cycles to Failure

Sine Wave	Trapezoidal Wave	
	One Minute	One Second
	103	
1 800	336	4 995
2 949	3 868	6 864
3 450	4 656	7 197
3 580	6 964	14 867
3 768	7 162	18 892
4 420	7 208	
4 602	7 493	
4 620	7 708	
5 450	8 167	
6 300	8 991	
6 312	9 946	
6 579	10 000 NF	
7 232	10 000 NF	
7 635	10 000 NF	
7 639		
8 169		

TABLE D11
TIME AT LOAD FATIGUE STUDY
RESULTS OF COUPONS CYCLED AT A MAXIMUM STRESS OF 310 MPa (45 KSI)
WITH A ONE MINUTE HOLD TIME

R = 0.0, f = 10 Hz, Room Temperature , Laboratory Air,
Average Moisture Content Approximately 0.6%

Coupon ID	Average Area		Cycles to Failure, N_f
	mm ²	in. ²	
1VX1391-A24	52.3	0.0811	10^4 NF ^a
-B10	51.9	0.0805	10^4 NF
-C25	52.5	0.0814	10^4 NF
-D6	52.8	0.0818	10^4 NF
2VX1392-A31	51.4	0.0796	10^4 NF
-C31	51.6	0.0800	10^4 NF

a = NF Indicates No Failure

TABLE D12
FATIGUE PRELOAD STUDY
RESULTS OF COUPONS PRELOADED TO 496 MPa (72 ksi) AND
CYCLED TO FAILURE AT 414 MPa (60 ksi)

R = 0.0, f = 10 Hz, Room Temperature, Laboratory Air,
Average Moisture Content Approximately 0.6%

Coupon ID	Average Area		Cycles to Failure, N_f
	mm ²	in. ²	
1VX1395-A15	52.3	0.0811	3 188
-B5	52.3	0.0811	2 923
-B9	52.1	0.0807	3 844
-C26	52.0	0.0806	5 045
-D17	51.9	0.0805	6 003
2VX1395-A16	52.0	0.0806	5 063
2VX1396-A5	52.1	0.0808	5 601
-D15	51.9	0.0805	6 215
-D17	52.1	0.0808	6 701
2VX1413-A29	52.3	0.0811	4 071
-C4	51.9	0.0805	9 078
-C13	52.2	0.0809	6 487

TABLE D13
FATIGUE PRELOAD STUDY
RESULTS OF COUPONS PRELOADED TO 496 MPa (72 ksi) AND
CYCLED TO FAILURE AT 310 MPa (45 ksi)

R = 0.0, f = 10 Hz, Room Temperature, Laboratory Air,
Average Moisture Content Approximately 0.6%

Coupon ID	Average Area		Cycles to Failure, N_f
	mm ²	in. ²	
1VX1395-A2	52.1	0.0808	328 802
-A29	51.6	0.0800	688 070
-B7	51.8	0.0803	971 000
-C8	52.1	0.0807	455 661
-C20	51.8	0.0803	166 931
-C24	52.9	0.0820	1 ^b
-D2	51.7	0.0802	296 460
-D18	51.9	0.0804	312 113
2VX1395-A22	52.3	0.0810	222 820
-A23	52.4	0.0812	1 ^b
-A24	53.0	0.0822	10 ⁶ NF ^a
-D30	52.3	0.0811	630 731
2VX1396-A16	51.9	0.0804	1 028 738
-A19	51.7	0.0802	1 ^b
-B4	52.2	0.0809	796 485
-B7	52.9	0.0820	654 432
-C4	52.2	0.0809	745 600
-C29	52.2	0.0809	793 064
2VX1413-A17	52.4	0.0812	585 800
-B6	52.5	0.0814	546 809

a = NF Indicates No Failure

b = Failed on Preload

1VX1395-C24 at 496 MPa (72.0 ksi), 2VX1395-A23 at 496 MPa (72.0 ksi),
2VX1396-A19 at 495 MPa (71.8 ksi)

TABLE D14
FATIGUE PRELOAD STUDY
RESULTS OF COUPONS PRELOADED TO 524 MPa (76 ksi) AND
CYCLED TO FAILURE AT 310 MPa (45 ksi)

R = 0.0, f = 10 Hz, Room Temperature, Laboratory Air,
Average Moisture Content Approximately 0.6%

Coupon ID	Average Area		Cycles to Failure, N_f
	mm ²	in. ²	
1VX1395-A3	52.0	0.0806	252 740
-A9	52.1	0.0807	311 700
-A10	51.9	0.0804	1 ^a
-A20	52.7	0.0817	329 500
-A22	51.0	0.0791	556 340 ^b
-A30	52.5	0.0813	10 ^b NF
-B6	51.4	0.0797	677 560
-B18	52.7	0.0817	1 ^a
-C29	52.5	0.0814	582 621
-D26	52.5	0.0814	10 ^b NF
1VX1395-B14	52.6	0.0815	1 ^a
-C22	52.6	0.0815	492 191
2VX1396-A10	52.0	0.0806	1 ^a
-C14	52.8	0.0819	657 894

a = Failed During Preload

1VX1395-A10 at 500 MPa (72.5 ksi), 1VX1395-B18 at 517 MPa (75.0 ksi)
2VX1395-B14 at 507 MPa (73.6 ksi), 2VX1396-A10 at 505 MPa (73.3 ksi)

b = NF Indicates No Failure

TABLE D15
FATIGUE BLOCK LOADING STUDY
RESULTS OF COUPONS CYCLED AT A MAXIMUM STRESS OF 310 MPa (45 ksi)
FOR 108,000 CYCLES AND AT 414 MPa (60 ksi) TO FAILURE

R = 0.0, f = 10 Hz, Room Temperature, Laboratory Air
Average Moisture Content Approximately 0.6%

Coupon ID	Average Area		Cycles to Failure, N_f
	mm ²	in. ²	
1VX1391-C14	52.1	0.0808	8 150
-D19	52.5	0.0813	3 386
2VX1392-B2	52.6	0.0815	4 669
-B8	52.5	0.0814	4 090
-D19	52.6	0.0816	3 480
2VX1395-A28	52.3	0.0810	1 480
-B2	52.4	0.0812	4 762
2VX1396-C8	52.8	0.0818	5 909
-D2	52.1	0.0807	4 970
-D18	52.7	0.0817	7 562
-D19	52.9	0.0820	5 944
-D27	51.9	0.0804	3 040
2VX1413-A24	53.0	0.0822	1 832
-B24	53.0	0.0822	5 200
-D31	52.5	0.0813	3 050

TABLE D16
FATIGUE BLOCK LOADING STUDY
RESULTS OF COUPONS CYCLED AT A MAXIMUM STRESS OF 310 MPa (45 ksi)
FOR 200,000 CYCLES AND AT 414 MPa (60 ksi) TO FAILURE

R = 0.0, f = 10 Hz, Room Temperature, Laboratory Air
Average Moisture Content Approximately 0.6%

Coupon ID	Average Area		Cycles to Failure, N_f
	mm ²	in. ²	
1VX1391-B18	52.3	0.0810	510
2VX1392-B17	52.6	0.0816	2 184
-B26	53.3	0.0826	140
-C13	53.3	0.0826	810
-D14	52.6	0.0815	4 340
1VX1395-A4	52.1	0.0807	3 560
2VX1395-A13	52.4	0.0812	2 250
-D10	51.7	0.0802	1 554
2VX1396-C13	52.8	0.0819	5 307
-D16	52.7	0.0817	575
2VX1413-A19	52.3	0.0810	7 157
-A27	52.3	0.0811	199
-B4	52.8	0.0818	2 050
-B19	52.2	0.0809	5 137
-C1	52.8	0.0819	5 306

TABLE D17
FATIGUE BLOCK LOADING STUDY
RESULTS OF COUPONS CYCLED AT A MAXIMUM STRESS OF 414 MPa (60 ksi)
FOR 1,360 CYCLES AND AT 310 MPa (45 ksi) TO FAILURE

R = 0.0, f = 10 Hz, Room Temperature, Laboratory Air
Average Moisture Content Approximately 0.6%

Coupon ID	Average Area		Cycles to Failure, N _f
	mm ²	in. ²	
1VX1391-B20	51.9	0.0805	10 ⁶ NF ^a
-C20	52.1	0.0807	336,088
-D7	52.3	0.0811	316 783
2VX1392-A28	52.3	0.0810	227 390
-B27	53.0	0.0821	336 822
2VX1395-B10	52.1	0.0808	948 790
-D18	52.6	0.0815	925 665
2VX1396-A2	52.4	0.0812	149 060
-A18	52.6	0.0816	339 275
-C9	52.7	0.0817	10 ⁶ NF
2VX1413-B30	52.6	0.0815	366 230
-C8	52.6	0.0815	844 340
-C14	52.5	0.0813	--b
-C31	52.5	0.0814	194 150
-D30	51.8	0.0803	195 708

a = NF indicates no failure

b = Failed after 1340 cycles while still at 414 MPa (60 ksi)

TABLE D1P
FATIGUE BLOCK LOADING STUDY
RESULTS OF COUPONS CYCLED AT A MAXIMUM STRESS OF 414 MPa (60 ksi)
FOR 1,800 CYCLES AND AT 310 MPa (45 ksi) TO FAILURE

R = 0.0, f = 10 Hz, Room Temperature, Laboratory Air
Average Moisture Content Approximately 0.6%

Coupon ID	Average Area		Cycles to Failure, N _f
	mm ²	in. ²	
2VX1391-C18	52.1	0.0807	612 650
-D24	52.5	0.0813	214 000
2VX1392-A14	52.6	0.0816	10 ⁶ NF ^a
-C1	52.9	0.0820	888 006
-D18	52.7	0.0817	813 816
1VX1395-B19	52.1	0.0808	947 958
-C17	52.8	0.0819	310 000
2VX1395-A1	50.8	0.0788	812 021
2VX1396-B31	52.4	0.0812	10 ⁶ NF
-C12	52.5	0.0813	10 ⁶ NF
-D10	52.1	0.0807	202 400
-D31	50.8	0.0787	832 258
2VX1413-A31	52.7	0.0817	135 870
-B2	53.5	0.0830	10 ⁶ NF
-D3	52.1	0.0808	292 169

a = NF indicates no failure

TABLE D19
FATIGUE OVERLOAD STUDY
RESULTS OF COUPONS CYCLED AT A MAXIMUM STRESS OF 310 MPa (45 ksi)
WITH A SINGLE CYCLE OVERLOAD OF 414 MPa (60 ksi) AT 108 000 CYCLES

R = 0.0, f = Hz, Room Temperature, Laboratory Air,
Average Moisture Content Approximately 0.6%

Coupon ID	Average Area		Cycles to Failure, N_f
	mm ²	in. ²	
1VX1395-A18	52.5	0.0813	947 000
-C9	52.4	0.0812	973 001 ^a
-C13	52.7	0.0817	108 001 ^a
-C19	52.7	0.0817	671 723
2VX1395-A5	52.4	0.0812	786 000
-D29	52.1	0.0807	519 000
2VX1396-B9	52.8	0.0818	10 ⁶ NF ^b
-B14	52.7	0.0817	441 971
-C17	52.6	0.0815	938 000
-C27	52.1	0.0808	298 002
-D3	52.6	0.0816	475 900
-D13	52.4	0.0812	10 ⁶ NF
2VX1403-A22	51.4	0.0797	93 930
2VX1413-A7	51.8	0.0803	10 ⁶ NF
-B18	52.9	0.0820	967 871

a = Coupon Failed on Overload

b = NF Indicates No Failure

TABLE D20
FATIGUE OVERLOAD STUDY
RESULTS OF COUPONS CYCLED AT A MAXIMUM STRESS OF 310 MPa (45 ksi)
WITH A SINGLE CYCLE OVERLOAD OF 483 MPa (70 ksi) AT 108 000 CYCLES

R = 0.0, f = Hz, Room Temperature, Laboratory Air,
Average Moisture Content Approximately 0.6%

Coupon ID	Average Area		Cycles to Failure, N _f
	mm ²	in. ²	
IVX1395-A27	51.5	0.0798	800 001
-C10	52.6	0.0815	108 001 ^a
-C15	52.7	0.0817	597 612
-C25	52.0	0.0806	108 001 ^a
2VX1395-B28	49.9	0.0773	10 ⁶ NF ^b
2VX1396-A26	51.9	0.0804	10 ⁶ NF
-B12	52.7	0.0817	10 ⁶ NF
-B20	52.6	0.0815	108 001 ^a
-D7	52.4	0.0811	10 ⁶ NF
-D13	52.4	0.0812	10 ⁶ NF
2VX1403-A28	52.1	0.0808	108 001 ^a
-C22	51.0	0.0791	108 001 ^a
2VX1413-C24	52.8	0.0818	709 001

a = Coupon Failed on Overload

b = NF Indicates No Failure

TABLE D21
FATIGUE OVERLOAD STUDY
RESULTS OF COUPONS CYCLED AT A MAXIMUM STRESS OF 310 MPa (45 ksi)
WITH A SINGLE CYCLE OVERLOAD OF 414 MPa (60 ksi) AFTER EVERY 100 CYCLES

R = 0.0, f = Hz, Room Temperature, Laboratory Air,
Average Moisture Content Approximately 0.6%

Coupon ID	Average Area		Cycles to Failure, N_f
	mm ²	in. ²	
2VX1395-B25	52.5	0.0813	80 295
-D16	52.4	0.0812	228 361
-D17	51.8	0.0803	101 606
-D25	52.0	0.0806	521 867
-D29	52.4	0.0812	122 513
2VX1396-B13	52.4	0.0812	149 480
-B15	54.3	0.0841	49 692
-B29	52.1	0.0807	128 068
-D5	52.5	0.0814	77 770
-D9	52.1	0.0807	75 649
2VX1413-A28	52.3	0.0810	182 608
-B21	52.9	0.0820	53 833
-C28	52.2	0.0809	101 202
-D8	52.2	0.0809	226 846

TABLE D22
FATIGUE OVERLOAD STUDY
RESULTS OF COUPONS CYCLED AT A MAXIMUM STRESS OF 310 MPa (45 ksi)
WITH A SINGLE CYCLE OVERLOAD OF 414 MPa (60 ksi) AFTER EVERY 1 000 CYCLES

R = 0.0, f = Hz, Room Temperature, Laboratory Air,
Average Moisture Content Approximately 0.6%

Coupon ID	Average Area		Cycles to Failure, N_f
	mm ²	in. ²	
1VX1395-C18	52.7	0.0817	112 112
2VX1395-A14	52.7	0.0817	140 140
-B8	52.0	0.0806	101 101
-C5	52.8	0.0818	337 337
-D8	52.7	0.0817	74 074
2VX1395-A8	52.7	0.0817	196 196
2VX1396-B19	52.6	0.0816	161 161
1VX1403-A15	51.7	0.0801	154 154
2VX1403-A30	52.8	0.0819	200 200
2VX1413-A13	53.0	0.0821	187 187
-A26	52.2	0.0809	202 200
-D17	52.6	0.0815	125 125
-D30	52.4	0.0812	278 278

TABLE D23
 FATIGUE OVERLOAD STUDY
 RESULTS OF COUPONS CYCLED AT A
 MAXIMUM STRESS OF 207 MPa (30 ksi)
 WITH A SINGLE CYCLE OVERLOAD OF 414 MPa (60 ksi) AFTER EVERY 100 CYCLES

Coupon ID	Average Area		Cycles To Failure At 414 MPa (60 ksi)
	mm ²	in. ²	
1VX1413-D1	52.1	0.0808	1 582
-D4	52.8	0.0819	1 360
-D9	52.8	0.0819	1 270
-D10	52.5	0.0814	1 241
2VX1414-C24	52.1	0.0807	1 132
-C27	52.6	0.0815	1 163
-C31	52.4	0.0813	1 604
2VX1425-B22	52.4	0.0813	950
-B25	52.0	0.0806	917
-B26	51.7	0.0802	918
-B31	51.4	0.0796	1 095
2VX1442-D20	52.6	0.0816	852

TABLE D24
 FATIGUE OVERLOAD STUDY
 RESULTS OF COUPONS CYCLED AT A
 MAXIMUM STRESS OF 138 MPa (20 ksi)
 WITH A SINGLE CYCLE OVERLOAD 414 MPa (60 ksi) AFTER EVERY 100 CYCLES

Coupon ID	Average Area		Cycles to Failure At 414 MPa (60 ksi)
	mm ²	in. ²	
1VX1413-C14	52.6	0.0816	1 262
-C15	52.3	0.0811	1 553
-C16	52.8	0.0818	1 730
-C17	52.6	0.0816	1 564
-C24	52.8	0.0818	1 429
2VX1414-C17	52.8	0.0819	1 770
-D2	52.4	0.0812	2 193
-D16	52.2	0.0810	1 176
-D17	52.3	0.0811	1 570
-D18	52.2	0.0810	1 653
-D19	52.2	0.0810	1 377
2VX1425-D2	52.0	0.0806	1 411

TABLE D25

RESULTS OF STRESS-LIFE SURVEY AT R = -1.0

ENVIRONMENT: ROOM TEMPERATURE, LABORATORY AIR; f = 10 Hz

Coupon IR	mm ²	Area in. ²	Maximum Stress Level		Cycles to Failure, NF	Bay In which Failure Occurred	Visible Delamination Extent at Failure No. of Bays
			MPa	ksi			
1VX1395-D10	52.1	0.0807	345	50	309	1	1
2VX1396-A28	51.9	0.0804			214	5	1
2VX1413-A21	53.2	0.0825			380	6	1
1VX1391-D16	52.6	0.0816	276	40	4 403	5	1
1VX1395-B4	52.0	0.0806			4 035	6	1
1VX1395-C1	51.0	0.0791			5 945	1	1
2VX1396-B12	52.7	0.0817			4 008	2	1
2VX1395-C31	52.1	0.0807	207	30	23 430	1	3
2VX1396-D22	52.1	0.0807			58 700	6	2
2VX1413-C6	52.2	0.0809			46 185	6	2
1VX1395-B13	52.6	0.0816	138	20	NF ^a	-	None
1VX1395-D31	50.8	0.0787			NF	-	None
2VX1413-B1	52.9	0.0820			NF	-	None

^aNF - indicates no failure a 1x10⁶ cycles.

TABLE D26
FATIGUE SCATTER STUDY
RESULTS OF STRESS LIFE SCAN AT R = -∞

f = 10 Hz, Room Temperature, Laboratory Air
Average Moisture Content Approximately 0.6%

Coupon ID	Max. Fatigue Stress MPa	ksi	Average Area mm ²	in. ²	Cycles To Failure	Failure in Fixture Bay No.
2VX1395-A27	-344	-50	51.9	0.0804	2 834	6
-B29	-344	-50	51.9	0.0804	318	1
2VX1396-D7	-344	-50	47.8	0.0741	13 140	3
2VX1395-D27	-310	-45	51.8	0.0803	19 840	6
2VX1412-C29	-310	-45	51.9	0.0805	15 239	1
2VX1413-D14	-310	-45	52.2	0.0809	32 870	4
2VX1395-A17	-276	-40	52.1	0.0807	15 440	5
2VX1396-C3	-276	-40	52.4	0.0812	150 508	4
2VX1413-A1	-276	-40	52.2	0.0809	104 870	1
1VX1395-B2	-241	-35	52.1	0.0807	497 089	2
2VX1395-B12	-241	-35	52.6	0.0816	10 ⁶ NF	- ^a
2VX1413-A12	-241	-35	52.3	0.0811	396 680	- ^b
1VX1395-B20	-207	-30	52.8	0.0818	10 ⁶ NF	-
2VX1396-C22	-207	-30	52.3	0.0810	10 ⁶ NF	-
2VX1413-C25	-207	-30	52.6	0.0815	10 ⁶ NF	-

a = NF Indicates No Failure

b = Fixture bay in which failure occurred was inadvertently not recorded

TABLE D27
FATIGUE SCATTER STUDY
RESULTS OF COUPONS TESTED AT A MINIMUM STRESS OF -241 MPa (-35 ksi)

R = ∞, f = 10 Hz, Room Temperature, Laboratory Air,
Average Moisture Content Approximately 0.6%

Coupon ID	Average Area		Cycles To Failure	Failure in Fixture Bay No.
	mm ²	in. ²		
1VX1395-A7	52.3	0.0810	10 ⁶ NF ^a	-
-A12	51.6	0.0800	10 ⁶ NF	-
-A16	52.5	0.0813	10 ⁶ NF	-
-A23	52.5	0.0813	10 ⁶ NF	-
-B2	52.1	0.0807	497 089	2
-B3	52.3	0.0811	262 086	5
-C2	52.5	0.0814	10 ⁶ NF	-
-C4	52.3	0.0811	10 ⁶ NF	-
2VX1395-B6	51.7	0.0801	10 ⁶ NF	-
-B12	52.6	0.0816	10 ⁶ NF	-
-D15	52.1	0.0807	10 ⁶ NF	-
2VX1396-B16	52.0	0.0806	718 800	1
-C1	52.1	0.0807	10 ⁶ NF	- ^b
-D20	51.8	0.0803	88 509	-
2VX1403-A1	52.6	0.0816		- ^c
-A24	52.3	0.0810	10 ⁶ NF	-
2VX1413-A12	52.3	0.0811	396 680	- ^b
-B3	52.3	0.0811	10 ⁶ NF	-
-B9	53.0	0.0821	259 450	- ^b
-C18	52.1	0.0807	10 ⁶ NF	-

a = NF indicates No Failure

b = Fixture Bay in which failure occurred was inadvertently not recorded

c = Coupon failed outside of equal bay length test section

TABLE D28
FATIGUE SCATTER STUDY
RESULTS OF COUPONS TESTED AT A MINIMUM STRESS OF -276 MPa (-40 ksi)

R = -∞, f = 10 Hz, Room Temperature, Laboratory Air,
Average Moisture Content Approximately 0.6%

Coupon ID	Average Area		Cycles To Failure	Failure in Fixture Bay No.
	mm ²	in. ²		
1VX1395-A8	52.5	0.0813	178 350	6
-B10	51.5	0.0798	330 570	4
-B14	52.6	0.0815	102 160	3
-B30	52.6	0.0815	123 030	6
-C12	52.4	0.0812	380 986	6
-D12	52.7	0.0817	66 110	5 _a
-D30	52.0	0.0806	40 459	- _a
2VX1395-A1	51.9	0.0805	187 690	1
-A17	52.1	0.0807	15 440	5
-B19	52.4	0.0812	148 470	2
-C6	52.5	0.0814	6 895	6
-D23	52.7	0.0817	101 039	4
2VX1396-A1	51.9	0.0805	56 000	2
-A4	51.9	0.0805	9 160	3
-A6	51.0	0.0791	206 113	5
-B17	52.7	0.0817	63 094	5
-B27	52.0	0.0806	780	1
-C3	52.4	0.0812	150 508	4 _a
-C26	52.6	0.0816	75 793	- _a
-D1	52.5	0.0814	250 300	1
2VX1413-A1	52.2	0.0809	104 870	1
-A14	52.9	0.0820	149 273	4 _a
-B14	53.4	0.0827	17 275	- _b
-C17	52.2	0.0809	546 000	- _b
-D29	52.6	0.0816	17 200	1

a = Coupon failed outside of equal bay length test section

b = Fixture bay in which failure occurred was inadvertently not recorded

TABLE D29
FATIGUE SCATTER STUDY
RESULTS OF COUPONS TESTED AT A MINIMUM STRESS OF -310 MPa (-45 ksi)

R = -∞, f = 10 Hz, Room Temperature, Laboratory Air,
Average Moisture Content Approximately 0.6%

Coupon ID	Average Area mm ² in. ²	Cycles To Failure	Failure in Fixture Bay No.
1VX1395-B17	52.5 0.0813	20 772	2
-B24	52.5 0.0814	30 420	1 ^a
-B26	51.9 0.0804	44 170	- ^a
-C23	52.7 0.0817	9 843	1
-C28	51.8 0.0803	328	1 ^b
-D6	52.3 0.0811	3 360	- ^b
2VX1395-A12	52.1 0.0807	13 890	6
-A25	52.2 0.0809	14 315	2
-C9	52.6 0.0816	31 520	1
-D6	50.3 0.0779	74 500	5
-D27	51.8 0.0803	19 840	6
2VX1396-A12	56.3 0.0873	7 009	5 ^b
-A29	51.6 0.0800	6 250	- ^b
-A31	50.1 0.0777	651	- ^b
2VX1403-A18	52.1 0.0808	77 289	6
2VX1412-C29	51.9 0.0805	15 239	1
2VX1413-D6	51.9 0.0804	19 105	1
-D14	52.2 0.0809	32 870	4 ^b
-D16	52.2 0.0809	14 251	- ^b

a = Fixture bay in which failure occurred was inadvertently not recorded

b = Coupon failed outside of equal bay length test section

c = Coupon failed before exact load was reached

TABLE D30
 COMPRESSION FAILURE STRENGTH STUDY
 RESULTS OF COUPONS TESTED IN COMPRESSION FATIGUE FIXTURE, MONOTONICALLY
 LOADED TO FAILURE IN SIXTY SECONDS

Room Temperature, Laboratory Air, Average Moisture Content Approximately 0.6%

Coupon ID	Average Area		Failure Stress		Failure in Fixture Bay No.
	mm ²	in. ²	MPa	ksi	
1VX1395-D19	51.6	0.0800	425	61.7	3
2VX1395-A29	51.9	0.0805	392	56.9	3
2VX1396-D14	52.3	0.0811	370	53.6	6
2VX1413-B27	52.5	0.0813	419	60.8	4
2VX1413-C3	51.9	0.0804	415	60.2	3

TABLE D31
 COMPRESSION FAILURE STRENGTH STUDY
 RESULTS OF COUPONS TESTED IN COMPRESSION FATIGUE FIXTURE,
 MONOTONICALLY LOADED TO FAILURE IN ONE SECOND

Room Temperature, Laboratory Air, Average Moisture Content Approximately 0.6%

Coupon ID	Average Area		Failure Stress		Failure in Fixture Bay No.
	mm ²	in. ²	MPa	ksi	
1VX1395-A28 -C6	51.5	0.0799	386	56.0	4,5
	52.1	0.0807	432	62.6	4
2VX1395-C26 -D8	52.0	0.0806	405	58.8	3 _a
	51.8	0.0803	423	61.4	-
2VX1403-B5	52.1	0.0808	425	61.7	4

a = Bay in which failure occurred was inadvertently not recorded

TABLE D32
 COMPRESSION FAILURE STRENGTH STUDY
 RESULTS OF COUPONS TESTED IN COMPRESSION FATIGUE FIXTURE,
 MONOTONICALLY LOADED TO FAILURE IN 0.1 SECONDS

Room Temperature, Laboratory Air, Average Moisture Content Approximately 0.6%

Coupon ID	Average Area		Failure Stress		Failure in Fixture Bay No.
	mm ²	in. ²	MPa	ksi	
2VX1395-A19 -D2	52.0	0.0806	480	69.6	1
	52.2	0.0809	441	64.0	4
2VX1396-B18	52.2	0.0809	435	63.1	2, 3, 4
2VX1413-C9	52.3	0.0810	436	63.3	5

TABLE D33
COMPARISON OF COMPRESSION FAILURE STRENGTHS OF
COUPONS WHICH FAILED IN THE COMPRESSION FATIGUE FIXTURE,
MONOTONICALLY LOADED AT VARIOUS LOADING RATES

Failure Time (Seconds)	Stress at Failure	
	MPa	ksi
60	370	53.6
	392	56.9
	415	60.2
	419	60.8
	425	61.7
1	386	56.0
	405	58.8
	423	61.4
	425	61.7
	432	62.6
0.1	435	63.1
	436	63.3
	441	64.0
	480	69.6

TABLE D34
PROGRESSIVE LOAD STUDY
RESULTS OF COUPONS PROGRESSIVELY LOADED TO FAILURE IN COMPRESSION
IN ONE MINUTE WITH SUPERIMPOSED SINE WAVE LOAD CYCLING

R = - ∞ , f = 10 Hz, Room Temperature, Laboratory Air,
Average Moisture Content Approximately 0.6%

Coupon ID	Average Area mm ²	in. ²	Cycles to Failure	Failure Stress MPa	ksi	Failure in Fixture Bay No.
1VX1395-A24	51.8	0.0803	598	-459	-66.5	2
-C22	51.3	0.0795	560	-434	-63.0	2,3
-D8	51.7	0.0801	562	-434	-62.9	3,4
-D15	51.9	0.0804	564	-432	-62.7	3
2VX1395-A4	51.5	0.0799	548	-421	-61.1	2
-A8	51.5	0.0799	572	-433	-62.8	3
-B18	52.6	0.0816	498	-352	-51.0	4
-B27	52.6	0.0815	578	-437	-63.4	3
-C19	51.6	0.0800	562	-431	-62.5	3
2VX1396-A24	52.8	0.0818	586	-432	-62.7	3
-A28	51.9	0.0805	566	-423	-61.3	3
-B22	51.4	0.0797	574	-432	-62.6	4
-C15	52.6	0.0815	568	-	-	3
2VX1413-A30	53.1	0.0823	586	-432	-62.6	3
-B17	52.1	0.0807	570	-428	-62.0	2
-C12	52.5	0.0813	554	-417	-60.5	5

TABLE D35
PROGRESSIVE LOAD STUDY
RESULTS OF COUPONS PROGRESSIVELY LOADED TO FAILURE IN COMPRESSION
IN ONE HOUR WITH SUPERIMPOSED SINE WAVE LOAD CYCLING

R = - ∞ , f = 10 Hz, Room Temperature, Laboratory Air,
Average Moisture Content Approximately 0.6%

Coupon ID	Average Area		Cycles to Failure	Failure Stress		Failure in Fixture Bay No.
	mm ²	in. ²		MPa	ksi	
1VX1395-A10	51.5	0.0799	35 340	-382	-55.4	1
-B27	51.6	0.0800	34 808	-384	-55.7	3
-C5	51.7	0.0801	35 568	-384	-55.7	2 ^a
-D7	51.5	0.0799	30 400	-379	-54.9	- ^a
2VX1395-A3	51.5	0.0798	33 532	-372	-53.9	- ^b
-C8	52.0	0.0806	35 264	-381	-55.3	3
-C10	51.5	0.0799	34 276	-379	-54.9	2
-C24	52.0	0.0806	34 504	-377	-54.7	2
-D14	52.1	0.0807	28 348	-389	-56.4	1
2VX1396-C18	52.2	0.0809	34 656	-505	-73.3	2
2VX1413-A8	51.6	0.0800	33 364	-355	-51.5	3
-C27	52.3	0.0810	34 732	-368	-53.3	1 ^a
-D27	52.2	0.0809	29 792	-363	-52.7	- ^a

a = Fixture bay in which coupon failed was inadvertently not recorded

b = Coupon failed outside of equal bay length test section

TABLE D36
BLOCK LOADING COMPRESSION
FATIGUE LIVES OF COUPONS CYCLED AT -241 MPa (-35 ksi)
AFTER PRIOR CYCLING AT -310 MPa (-45 ksi)

R = - ∞ , f = 10 Hz, Room Temperature, Laboratory Air,
Average Moisture Content Approximately 0.6%

No Prior Cycling	5 000 Cycles At -310 MPa (-45 ksi)	15 000 Cycles at -310 MPa (-45 ksi)
262 086	505	3 479
295 450	3 295	14 069
396 680	93 600	211 780
497 089	313 984	388 642
718 800	537 425	676 000
10 ⁶ NF ^a	682 914	10 ⁶ NF
10 ⁶ NF	763 556	10 ⁶ NF
10 ⁶ NF	829 000	10 ⁶ NF
10 ⁶ NF	10 ⁶ NF	10 ⁶ NF
10 ⁶ NF	10 ⁶ NF	10 ⁶ NF
10 ⁶ NF	10 ⁶ NF	10 ⁶ NF
10 ⁶ NF	10 ⁶ NF	10 ⁶ NF
10 ⁶ NF	10 ⁶ NF	10 ⁶ NF
10 ⁶ NF	10 ⁶ NF	10 ⁶ NF
10 ⁶ NF		
10 ⁶ NF		

a = NF indicates No Failure

TABLE D37
BLOCK LOADING COMPRESSION
FATIGUE LIVES OF COUPONS CYCLED AT -310 MPa (-45 ksi)
AFTER PRIOR CYCLING AT -241 MPa (-35 ksi)

R = - ∞ , f = 10 Hz, Room Temperature, Laboratory Air,
Average Moisture Content Approximately 0.6%

No. Prior Cycling	200 000 Cycles at - 241 MPa (-35 ksi)
382	73
651	170
3 360	1 053
7 009	3 572
9 843	5 214
13 890	7 967
14 251	10 494
14 315	16 860
15 239	17 719
19 105	46 809
19 840	47 358
20 772	57 505
26 647	64 726
30 420	171 879
31 520	227 912
32 870	
44 170	
74 500	
77 289	

TABLE D38
BLOCK FATIGUE STUDY
RESULTS OF COUPONS CYCLED AT -310 MPa (-45 ksi) FOR 5 000 CYCLES
AND CYCLED TO FAILURE AT -241 MPa (-35 ksi)

R = - ∞ , f = 10 Hz, Room Temperature, Laboratory Air,
Average Moisture Content Approximately 0.6%

Coupon ID	mm ²	Average Area in. ²	Cycles To Failure	Failure in Fixture Bay No.
1VX1395-A31	50.7	0.0786	763 556	- ^a
-B1	51.7	0.0802	829 000	2
-B22	51.0	0.0790	93 600 ^b	2
-C7	51.5	0.0798	10 ⁶ NF	-
2VX1395-B15	51.7	0.0801	10 ⁶ NF	-
-C30	51.9	0.0804	313 984	6
2VX1396-A13	52.0	0.0806	10 ⁶ NF	-
-A22	51.7	0.0801	682 914	c
-A27	51.9	0.0804	10 ⁶ NF	-
-B23	52.0	0.0806	10 ⁶ NF	-
-B28	51.6	0.0800	505	c
-C19	52.2	0.0809	10 ⁶ NF	-
2VX1403-C27	51.7	0.0801	3 295	6
2VX1413-C30	52.6	0.0816	537 425	2

a = Fixture bay in which failure occurred was inadvertently not recorded

b = NF indicates No Failure

c = Coupon failed outside of equal bay length test section

TABLE D39
BLOCK FATIGUE STUDY
RESULTS OF COUPONS CYCLED AT -310 MPa (-45 ksi) FOR 15 000 CYCLES
AND CYCLED TO FAILURE AT -241 MPa (-35 ksi)

R = - α , f = 10 Hz, Room Temperature, Laboratory Air,
Average Moisture Content Approximately 0.6%

Coupon ID	Average Area mm ² in. ²		Cycles To Failure	Failure in Fixture Bay No.
1VX1395-B16	52.1	0.0808	10 ⁶ NF ^a	-
-C16	52.6	0.0816	10 ⁶ NF	-
-D1	52.1	0.0807	10 ⁶ NF	-
-D3	52.5	0.0814	10 ⁶ NF	-
-D14	51.7	0.0802	10 ⁶ NF	- ^b
-D28	52.1	0.0808	14 064	-
2VX1395-D22	51.5	0.0799	10 ⁶ NF	-
2VX1396-A17	52.6	0.0815	10 ⁶ NF	-
-B2	52.1	0.0808	10 ⁶ NF	-
-B30	52.6	0.0816	676 000	1
-C5	53.4	0.0828	211 780	5
-C20	52.4	0.0812	10 ⁶ NF	-
-C31	49.9	0.0774	388 642	3 ^b
-D23	52.7	0.0817	3 479	-

a = NF indicates No Failure

b = Coupon failed outside of equal bay length test section

TABLE D40
BLOCK FATIGUE STUDY
RESULTS OF COUPONS CYCLED AT -241 MPa (-35 ksi) FOR 200 000 CYCLES
AND CYCLED TO FAILURE AT -310 MPa (-45 ksi)

R = - ∞ , f = 10 Hz, Room Temperature, Laboratory Air,
Average Moisture Content Approximately 0.6%

Coupon ID	Average Area		Cycles To Failure	Failure in Fixture Bay No.
	mm ²	in. ²		
2VX1395-A20	52.2	0.0809	3 572	6
-B8	52.8	0.0819	227 912	4
-B9	52.5	0.0813	10 494	3
-B26	51.6	0.0800	171 879	1
-B30	51.8	0.0803	1 053	3 ^a
-C13	51.8	0.0803	73	- ^a
-C14	52.6	0.0816	47 358	2
-D5	52.1	0.0807	64 726	1
2VX1396-A7	51.4	0.0797	16 860	2 ^a
-A15	52.1	0.0808	5 214	- ^a
-B1	52.6	0.0815	17 719	2
-B6	51.6	0.0800	170	2
-C10	52.5	0.0813	7 967	1 ^a
-C23	51.5	0.0799	46 809	- ^a
-D25	51.7	0.0802	57 505	5

a = Coupon failed outside of equal bay length test section

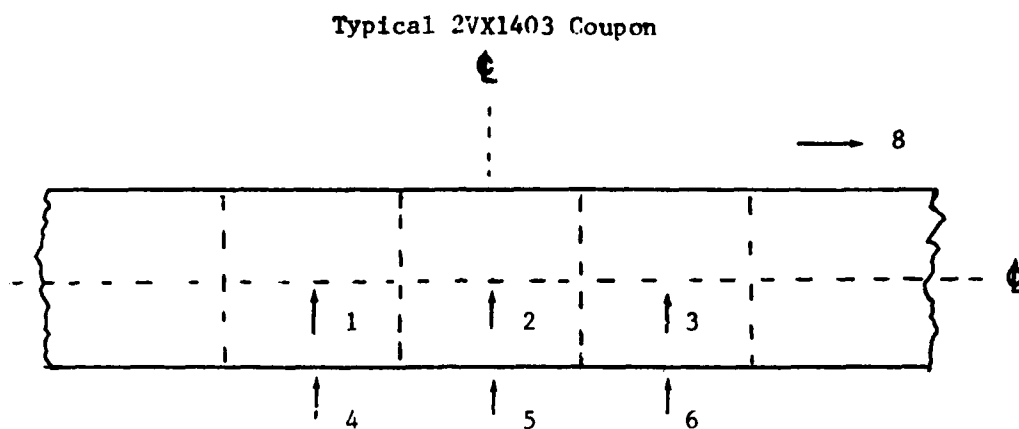
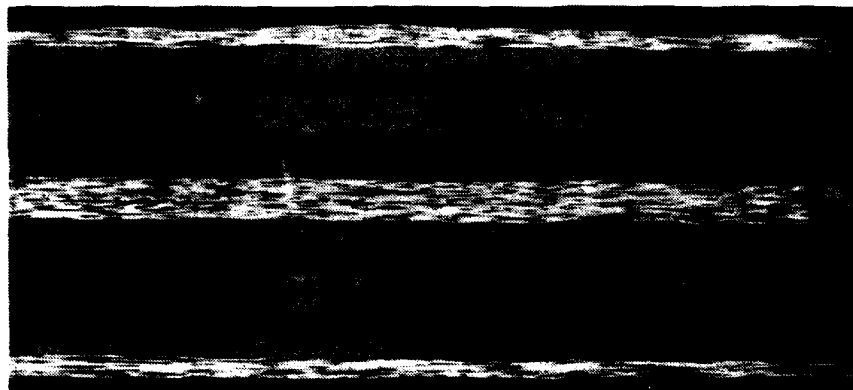
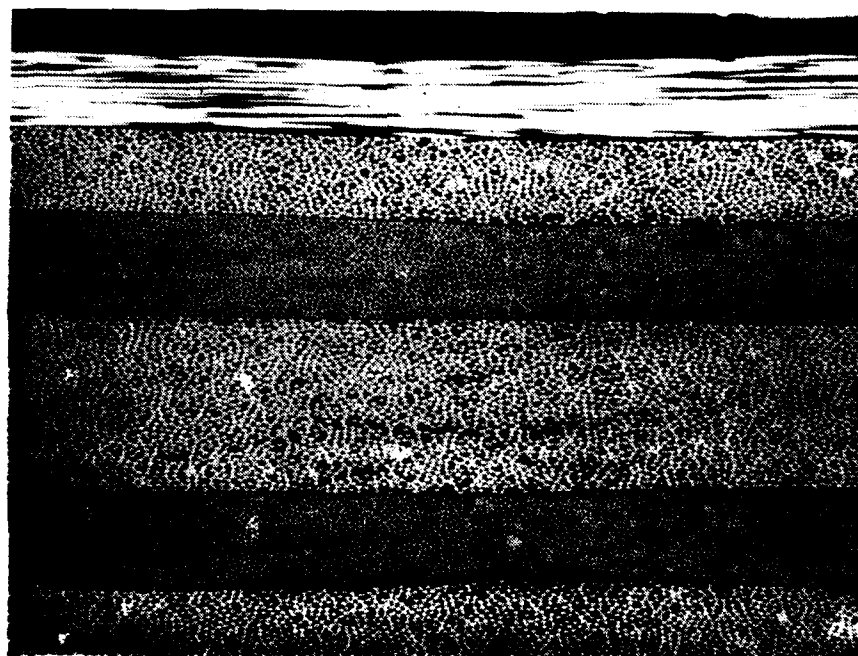


Figure D1: Photographs of Typical Cross-Sections of Coupons Monotonically Loaded in Tension to Various Percentages of the Average Ultimate Strength.

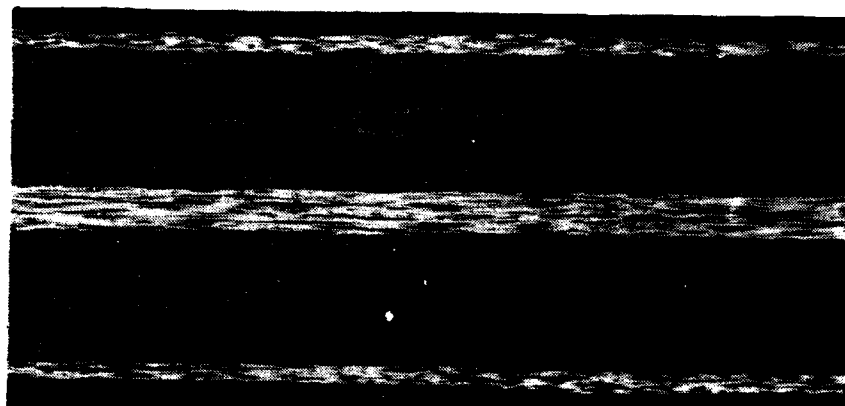


25X

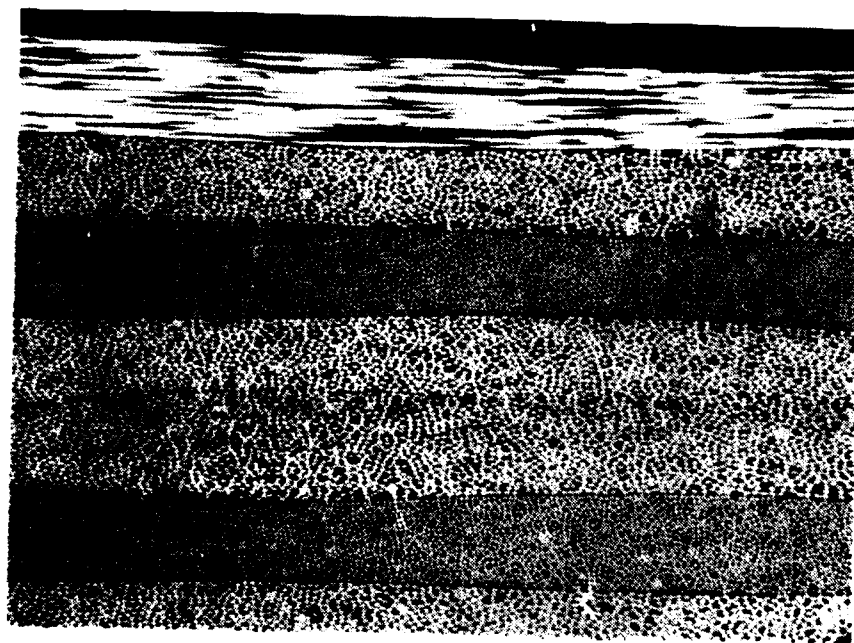


100X

Dla: Coupon 2VX1403-D23, Area 1, 20 Percent

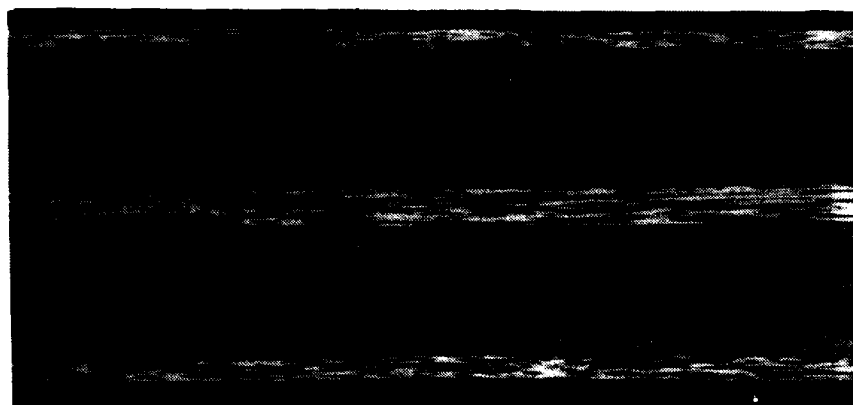


25X

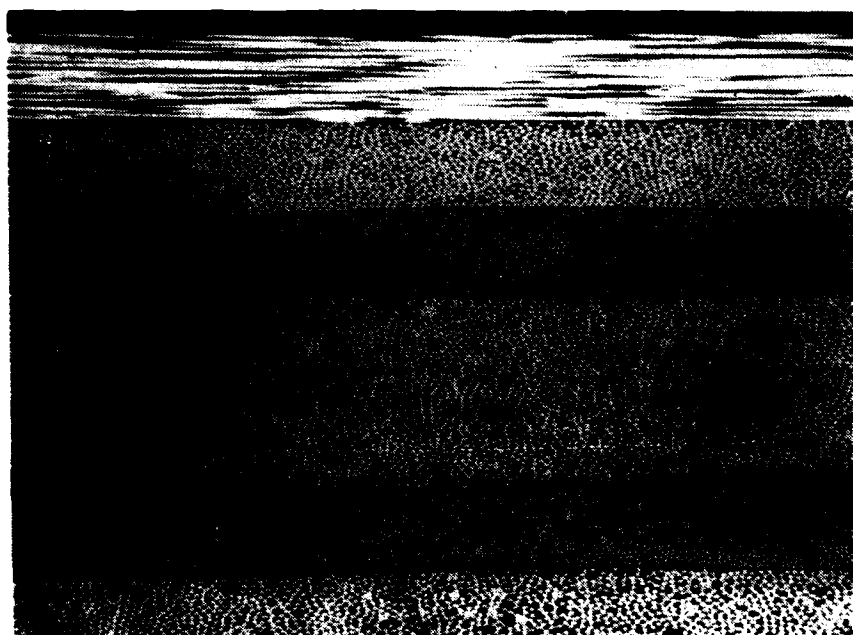


100X

D1b: Coupon 2VX1403-D23, Area 2, 20 Percent

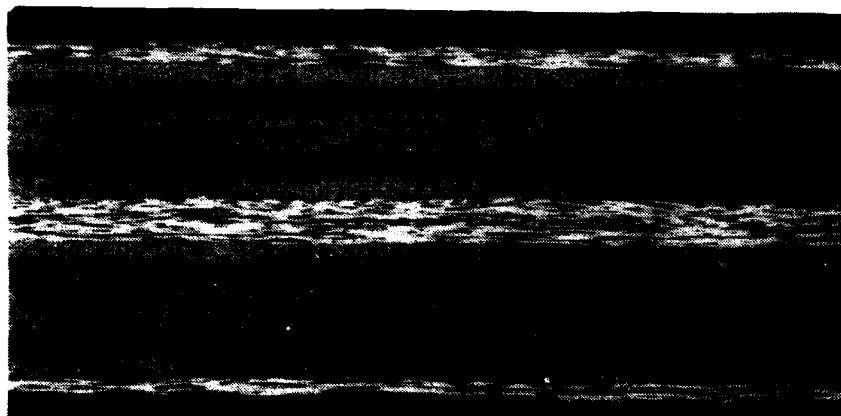


25X

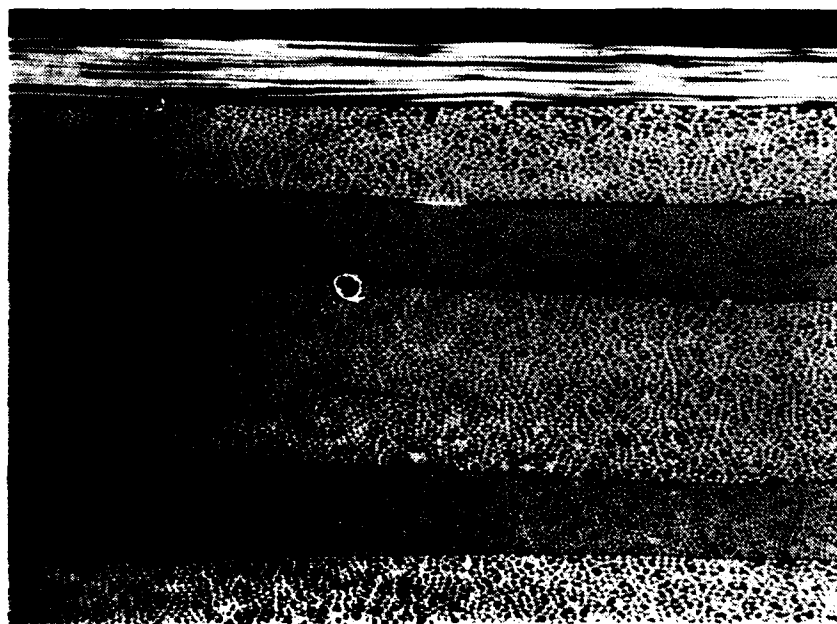


100X

Dlc: Coupon 2VX1403-B29, Area 1, 40 Percent

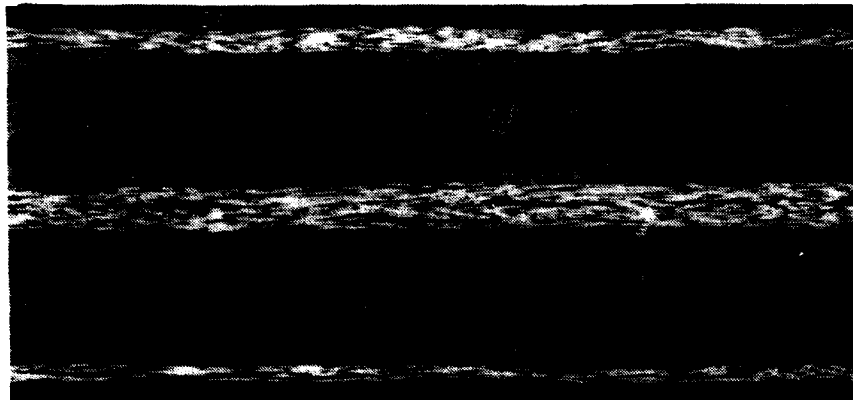


25X

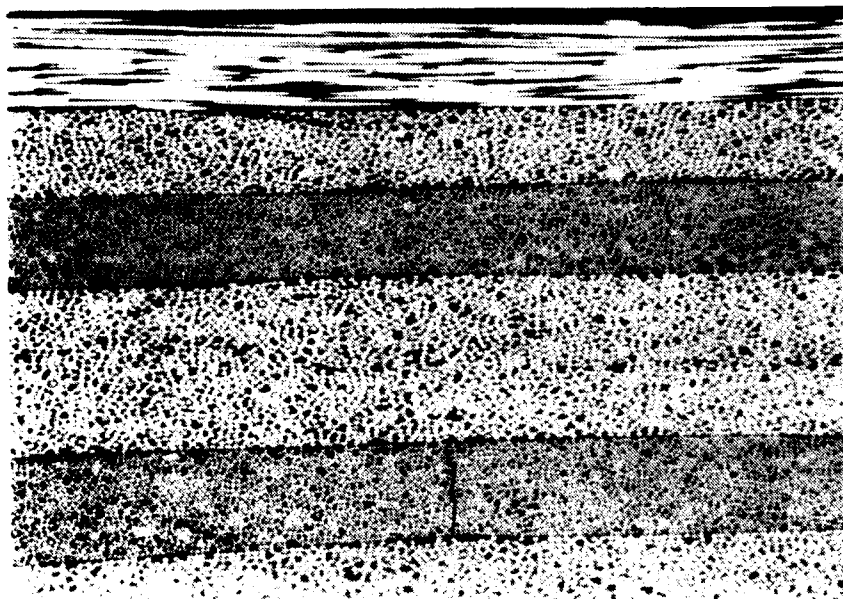


100X

Dld: Coupon 2VX1403-B29, Area 2, 40 Percent

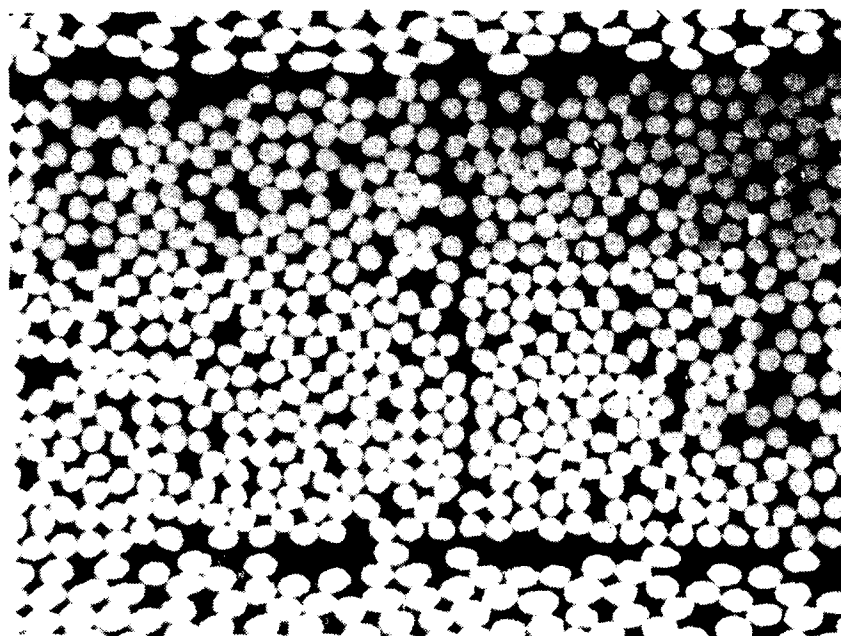


25X



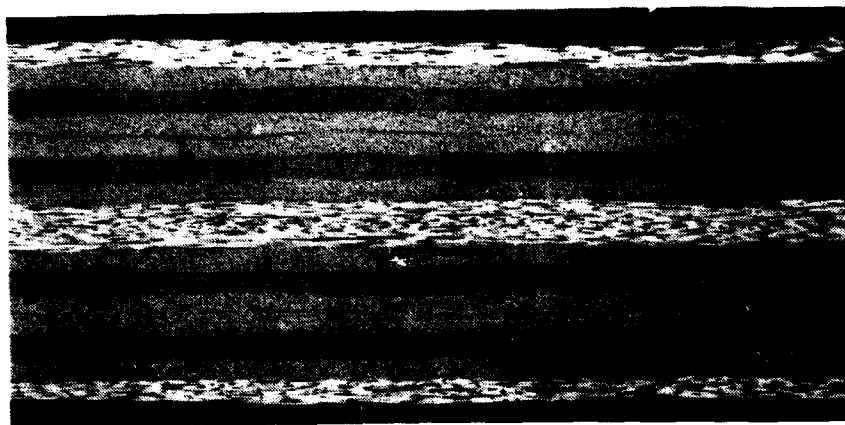
100X

Dle: Coupon 2VX1403-D17, Area 1, 60 Percent

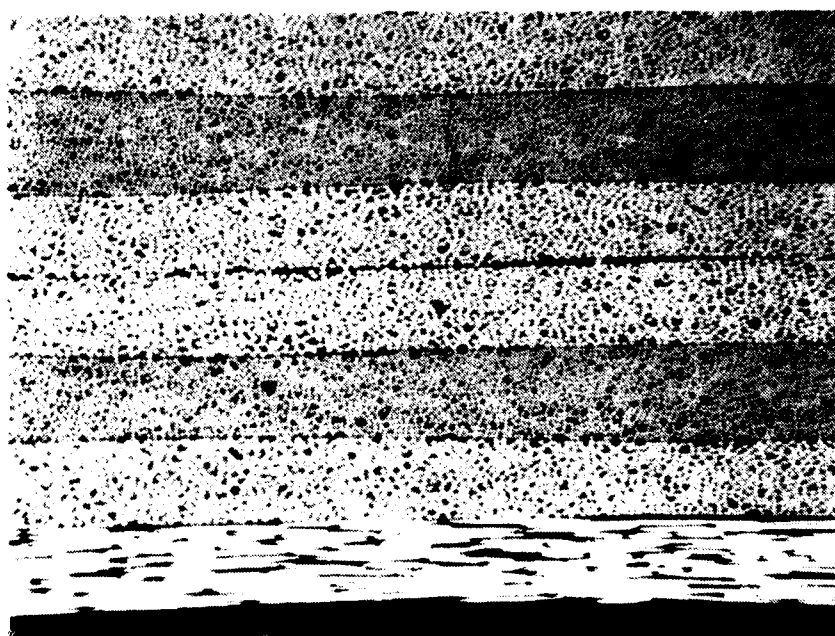


500X

Dlf: Coupon 2VX1403-D17, Area 1, 60 Percent

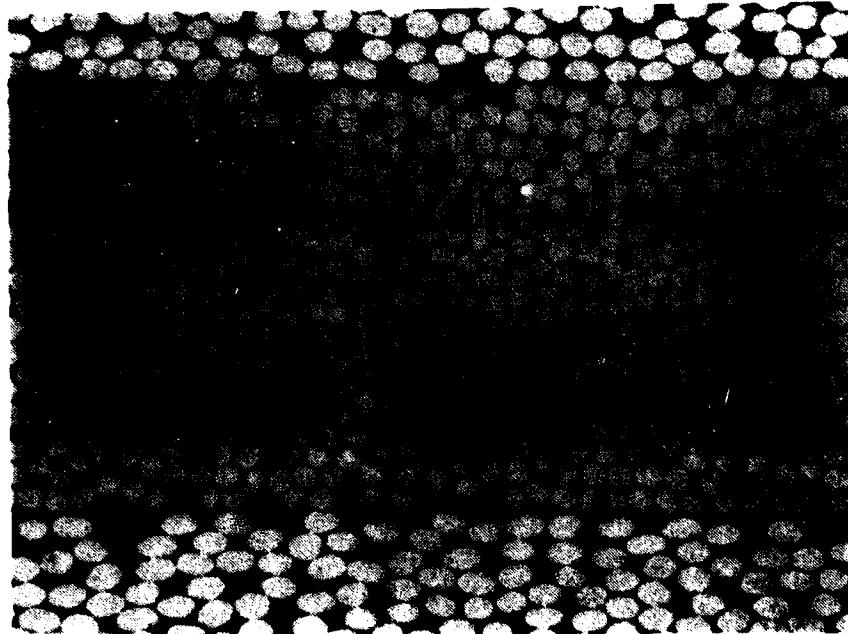


25X



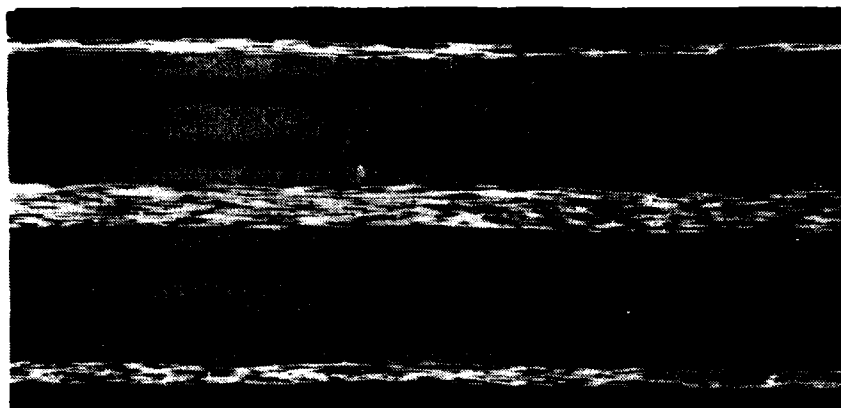
100X

Dlg: Coupon 2VX1403-D17, Area 2, 60 Percent

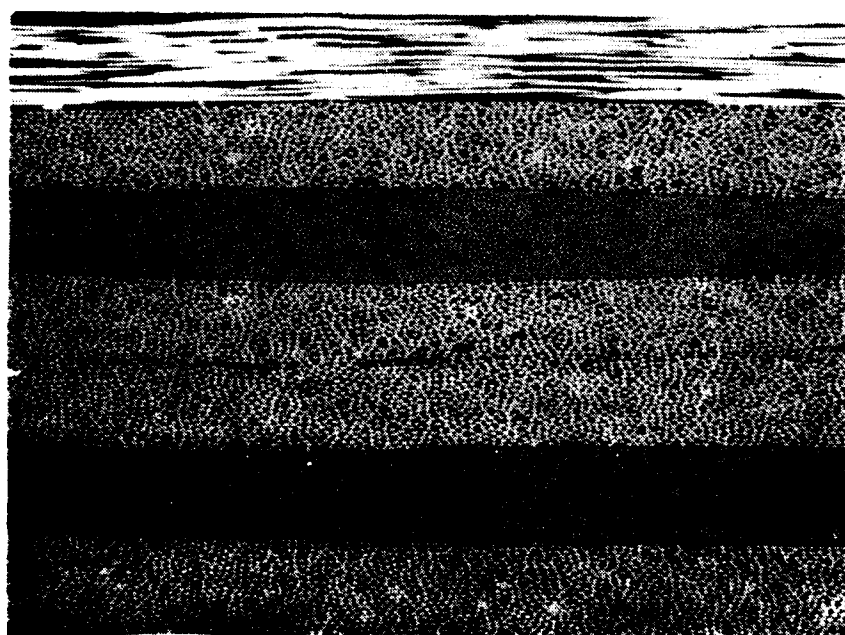


500X

Dlh: Coupon 2VX1403-D17, Area 2, 60 Percent

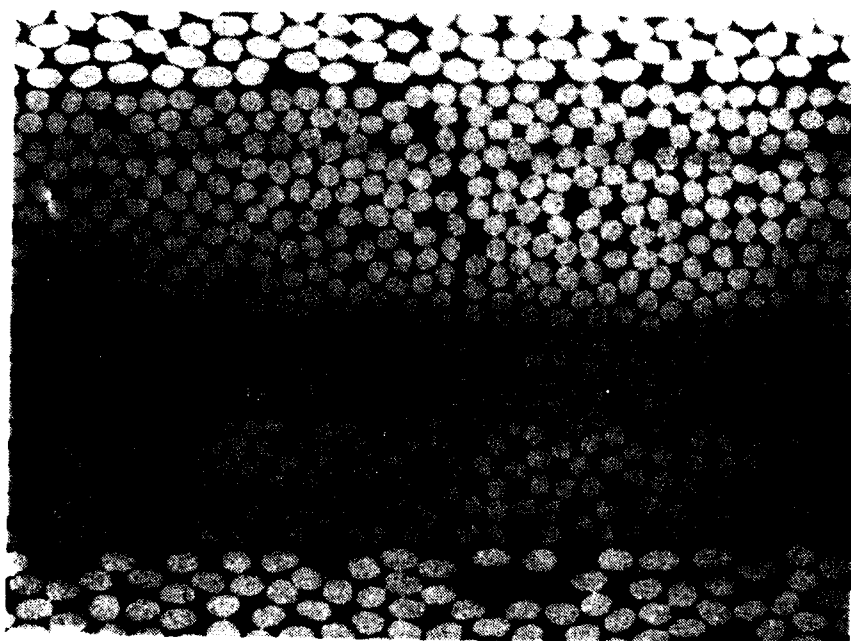


25X



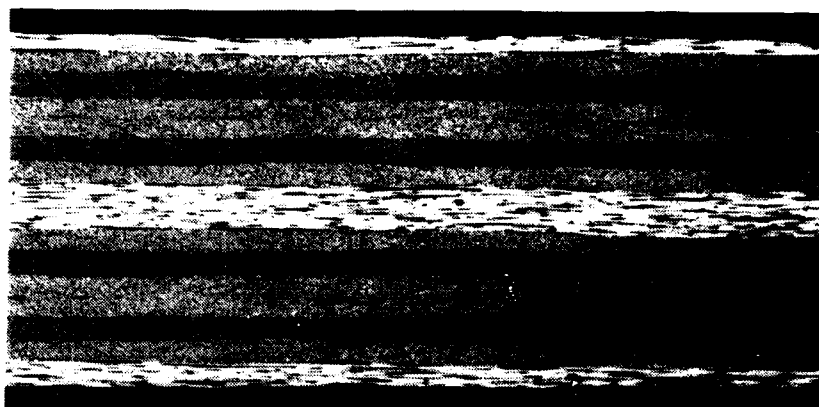
100X

D1i: Coupon 2VX1403-D27, Area 2, 80 Percent

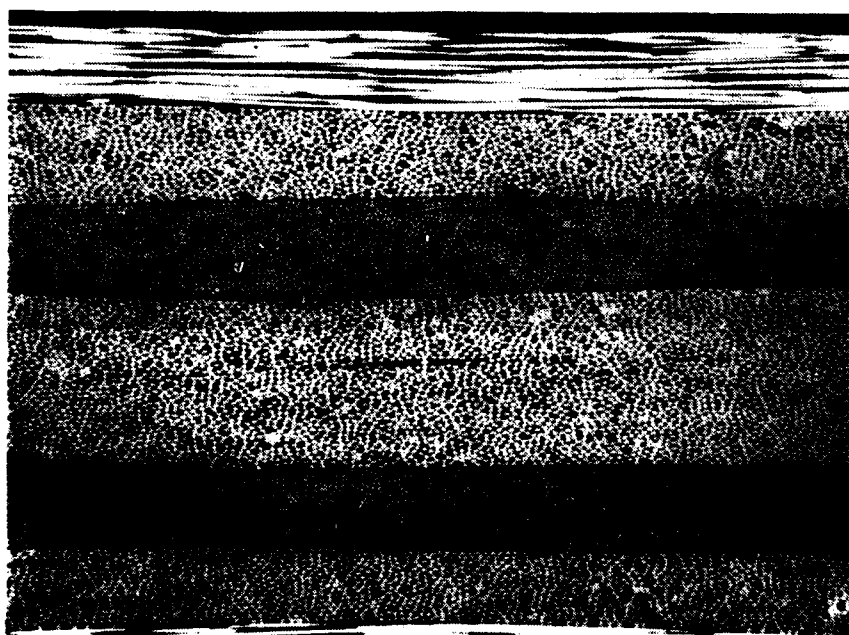


500X

D1j: Coupon 2VX1403-D27, Area 2, 80 Percent

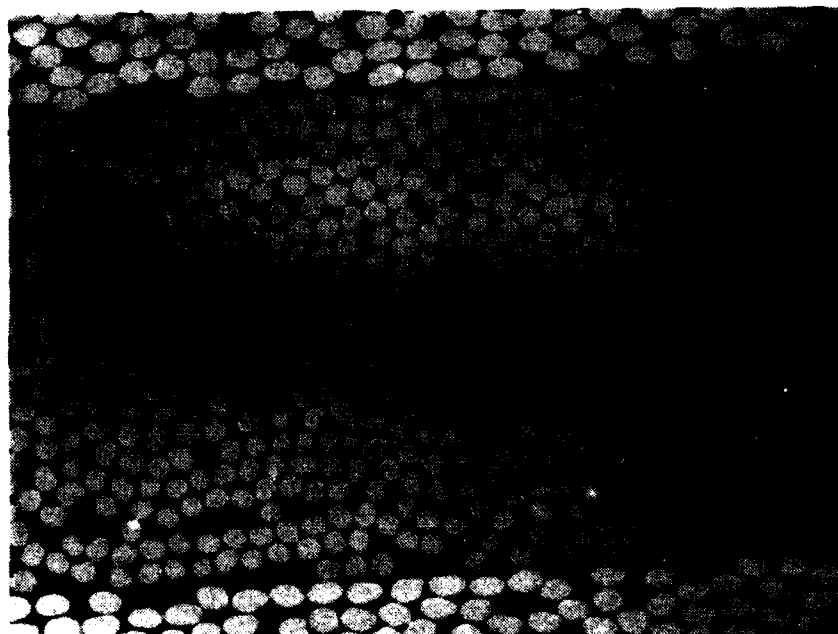


25X



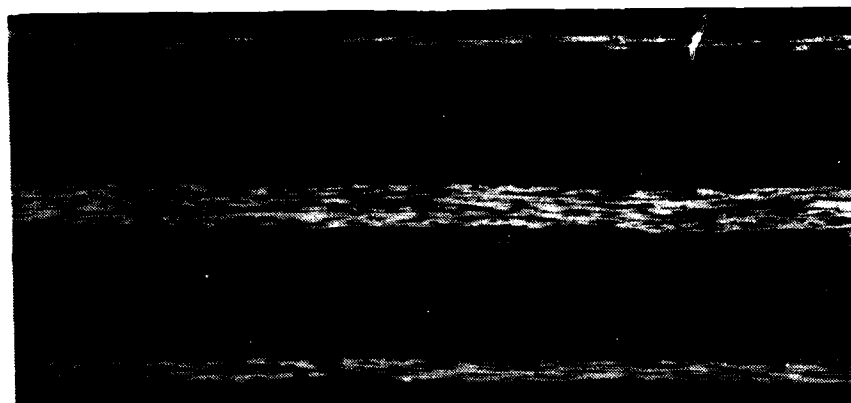
100X

Dlk: Coupon 2VX1403-D27, Area 3, 80 Percent

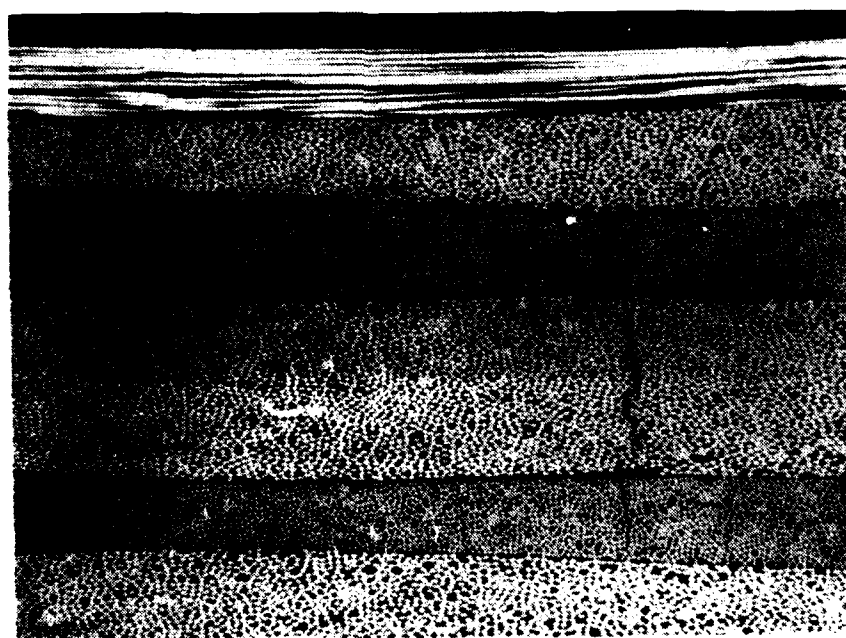


500X

D114: Coupon 2VX1403-D27, Area 3, 80 Percent

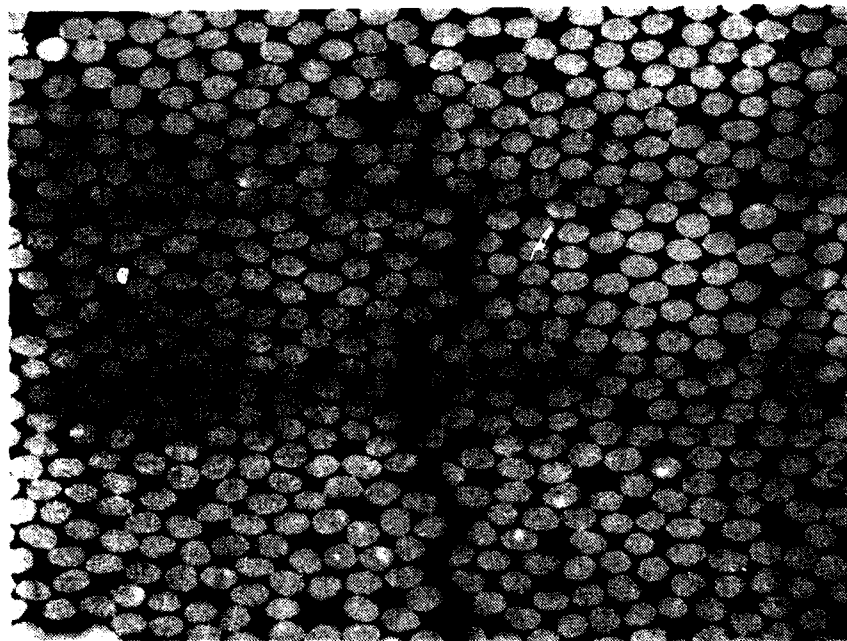


25X



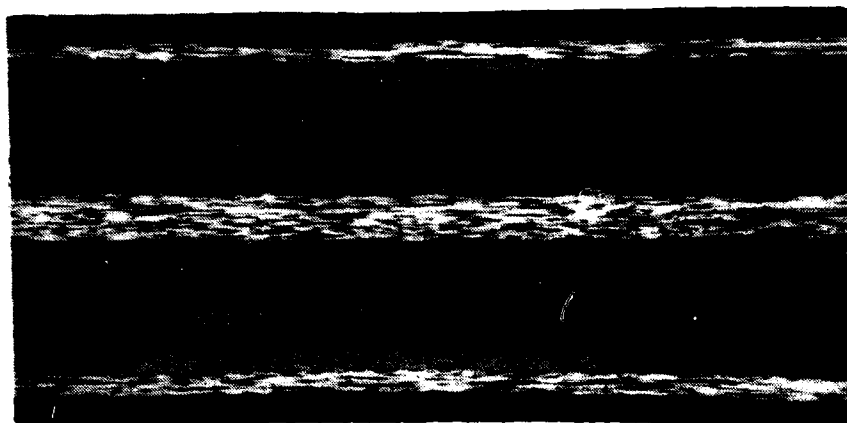
100X

Dlm: Coupon 2VX1403-D14, Area 1, 90 Percent

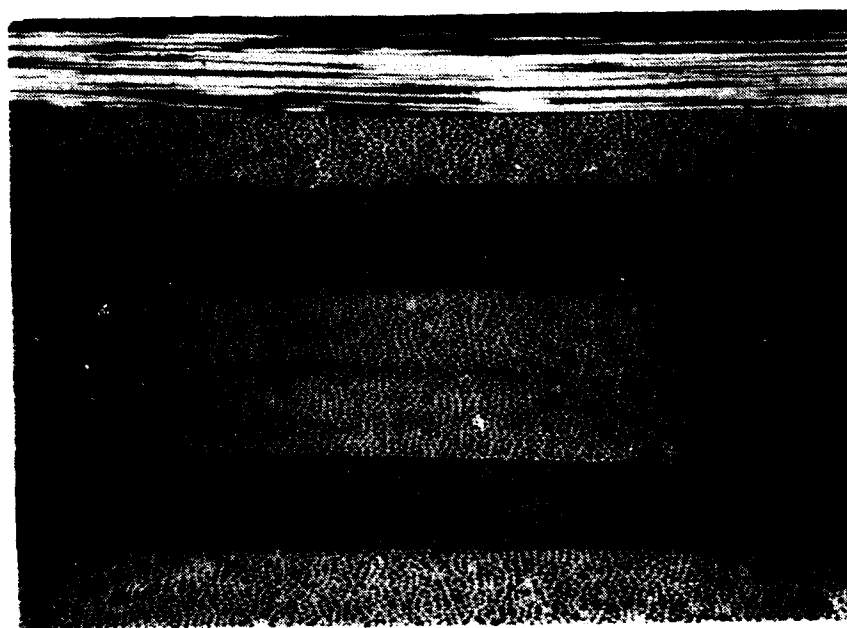


500X

Dln: Coupon 2VX1403-D14, Area 1, 90 Percent

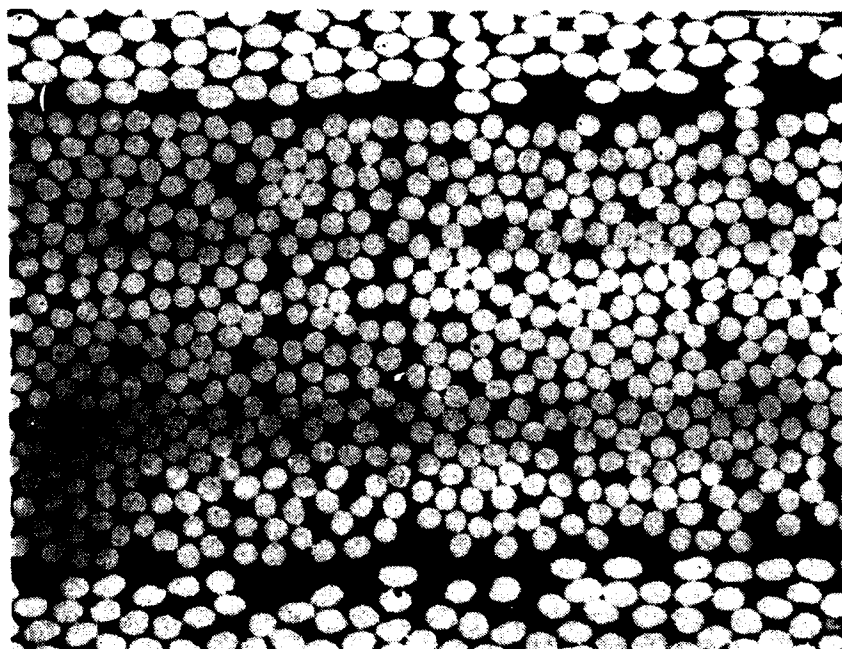


25X



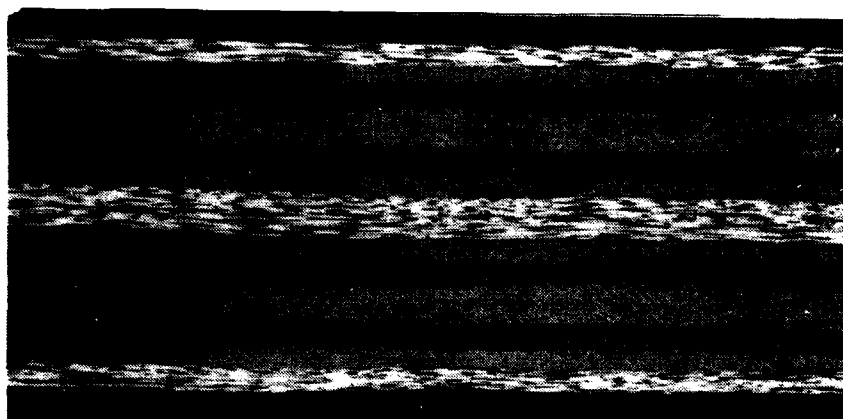
100X

Dlo: Coupon 2VX1403-D14, Area 2, 90 Percent

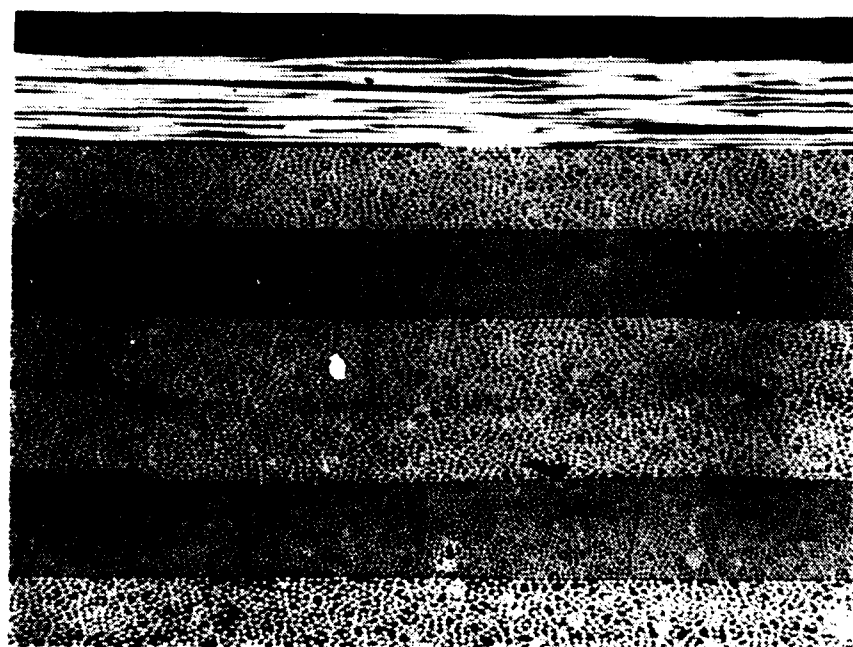


500X

Dlp: Coupon 2VX1403-D14, Area 2, 90 Percent

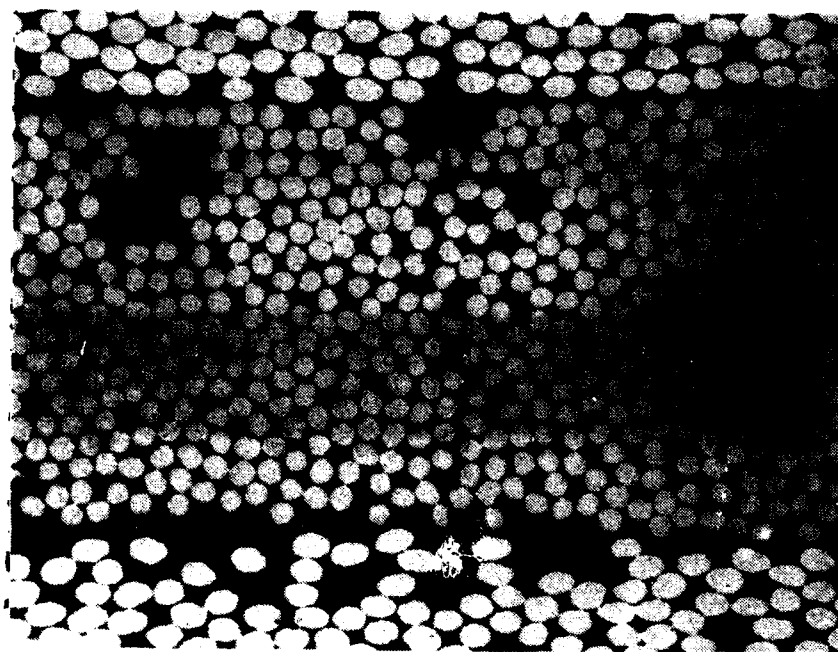


25X



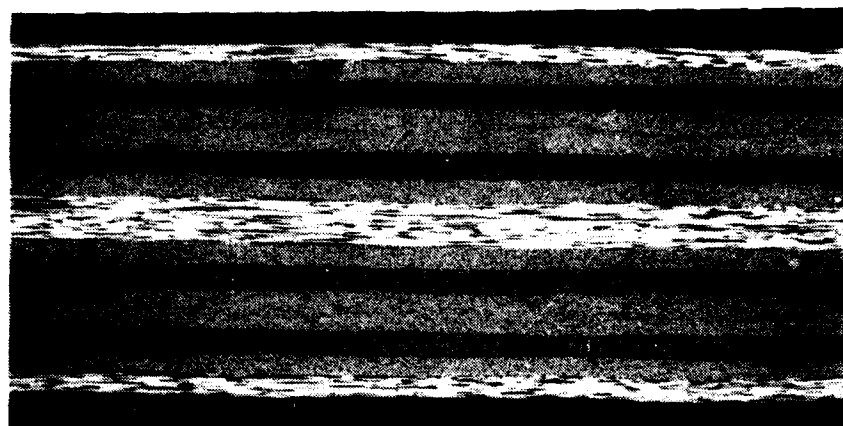
100X

Dlq: Coupon 2VX1403-D29, Area 1, 95.Percent

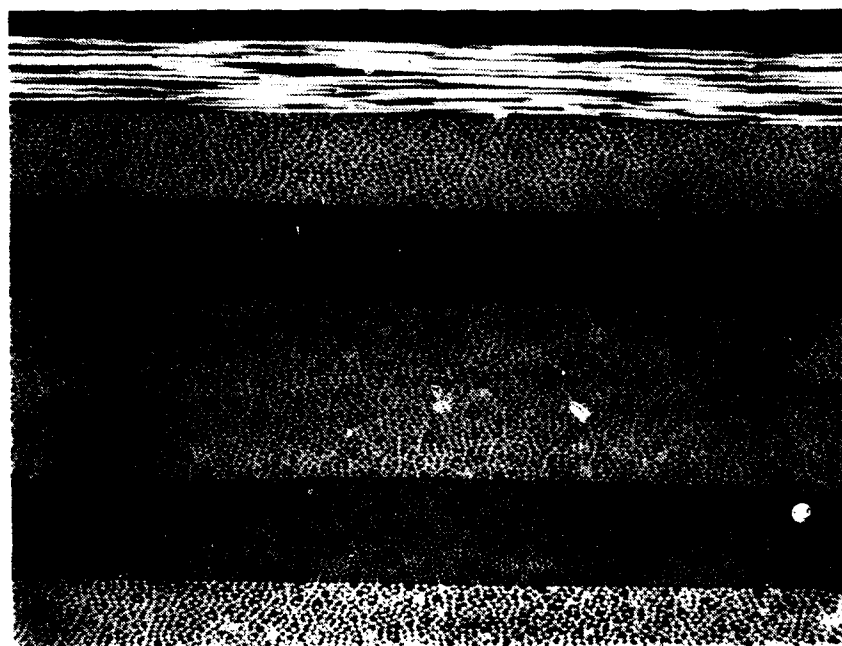


500X

Dlr: Coupon 2VX1403-D29, Area 1, 95 Percent



25X



100X

Dls: Coupon 2VX1403-D29, Area 2, 95 Percent

AD-A118 084

LOCKHEED-CALIFORNIA CO BURBANK RYE CANYON RESEARCH LAB

F/G 11/4

EFFECT OF LOAD HISTORY ON FATIGUE LIFE.(U)

DEC 81 J T RYDER, K N LAURAITIS

F33615-78-C-5090

UNCLASSIFIED

LR-29586-1

AFWAL-TR-81-4155

NL

4 1/4

4 1/4



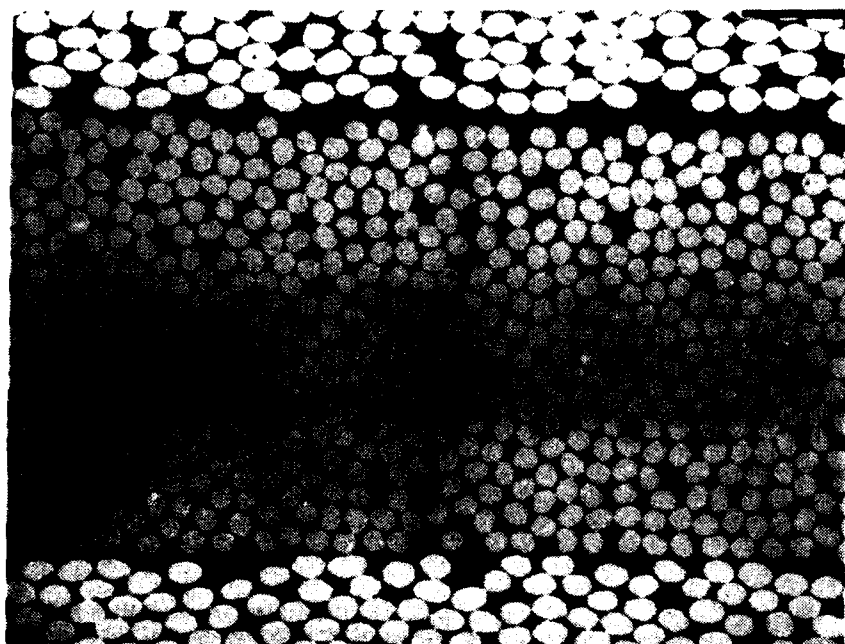
END

DATE

FILED

9 82

DTIC



500X

Dlt: Coupon 2VX1403-D29, Area 2, 95 Percent

FILME
— 8